

**Asymmetric Hydrogenation of Alkenes with Cationic
Iridium(I) Complexes of 2-Phosphino-1-Aminoferrocene
Ligands**

by

Lori Van Belle, B. Sc., University of Ontario Institute of Technology

A Thesis

submitted to the Department of Chemistry

in partial fulfillment of the requirements for the degree of

Master of Science

Supervised by

Professor Costa Metallinos

August 2010

Brock University

St. Catharines, Ontario

© Lori Van Belle 2010

Abstract

Iridium complexes with bidentate *P,N* ligands represent a class of catalysts that significantly expand the application range of asymmetric hydrogenation. New substrate classes, for which there have previously been no suitable catalysts, can now be efficiently hydrogenated in high conversion and enantioselectivity. These substrates are often of synthetic importance, thus iridium catalysis represents a significant advance in the field of asymmetric catalysis.

Planar chiral ferrocenyl aminophosphine ligands in which both heteroatoms were directly bound to the cyclopentadienyl ring were prepared by BF_3 -activated lithiation-substitution in the presence of a chiral diamine in 49-59% yield and 75-85% enantiomeric excess. Some of these ligands were recrystallized to enantiomeric purity via ammonium fluoroborate salt formation of the phosphine sulfide. A crystal structure of one of these compounds was obtained and features an intramolecular hydrogen bond between the nitrogen, hydrogen, and sulfur atoms. Neutralization, followed by desulfurization, provided the free ligands in enantiomeric purity. Iridium complexes with these ligands were formed via reaction with $[\text{Ir}(\text{COD})\text{Cl}]_2$ followed by anion exchange with NaBAr_F . These complexes were successfully applied in homogeneous hydrogenation of several prochiral substrates, providing products in up to 92% enantiomeric excess. Variation of the dimethylamino group to a pyrrolidine group had a negative effect on the selectivity of hydrogenation. Variation of the substituents on phosphorus to bulkier *ortho*-tolyl groups had a positive effect, while variation to the more electron rich dicyclohexyl phosphine had a negative effect on selectivity.

Acknowledgments

First and foremost, I would like to thank my family. They have always supported my pursuit of knowledge and a higher education, and encouraged me to follow my dreams wherever they take me.

Second, I would like to thank past Metallinos group members for their guidance and support throughout my two years here at Brock. In particular I would like to thank Josh Zaifman for always helping me both in the lab and with any questions I had. He was a great asset to me professionally and a great friend and confidant.

Third, I would like to acknowledge my supervisor, Dr. Costa Metallinos. Without his guidance, support, and encouragement this project would not have gone as smoothly. His constant push to get new results and explain my findings has made me a better scientist.

Last, I would like to thank the other professors here at Brock University. In particular, my committee members, Dr. van der Est and Dr. Yan for their questions, suggestions, and encouragement during my time here, as well as Dr. Hudlicky for always encouraging me to set higher expectations for myself, to be inquisitive and critical of the literature, and to keep striving for greater things.

Table of Contents

Acknowledgments.....	ii
Table of Contents	iii
List of Tables	v
List of Figures	vi
List of Schemes.....	x
Chapter 1: Introduction and Historical Background.....	1
1.1 Catalysis, Ligands, and Complexes.	1
1.1.1 Chiral Ligands and Complexes.....	4
1.2 <i>P,N</i> Donor Ligands.	5
1.2.1 Amine <i>N</i> , Phosphine <i>P</i> Ligands.....	7
1.2.2 Imine <i>N</i> , Phosphine <i>P</i> Ligands.....	15
1.2.3 Imine <i>N</i> , Heteroatom Bound <i>P</i> Ligands.....	25
1.3 Catalytic Homogeneous Hydrogenation.....	26
1.3.1 Structural Types of Alkenes in Asymmetric Homogenous Hydrogenation. ...	30
1.3.2 Iridium-Catalyzed Homogeneous Hydrogenation.	31
1.3.3 Further Development of Iridium Catalysts.	35
1.3.4 Mechanistic Studies of Ir-Catalyzed Hydrogenation.....	38
1.3.5 Applications of Ir-Catalyzed Hydrogenation.....	50
1.4 Planar Chiral Ferrocene Ligands.	58
1.4.1 1,2-Substituted Planar Chiral Ferrocenes.	58

1.4.2 Stereoselective Synthesis of Planar Chiral <i>P,N</i> Ferrocenes and Aminoferrocenes.....	58
1.4.3 Applications of Planar Chiral <i>P,N</i> Ferrocene Ligands.....	67
1.5 Aims and Objectives.....	69
Chapter 2: Results and Discussion.....	72
2.1 Synthesis of Aminoferrocenes.....	72
2.2 2-Phosphino-1-aminoferrocene Ligand Synthesis.....	74
2.3 Synthesis of Iridium Complexes.....	76
2.4 Hydrogenation of Alkenes with Racemic Iridium(COD) Complex 221	81
2.5 Synthesis of Enantiopure 2-Phosphino-1-aminoferrocenes and their Iridium Complexes.....	87
2.6 Synthesis of Enantiopure Iridium Complexes.....	93
2.7 Asymmetric Hydrogenation of Alkenes with Enantioenriched / Enantiopure Iridium(COD)[BAR _F] Complexes (<i>S</i>)- 221 , (<i>S</i>)- 234 , (<i>S</i>)- 235 , and (<i>S</i>)- 236	95
2.8 Proposed Mechanism of Hydrogenation.....	99
Chapter 3: Conclusions	107
Chapter 4: Future Work	109
Chapter 5: Experimental	112
Chapter 6: References	186
Chapter 7: Appendices.....	198
7.1 Appendix 1 – NMR data.....	198
7.2 Appendix 2 – X-ray data.....	242

List of Tables

Table 1. Pd-catalyzed asymmetric allylic alkylations with various nucleophiles with phosphinooxazoline ligand 50 (reproduced from ref 32).	20
Table 2. Asymmetric transfer hydrogenation with ferrocenyl phosphinooxazoline Ru complex 63 (reproduced from ref 41).	23
Table 3. Ir-catalyzed asymmetric hydrosilylations of imines and ketones with ferrocenyl phosphinooxazoline ligands 66 and 67 (reproduced from ref 42).	24
Table 4. Turnover frequencies (mol substrate reduced (mol catalyst) ⁻¹ h ⁻¹) for several olefins with various catalysts (reproduced from ref 56).	32
Table 5. Steroid derivatives reduced with Crabtree's iridium complex.	35
Table 6. Selectivities of several chiral catalysts (reproduced from ref 76).	51
Table 7. Pd-catalyzed Suzuki-Miyaura cross coupling (reproduced from ref 111).	75
Table 8. Pd-catalyzed Buchwald-Hartwig aminations (reproduced from ref 111).	76
Table 9. Iridium catalyzed hydrogenation of disubstituted alkenes.	82
Table 10. Racemic Ir-catalyzed hydrogenation of prochiral alkenes.	84
Table 11. Asymmetric hydrogenation results with complexes (<i>S</i>)- 221 , (<i>S</i>)- 234 , (<i>S</i>)- 235 , and (<i>S</i>)- 236	95
Table 12. Additional asymmetric hydrogenation results with complex (<i>S</i>)- 221	96

List of Figures

Figure 1. Ligand bite angle formed upon coordination of heteroatoms X and Y with metal M.	2
Figure 2. Different categories of chirality.....	4
Figure 3. PPFA and MPFA ligands.	7
Figure 4. Mechanism of Ni-catalyzed asymmetric Grignard cross coupling with β -aminoalkylphosphines (adapted from ref 16).	9
Figure 5. Mechanism of Ni-catalyzed asymmetric Grignard cross coupling with ferrocene <i>P,N</i> ligands (adapted from ref 17).....	10
Figure 6: Diphenylphosphinoxazoline ligand structure.....	19
Figure 7. Catalytic H ₂ and transfer hydrogenations.....	27
Figure 8. Enantiofacial differentiation of alkenes during asymmetric hydrogenation.	28
Figure 9. Classes of alkenes used in asymmetric iridium catalyzed hydrogenations.	31
Figure 10. Crabtree and Morris' cationic iridium complex.	31
Figure 11. Hydrogen absorption curves for several alkenes with [Ir(COD)(Pi-Pr ₃)(py)]PF ₆ (rates expressed in mol H ₂ (mol Ir) ⁻¹ h ⁻¹) (used with permission from ref 56).	33
Figure 12. Structure of Crabtree deactivated complexes (used with permission from ref 56).	34
Figure 13. BAr _F counterion.....	36
Figure 14. Complexes containing chiral Δ -TRISPHAT anion with achiral (104) and chiral (105) cations.....	38

Figure 15. Crabtree's dihydride complex (measured at $-80\text{ }^{\circ}\text{C}$ in CD_2Cl_2) (reproduced from ref 63c).	39
Figure 16. Pfaltz's dihydride complex (measured at $-40\text{ }^{\circ}\text{C}$ in $d_8\text{-THF}$) (used with permission from ref 65).	40
Figure 17. NOE observations and spectrum for dihydride intermediate 111 (used with permission from ref 65).	41
Figure 18. Calculated energies for dihydride species (used with permission from ref 65).	42
Figure 19. Pfaltz's solvated (THF) hydride complexes (used with permission from ref 65).	43
Figure 20. NOE observation for dihydride intermediate 115 (used with permission from ref 65).	44
Figure 21. Calculated energies for solvated (CH_3Cl) complexes (used with permission from ref 65).	44
Figure 22. Ir(I) / Ir(III) (left) and Ir(III) / Ir(V) (right) catalytic cycles.	46
Figure 23. Steric influence on enantioselectivity (used with permission from ref 73).	47
Figure 24. Steric and electronic influences during enantiodetermining migratory insertion step (used with permission from ref 73).	48
Figure 25. Calculated transition states for migratory insertion: A – sterically and electronically favoured hydride addition to the β -carbon of <i>trans</i> - β -methyl cinnamate; B – sterically and electronically unfavoured hydride addition to the α -carbon of <i>trans</i> - β -methyl cinnamate; C – sterically favoured, electronically unfavoured hydride addition to the α -carbon of <i>trans</i> - α -methyl cinnamate; D – sterically unfavoured, electronically	

favoured hydride addition to the β -carbon of <i>trans</i> - α -methyl cinnamate (used with permission from ref 73).	49
Figure 26. <i>P,N</i> ligands used in asymmetric Ir-catalyzed hydrogenation.	50
Figure 27. Standard test substrate alkenes for asymmetric Ir-catalyzed hydrogenations.	51
Figure 28. Hydrogenation results of terminal, purely alkyl-substituted, and tetrasubstituted alkenes.	53
Figure 29. Hydrogenation results of diaryl- and trifluoromethyl-substituted alkenes.....	54
Figure 30. Planar chirality of 1,2-substituted ferrocenes.	58
Figure 31. Strategies for synthesizing planar chiral ferrocene compounds.	60
Figure 32. ORTEP plot of alcohol (<i>S</i>)- 193 at 50% probability; all H atoms except H1 are omitted for clarity.	66
Figure 33. Pro- <i>R</i> and Pro- <i>S</i> <i>ortho</i> protons of aminoferrocenes.	67
Figure 34. Proposed variations of 2-phosphino-1-aminoferrocene ligand.	71
Figure 35. ^{31}P NMR spectra of the free ligand 204 and iridium complex 221	78
Figure 36. ^1H NMR spectra of NMe ₂ group in free ligand 204 and iridium complex 221	78
Figure 37. ORTEP plot of Ir complex 221 at 50% probability; all H atoms and the BAr _F counterion have been omitted for clarity.	80
Figure 38. ORTEP plot of crystal packing of Ir complex 221 at 50% probability; all H atoms have been omitted for clarity.	80
Figure 39. Attempted hydrogenation reactions with no conversion.	85
Figure 40. Attempted hydrogenation reactions with incomplete hydrogenation.	86

Figure 41. ORTEP plot of ammonium tetrafluoroborate salt 230 ·HBF ₄ at 50% probability; all H atoms except H1a are omitted for clarity.	90
Figure 42. Formation of catalytically active Ir-dihydride solvent species.....	100
Figure 43. Quadrant system for selective binding of substrate alkene.	101
Figure 44. Alkene coordination modes for β -methyl ethyl cinnamate.	102
Figure 45. Migratory insertion modes for β -methyl ethyl cinnamate.....	103
Figure 46. Alkene coordination modes for α -methyl ethyl cinnamate.	104
Figure 47. Migratory insertion modes for α -methyl ethyl cinnamate.....	105

List of Schemes

Scheme 1. Rh-catalyzed asymmetric hydrosilylation using MPFA.	8
Scheme 2. Ni-catalyzed asymmetric Grignard cross coupling with β -aminoalkylphosphine ligand.	8
Scheme 3. Ni-catalyzed asymmetric Grignard cross coupling with ferrocene ligands. ...	10
Scheme 4. Pd-catalyzed asymmetric Grignard cross coupling with constrained planar / central chiral ferrocene <i>P,N</i> ligand.	11
Scheme 5. Pd-catalyzed allylic alkylation with axial chiral <i>P,N</i> ligand.	12
Scheme 6. Pd-catalyzed asymmetric allylic alkylation with <i>P,N</i> ligand with different <i>N</i> substituents.	13
Scheme 7. Asymmetric Heck reaction with pyrrolidine based <i>P,N</i> ligand.	13
Scheme 8. Pd-catalyzed allylic alkylation with pyrrolidine based <i>P,N</i> ligand.	14
Scheme 9. Ag-catalyzed asymmetric allylation with axial chiral pyrrolidine ligand.	14
Scheme 10. Pd-catalyzed allylic alkylation with oxazolidine and imidazolidine based <i>P,N</i> ligands.	15
Scheme 11. Pd-catalyzed asymmetric allylic alkylation with iminophosphine ligand.	16
Scheme 12. Pd-catalyzed asymmetric allylic alkylation with iminophosphine ligand with ferrocene substituent.	16
Scheme 13. Rh-catalyzed asymmetric hydrosilylation with a central and planar chiral ferrocenyl iminophosphine ligand.	17
Scheme 14. Cu-catalyzed synthesis of propargylamines with QUINAP ligand.	17

Scheme 15. Pd-catalyzed asymmetric allylic amination with ferrocenyl-QUINAP analogue.	18
Scheme 16. Pd-catalyzed asymmetric allylic alkylation with amidine ligands.	18
Scheme 17. Pd-catalyzed asymmetric Heck reactions with phosphinooxazoline ligand 50e.	21
Scheme 18. Pd-catalyzed asymmetric Diels-Alder reaction with phosphine-oxazoline ligand.	22
Scheme 19. Pd-catalyzed asymmetric Heck reaction with ferrocenyl phosphinooxazoline ligand 78	24
Scheme 20. Pd-catalyzed allylic amination with axial chiral phosphinooxazoline ligand 81	25
Scheme 21. Pd-catalyzed asymmetric allylic alkylation with phosphinitooxazoline ligand 83	26
Scheme 22: Pd-catalyzed asymmetric allylic alkylation with pyrrolidine-bound phosphine oxazoline ligand 84	26
Scheme 23. Monsanto synthesis of <i>L</i> -DOPA.	29
Scheme 24. Key asymmetric hydrogenation step in the synthesis of (<i>S</i>)-metolachlor.	30
Scheme 25. Asymmetric synthesis of lilial using Ir-PHOX complex 151	55
Scheme 26. Asymmetric synthesis of γ -tocopheryl acetate 156	56
Scheme 27. Total synthesis of (+)- and (–)-mutisianthol.	57
Scheme 28. Ligands derived from Ugi's amine.	61
Scheme 29. Synthesis of Fc-PHOX ligands via diastereoselective lithiation.	62

Scheme 30: Synthesis of aminoferrocene ligand 173 via diastereoselective lithiation of Kagan's sulfoxide.	62
Scheme 31. Togni's synthesis of a substituted aminoferrocene.	63
Scheme 32. Enantioselective synthesis of 1,2-substituted ferrocenes in the presence of TMCDA.	64
Scheme 33. Enantioselective synthesis of 1,2-substituted ferrocenes in the presence of (–)-sparteine.	64
Scheme 34. Enantioselective synthesis of 1,2-substituted ferrocenes in the presence of chiral LDA derivative.	64
Scheme 35. Enantioselective synthesis of 1,2-substituted ferrocenes by BF ₃ -activated lithiation with chiral diamine ligand.	65
Scheme 36. Synthesis of alcohol (<i>S</i>)- 193 with (<i>S,S</i>)-diamine ligand 191	66
Scheme 37. Rh-catalyzed asymmetric hydrogenation with methyl-BoPhoz.	68
Scheme 38. Ru-catalyzed hydrogenation with ferrocenyl phosphinooxazoline ligand.	69
Scheme 39. Proposed preparation of ferrocenyl aminophosphine ligands.	70
Scheme 40. Proposed preparation of iridium complex with ferrocenyl aminophosphine ligands.	70
Scheme 41. Proposed hydrogenation of alkenes with iridium complex.	71
Scheme 42. Aminoferrocene preparation.	73
Scheme 43. Preparation of tertiary aminoferrocenes 192 and 213	73
Scheme 44. Synthesis of racemic ligand 204	74
Scheme 45. Synthesis of iridium BAr _F complex 221 from ligand 204	77
Scheme 46. Synthesis of NaBAr _F	77

Scheme 47. Hydrogenation of stilbene.	81
Scheme 48. Synthesis of enantioenriched (<i>S</i>)-2-diphenylphosphinothionyl-1-dimethylaminoferrocene 230	87
Scheme 49. Formation of ammonium tetrafluoroborate salt 230 ·HBF ₄	88
Scheme 50. Neutralization and desulfurization to enantiopure ligand (<i>S</i>)- 204	91
Scheme 51. Synthesis of ortho-tolyl derivative 205	92
Scheme 52. Synthesis of cyclohexyl derivative 206	92
Scheme 53. Synthesis of N-ferrocenylpyrrolidine ligand (<i>S</i>)- 207	93
Scheme 54. Synthesis of enantioenriched cationic Ir(COD)[BAr _F] complexes (<i>S</i>)- 221 , (<i>S</i>)- 234 , (<i>S</i>)- 235 , and (<i>S</i>)- 236	94

Abbreviations

BAr_F = tetrakis[3,5-bis(trifluoromethyl)phenyl]borate

BINAP = 2,2'-bis(diphenylphosphino)-1,1'-binaphthyl

COD = cyclooctadiene

Cp = cyclopentadienyl

DCM = dichloromethane

DFT = density functional theory

DMAE = dimethylaminoethanol

DME = dimethoxyethane

DPPF = 1,1'-bis(diphenylphosphino)ferrocene

HOMO = highest occupied molecular orbital

i-PrLi = *isopropyl*lithium

i-PrOH = *isopropanol*

Fc = ferrocene/ferrocenyl

Fc-PHOX = Ferrocenyl phosphino-oxazoline

LUMO = lowest unoccupied molecular orbital

Methyl-BoPhoz = (*R*)-*N*-Methyl-*N*-diphenylphosphino-1-[(*S*)-2 diphenylphosphino)

ferrocenyl]ethylamine

MPFA = [2-dimethylphosphinoferrocenyl]ethyldimethylamine

NOE = nuclear Overhauser effect

Op = optical purity

PHOX = phosphinooxazoline

P,N = aminophosphine

PPFA = [2-diphenylphosphinoferrocenyl]ethyldimethylamine

QUINAP = 1-(2-diphenylphosphino-1-naphthyl)isoquinoline

t-BuOMe = *tert*-butyl methyl ether

TOF = turnover frequency

TON = turnover number

THF = tetrahydrofuran

TTN = thallium(III) trinitrate

Chapter 1: Introduction and Historical Background

1.1 Catalysis, Ligands, and Complexes.

The importance of stereochemical purity in pharmaceutical products has been a prominent driving force in the pursuit of improved control over the stereochemical output of organic reactions.¹ To this end, new catalysts, ligands, and applications are reported every year to satisfy the need to embrace a wider range of reactions and to improve the efficiency of existing processes. A catalyst is defined as a substance that changes the rate of a chemical reaction without itself being consumed. Today, precatalysts are often used which are activated *in situ* to form an active catalyst complex. The active catalyst will pass through a number of intermediates during a catalytic cycle, but can mediate a reaction many times, in effect remaining unaltered, and thus these molecules are also classified as catalysts.²

Homogeneous catalysis refers to a catalytic system in which the substrate and catalyst are brought together in the same phase where the reaction takes place. The number of times a catalyst goes through the cycle is termed the turnover number (TON) and is defined as the total number of substrate molecules that a catalyst converts into product molecules. The turnover frequency (TOF) is the number of substrate molecules that a catalyst converts into product molecules in a period of time and is often reported in moles of substrate molecule per mole of catalyst per hour.³

A ligand is a molecule that bonds to a central metal atom to form a coordination complex that may be used as a catalyst or precatalyst. Bonding generally involves donation of one or more pairs of electrons from the ligand HOMO to the LUMO of the

metal.⁴ The metal-ligand bond can be further stabilized by back donation from filled metal orbitals into the LUMO of the ligand. By linking a metal center and an organic fragment together to form a complex, the properties of both components change greatly. The identity, charge, size, and hapticity of the ligand dictate the reactivity of the complex. Ligands that are bound directly to the metal center form the first coordination, or inner, sphere of the complex. Outer sphere ligands are not directly bound to the metal, but are generally weakly bound to the inner ligands.⁵ Ligands that bind via more than one donor atom are called chelating ligands with the most favourable chelate ring size being five or six atoms. Ligands with two donor atoms are termed bidentate ligands, and are characterized by their bite angle. Bite angle refers to the angle between the two donor atoms created upon complexation (θ , Figure 1). The bite angle is affected by the cone angle of each donor atom, the distance between the donor atoms, the size and flexibility of the backbone, and the orientation in which chelation to the metal occurs (which is affected by steric repulsion between substituents on the donor atom and backbone).⁶ Electronic properties play a role on the metal-donor atom bond length, another factor influencing the bite angle. In addition, other ligands attached to the metal center can influence the bite angle if they are bulky or have a strong influence on the metal orbitals. Ligand bite angle is often related to catalytic performance and selectivity.³

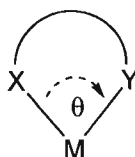


Figure 1. Ligand bite angle formed upon coordination of heteroatoms X and Y with metal M.

Chelating ligands are less easily displaced than their corresponding monodentate analogues, as they are entropically favoured. Chelation not only makes the complex more stable, but also forces the donor atoms to take up adjacent, or *cis*, sites in the resulting complex. *Trans* ligands are those that occupy opposite vertices of a complex. Werner first recognized that certain ligands affect the reactions of groups opposite to them in 1893 and termed the principle “*trans*-elimination”.⁶ Chernyaev later described the “*trans*-effect rule” based on studies of square planar Pt(II) complexes. The *trans*-effect rule described the property that certain ligands, L^t , aided in the dissociation of a second ligand, L , *trans* to the first, and their replacement by an external ligand. L^t ligands were said to have a higher *trans* effect.⁷ The *trans* effect occurs because two *trans* ligands compete with each other for electron density as they use the same metal orbitals for bonding. Ligands with high *trans* effect properties often have strong σ interactions with the metal center (such as H^- , Me^- , and $SnCl_3^-$) or strong π interactions with the metal center (such as CO, C_2H_2 , and $(NH_2)_2CS$).⁸ These ligands weaken the metal-ligand bonds *trans* to them as seen in the lengthening of the M-L distances, or changes in the M-L coupling in NMR spectroscopy or $\nu(M-L)$ stretching frequency in IR spectroscopy.⁹ The *trans* effect is a kinetic phenomenon, different from the *trans* influence, which describes a change in the ground state thermodynamic properties of complexes with certain ligands.¹⁰ Thus, by chelation of a bidentate ligand with differing heteroatoms in *cis* orientation, different *trans* effects can occur during catalysis.

1.1.1 Chiral Ligands and Complexes.

Chiral ligands used in asymmetric synthesis can contain central, axial, or planar chirality, or a combination of these (Figure 2).

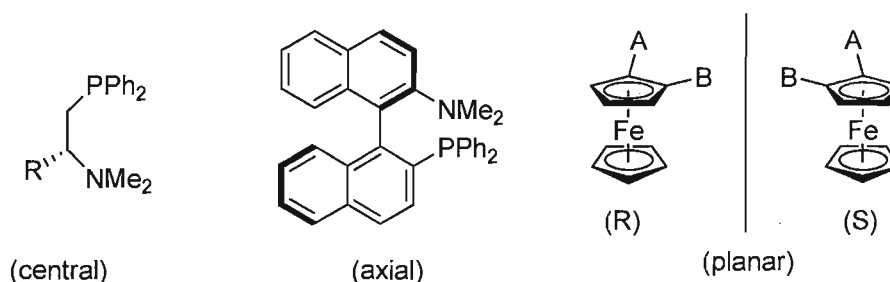


Figure 2. Different categories of chirality.

Bidentate chiral ligands coordinate to a metal center to form a chiral complex which may transfer its chirality to a substrate during a catalytic process. Enantiofacial differentiation can be enhanced by using bidentate ligands, as they display greater conformational rigidity since the chiral backbone forces the ligand into a single or restricted conformation. Chiral ligands can induce asymmetry in a reaction through steric interactions between the ligand and the substrate, as well as by creating electronic asymmetry around a metal center through the presence of different donor atoms. Variation of these steric and electronic influences can affect the binding of substrates, and thus the stereochemical outcome of the reaction.¹¹

Transition metal mediated asymmetric catalysis has applications ranging from bench top research to the preparation of compounds on an industrial scale. In principle, the use of chiral ligands in synthesis enables the preparation of large amounts of chiral compounds from achiral precursors in a reliable and highly enantioselective manner,

generally in good yields and with only a very small amount of chiral catalyst required. Ideally, these chiral catalysts (or the chiral ligands used to prepare them) are readily accessible or commercially available. Additionally, asymmetric catalysis can be used to construct the skeleton of the target molecule, or to prepare optically pure starting materials that induce asymmetry in the remaining stereogenic centers of a complex target.¹¹

Despite much progress in the field of asymmetric catalysis, the design of suitable ligands for a particular application still remains a challenging task. The complexity of most catalytic processes prevents a purely rational design of chiral ligands. However, understanding of reaction mechanisms and how steric and electronic factors affect intermediates, identified through both analysis of experimental results and computational modeling, can allow for a semirational approach to ligand design. Moreover, the investigation of new ligands with frameworks that differ from previous cases may provide further insight and possibly catalysts that are able to surmount the limitations of known systems.

1.2 *P,N* Donor Ligands.

Aminophosphine, or *P,N*, ligands contain nitrogen and phosphorus donor atoms and are prominent bidentate ligands in many transition metal mediated synthetic processes. The π acceptor character of phosphorus stabilizes a metal center in low oxidation states and the σ donor ability of nitrogen makes the metal more susceptible to oxidative addition reactions.³ The markedly different characteristics of nitrogen and

phosphorus provide a class of ligands that are electronically desymmetrized, allowing the possibility for preferential coordination of substrates to the metal center of their complexes. The combination of these two heteroatoms in a ligand motif can help to stabilize intermediate oxidation states or geometries formed during the catalytic cycle in which the substrate is transformed into the desired product.¹²

Many modifications can be made to alter both the steric and electronic characteristics of these ligands. For example, an additional stereogenic element can be created by having different groups on a donor atom¹³ (for example see Scheme 6, Section 1.2.1). Established chirality in the backbone can induce a preferential orientation of the different substituents on the donor atom upon binding to the metal. When adding an additional stereogenic element to an already chiral ligand, there is the possibility for match / mismatch interactions where selectivity can be enhanced or hindered by the additional stereogenic element. Bonding the phosphorus donor directly to a more electronegative atom such as oxygen or nitrogen (as in phosphinite or phosphoramidine ligands) can lessen its electron donating ability while enhancing its π acceptor capacity, thereby enhancing the electrophilicity of the metal. Utilizing an imino rather than an amino group normally results in greater σ donating capabilities making the metal more susceptible to oxidative addition reactions. These factors can create a greater electronic disparity between the donor atoms.¹⁴

P,N ligands can be split into three modules, the phosphorus moiety, nitrogen moiety, and backbone linker. The most popular and successful designs for *P,N* ligands feature an achiral phosphorus moiety, an achiral amino or imino nitrogen moiety, and a chiral backbone. The ability to modularly alter the structure of *P,N* ligands has made

them a popular ligand motif, as it allows for fine tuning of a generalized structure to suit a specific process or substrate.

1.2.1 Amine *N*, Phosphine *P* Ligands.

Kumada and Hayashi were the first to prepare and utilize chiral aminophosphine ligands with the planar chiral ferrocenes (*S*)- α -(*R*)-[2-diphenylphosphinoferrocenyl] ethyldimethylamine (PPFA) (**1**) and (*R*)- α -(*S*)-[2-dimethylphosphinoferrocenyl] ethyldimethylamine (MPFA) (**2**) (Figure 3).¹⁵ These ligands contained both planar and central chirality and were utilized in Rh-catalyzed hydrosilylations with low catalyst loadings (0.5 mol %) (Scheme 1).¹⁵ Although low to moderate enantioselectivities (up to 49% optical purity) were obtained with these early *P,N* ligands, they demonstrated the utility of chiral aminophosphine ligands. For example, MPFA gave higher selectivity in the hydrosilylation of acetophenone (**3** \rightarrow **4**) than diphosphine ligands of the time.¹⁵

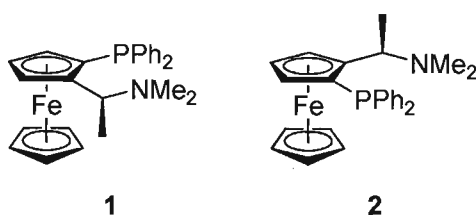
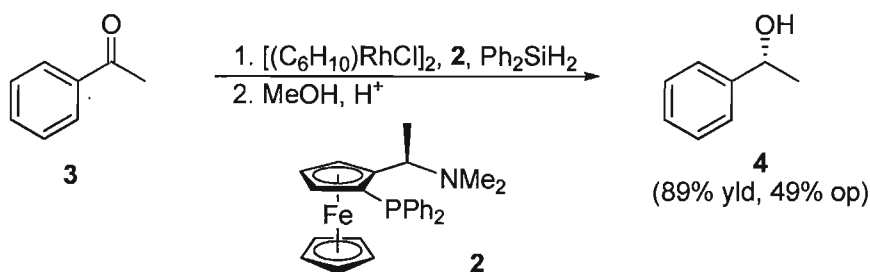
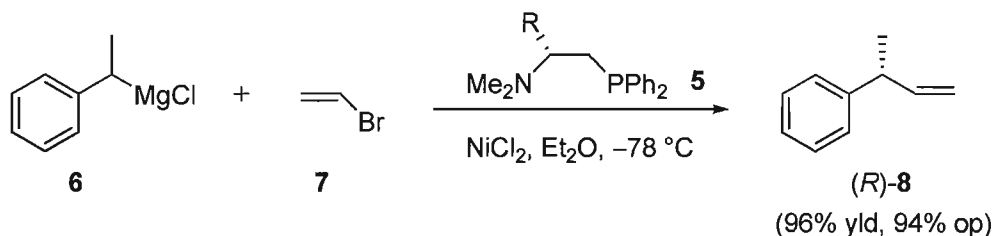


Figure 3. PPFA and MPFA ligands.



Scheme 1. Rh-catalyzed asymmetric hydrosilylation using MPFA.

Kumada and Hayashi later utilized central chiral β -aminoalkylphosphine (**5**) *P,N* ligands derived from chiral amino acids in Ni-catalyzed asymmetric Grignard cross couplings of 1-phenylethylmagnesium chloride (**6**) and vinyl bromide (**7**).¹⁶ The best results were obtained with a *t*-Bu group as the substituent with (*R*) configuration, giving (*R*)-**8** in 94% optical purity (Scheme 2).



Scheme 2. Ni-catalyzed asymmetric Grignard cross coupling with β -aminoalkylphosphine ligand.

It was found that the larger the substituent at the chiral carbon atom, the higher the asymmetric induction: (*R* = *t*-Bu) > (*R* = *i*-Pr) > (*R* = CH₂Ph) = (*R* = Ph) > (*R* = Me). It was also found that switching the positions of the phosphino and amino groups resulted in lower selectivity. Analogous diphosphines provided only racemic product, indicating

that the nitrogen substituent was crucial for asymmetric induction. Asymmetry was thought to be induced by the dissociation of nitrogen from the nickel complex (**9** \rightarrow **10**) during the reaction to preferentially bind one enantiomer of the Grignard reagent, forming a diastereomeric transition state and fixing the conformation of the benzylic carbon (**10** \rightarrow **11**) before reductive elimination gave the product and regenerated the catalyst (**11** \rightarrow **9**) (Figure 4).¹⁶

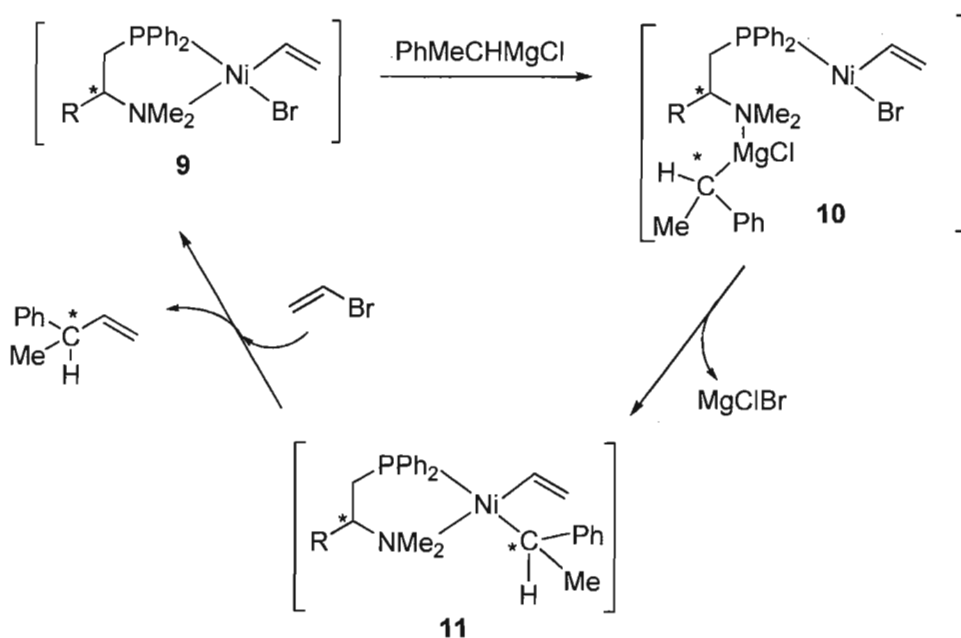
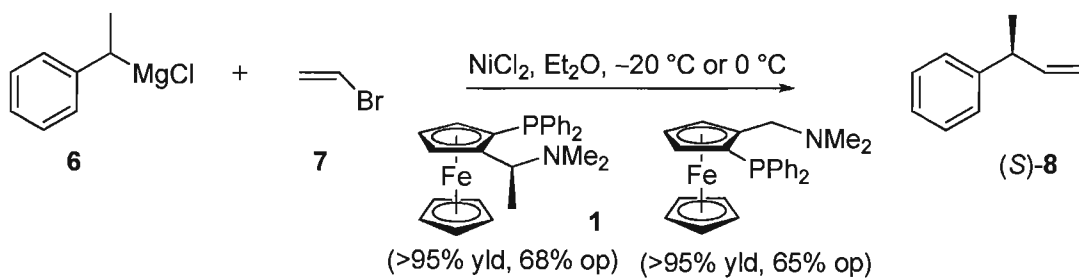


Figure 4. Mechanism of Ni-catalyzed asymmetric Grignard cross coupling with β -aminoalkylphosphines (adapted from ref 16).

Kumada and Hayashi compared the ferrocenyl aminophosphine ligands in the nickel catalyzed Grignard reactions, obtaining up to 68% optical purity with PPFA (**1**, Scheme 3).¹⁷ It was found that the planar chirality was more important to the selectivity than the carbon central chirality, the dimethylamino group was required for high stereoselectivity, and the same type of mechanism was suggested (Figure 5).¹⁷ It was also

shown that ferrocene ligand **12** could facilitate this transformation in 65% optical purity, showing that the planar chirality of ferrocene can induce asymmetry without the added central chiral unit.



Scheme 3. Ni-catalyzed asymmetric Grignard cross coupling with ferrocene ligands.

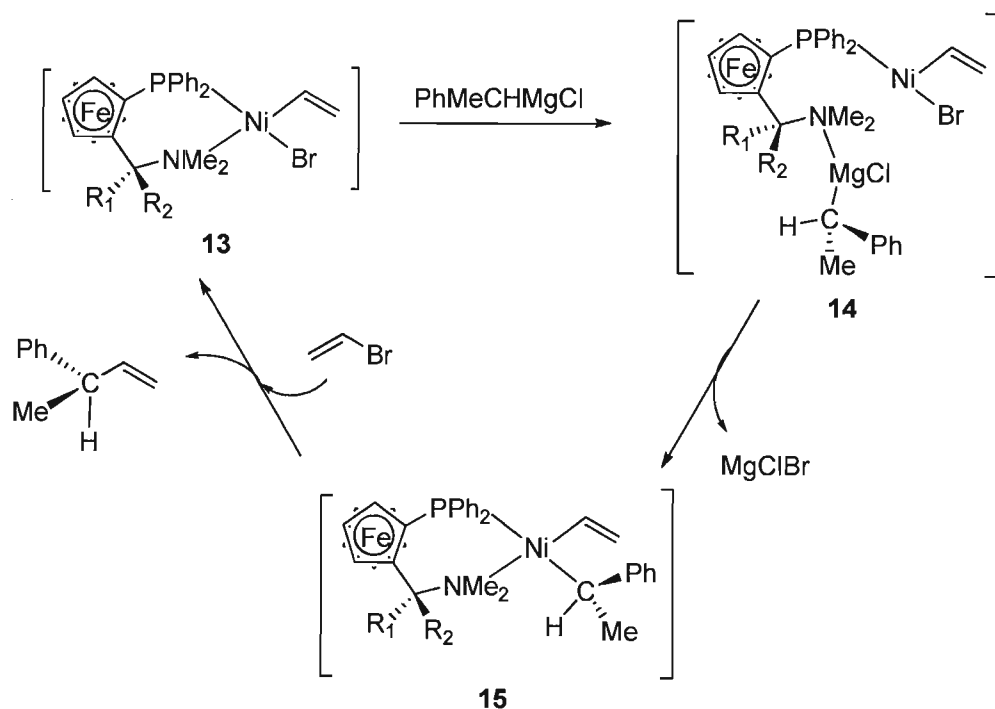
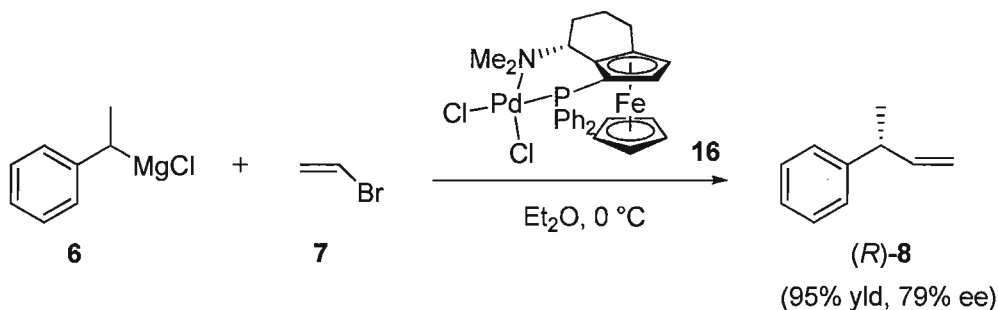


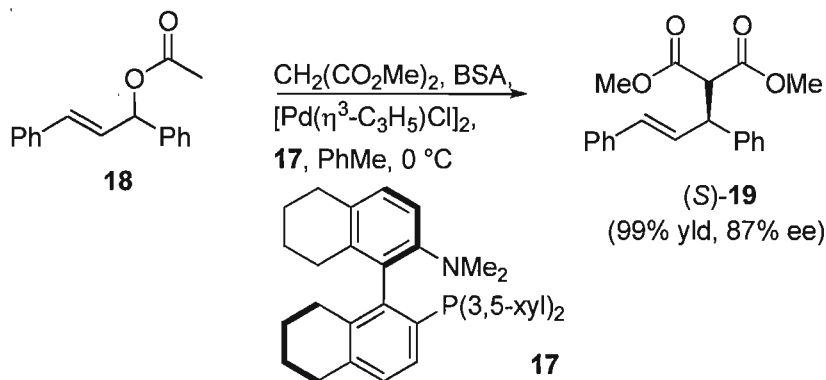
Figure 5. Mechanism of Ni-catalyzed asymmetric Grignard cross coupling with ferrocene *P,N* ligands (adapted from ref 17).

Weissensteiner *et al.*¹⁸ prepared planar chiral ferrocene ligands constraining the additional central chiral element within a ring (**16**), making the ligand less flexible and more bulky than PPFA. These were used in asymmetric Pd-catalyzed Grignard cross couplings resulting in increased selectivity of 79% ee for (*R*)-**8** (Scheme 4).



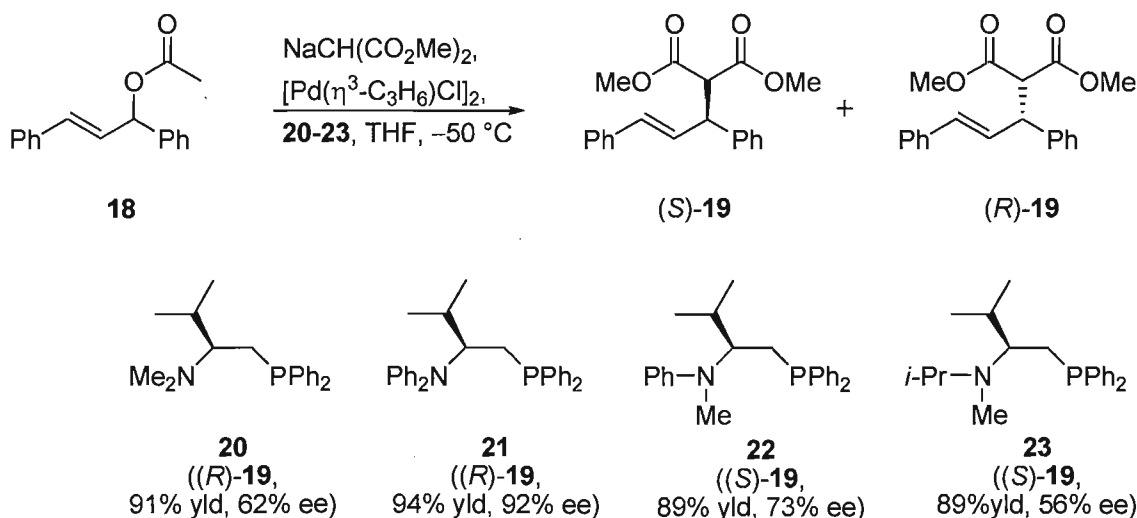
Scheme 4. Pd-catalyzed asymmetric Grignard cross coupling with constrained planar / central chiral ferrocene *P,N* ligand.

Axial chirality is another form of chirality used in ligands, often achieved using the binaphthalene backbone or derivatives thereof, such as H_8 -binaphthalene derivative **17**. Ligand **17** was found to have a larger bite angle than the fully aromatic binaphthalene analogue, and gave (*S*)-**24** in 87% ee in the Pd-catalyzed asymmetric allylic alkylation of 1,3-diphenylprop-2-en-1-yl acetate (**18**) with dimethyl malonate (Scheme 5).¹⁹



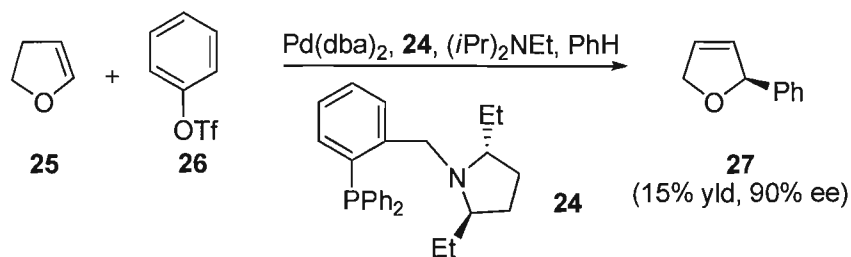
Scheme 5. Pd-catalyzed allylic alkylation with axial chiral *P,N* ligand.

In addition to dimethylamino substituted ligands, different substituents at nitrogen may be used to give an extra stereogenic element upon coordination to a metal. For example, Anderson *et al.* applied β -aminoalkylphosphine ligands with various nitrogen donor groups in Pd-catalyzed allylic alkylations (Scheme 6).¹³ It was found that the chirality in the backbone induced a preferential orientation of the amino substituents upon chelation to the metal, rendering the nitrogen atom stereogenic. This caused different diastereomers to be formed depending on the substitution at nitrogen. For example, when using identical amino substituents (ligands **20** (R=Me) and **21** (R=Ph)), the product of alkylation of (*E*)-1,3-diphenylpropenyl acetate (**18**) had (*R*) configuration ((*R*)-**19**), while (*S*)-**19** was obtained when using ligands with two different amino substituents (ligands **22** (R=Me, Ph) and **23** (R=Me, *i*-Pr)). This added nitrogen stereogenic element did not, however, enhance the enantioselectivity of the reaction – 62% ee for **20**, 92% for **21**, 73% for **22**, and 56% for **23**, probably due to mismatch diastereomeric interactions.

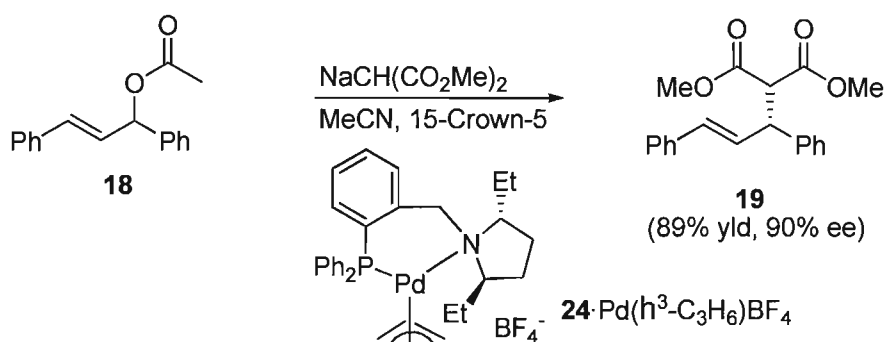


Scheme 6. Pd-catalyzed asymmetric allylic alkylation with *P,N* ligand with different *N* substituents.

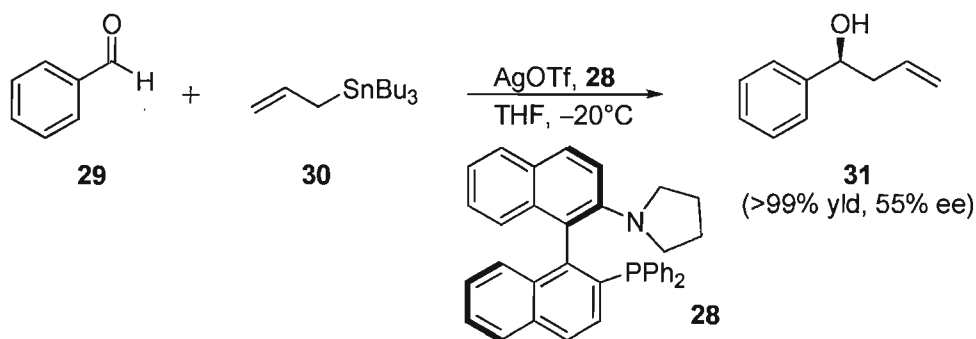
Restriction of the nitrogen donor within a ring has been used to orient substituents on the ligand and give rise to differing steric effects. Pyrrolidine ligands are the most common cycles used, working best with an aromatic backbone between the nitrogen and phosphorus atoms. For example, asymmetric Heck reactions were conducted in up to 90% ee (Scheme 7) with pyrrolidine ligand **24**.²⁰ With the same ligand, Pd-catalyzed allylic alkylations were performed, again with excellent results, 90% ee for compound **19** (Scheme 8).²¹ With axial chiral pyrrolidine ligand **28**, the silver-catalyzed allylation of benzaldehyde was achieved in 55% ee (Scheme 9).²²



Scheme 7. Asymmetric Heck reaction with pyrrolidine based *P,N* ligand.

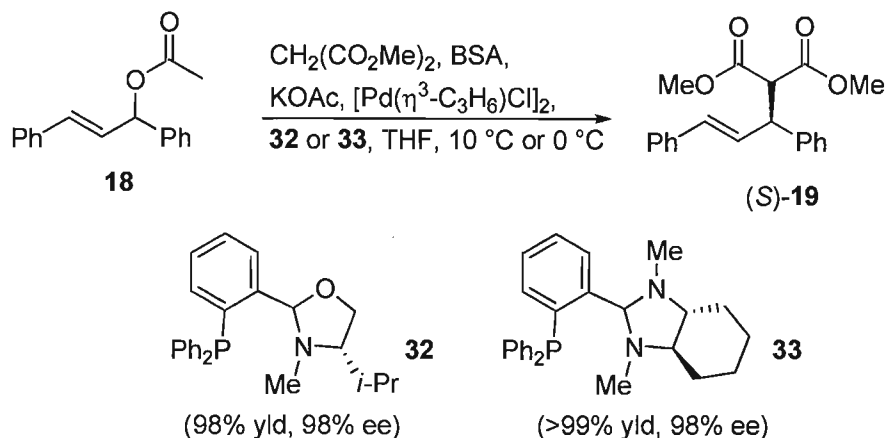


Scheme 8. Pd-catalyzed allylic alkylation with pyrrolidine based P,N ligand.



Scheme 9. Ag-catalyzed asymmetric allylation with axial chiral pyridine ligand.

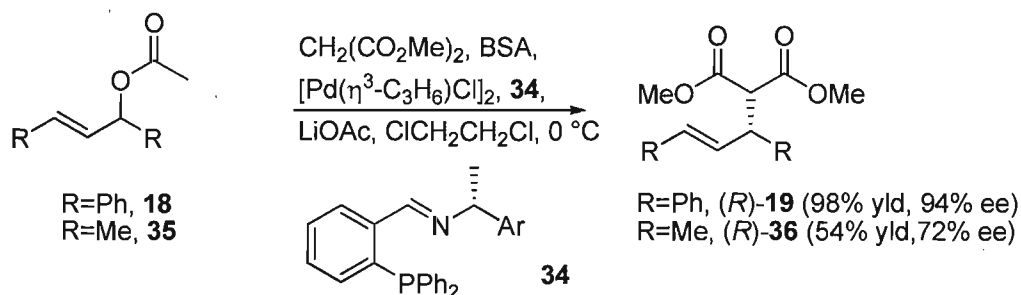
Oxazolidine ligands are similar to pyrrolidine ligands yet provide a slightly different steric and electronic environment because of the added oxygen atom. Jin *et al.*²³ used oxazolidine ligand **32** in Pd-catalyzed allylic alkylations, obtaining excellent enantioselectivities of 98% ee for **19** (Scheme 10). Imidazolidine ligands, with two nitrogen atoms in the ring were also evaluated in this reaction, again with excellent results, for example, providing (*S*)-**19** in 98% ee with ligand **33**.²⁴



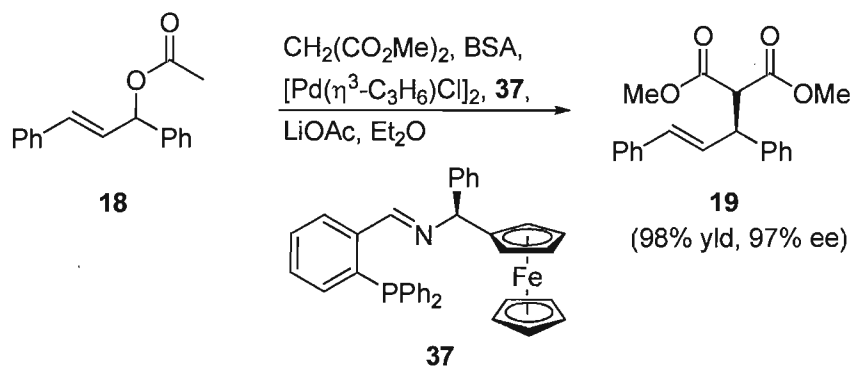
Scheme 10. Pd-catalyzed allylic alkylation with oxazolidinone and imidazolidine based *P,N* ligands.

1.2.2 Imine *N*, Phosphine *P* Ligands.

Sp^2 -hybridized nitrogen donors are stronger electron donors than their sp^3 analogues (as there is more electron density on the nitrogen available for donation to the metal) and as such often provide for stronger bonding to a metal. Iminophosphine ligands **34** were prepared by Hashimoto²⁵ and utilized in Pd-catalyzed allylic alkylations. The bulky mesityl analogue (Ar = Mes) was found to be the best ligand, giving **(R)-19** in 94% ee. Ligand **34** was also used on the more difficult dimethyl substrate **35**, giving **(R)-36** in 72% ee (Scheme 11).²⁵ Similarly, Iwao developed iminophosphine ligands with bulky ferrocene substituents, with ligand **37** giving **(S)-19** in 97% ee (Scheme 12).²⁶

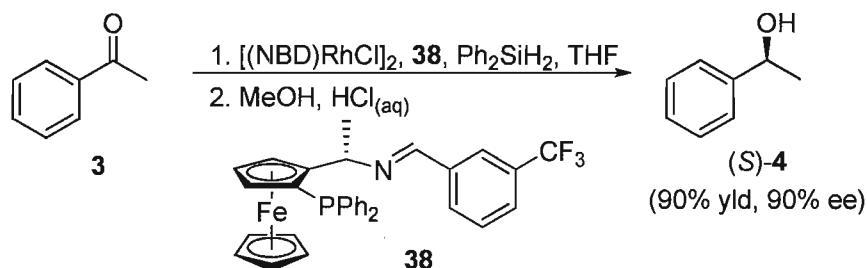


Scheme 11. Pd-catalyzed asymmetric allylic alkylation with iminophosphine ligand.



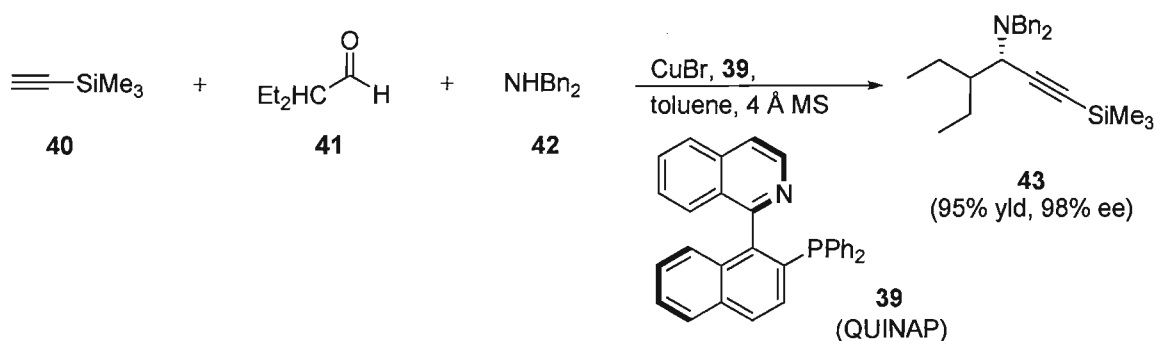
Scheme 12. Pd-catalyzed asymmetric allylic alkylation with iminophosphine ligand with ferrocene substituent.

Hayashi prepared analogues with planar and central chirality (**38**), and utilized them in the Rh-catalyzed asymmetric hydrosilylation of acetophenone, providing (*S*)-**4** in 90% ee²⁷ (Scheme 13), a large improvement from the early MPFA ligand (**2**, Scheme 1, Section 1.2.1).



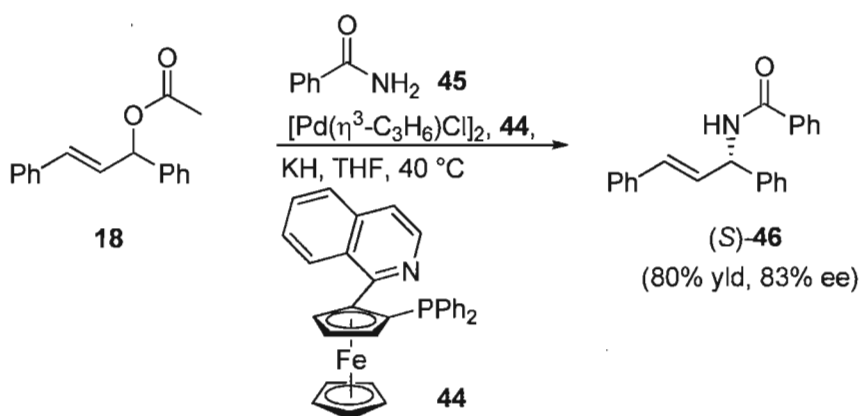
Scheme 13. Rh-catalyzed asymmetric hydrosilylation with a central and planar chiral ferrocenyl iminophosphine ligand.

Axial chiral iminophosphine ligands have also been used. For example, 1-(2-diphenylphosphino-1-naphthyl)isoquinoline (QUINAP) ligand **39** has been used by Knochel²⁸ in the Cu-mediated one-pot three-component reaction of terminal alkynes (**40**), aldehydes (**41**), and secondary amines (**42**) to form synthetically important propargylamines (**43**) in up to 98% ee (Scheme 14).



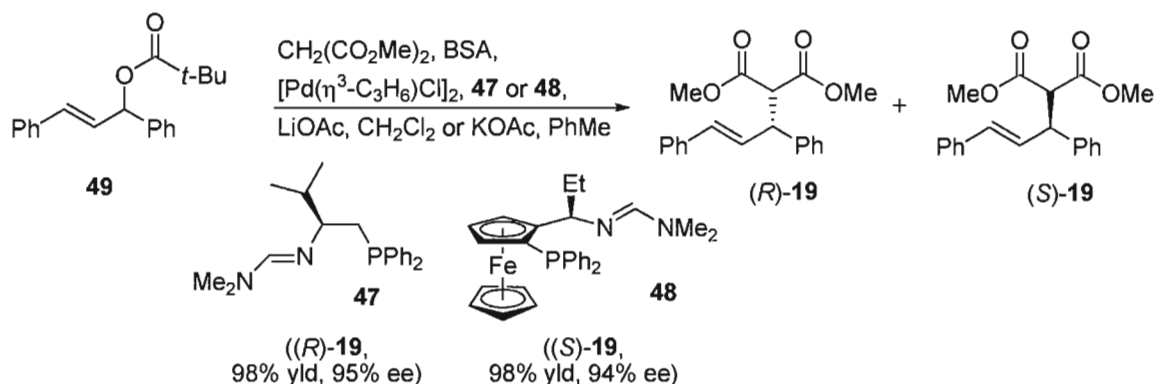
Scheme 14. Cu-catalyzed synthesis of propargylamines with QUINAP ligand.

Planar chiral ferrocenyl QUINAP analogues were also prepared by Knochel and utilized in Pd-catalyzed allylic aminations with ligand **44** providing (*S*)-**46** in 83% ee (Scheme 15).²⁹



Scheme 15. Pd-catalyzed asymmetric allylic amination with ferrocenyl-QUINAP analogue.

Similar in structure to the β -aminoalkylphosphine ligands (**5**, Scheme 2, Section 1.2.1), amidine ligand **47**, based on the amino acid valine, was prepared by Morimoto *et al.* and utilized in Pd-catalyzed allylic alkylation of (*E*)-1,3-diphenylprop-2-enyl pivalate (**49**) giving **19** in 95% ee with (*R*) selectivity (Scheme 16).³⁰ Zheng *et al.* prepared similar ferrocenylphosphine-amidine ligands, and obtained (*S*)-**19** in 94% ee with ligand **48**.³¹



Scheme 16. Pd-catalyzed asymmetric allylic alkylation with amidine ligands.

As with amino nitrogen donor ligands, constraining the imino nitrogen within a ring changes the steric and electronic environment of the ligand. Oxazoline rings, such as in phosphinooxazoline (PHOX) ligands, are the most common and have become one of the most popular *P,N* ligand motifs. They were introduced independently by Pfaltz³², Helmchen³³, and Williams³⁴ in 1993. In particular, the diphenylphosphinooxazolines (**50**, Figure 6) are highly modular and can be easily synthesized from commercially available amino acids.

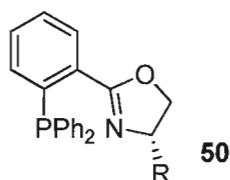


Figure 6: Diphenylphosphinooxazoline ligand structure

Since its introduction, many researchers have utilized this ligand motif in a large variety of catalytic processes. For example, Pd-catalyzed allylic substitution can be accomplished with a number of different nucleophiles in excellent enantioselectivities (Table 1).³² Ligand **50e** was also applied successfully in Pd-catalyzed asymmetric Heck reactions in which only the kinetic 2,5-dihydropyran product ((*R*)-**27**) was obtained in excellent selectivity (97% ee) upon phenylation of 2,3-dihydrofuran (**25**).³⁵ Other derivatives could also be prepared in good to excellent enantioselectivities (Scheme 17). It was speculated that the kinetic specificity was due to the π -complex between the PHOX-palladium hydride and the olefin (formed after the first β -hydride elimination)

being less stable than the corresponding complexes with other ligands, enabling dissociation to the product faster than insertion of the olefin into the Pd–H bond.³⁵

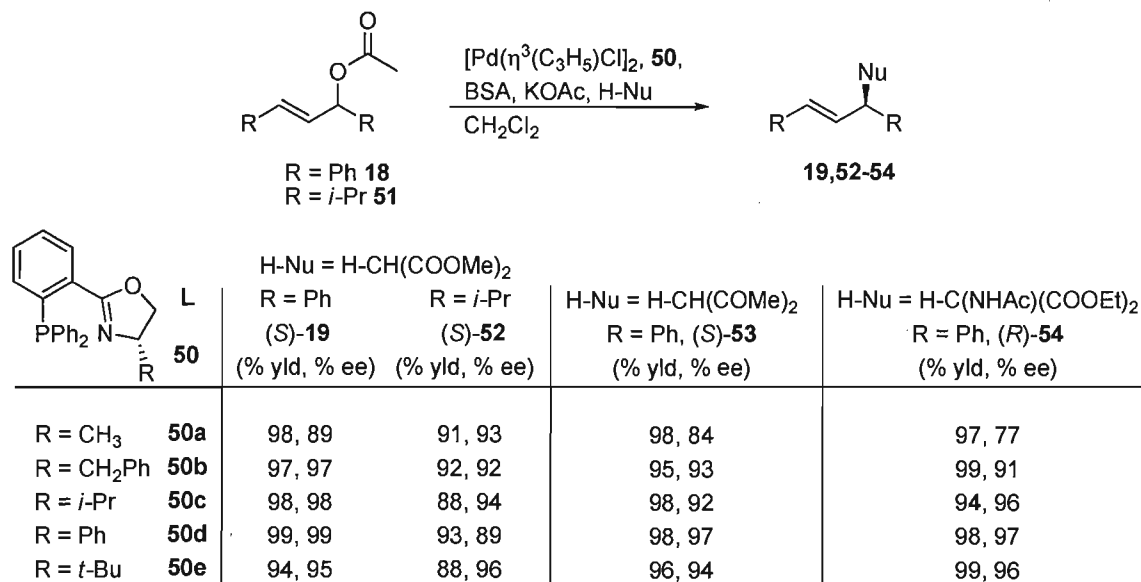
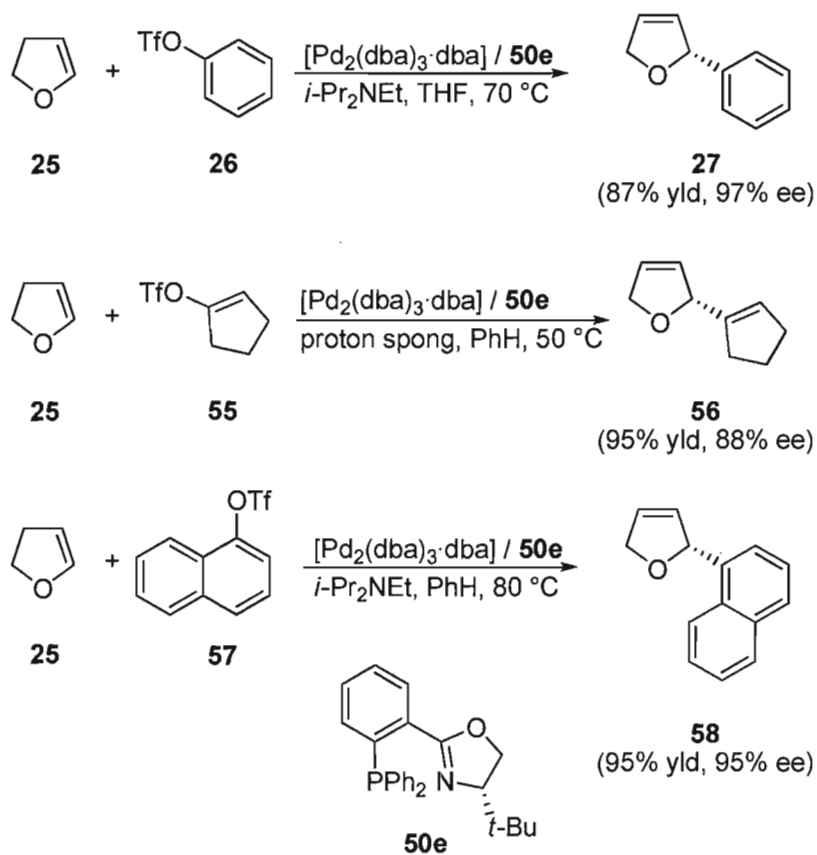
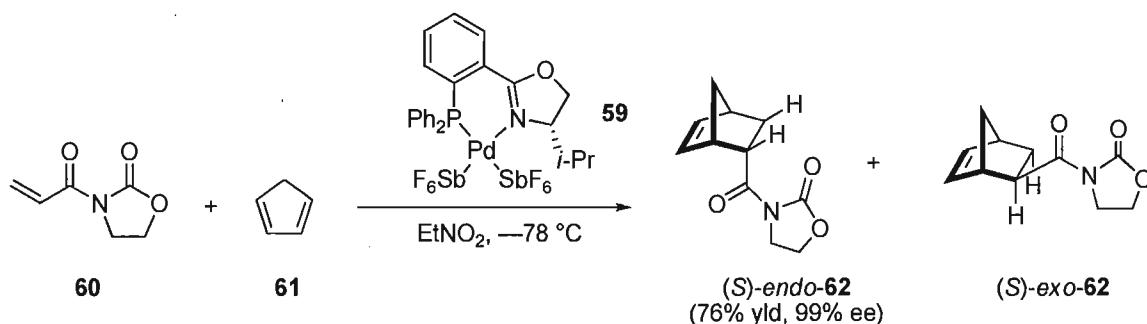


Table 1. Pd-catalyzed asymmetric allylic alkylations with various nucleophiles with phosphino-oxazoline ligand **50** (reproduced from ref 32).



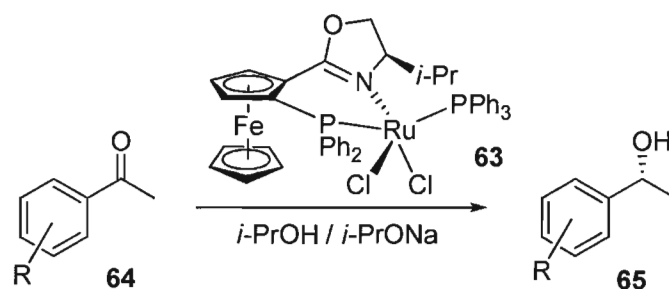
Scheme 17. Pd-catalyzed asymmetric Heck reactions with phosphinooxazoline ligand **50e**.

Additionally, these ligands have found application in Pd-catalyzed enantioselective Diels-Alder reactions, providing a high *endo/exo* ratio (97:3) and the (*S*)-*endo*-**62** product in high enantioselectivity (99% ee) with complex **59** (Scheme 18).³⁶



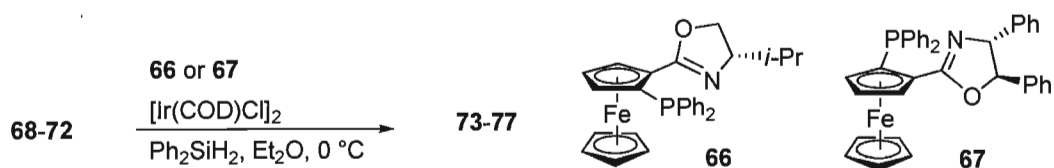
Scheme 18. Pd-catalyzed asymmetric Diels-Alder reaction with phosphine-oxazoline ligand.

Several derivatives based on the phosphinooxazoline framework have been prepared. For example, planar chiral ferrocene analogues were prepared independently by Uemura³⁷, Richards³⁸, and Sammakia³⁹ in 1995 and shown to provide excellent enantioselectivities in many catalytic reactions⁴⁰ such as Ru-catalyzed transfer hydrogenations (Table 2)⁴¹, Ir-catalyzed hydrosilylations (Table 3)⁴², and Pd-catalyzed asymmetric Heck reactions (Scheme 19).⁴³ Axial chiral phosphinooxazoline **81** with binaphthalene backbone was used in allylic aminations with up to 99% ee (Scheme 20).⁴⁴ Possibly the largest application of the PHOX ligands continues to be in Ir-catalyzed asymmetric hydrogenation (see Section 1.3.5).



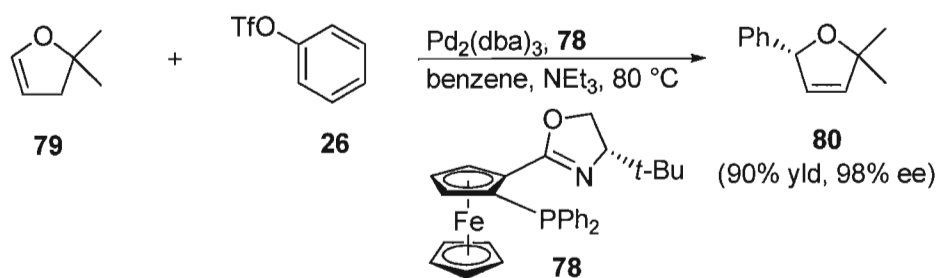
	R	Time, h	Product, % Yield		% ee
3	H	2	4	94	99.6
64a	<i>o</i> -Me	1	65a	99	99.9
64b	<i>o</i> -Cl	1	65b	99	99.7
64c	<i>m</i> -Me	1	65c	98	99.9
64d	<i>m</i> -Cl	2	65d	99	99.7
64e	<i>p</i> -Me	4	65e	98	99.3
64f	<i>p</i> -Cl	2	65f	99	98.7

Table 2. Asymmetric transfer hydrogenation with ferrocenyl phosphinooxazoline Ru complex **63** (reproduced from ref 41).

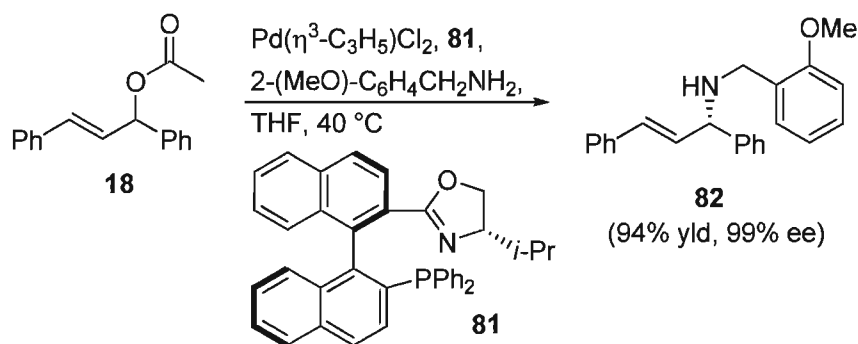


	Substrate	Ligand	Reaction time	Product	Yield, %	% ee
68		66	20 h	73	95	85
69		66	60 h	74	56	89
3		67	15 h	4	100	96
70		67	15 h	75	100	92
71		67	15 h	76	100	81
72		67	15 h	77	100	84

Table 3. Ir-catalyzed asymmetric hydrosilylations of imines and ketones with ferrocenyl phosphinooxazoline ligands **66** and **67** (reproduced from ref 42).



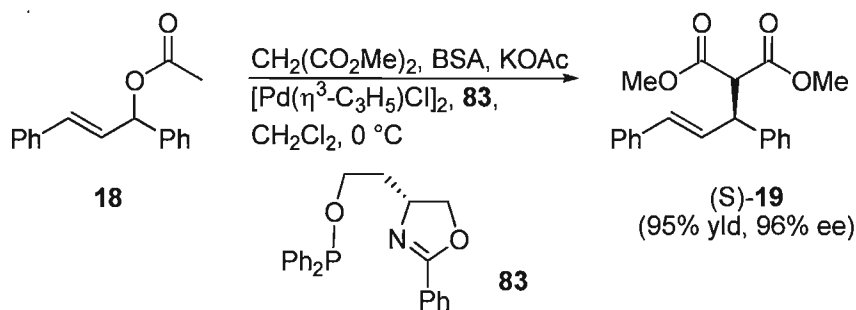
Scheme 19. Pd-catalyzed asymmetric Heck reaction with ferrocenyl phosphinooxazoline ligand **78**.



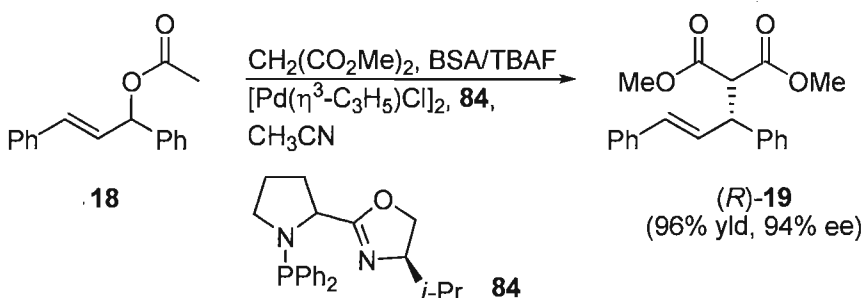
Scheme 20. Pd-catalyzed allylic amination with axial chiral phosphinooxazoline ligand **81**.

1.2.3 Imine *N*, Heteroatom Bound *P* Ligands.

Placing an electronegative atom on the phosphorus donor atom increases its π -accepting qualities. Most work in this area involves oxazoline nitrogen donor groups, and either nitrogen or oxygen substituted phosphorus donor groups. This often makes these types of ligands more effective than traditional phosphine ligands. For example, phosphinitooxazolines have been found to offer better substrate scope in Ir-catalyzed asymmetric hydrogenation than traditional PHOX ligands (see Table 6, Section 1.3.5).^{45,46} Additionally, Richards used phosphinitooxazolines, such as ligand **83** in Pd-catalyzed asymmetric allylic alkylation of **18** and obtained (*S*)-**19** in excellent yield and 96% ee (Scheme 21).⁴⁷ Gilbertson prepared ligand **84** with a pyrrolidine-bound phosphorus donor atom. This ligand provided product (*R*)-**19** in excellent yield and 94% ee (Scheme 22).⁴⁸



Scheme 21. Pd-catalyzed asymmetric allylic alkylation with phosphinitooxazoline ligand **83**.



Scheme 22: Pd-catalyzed asymmetric allylic alkylation with pyrrolidine-bound phosphine oxazoline ligand **84**.

1.3 Catalytic Homogeneous Hydrogenation.

Hydrogenation in organic synthesis involves the addition of two or more hydrogen atoms across a multiple bond. Hydrogen gas addition to an olefin is often termed H_2 -catalytic hydrogenation, while transfer of hydrogen from one molecule (usually an alcohol) to a double bond (usually a carbonyl) is termed catalytic transfer hydrogenation (Figure 7). In the absence of catalysts, molecular hydrogen is stable, with a bond energy of 104 kcal/mol, and does not react with organic molecules. However, in the presence of transition metals or their complexes, H_2 can be activated to participate in

hydrogenation of unsaturated organic molecules. The nature and reactivity of the intermediate transition metal species depends on the central metal atom as well as the electronic and steric properties of attached ligands.⁴⁹

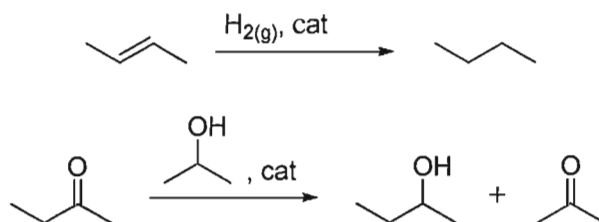
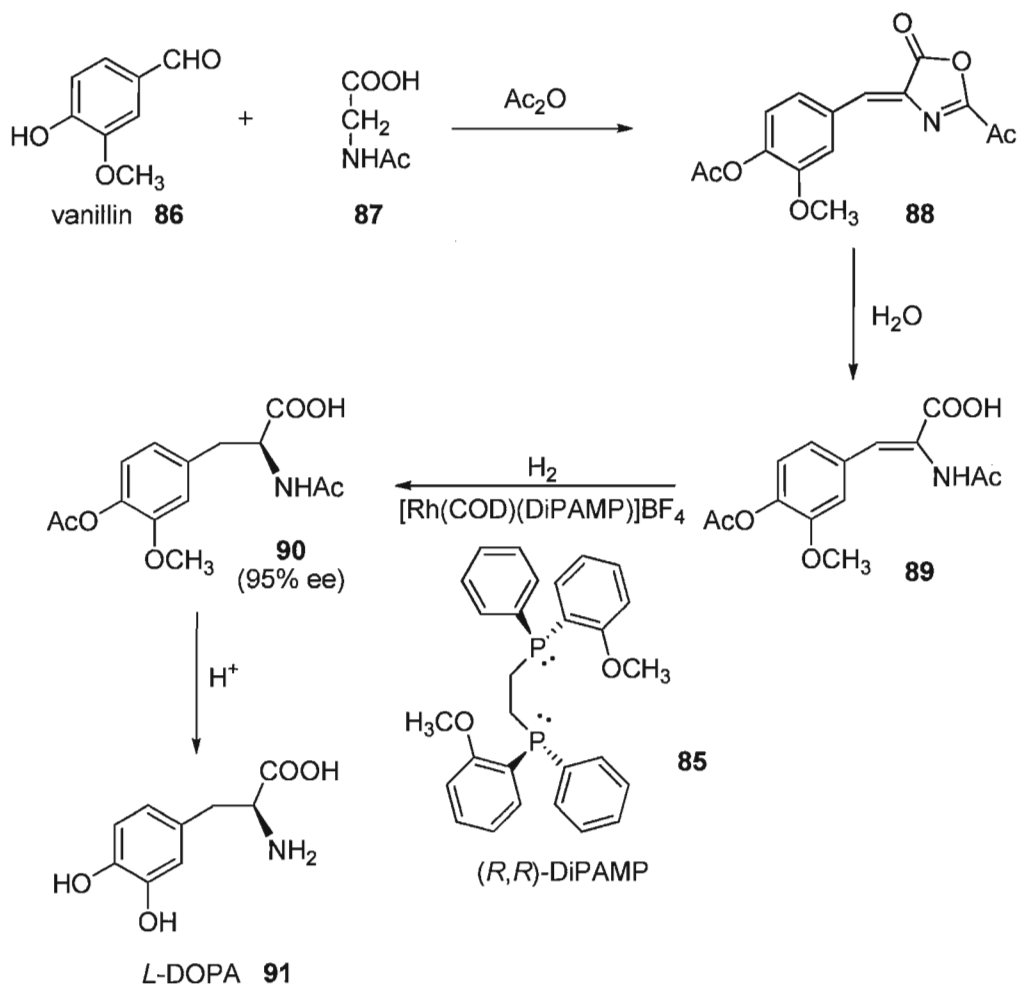


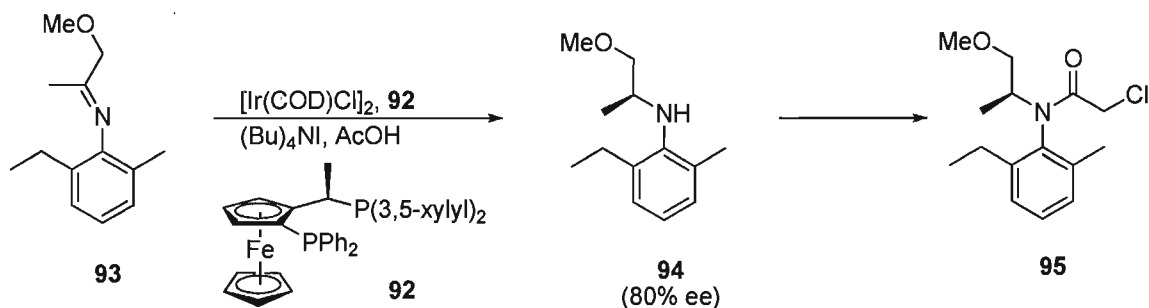
Figure 7. Catalytic H_2 and transfer hydrogenations.

Alkenes that can give two enantiomers upon hydrogenation are termed prochiral alkenes. The two faces of the prochiral alkene can be defined as *re* or *si*; one face has a clockwise arrangement of substituents R, R', and alkene about the trisubstituted sp^2 carbon (*re*), while the other face has a counterclockwise arrangement of the same substituents (*si*). Upon coordination with a metal complex, diastereomers are formed based on the face of coordination. Thus, when H_2 is exclusively added from one face, one enantiomer is formed; when added from the other, the opposite enantiomer is formed (Figure 8).⁸



Scheme 23. Monsanto synthesis of *L*-DOPA.

The largest scale enantioselective catalytic process in industry is the synthesis of a precursor to the herbicide (*S*)-metolachlor (**95**) by Xyliphos (**92**) Ir-catalyzed asymmetric imine hydrogenation with a TON of 2 000 000, TOF 600 000 / hour, and with more than 10 000 tons prepared per year. This reaction is one of the fastest homogeneous systems known (S/C 10⁶) giving precursor **94** in 80% ee, a sufficient enantiopurity for this process (Scheme 24).⁵³



Scheme 24. Key asymmetric hydrogenation step in the synthesis of (*S*)-metolachlor.

1.3.1 Structural Types of Alkenes in Asymmetric Homogenous Hydrogenation.

Alkenes can be divided into several different categories – functionalized, largely unfunctionalized, and unfunctionalized (Figure 9).⁵⁴ Often certain catalysts will work well for one class of olefin, but not for another. Functionalized olefins, including α,β -unsaturated carboxylic acids and amides, have functional groups that often bind to metal centers and orient the substrates in the catalytic intermediates. Largely unfunctionalized olefins, including α,β -unsaturated esters, contain a functional group that is directly conjugated to the alkene but that does not coordinate to the metal center. Unfunctionalized olefins involve functional groups that do not coordinate to metal centers, nor contain polarized double bonds, and include those with aromatic or alkyl substituents. A large portion of the useful largely unfunctionalized alkene substrates for asymmetric hydrogenations are tri- and tetra-substituted alkenes.⁵⁴

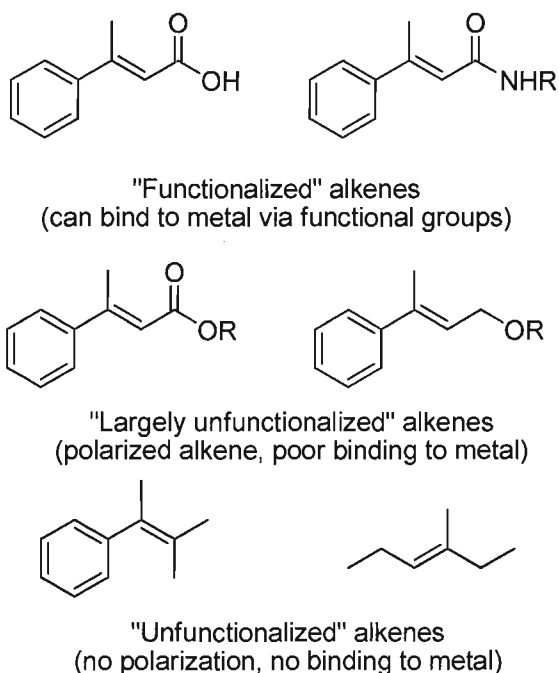


Figure 9. Classes of alkenes used in asymmetric iridium catalyzed hydrogenations.

1.3.2 Iridium-Catalyzed Homogeneous Hydrogenation.

Iridium complexes were first discovered to promote catalytic hydrogenation by Crabtree and Morris in 1977.⁵⁵ They utilized a cationic iridium complex composed of tricyclohexylphosphine, pyridine, and cyclooctadiene ligands, with a hexafluorophosphate (PF_6) counterion (**96**, Figure 10). Reactions were performed in non-coordinating solvents such as dichloromethane.⁵⁵

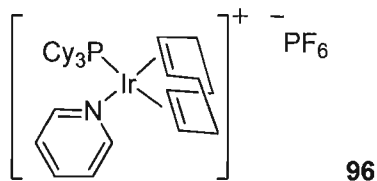


Figure 10. Crabtree and Morris' cationic iridium complex.

Several factors were found to be crucial for the iridium complexes to be active. In particular was the electrophilic nature of the cationic complex, which can be affected by the number and identity of ligands associated with the metal center.⁵⁵ Other important factors included the use of non-coordinating solvents and bulky, weakly coordinating anions. Coordinating solvents and stronger anions (such as halides) were found to form complexes that were too stable to promote hydrogenation (i.e. dissociation of any ligands needed to create a vacant site for the substrate does not occur).^{55,56} By combining non-coordinating solvents with non-coordinating counterions, as well as the COD ligand (which can be easily released from the Ir complex via hydrogenation thus irreversibly providing vacant sites), active iridium complexes were developed. Catalysts with two pyridine ligands were found to be inactive, while those with two phosphine ligands were found to be less active than the mixed pyridine/phosphine complexes which exhibited high TOFs, particularly for hindered (e.g. tetrasubstituted) alkenes (Table 4 and Figure 11).⁵⁶ While these initial complexes were achiral, they showed how tremendously effective iridium(I) was at catalyzing this class of reaction.

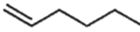
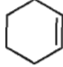
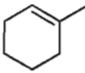
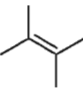
catalyst precursor	temp, °C	solvent				
[Ir(COD)PCy ₃ (py)]PF ₆	0	CH ₂ Cl ₂	6400	4500	3800	4000
[Ir(COD)(PMePh ₂) ₂]PF ₆	0	CH ₂ Cl ₂	5100	3800	1900	50
	0	Me ₂ CO	~10	0	0	0
[Rh(COD)(PPh ₃) ₂]PF ₆	25	CH ₂ Cl ₂	4000	10	-	0
[RuHCl(PPh ₃) ₃]	25	C ₆ H ₆	9000	7	-	0
[RhCl(PPh ₃) ₃]	25	C ₆ H ₆ / EtOH	650	700	13	0
	0	C ₆ H ₆ / EtOH	60	70	-	0

Table 4. Turnover frequencies (mol substrate reduced (mol catalyst)⁻¹ h⁻¹) for several olefins with various catalysts (reproduced from ref 56).

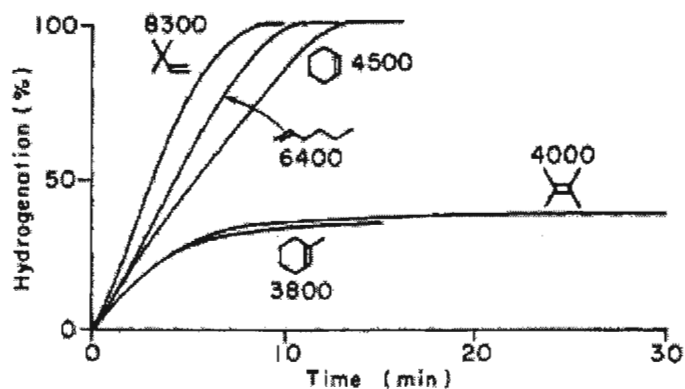


Figure 11. Hydrogen absorption curves for several alkenes with $[\text{Ir}(\text{COD})(\text{Pi-Pr}_3)(\text{py})]\text{PF}_6$ (rates expressed in $\text{mol H}_2 (\text{mol Ir})^{-1} \text{h}^{-1}$) (used with permission from ref 56).

Unfortunately, Crabtree's catalyst suffered from deactivation after, or in some cases before, full conversion was reached. Deactivation was found to occur via the formation of trimers of the catalyst (Figure 12). Crabtree stated that "the fact that the deactivation products are polynuclear clusters suggests that by keeping the catalyst species apart from one another, deactivation can be prevented or at least slowed down. One effective method is simply to inject a dilute catalyst solution dropwise into the reaction vessel as the hydrogenation proceeds. Choosing ligands so large that they prevent dimerization also works, but at the cost of almost complete loss of activity".⁵⁶

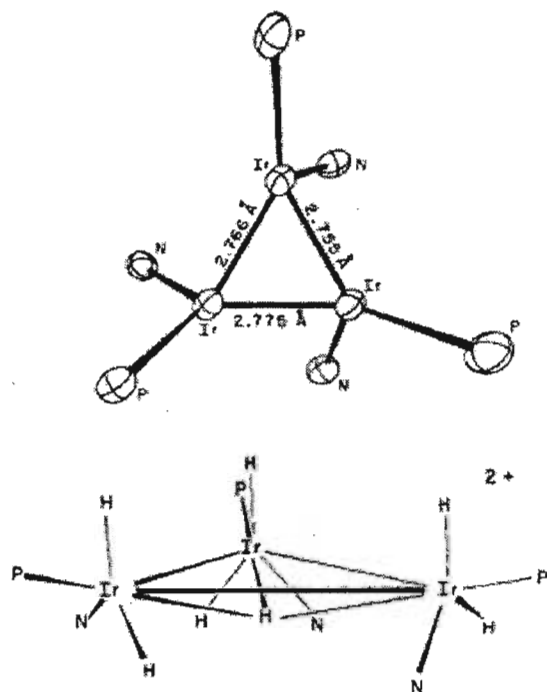
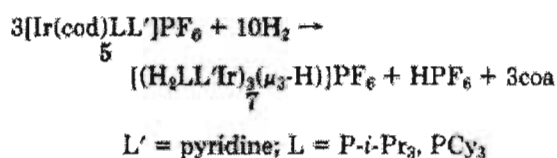


Figure 12. Structure of Crabtree deactivated complexes (used with permission from ref 56).

Suggs and Crabtree demonstrated the usefulness of these iridium complexes in hydrogenation of hindered steroidal alkenes. Several Δ^4 -3-ketosteroids could be hydrogenated to the desired 5α -3-ketosteroids (Table 5).⁵⁷ Heterogeneous catalysts gave mixtures of the 5α - and 5β -steroids, with the undesired 5β isomer predominating. Wilkinson's catalyst ($\text{RhCl}(\text{PPh}_3)_3$) did selectively hydrogenate from the α face, but the reduction required long reaction times and yields were low.⁵⁸ Consequently, $[\text{Ir}(\text{COD})\text{PCy}_3(\text{py})]\text{PF}_6$ showed higher activity than Wilkinson's catalyst while retaining the 5α selectivity, providing the steroids in good to excellent yields.

	Substrate	Product	Yield
97		100	73
98		101	70
99		102	90

Table 5. Steroid derivatives reduced with Crabtree's iridium complex.

1.3.3 Further Development of Iridium Catalysts.

Subsequent studies have focused on the preparation of chiral bidentate *P,N* ligands for use in asymmetric applications. Iridium complexes with *P,N* ligands represent a class of catalysts that significantly expand the application range of asymmetric hydrogenation. Iridium complexes are advantageous over rhodium or ruthenium complexes because they are generally more stable to oxidizing conditions that normally deactivate the latter. Additionally, in contrast to chiral rhodium- or ruthenium-phosphine catalysts, iridium catalysts do not require the presence of a polar functional group conjugated to the C=C double bond, although these functionalized alkenes can be

hydrogenated as well. This makes the application range of iridium catalysts largely complementary to chiral rhodium and ruthenium catalysts.⁵⁹

Pfaltz expanded the field of Ir-catalyzed asymmetric hydrogenation with the discovery that the BAr_F counterion {tetrakis[3,5-bis(trifluoromethyl)phenyl]borate} (**103**) (Figure 13) made iridium complexes much more active, air and moisture stable, and less prone to deactivation prior to full conversion of the olefin.⁶⁰

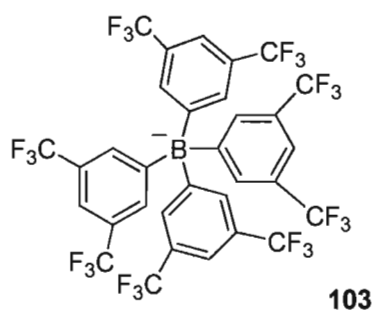


Figure 13. BAr_F counterion.

Pfaltz further showed that the reaction kinetics, and thus the catalytic activity and productivity of PHOX-iridium complexes, were largely influenced by the counterion. The reaction rate for methyl stilbene hydrogenation was found to decrease strongly over the series $[\text{Al}\{\text{OC}(\text{CF}_3)_3\}_4]^- > \text{BAr}_\text{F}^- > [\text{B}(\text{C}_6\text{F}_5)_4]^- > \text{PF}_6^- \gg \text{BF}_4^- > \text{CF}_3\text{SO}_3^-$.⁵⁶ Full conversions were found with the aluminate, BAr_F⁻, and perfluorotetraphenylborate anions, while 50% conversion was observed with the hexafluorophosphate anion. High turnover frequencies were found with the aluminate, BAr_F⁻, and perfluorinated tetraphenylborate anions with $[\text{Al}\{\text{OC}(\text{CF}_3)_3\}_4]^-$ being ~10% faster than BAr_F⁻, and the $[\text{B}(\text{C}_6\text{F}_5)_4]^-$ found to be ~17% slower than BAr_F⁻. It was also observed that the aluminate,

BArF^- , and $[\text{B}(\text{C}_6\text{F}_5)_4]^-$ salts remained active after full conversion of the substrate was reached, while the PF_6^- salt had lost its activity.⁶¹

Following a short induction period involving gas transfer to the liquid phase and generation of the active catalyst by hydrogenation and dissociation of COD, a linear uptake of hydrogen was observed until the reaction was complete. Kinetic data showed that there was an approximately first order rate dependence on the hydrogen pressure, indicating that dihydrogen is involved in the rate-determining step.⁶¹ It was also shown that at low alkene concentrations, a rate order of approximately one was observed for the PF_6^- salt, suggesting that the alkene is involved in the rate-determining step with PF_6^- complexes. This was not the case for the BArF^- salt. This data suggests that the counterion effect was due to the significantly faster reaction of the alkene with the BArF^- containing catalyst compared to the PF_6^- salt. Thus, stronger coordination to the PF_6^- counterion blocks coordination of the alkene substrate to iridium.⁶¹ Crabtree's initial complex became even more active with the BArF^- counterion, and the deactivation problems observed with the PF_6^- counterion were eliminated.⁶²

Pfaltz also showed that enantioselectivity does not vary during the reaction. An experiment where several samples were taken throughout the reaction (ranging from 9 to 84% conversion) was conducted, and showed that the enantiomeric excess remained constant throughout the reaction. Additionally, the effect of a chiral anion in asymmetric hydrogenation of methyl stilbene was examined. Complex **104** with the chiral anion Δ -TRISPHAT and achiral cation produced product in racemic form. Conversely, complex **105** with Δ -TRISPHAT anion and chiral cation provided product in the same

enantioselectivity as the corresponding BAr_F^- complex (Figure 14), thus indicating that it was the ligand chirality that determined the enantioselectivity of the reaction.⁶¹

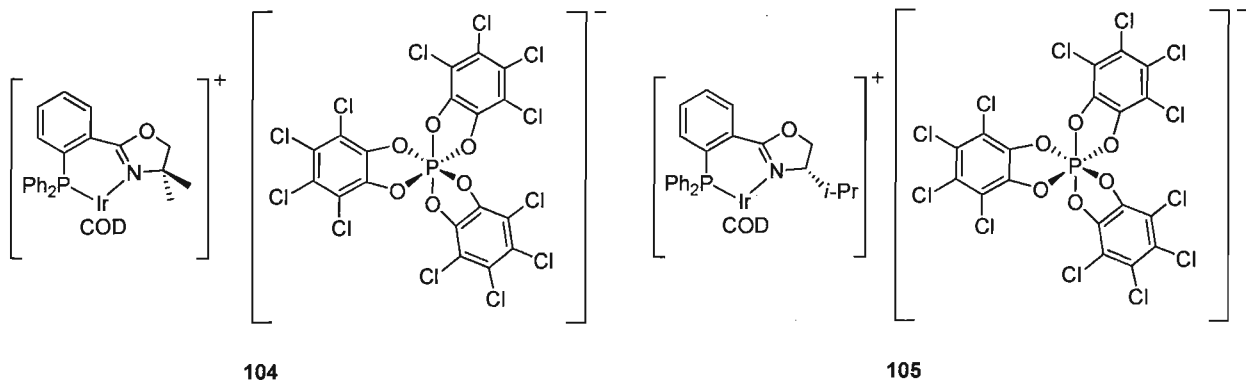


Figure 14. Complexes containing chiral Δ -TRISPHAT anion with achiral (**104**) and chiral (**105**) cations.

1.3.4 Mechanistic Studies of Ir-Catalyzed Hydrogenation.

The earliest mechanistic studies of iridium catalyzed hydrogenation were conducted by Crabtree *et al.* who used low temperature NMR spectroscopy to identify intermediates.⁶³ The mechanism of hydrogenation involves the oxidative addition of dihydrogen to the square planar Ir(I) precatalyst to provide the thermodynamically and kinetically more stable octahedral Ir(III) dihydride species (**101**, Figure 14). Hydrogen oxidatively adds two hydrides *trans* to the electronically more donating group (pyridine in this case), and *cis* to the olefin group (whether that be the initial COD ligand or the substrate alkene) in order to achieve co-planarity.^{63c} As hydride is a strong σ donor, the two hydrides do not occupy *trans* positions to one another, nor do they occupy sites *trans* to the next strongest *trans* effect ligand, the phosphine,⁶⁴ further explaining the preference

for species **106**. Crabtree and Morris showed that these octahedral dihydride complexes could be formed reversibly if hydrogen was added and then quickly removed from the system at low temperature.^{63c} Also, dihydride intermediates could be identified by low temperature NMR spectroscopy (Figure 15). In the proton NMR spectrum (CD₂Cl₂ at –80 °C), H_A appeared as a doublet at –18.0 ppm and H_B as a doublet at –12.7 ppm, with coupling constants of 18 and 20 Hz, respectively, consistent with *cis* phosphorus–hydride coupling. The identities of H_A and H_B were established based on chemical shifts, based on the effect of the ligand *trans* to them. Inequivalence of the COD vinyl protons was also observed, further confirming the stereochemistry of species **106** seen in Figure 15.^{63c}

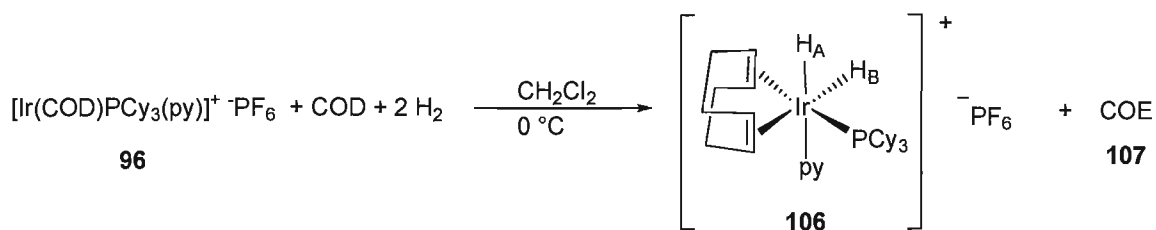


Figure 15. Crabtree's dihydride complex (measured at –80 °C in CD₂Cl₂) (reproduced from ref 63c).

Pfaltz *et al.* also conducted low temperature NMR studies with a [Ir(PHOX)COD]BAR_F catalyst and found that a single olefin dihydride intermediate was formed at –40 °C in THF.⁶⁵ The addition of H₂ was highly stereoselective, resulting from both steric and electronic influences of the PHOX ligand. Two new signals appeared in the hydride region at –12.7 and –15.6 ppm, with coupling constants to phosphorus of approximately 20 Hz (again consistent with *cis* coupling), represented by structure **111** in Figure 16. Isomer **111** is favoured both electronically and sterically. Dihydrogen addition

to this face provided a structure with the least amount of steric strain between the chelating COD and PHOX ligands. Additionally, in accordance with Crabtree's observations, addition of dihydrogen occurred *trans* to nitrogen.^{63b,c} This structural isomer was also confirmed by 2D-NMR experiments where NOE contacts between the hydride in the apical position (H1) and both the isopropyl hydrogen (H3) and the *ortho* hydrogen on the *P*-phenyl ring (H5) were observed (Figure 17).⁶⁵

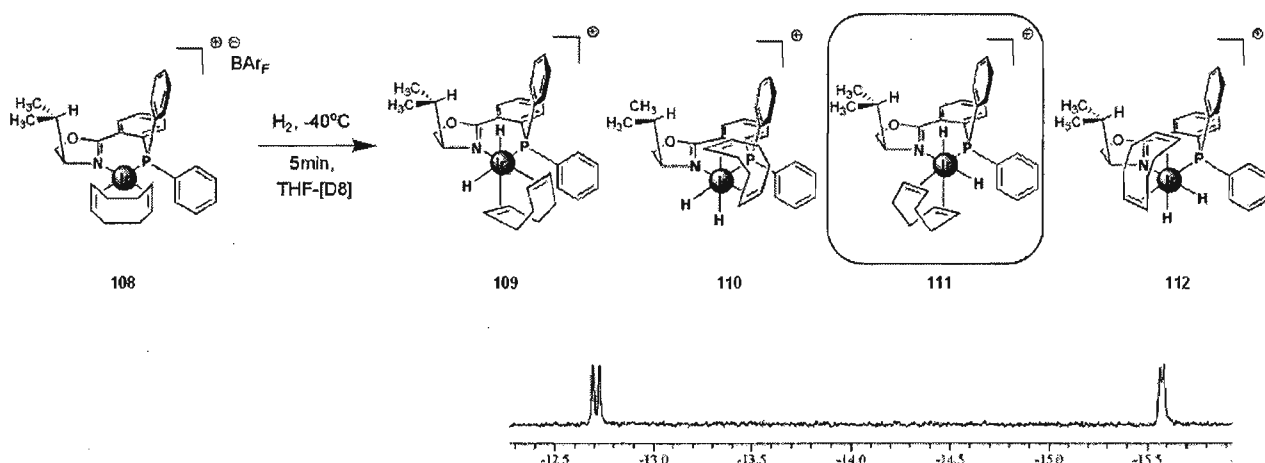
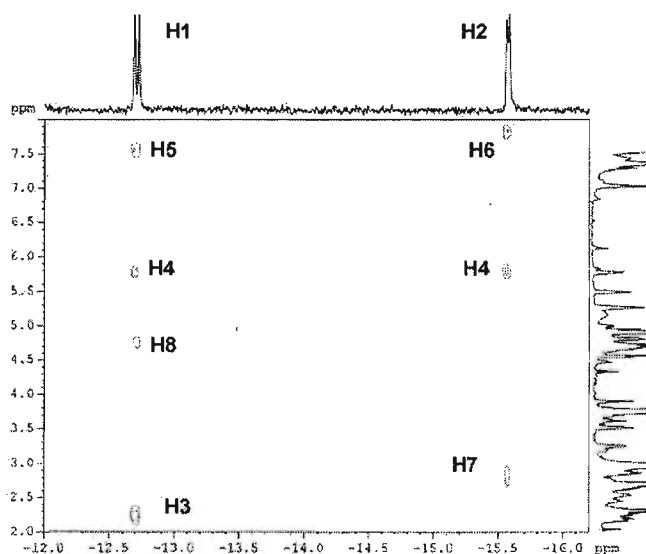


Figure 16. Pfaltz's dihydride complex (measured at -40 °C in *d*₈-THF) (used with permission from ref 65).



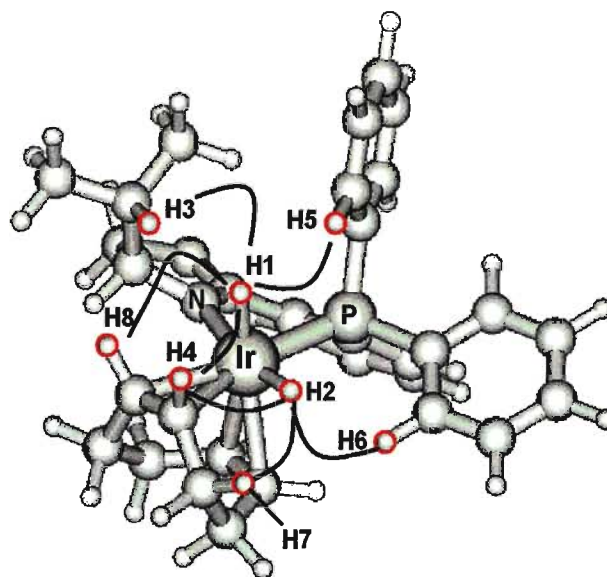


Figure 17. NOE observations and spectrum for dihydride intermediate **111** (used with permission from ref 65).

These structures were also studied via computational modeling (DFT calculations) where it was predicted that experimentally observed isomer **111** was thermodynamically the most stable isomer (Figure 18), and that the ligand played a crucial role in the geometry of the Ir-hydride complexes. The +4.9 kcal/mol energy difference between isomer **111** and **112** was explained by unfavourable steric interactions between the COD ligand and the oxazoline portion of the ligand. The +10.6 kcal/mol energy difference between isomer **111** and **109** was explained by the unfavourable coordination of the hydride *trans* to phosphorus instead of nitrogen. Isomer **110** was both sterically and electronically disfavoured.⁶⁵

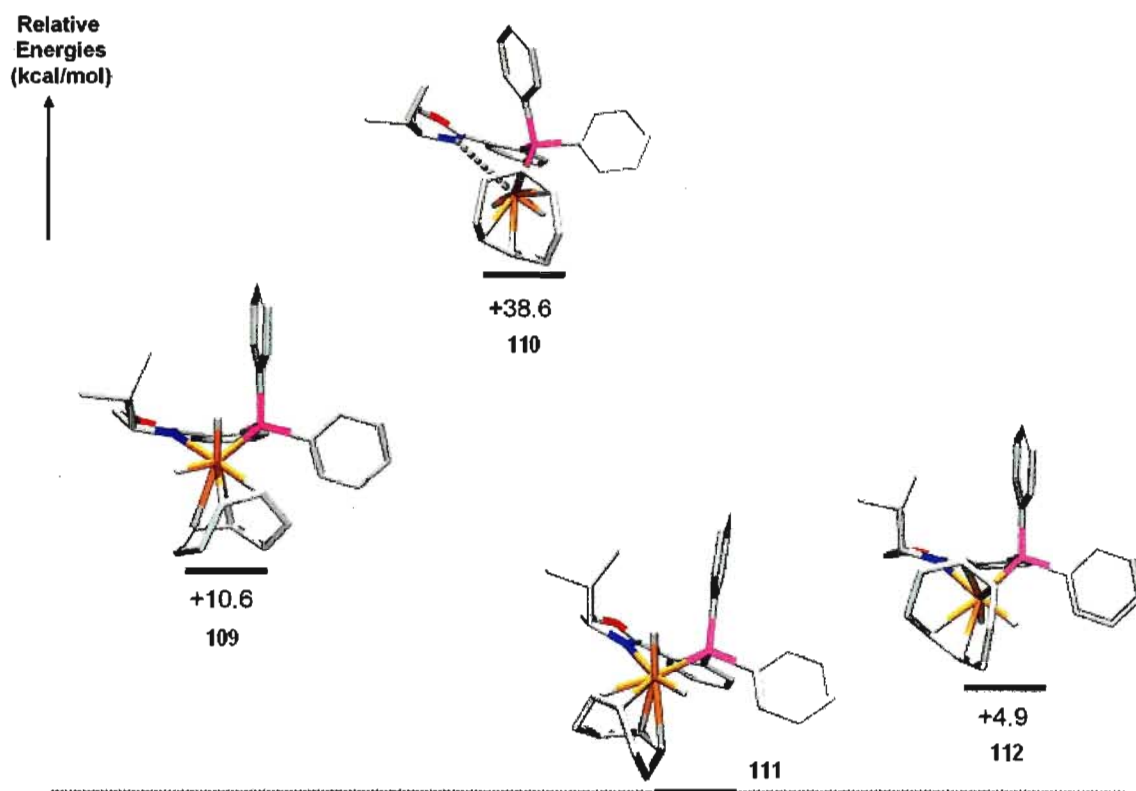


Figure 18. Calculated energies for dihydride species (used with permission from ref 65).

No spectral changes were observed upon slowly warming the solution of catalyst from -40 to 0 °C in the absence of hydrogen, indicating that the kinetically preferred product was also thermodynamically favoured. Upon warming from -40 to 0 °C in the presence of hydrogen, gradual consumption of isomer **111** was observed, accompanied with formation of solvated complexes **115** and **116** and free cyclooctane, confirming hydrogenation of the COD ligand (Figure 19).⁶⁵ These isomers were established based on chemical shifts (-17 and -29 ppm), coupling constants ($J_{\text{H}^{31}\text{P}}^1 \sim 19$ Hz), and NOE observations. The highly negative chemical shift of one hydride ligand indicated that it was located *trans* to a weak ligand, the coupling constants are consistent with *cis*-phosphine coupling, and complex **115** has an NOE contact between the apical hydride

and the hydrogen on the *isopropyl* substituent (Figure 20).⁶⁵ It should be noted that the NMR reactions were run in $[D_8]THF$, a more coordinating solvent than used standard catalytic conditions, as attempts to follow the reaction under H_2 in CD_2Cl_2 were unsuccessful and a complex mixture of hydrido species observed which could not be analyzed. Pfaltz later stated that an iridium dihydride solvate species had been characterized in dichloromethane, but no experimental details or discussion of structure have been published to this point.⁶⁶

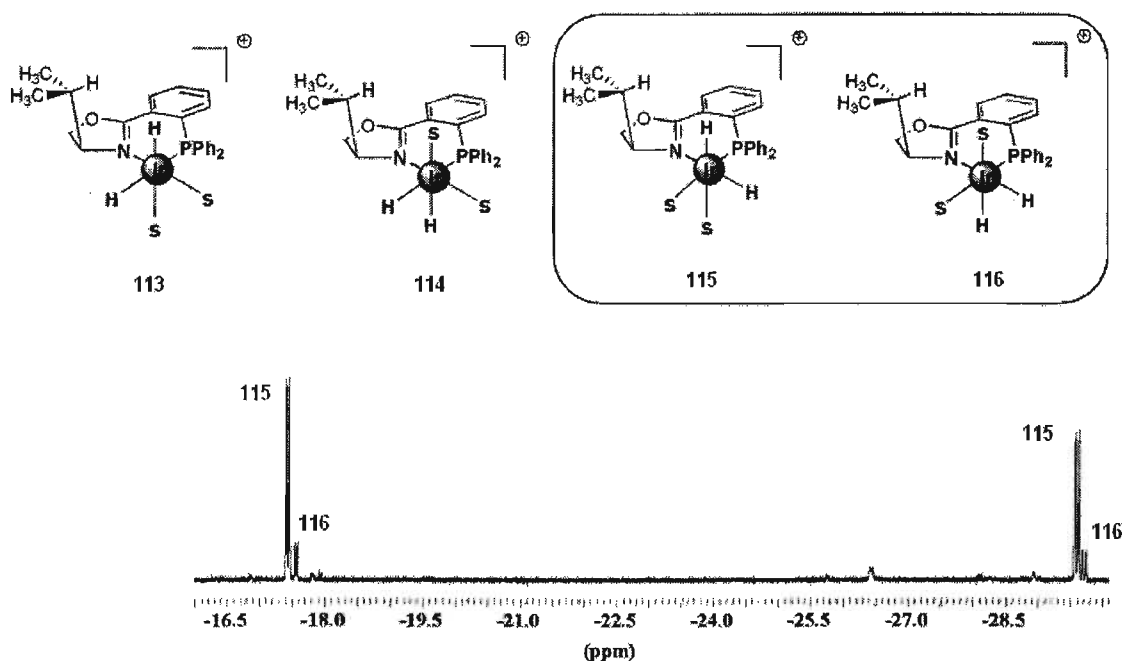


Figure 19. Pfaltz's solvated (THF) hydride complexes (used with permission from ref 65).

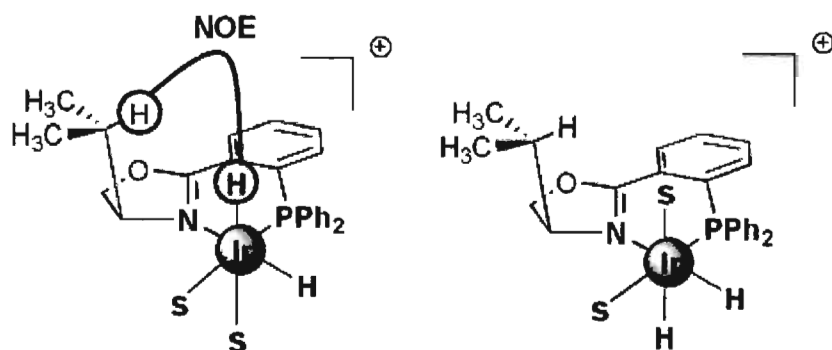


Figure 20. NOE observation for dihydride intermediate **115** (used with permission from ref 65).

These complexes were again studied computationally with methyl chloride molecules used to simulate the dichloromethane generally used as solvent in actual hydrogenation reactions, and again the predicted lowest energy conformation was consistent with the main observed isomer, **115** (Figure 21).⁶⁵

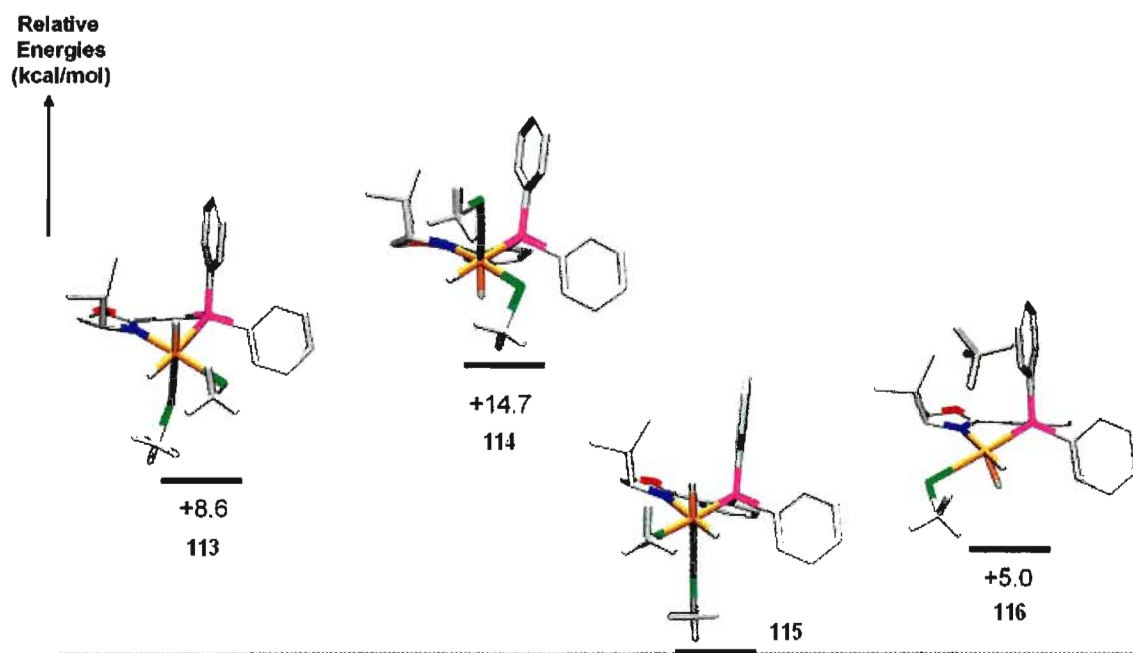


Figure 21. Calculated energies for solvated (CH_3Cl) complexes (used with permission from ref 65).

Once transfer of hydrogen to the COD ligand and oxidative addition of another H₂ molecule has occurred, two open coordination sites are left, which are subsequently occupied by solvent to produce species **117**. Both the oxidative addition and solvent coordination steps were found to be energetically favoured in calculations by Brandt.⁶⁷ Dissociation of solvent with simultaneous coordination of alkene gave an intermediate Ir(III)-dihydride-alkene complex with olefin coordinated *trans* to the stronger *trans* effect terminus, the phosphine donor group (**118** or **122**, Figure 22).^{66,67} The *trans* effect occurs because two *trans* ligands compete with each other for electron density as they use the same metal orbitals for bonding. Thus, *trans* ligands can exert an effect on one another dictating the order in which ligands bind or are displaced (kinetic effect – see Section 1.1). The order of *trans* influence for phosphines is as follows: P(OMe)Ph₂ > PPh₃ > P(Me)Ph₂ > PEt₃ > P(*i*-Pr)₃ > PCy₃.⁶⁸

Following coordination of the alkene, two pathways have been studied. The first follows a similar mechanism as rhodium diphosphine catalyzed hydrogenation of alkenes,⁶⁹ and involves Ir(I) / Ir(III) intermediates (Figure 22, left). In this mechanism, transfer of one hydride to the alkene via 1,2-hydride migratory insertion occurs giving an Ir(III) ethane complex (**119**). A coplanar M(C=C)H system is required in order for insertion of the coordinated olefin into the M-H bond.⁷⁰ After this, transfer of the second hydride with simultaneous dissociation of the alkane (reductive elimination) gives an Ir(I) species (**120**) which undergoes solvent coordination and rapid oxidative addition of dihydrogen to reform the active Ir(III) solvated dihydride species (**117**). Alternatively, an Ir(III) / Ir(V) catalytic cycle has been proposed based on computationally studies (Figure 22, right).⁶⁷ Dihydrogen and substrate alkene coordination to intermediate **117** with

dissociation of two solvent molecules, forms Ir(III) species **121** with η^2 coordinated dihydrogen.⁶⁷ Migratory insertion of the alkene into the axial Ir-H bond accompanied by simultaneous oxidative addition of the attached H₂ gives Ir(V) complex **122**. This complex rapidly undergoes reductive elimination of the alkane to produce Ir(III) dihydride species **123**, and ligand substitution of the alkane with solvent reforms Ir(III) dihydride solvent species **117**. Both of these mechanisms may be active during hydrogenation, especially as different factors will influence the transition states involved. These include the temperature of the reaction, the hydrogen pressure used, the catalyst loading, the concentration of both substrate and catalyst, the solvent, and the substrate for hydrogenation.⁷¹

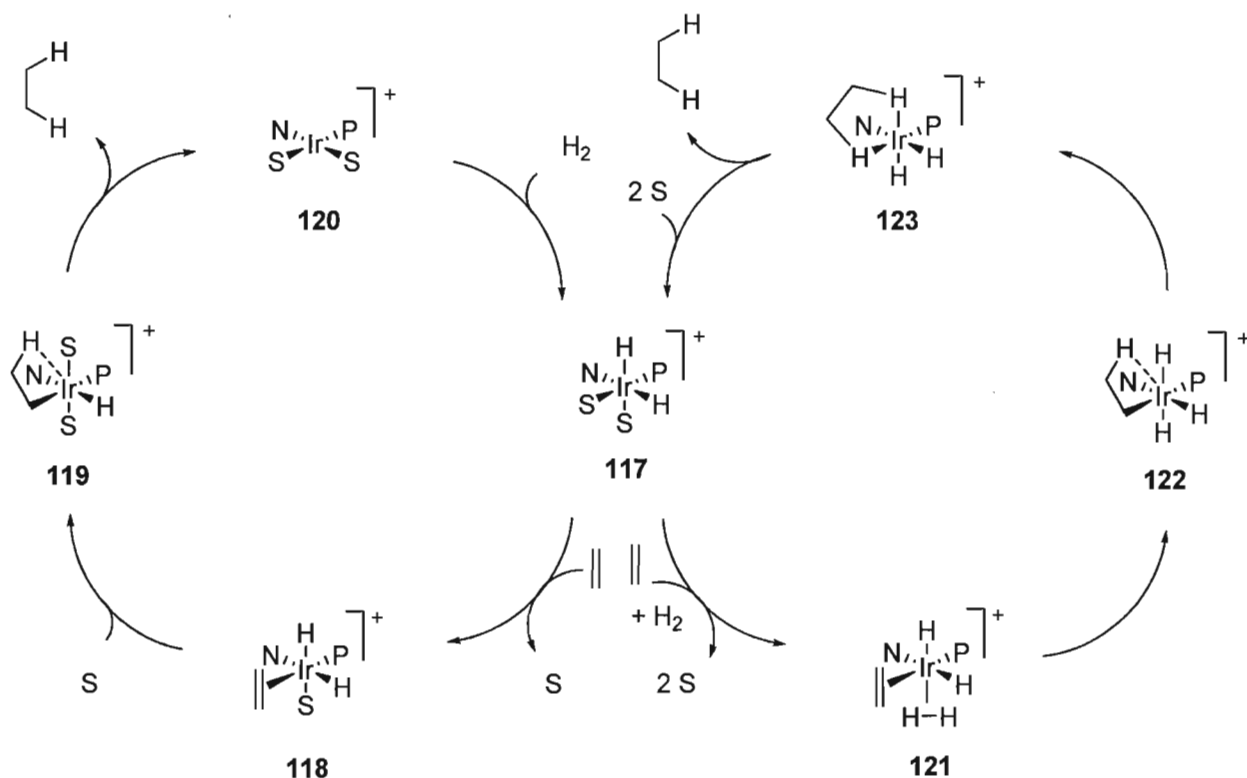


Figure 22. Ir(I) / Ir(III) (left) and Ir(III) / Ir(V) (right) catalytic cycles.

The origin of enantioselectivity was found to depend on a combination of two factors, the facial selectivity of the alkene upon complexation with iridium, and the relative rates of the hydride migratory insertion step. Olefin coordination can occur either in the plane of the ligand (i.e. *trans* to the ligand plane) or in the axial position (i.e. *cis* to the ligand plane). Calculations by Brandt⁶⁷ and Burgess and Hall⁷² have shown that the olefin preferentially lies in the equatorial plane. Upon coordination in the equatorial plane, the alkene is *cis* to the nitrogen group (which is generally the terminus with the bulky chiral group), and as such the alkene prefers to bind with its smallest substituent pointing toward the bulky group, with larger groups preferring unhindered regions (Figure 23).^{67,72,73} Having steric bulk on phosphorus can also aid in selectivity by forcing the more substituted carbon of the alkene *trans* to phosphorus.

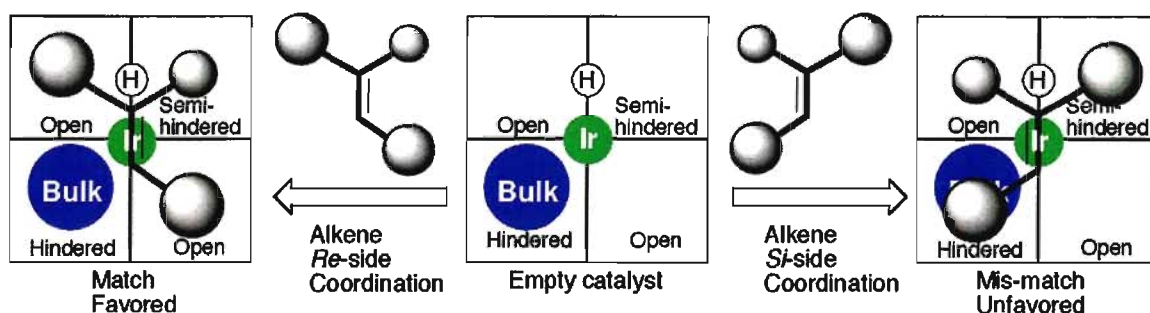


Figure 23. Steric influence on enantioselectivity (used with permission from ref 73).

In the transition state for the hydride migratory insertion step, the olefin becomes tilted towards the hydride. The hydride addition becomes sterically favoured if the olefin is tilting away from the ligand bulk, and disfavoured if tilting toward the ligand bulk.⁷⁴ Additionally, while non-coordinating functional groups do not direct hydrogenation by chelation as with rhodium and ruthenium catalysis, they have been found to influence the

stereoselectivity by polarization of the double bond.⁷⁴ Hydride addition then becomes preferentially selective towards the δ^+ carbon (electronically favoured). These steric and electronic factors during hydride insertion can work synergistically or counteract each other (Figure 24).

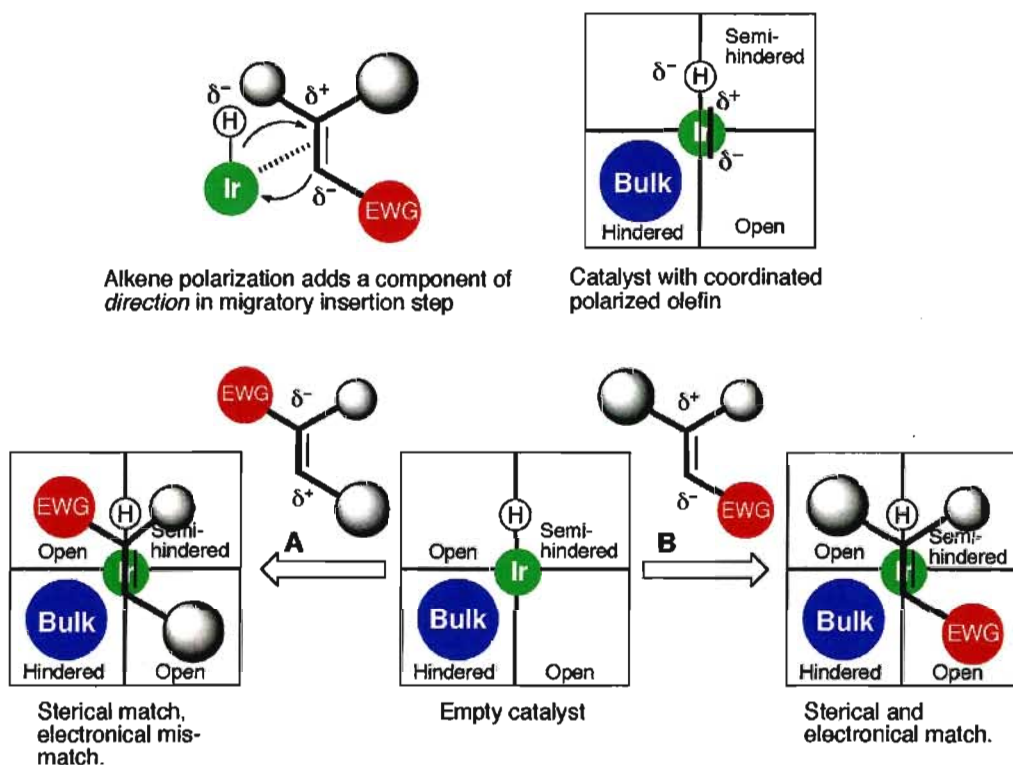


Figure 24. Steric and electronic influences during enantiodetermining migratory insertion step (used with permission from ref 73).

For example, Andersson has shown that hydrogenation of β -methyl cinnamate was both sterically and electronically favoured, while hydrogenation of the α -substituted ester was sterically favoured, but electronically unfavoured. Computational modeling of the enantiodetermining migratory insertion transition states with Andersson's thiazole complex explained the levels of enantioselectivities and why higher levels of selectivity were obtained with β -substituted cinnamates (Figure 25).⁷³

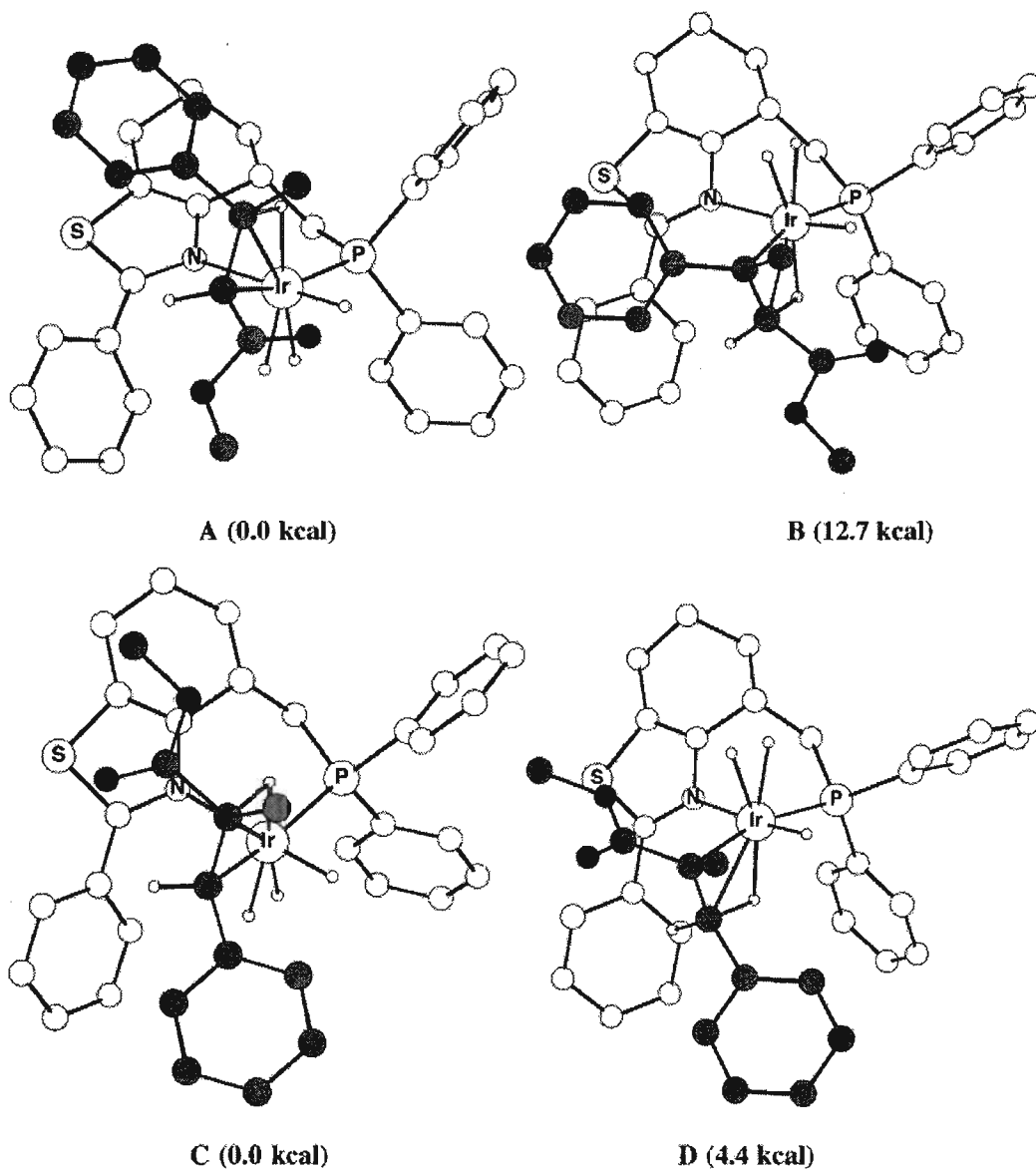


Figure 25. Calculated transition states for migratory insertion: A – sterically and electronically favoured hydride addition to the β -carbon of *trans*- β -methyl cinnamate; B – sterically and electronically unfavoured hydride addition to the α -carbon of *trans*- β -methyl cinnamate; C – sterically favoured, electronically unfavoured hydride addition to the α -carbon of *trans*- α -methyl cinnamate; D – sterically unfavoured, electronically favoured hydride addition to the β -carbon of *trans*- α -methyl cinnamate (used with permission from ref 73).

1.3.5 Applications of Ir-Catalyzed Hydrogenation.

There are numerous chiral ligands that have been employed in Ir-catalyzed hydrogenation with excellent results (several examples are given in Figure 26).⁷⁵ When new ligands are prepared, they are tested against several standard substrates for both activity and selectivity. Some of these substrates are shown in Figure 27, and include methyl stilbenes (**124**), alkyl substituted alkenes (**125**, **126**), trisubstituted cyclic alkenes (**127**), α,β -unsaturated esters (**128**), and allylic alcohols (**129**). In general, different substrates require different ligands for optimum enantioselectivity, while tetrasubstituted and purely alkyl substituted olefins remain difficult to hydrogenate even with the best ligands. Additionally, aromatic substituents attached to the C=C bond seem to have a beneficial effect on enantioselectivity, and thus these are often present in the standard substrates.⁵⁹ *p*-Methoxy phenyl is also a common substituent as it aids in enantioselectivity determination by chiral stationary phase HPLC or GC.

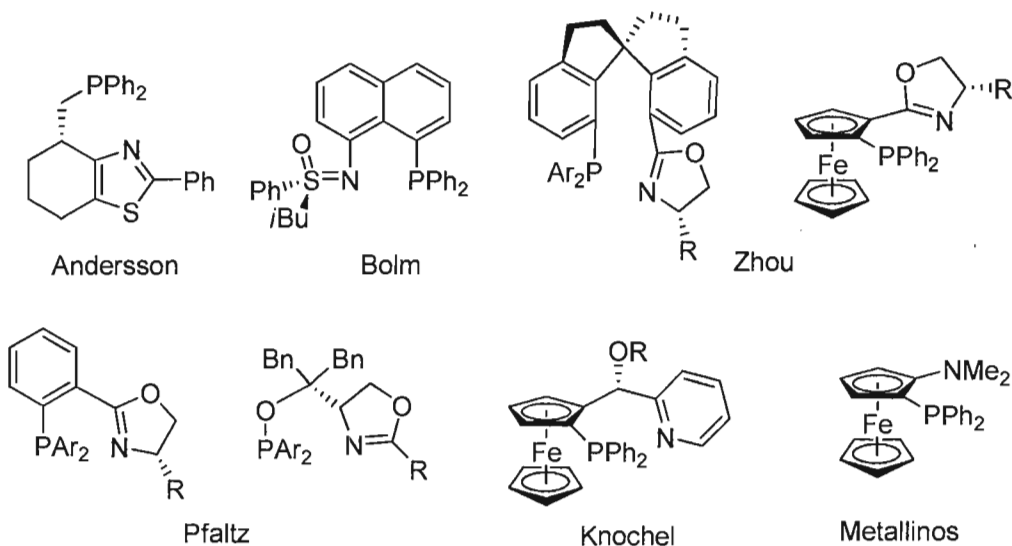


Figure 26. *P,N* ligands used in asymmetric Ir-catalyzed hydrogenation.

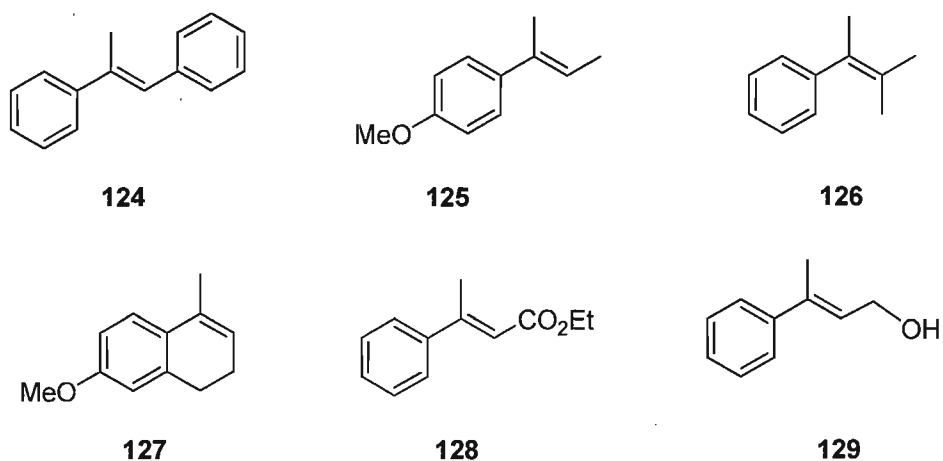


Figure 27. Standard test substrate alkenes for asymmetric Ir-catalyzed hydrogenations.

Several catalysts exist that can hydrogenate olefins in Figure 27 with near quantitative yields and high enantioselectivities. A few representative examples are given in Table 6.⁷⁶

		 130	 131	 132	 133
124		97	97	89	98
125		61	89	/	91
128		84	95	82	94
129		96	94	99	97

Table 6. Selectivities of several chiral catalysts (reproduced from ref 76).

The development of the PHOX and phosphinitooxazoline ligands along with the discovery of more active iridium complexes using the BAr_F counterion sparked vast interest in the area of asymmetric iridium catalyzed hydrogenation. Many new chiral *P,N* ligands are introduced every year by various groups employing modifications of this and other structural motifs. No one ligand is effective for every substrate, thus the search for a catalyst with a wide or complementary substrate range is ongoing. Several types of functionalized and unfunctionalized alkenes can be hydrogenated with excellent turnover frequencies ($> 5000 \text{ h}^{-1}$) and enantioselectivities, while some improvement is still needed with tetrasubstituted olefins. New substrate classes for which there have previously been no suitable catalysts are frequently being reported with good conversions and enantioselectivities. These substrates are often key intermediates in the synthesis of complex molecules. For example, Pfaltz reported the hydrogenation of terminal alkenes,⁷⁷ purely alkyl substituted alkenes,⁷⁸ and tetrasubstituted alkenes⁷⁹ in 2005, 2006, and 2007, respectively, using oxazoline or pyridine derived *P,N* ligands (Figure 28). Full conversions and high selectivities were found with the terminal and alkyl alkenes, while varying conversions, and moderate to high enantioselectivities were obtained with tetrasubstituted alkenes.

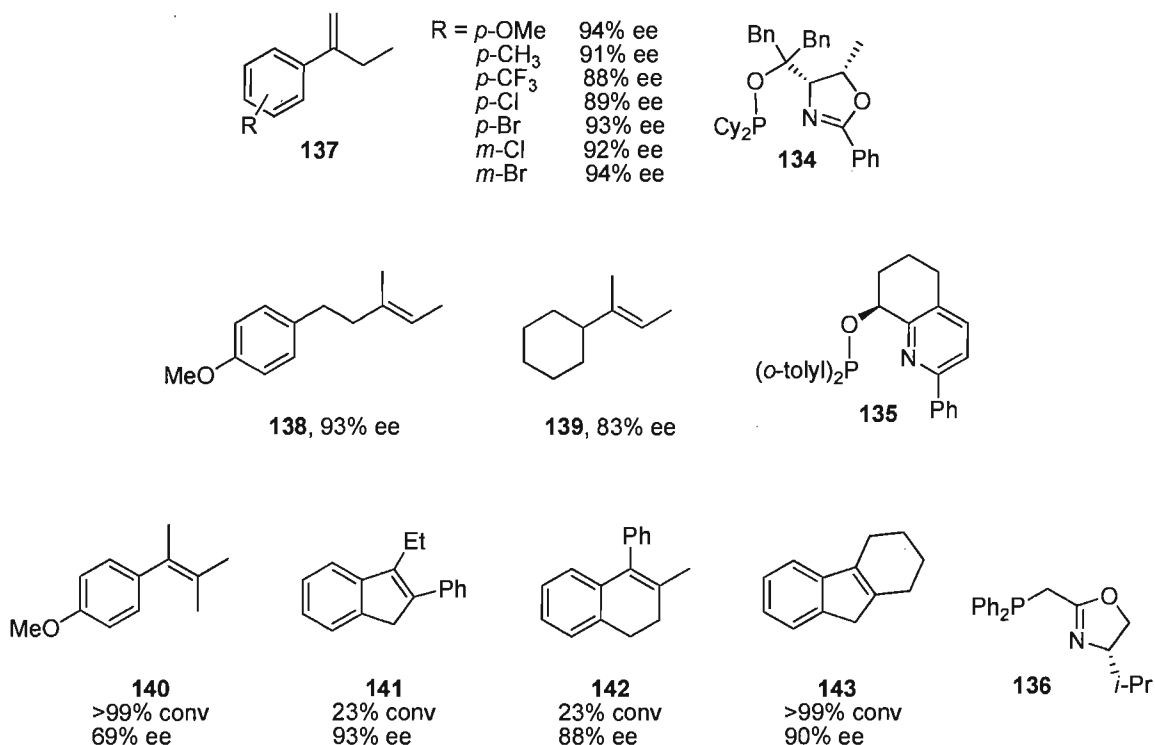


Figure 28. Hydrogenation results of terminal, purely alkyl-substituted, and tetrasubstituted alkenes.

Andersson reported the hydrogenation of diaryl substituted alkenes in 2009, providing products which are prevalent in medicinal chemistry. His thiazole based *P,N* ligand (**144**, Figure 29) was able to achieve high conversions and excellent enantioselectivities for a broad range of diaryl alkenes, with some limitations and high pressures and temperatures needed in some cases.⁸⁰ Andersson also applied the same thiazole catalyst in the hydrogenation of trifluoromethyl substituted alkenes, products of which have applications ranging from agrochemical to pharmaceuticals and materials chemistry. Products were obtained in high enantioselectivity, although high pressures (100 bar) were needed for good conversions (Figure 29).⁸¹ Other uncommon classes of hydrogenation substrates include quinolines by Zhou,⁸² *N*-protected indoles by Pfaltz,⁸³

chromenes by Pfaltz,⁸⁴ as well as α,β -unsaturated ketones,⁸⁵ amides,⁸⁶ and carboxylic acids.⁸⁷

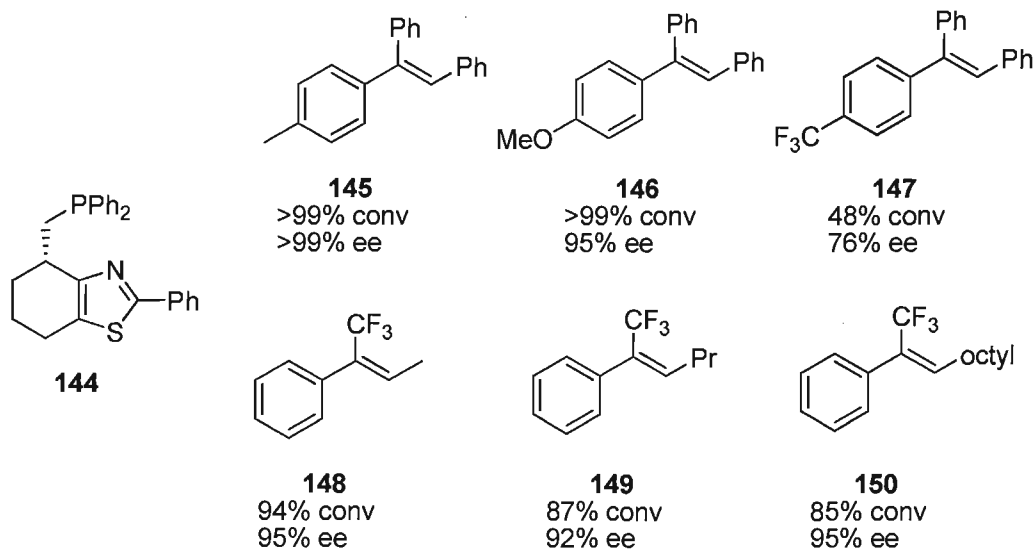
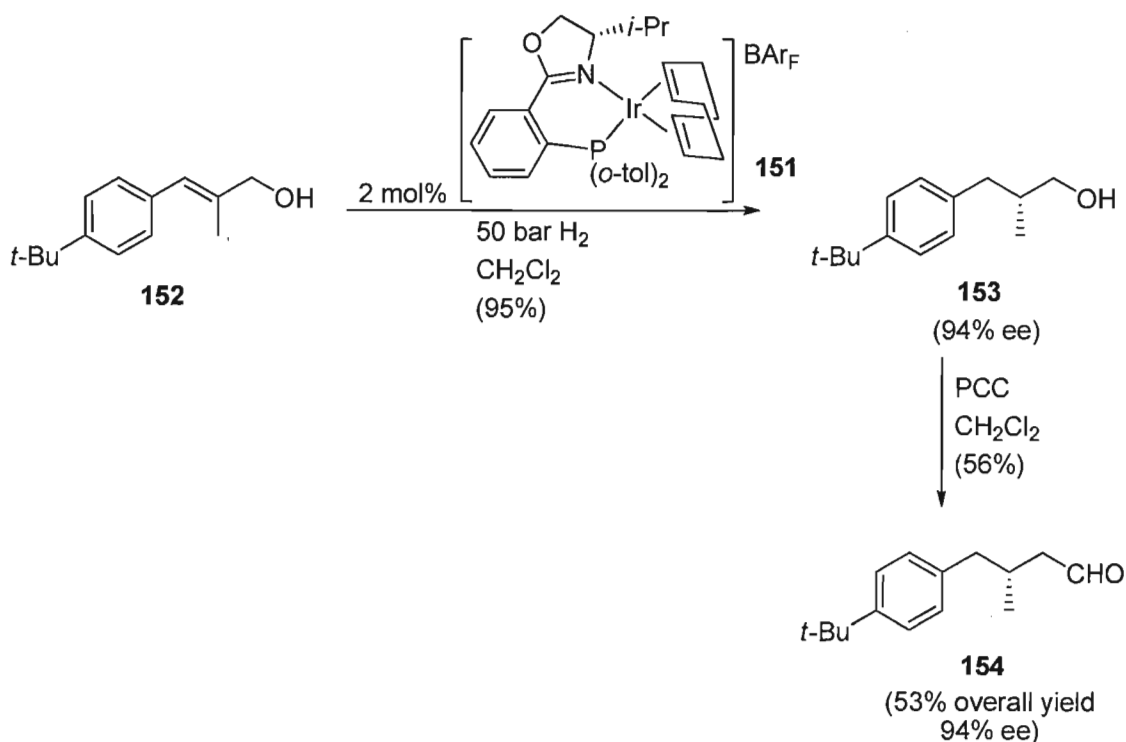


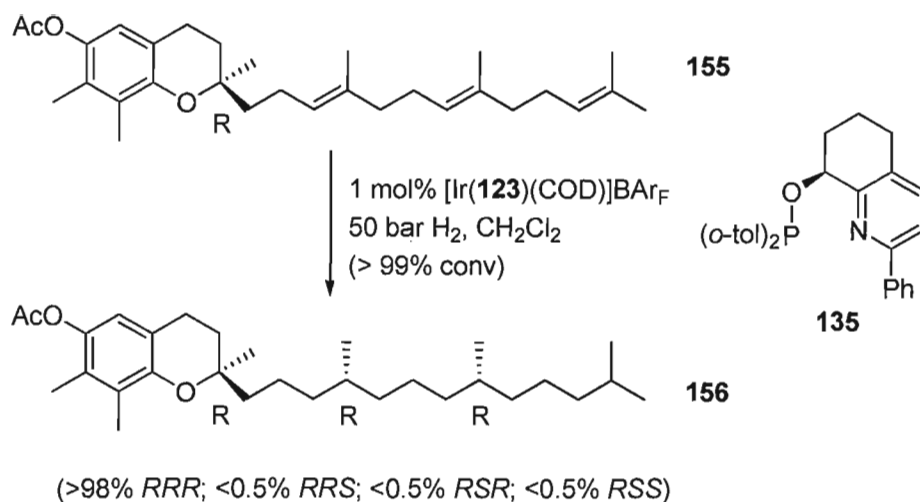
Figure 29. Hydrogenation results of diaryl- and trifluoromethyl-substituted alkenes.

Iridium catalyzed asymmetric hydrogenation using *P,N* ligands has been used in numerous asymmetric total syntheses of natural products and drug leads. One of the earliest examples was Pfaltz's synthesis of lilial in 1998. Lilial (**154**) was obtained in 94% ee and 53% overall yield in two steps from allylic alcohol **152** (Scheme 25).⁸⁸ In 2006, Pfaltz synthesized γ -tocopheryl acetate via hydrogenation of triene **155**, a rare example of hydrogenation of a purely alkyl substituted alkene (Scheme 26).⁸⁹ The tocopherol family of molecules are the main components in vitamin E and are biologically and economically important fat-soluble antioxidants. In the reaction, three C=C bonds are hydrogenated with two new stereocenters created. When starting with the two prochiral double bonds in the (*E*) configuration (**155**), the expected sense of

induction will be either (*R,R*) or (*S,S*), depending on the configuration of the catalyst used. Using pyridine-phosphinite ligand **135**, the natural (*R,R,R*)-tocopheryl acetate **156** was obtained in 98% dr and nearly quantitative conversion from triene **155**. Thus, asymmetric iridium catalyzed hydrogenation provides a highly effective stereoselective route to this important class of bioactive antioxidants with installation of the *R,R* configuration established in one step.⁸⁹

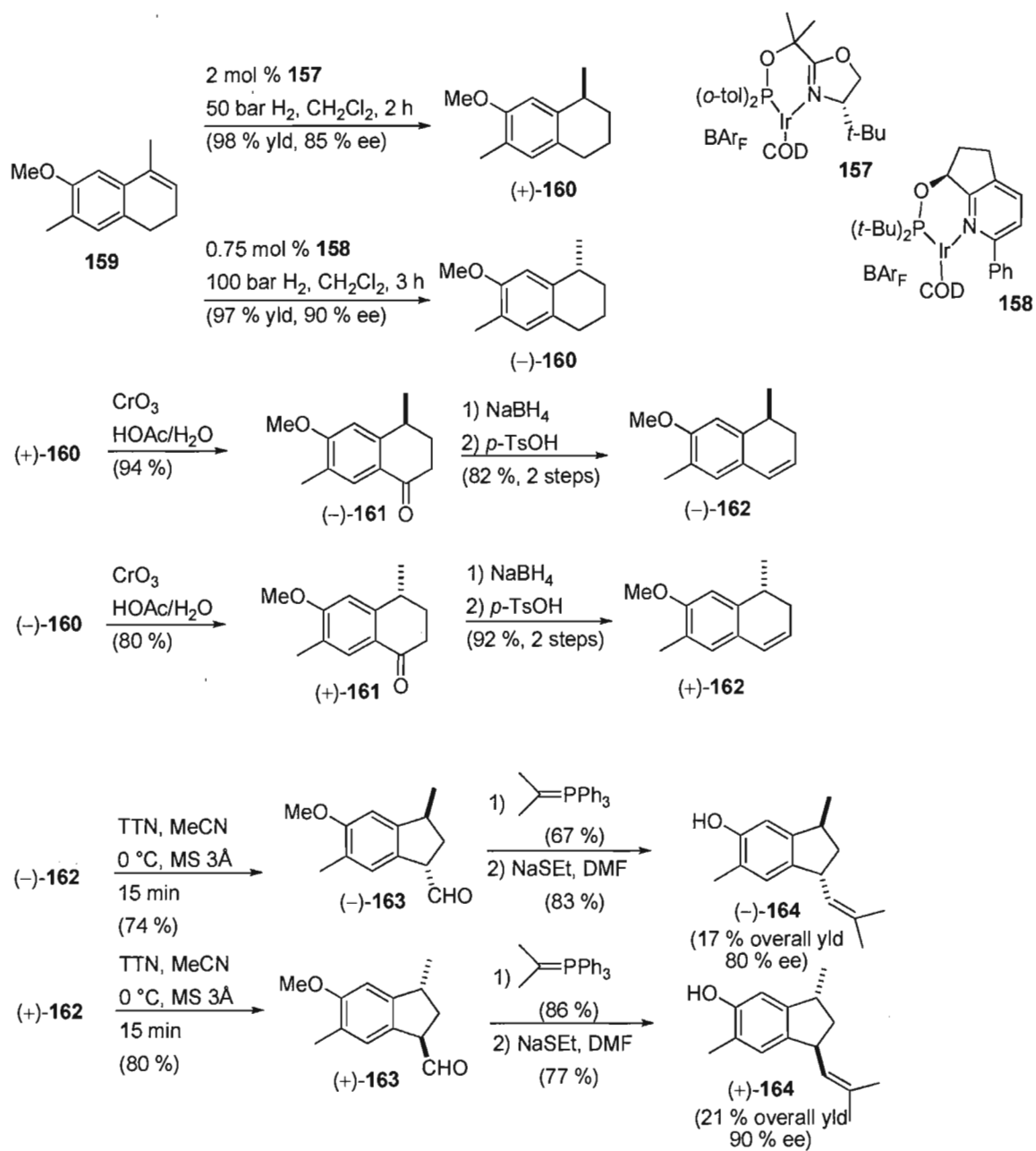


Scheme 25. Asymmetric synthesis of linal using Ir-PHOX complex **151**.



Scheme 26. Asymmetric synthesis of γ -tocopheryl acetate **156**.

A further example was given by Pfaltz in 2009, where he utilized asymmetric iridium hydrogenation as the key step in the synthesis of (+)- and (–)-mutisianthol, a phenolic sesquiterpene with moderate antitumor activity (Scheme 27).⁹⁰ Utilizing two different catalysts (**157** or **158**), both enantiomers of intermediate **160** could be obtained after asymmetric hydrogenation of trisubstituted cyclic olefin **159**. From here, selective oxidation of the benzylic position, followed by reduction/dehydration provided intermediate **162**. This intermediate was then subjected to a ring contraction reaction using thallium(III) trinitrate (TTN) to give the aldehyde intermediate **163**. This intermediate underwent Wittig olefination, followed by demethylation to afford (+)- and (–)-mutisianthol (**164**) in good overall yield and selectivity. As seen previously, asymmetric iridium catalyzed hydrogenation proved to be a vital step in the synthesis to set the initial stereochemistry of the molecule.⁹¹



Scheme 27. Total synthesis of (+)- and (-)-mutisianthol.

1.4 Planar Chiral Ferrocene Ligands.

1.4.1 1,2-Substituted Planar Chiral Ferrocenes.

Ferrocenyl compounds substituted with different groups at the 1 and 2 positions exhibit planar chirality due to the loss of both the σ_v plane of symmetry and inversion axis, and as such may be synthesized in enantiopure form.⁹² The absolute configuration is assigned by looking along the C_5 axis of ferrocene with the more substituted ring directly towards the observer (Figure 30). When $R_1 > R_2$, the compound has (*R*) planar chiral configuration; when $R_2 > R_1$, the compound has (*S*) planar chiral configuration.⁹³

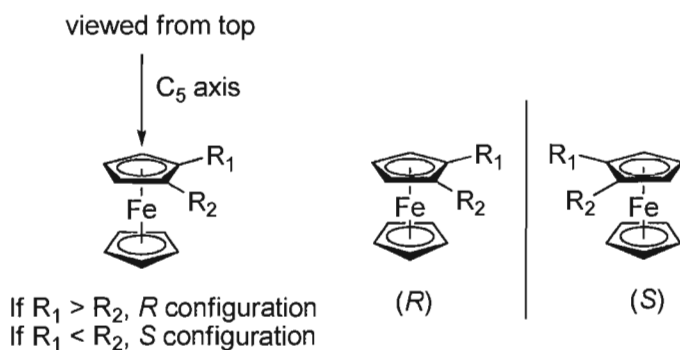


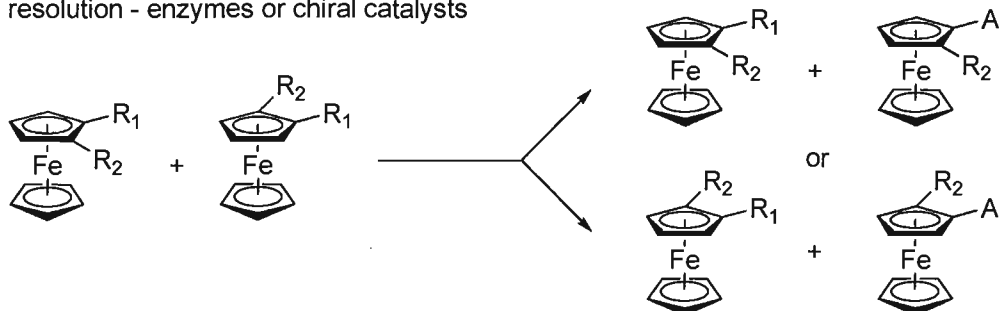
Figure 30. Planar chirality of 1,2-substituted ferrocenes.

1.4.2 Stereoselective Synthesis of Planar Chiral *P,N* Ferrocenes and Aminoferrocenes.

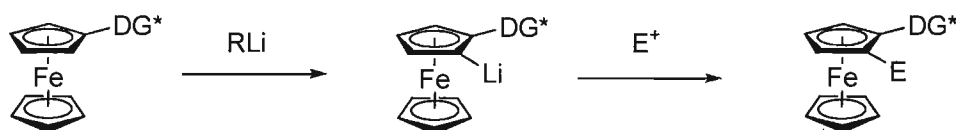
The three main strategies for obtaining enantiomerically enriched planar chiral ferrocenes are resolution of racemic 1,2-substituted ferrocenes, diastereoselective *ortho*-lithiation of 1-substituted ferrocenes containing an appropriate chiral *ortho*-directing

group and subsequent in situ trapping with an electrophile, and enantioselective lithiation with a chiral additive (Figure 31).⁹³ Resolution can either be accomplished by enzymatic kinetic resolution⁹⁴ (using for example lipase) or by non-enzymatic routes (such as using a chiral catalytic reaction like Sharpless asymmetric dihydroxylation or asymmetric ring closing metathesis.⁹⁵ In either case, the resolving species reacts preferentially with one enantiomer of the starting racemic mixture over the other, thereby providing one enantiomer in enriched form, with the other being converted to another separable species. In diastereoselective lithiation, an attached chiral directing group coordinates to the lithiating reagent, thereby differentiating the two prochiral *ortho* positions on the Cp ring.⁹⁶ In enantioselective lithiation, a chiral additive coordinates with an alkyl lithium to create a chiral lithiating species that differentiates the two prochiral *ortho* positions on the Cp ring.

resolution - enzymes or chiral catalysts

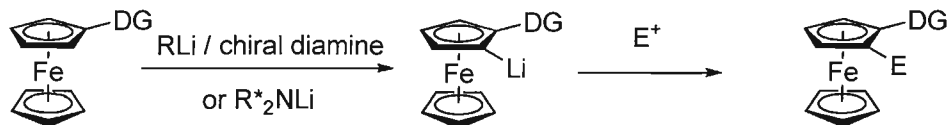


diastereoselective directed *ortho* metalation



optically pure

enantioselective directed *ortho* metalation

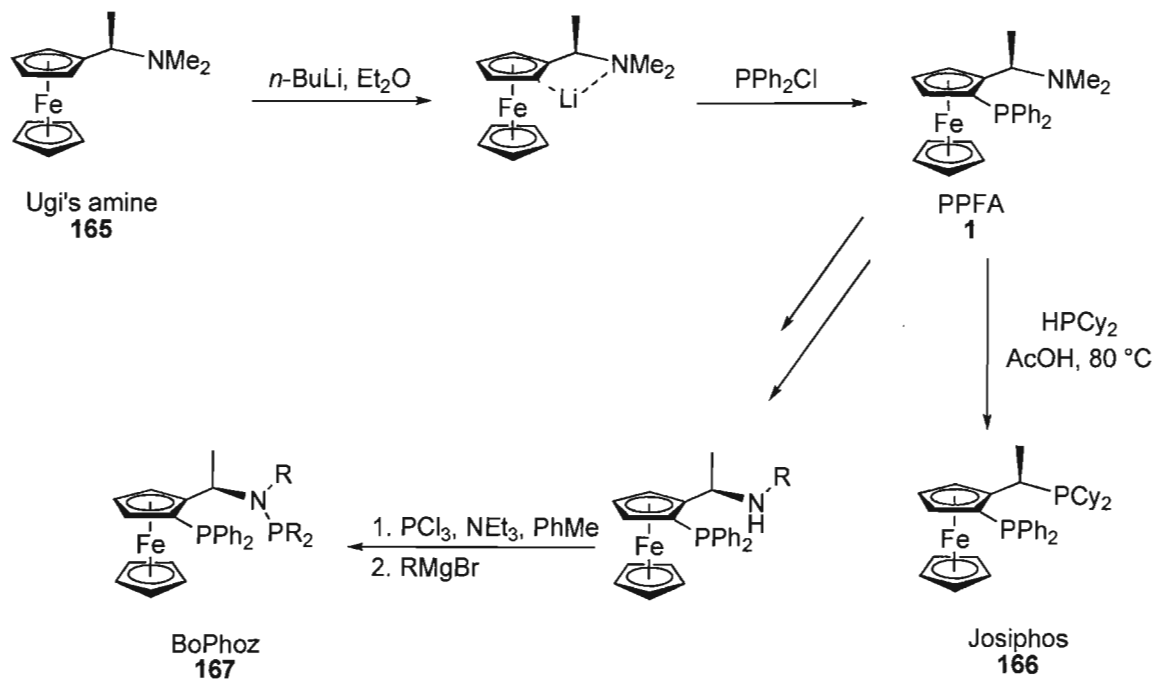


achiral

Figure 31. Strategies for synthesizing planar chiral ferrocene compounds.

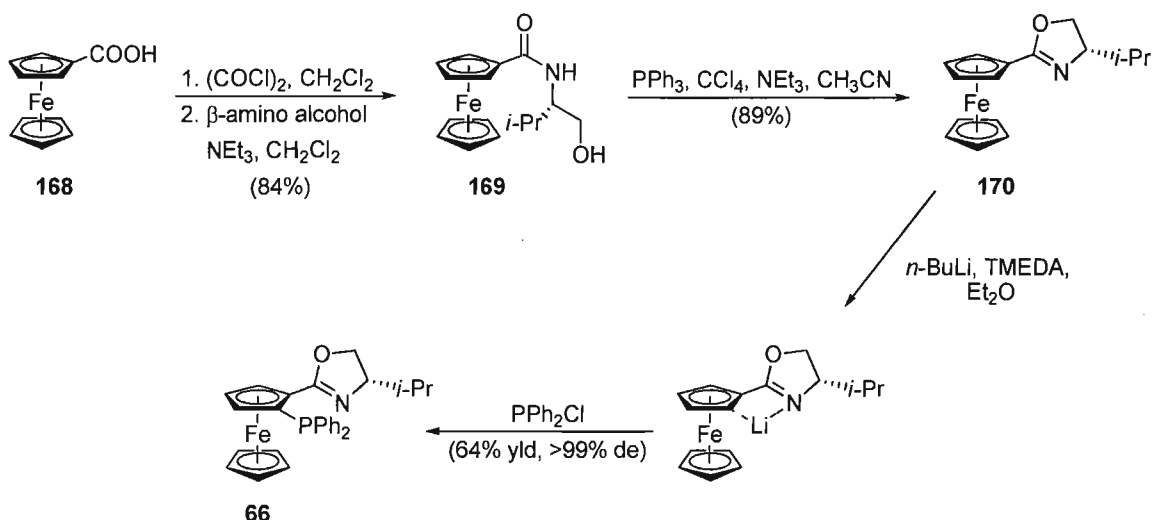
Compounds prepared from diastereoselective lithiation of Ugi's amine⁹⁷ (**165**, Scheme 28) can undergo further stereoselective S_N1 type reactions of the dimethylamino moiety with different nucleophiles while retaining the set configuration. For example, the early *P,N* ligand PPFA (**1**) was prepared by the reaction of the lithiated intermediate of Ugi's amine with chlorodiphenylphosphine (Scheme 28).⁹⁷ Josiphos (**166**, 1-(dicyclohexylphosphino)ethyl-2-(diphenylphosphino)ferrocene) was synthesized by S_N1 type reaction of the dimethylamino group from Ugi's amine with secondary phosphines.⁹⁸ Additionally, BoPhoz type ligands (**167**) are prepared by reaction of the 2-phosphino

derived secondary amine with $\text{PCl}_3/\text{NEt}_3$ followed by Grignard reaction to form phosphine-aminophosphines (Scheme 28).⁹⁹



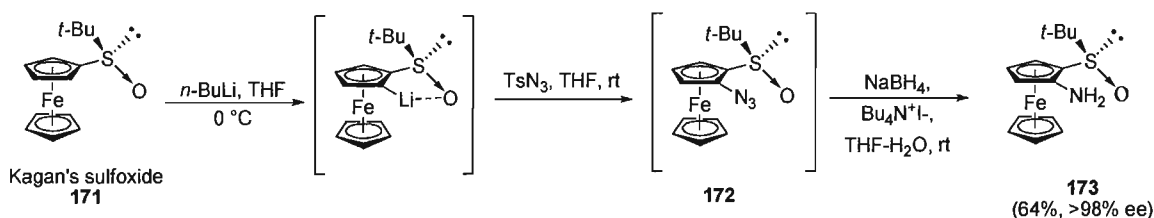
Scheme 28. Ligands derived from Ugi's amine.

Chiral oxazoline directing groups¹⁰⁰ provide the added advantage of being used directly as ligands (i.e. no need to remove / transform the group). Enantiopure ferrocenyl oxazolines are easily prepared from ferrocenyl carboxylic acid or cyanide and optically pure amino alcohols.¹⁰¹ Ferrocenyl phosphinooxazoline (Fc-PHOX) ligands were synthesized by diastereoselective *ortho*-lithiation / phosphorylation of chiral ferrocenyl oxazolines (Scheme 29).¹⁰²



Scheme 29. Synthesis of Fc-PHOX ligands via diastereoselective lithiation.

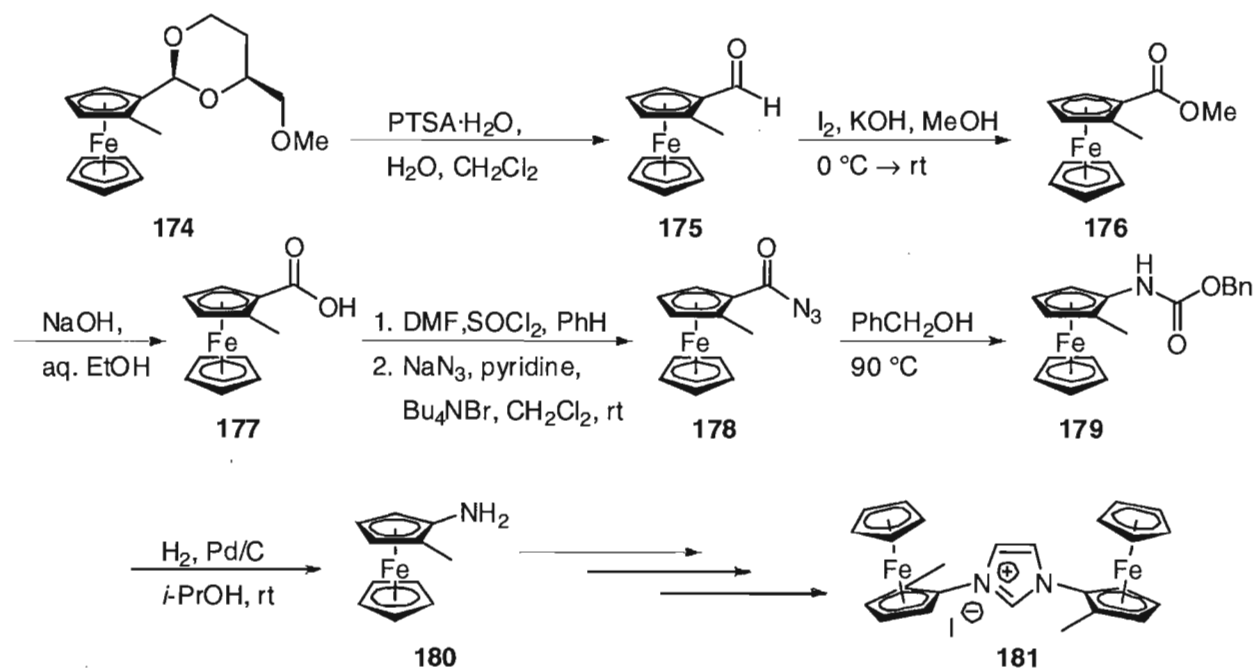
Compounds generated through Kagan's sulfoxide¹⁰³ route have also been used as ligands directly. For example, aminoferrocene **173**, a rare example of a directly bound amino group, was prepared from sulfoxide **171** (Scheme 30).¹⁰⁴



Scheme 30: Synthesis of aminoferrocene ligand **173** via diastereoselective lithiation of Kagan's sulfoxide.

Another example of a planar chiral aminoferrocene is the synthesis of an *N*-ferrocenyl-linked *N*-heterocyclic carbene (**181**) by Togni, *et al.* (Scheme 31).¹⁰⁵ This synthesis begins with the installation of the 1,2-stereochemistry via diastereoselective *ortho*-lithiation using the acetal directing group.¹⁰⁶ Several steps must then be taken to

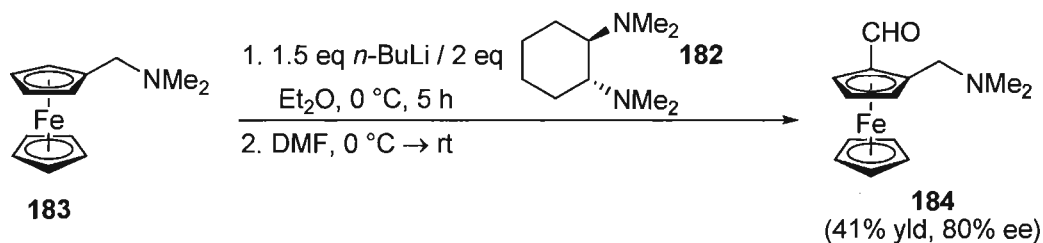
remove the acetal and install the nitrogen-ferrocene bond via a Curtius rearrangement of a ketyl azide (**178** → **179**). Togni states that a major challenge in the synthesis of the ferrocenyl imidazolium ligand was the generation of the nitrogen ferrocene bond.¹⁰⁵



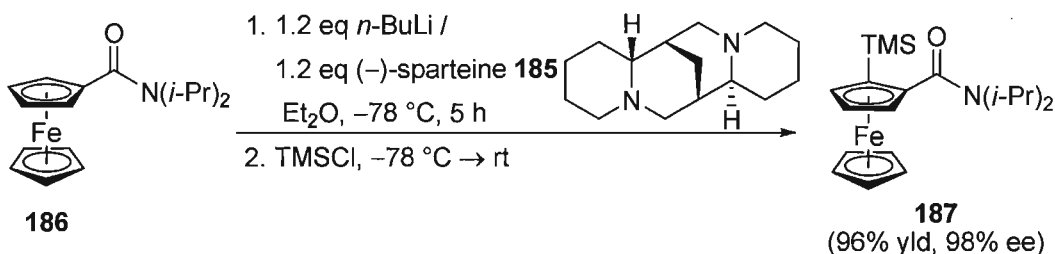
Scheme 31. Togni's synthesis of a substituted aminoferrocene.

Use of an external source of chirality for enantioselective *ortho*-lithiation on prochiral ferrocenes without a chiral directing group would provide solely planar chiral ferrocene derivatives. This approach was investigated by Uemura *et al.* who prepared 2-substituted *N,N*-(dimethylamino)methylferrocenes via *ortho*-lithiation of **183** in the presence of TMEDA (**182**). The best results were obtained with *n*-BuLi (1.5 eq) at 0 °C with 2 eq. of TMEDA, providing products in up to 80% ee (Scheme 32).¹⁰⁷ Snieckus performed enantioselective lithiation of ferrocenyl carboxamides (**186**) in the presence of

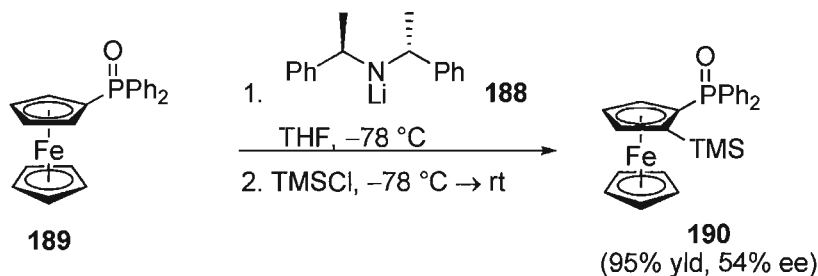
(-)-sparteine (**185**), obtaining products ranging from 81% to up to 99% ee (Scheme 33).¹⁰⁸ Simpkins also accomplished enantioselective lithiation, this time using a chiral lithium amide analogue (**188**), starting from ferrocenyl diphosphine oxides (**189**), providing products in up to 54% ee (Scheme 34).¹⁰⁹



Scheme 32. Enantioselective synthesis of 1,2-substituted ferrocenes in the presence of TMCD.

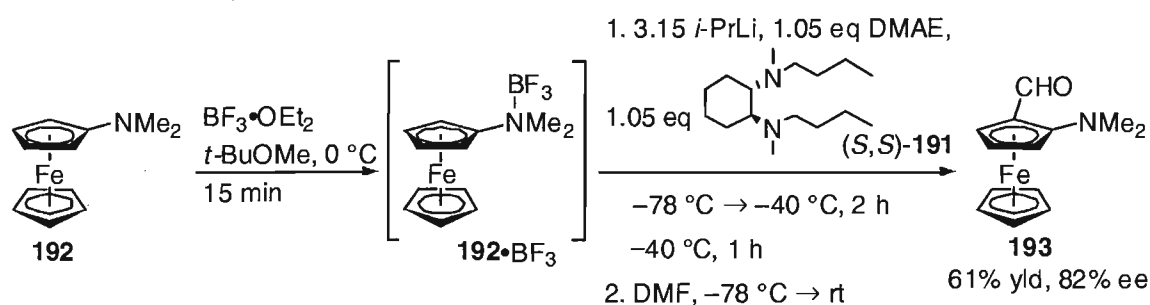


Scheme 33. Enantioselective synthesis of 1,2-substituted ferrocenes in the presence of (-)-sparteine.



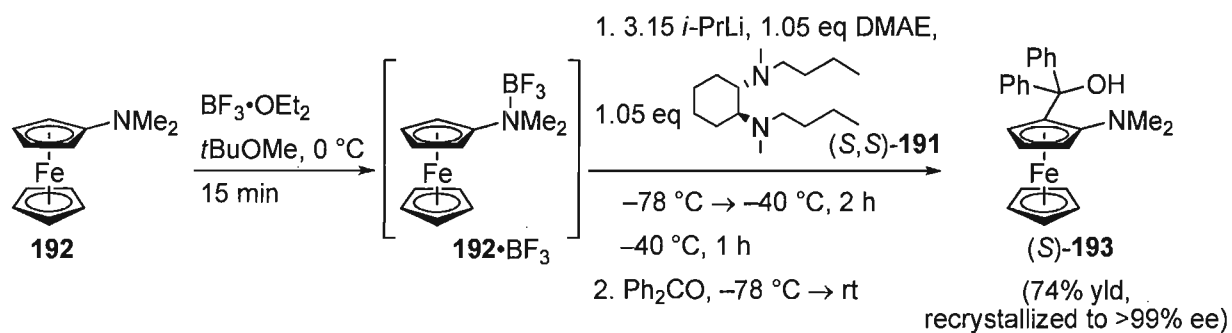
Scheme 34. Enantioselective synthesis of 1,2-substituted ferrocenes in the presence of chiral LDA derivative.

A complementary method has been developed by the Metallinos group that allows for the direct synthesis of 1,2-substituted aminoferrocenes with the amino group directly attached to the cyclopentadienyl ring, a class of ligands that has yet to be explored fully in catalysis.^{110,111,112} Thus, the Metallinos procedure starts with the nitrogen-ferrocene bond in place (**192**) and installs the 1,2-substitution via an enantioselective lithiation of boron trifluoride-complexed tertiary aminoferrocenes. Optimal results were obtained in *t*-BuOMe at $-78\text{ }^{\circ}\text{C}$ using 2.1 eq *i*-PrLi with bulkyl cyclohexyldiamine derivatives (such as (*S,S*)-**191**). A wide variety of electrophiles could be installed in good yields and enantioselectivities up to 82% (Scheme 35).¹¹³



Scheme 35. Enantioselective synthesis of 1,2-substituted ferrocenes by BF_3 -activated lithiation with chiral diamine ligand.

The stereochemistry of the lithiation was verified with the crystal structure of alcohol (*S*)-**192** (Figure 32), which was prepared with (*S,S*)-diamine ligand **191** (Scheme 36) and recrystallized to enantiomeric purity in one crystallization from diethyl ether.¹¹² The X-ray confirmed that the pro-*S* hydrogen (Figure 33) was removed during lithiation.



Scheme 36. Synthesis of alcohol (S)-**193** with (S,S)-diamine ligand **191**.

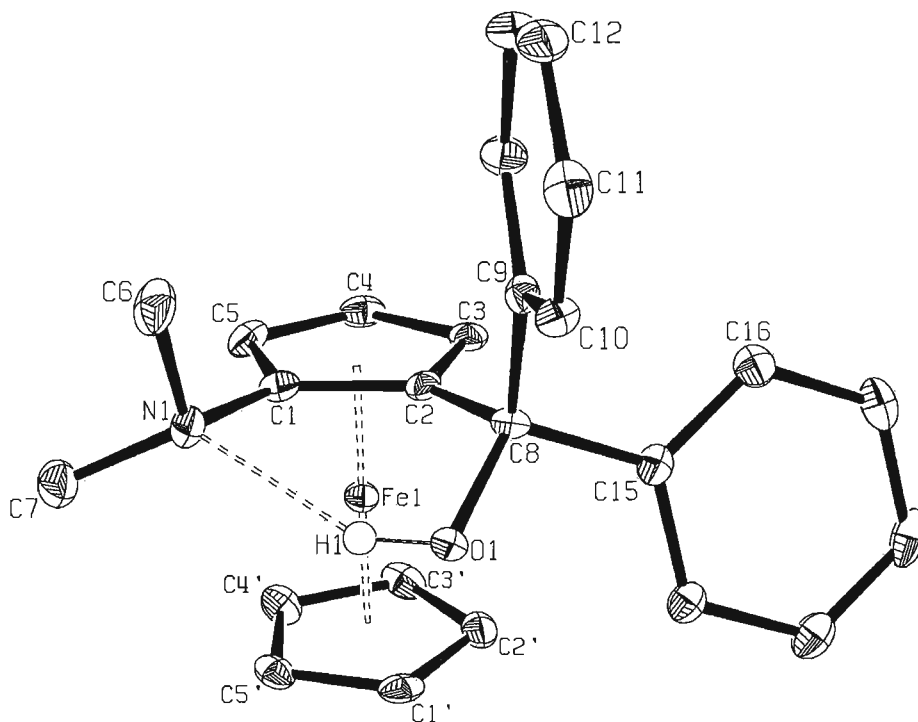


Figure 32. ORTEP plot of alcohol (S)-**193** at 50% probability; all H atoms except H1 are omitted for clarity.

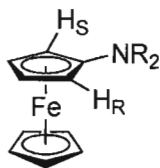
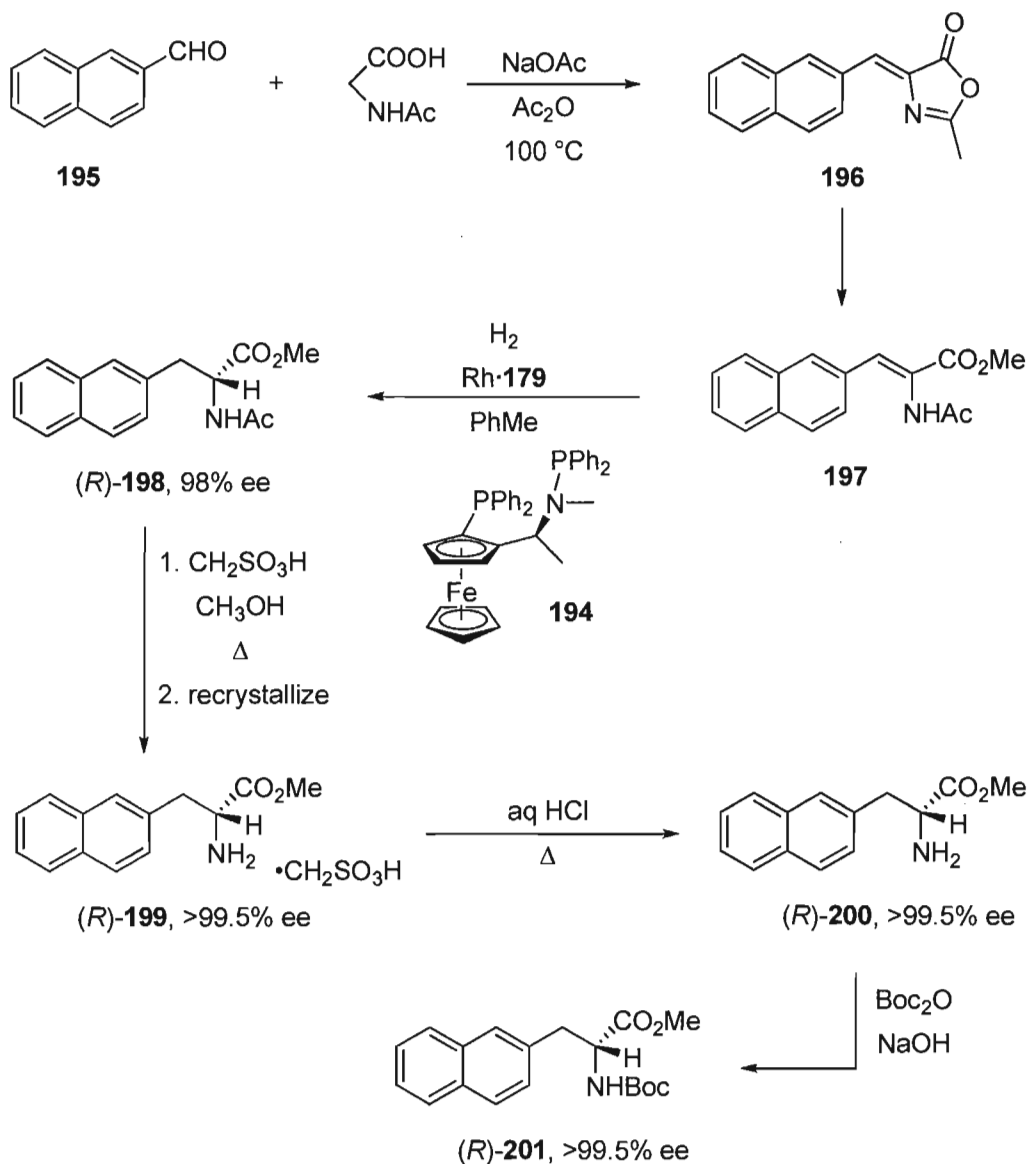


Figure 33. Pro-*R* and Pro-*S* *ortho* protons of aminoferrocenes.

With this new method for synthesizing planar chiral 1,2-substituted aminoferrocenes available, the potential to investigate 1,2-substituted aminoferrocene compounds as ligands in asymmetric transformations is possible.

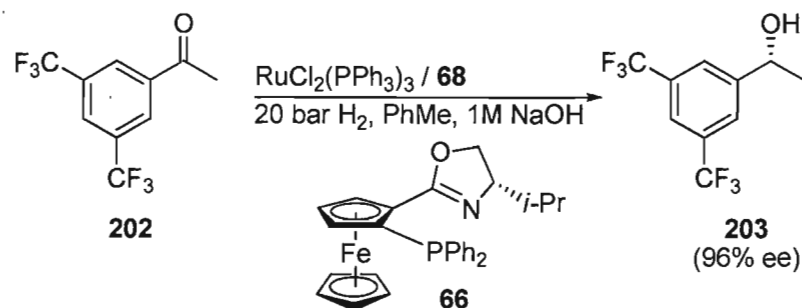
1.4.3 Applications of Planar Chiral *P,N* Ferrocene Ligands.

The applications of planar chiral ferrocenes are of interest to both academia and industry.¹¹⁴ For example, the largest scale enantioselective catalytic process in industry is the synthesis of a precursor to the herbicide (*S*)-metolachlor by an Xyliphos (ferrocenyl *P,P* ligand) Ir-catalyzed asymmetric imine hydrogenation (see Scheme 24, Section 1.3).⁵³ Another industrial example is the synthesis of non-natural α -amino acids on a multikilogram scale using a Rh-catalyzed asymmetric hydrogenation with methyl-BoPhoz **194** (ferrocenyl *P,P* ligand) to make (*R*)-2-naphthylalanine (**200**) and (*R*)-*N*-tert-butoxycarbonyl-2-naphthylalanine (**201**) with a S/C ratio of 2000 and enantiopurity of greater than 99.5% (Scheme 37).¹¹⁵



Scheme 37. Rh-catalyzed asymmetric hydrogenation with methyl-BoPhoz.

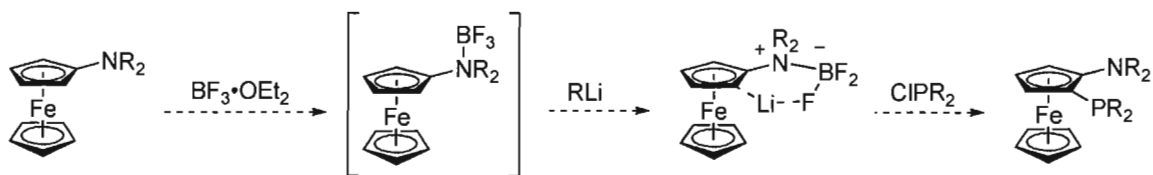
The first industrial catalytic process with a ferrocenyl oxazoline (*P,N*) ligand was the ruthenium catalyzed hydrogenation of 3,5-bis(trifluoromethyl)acetophenone (**202**) on a 140 kg scale (4000 L reactor) with S/C ratio of 20,000 giving a TOF of 1660 h⁻¹ and the product (**203**) in 96% ee in full conversion after 15 hours (Scheme 38).¹¹⁶



Scheme 38. Ru-catalyzed hydrogenation with ferrocenyl phosphinooxazoline ligand.

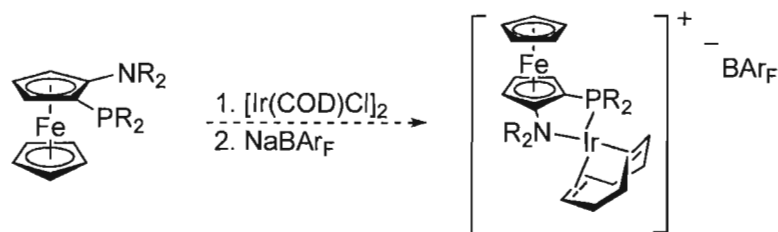
1.5 Aims and Objectives.

As seen in the introduction, *P,N*-donor ligands are predominant in asymmetric iridium catalyzed hydrogenation reactions. Despite this, sp^3 -hybridized amine donor groups are relatively uncommon structural features of such ligands, which normally have sp^2 -hybridized nitrogen donors. In addition, in ferrocene ligands, the *N* donor is usually part of a pendant group, not directly attached to the Cp ring. Moreover, ligands with exclusively planar chirality have also not been investigated to their full potential. The objective of this thesis project is to assess the catalytic activity of planar chiral 2-phosphino-1-aminoferrocene ligands in iridium catalyzed hydrogenation reactions. This type of ligand has been poorly investigated in catalytic applications in the past because of a lack of convenient synthetic methods to prepare them. In response to this problem, the ligands to be investigated are to be prepared using the Metallinos method, wherein BF_3 -activated tertiary aminoferrocenes undergo asymmetric lithiation in the presence of chiral diamine ligands and the phosphorus group installed by addition of a chlorophosphine to the lithiated intermediate (Scheme 39).

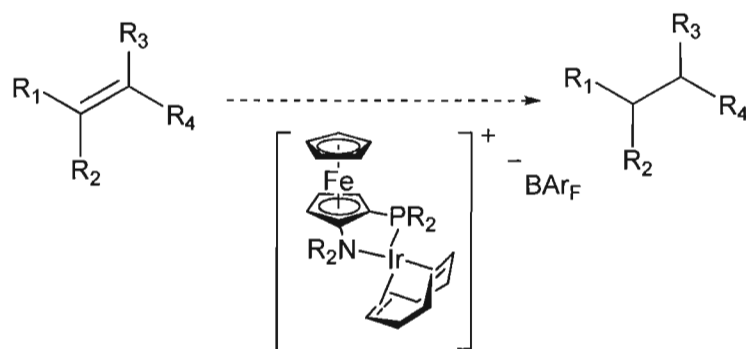


Scheme 39. Proposed preparation of ferrocenyl aminophosphine ligands.

Coordination chemistry of ligands of this series with Ir(I) will be investigated (Scheme 40) via formation of cationic iridium complexes with chloride or BAr_F counterions. Assessment of the catalytic activity of these complexes in iridium-catalyzed hydrogenations (Scheme 41), as well as the asymmetric induction that these ligands impart, will be carried out. Various prochiral alkenes will be prepared and hydrogenated using the enantioenriched catalysts to test the scope of activity and selectivity.



Scheme 40. Proposed preparation of iridium complex with ferrocenyl aminophosphine ligands.



Scheme 41. Proposed hydrogenation of alkenes with iridium complex.

Finally, variation of substituents on the ligand will be carried out in order to optimize enantioselectivity. For example, the phenyl substituent on the phosphorus donor atom may be altered to *ortho*-tolyl or cyclohexyl to establish the steric and electronic influences of the phosphorus donor on catalysis. Substituents on the nitrogen donor atom may be varied from a dimethylamino group to pyrrolidine to determine the steric influence of the nitrogen moiety on catalysis (Figure 34).

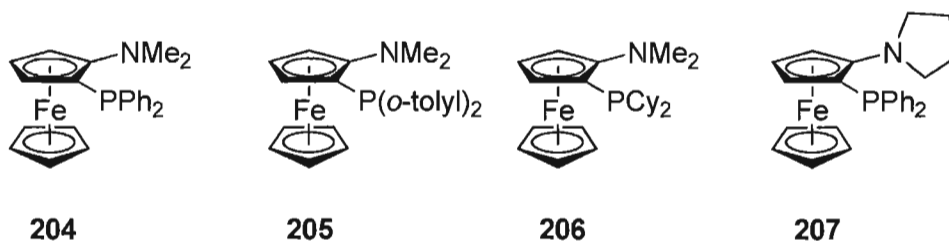
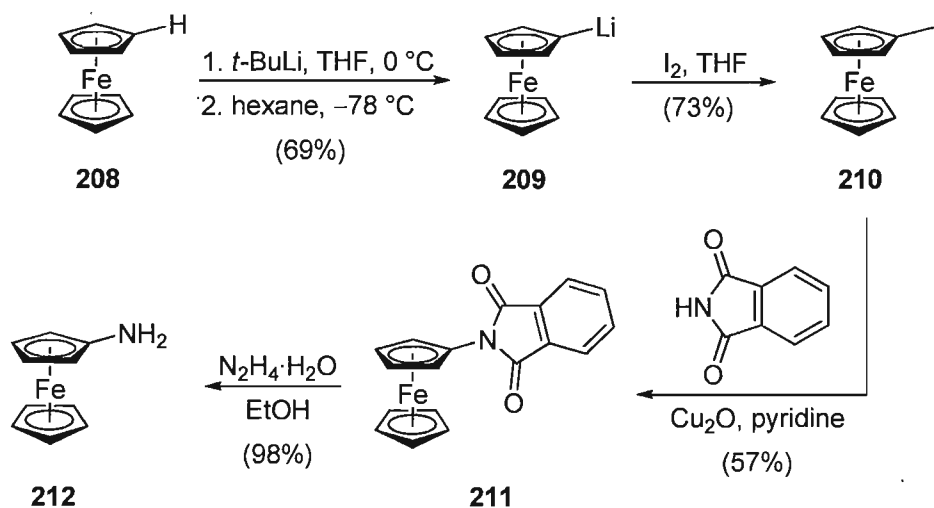


Figure 34. Proposed variations of 2-phosphino-1-aminoferrocene ligand.

Chapter 2: Results and Discussion

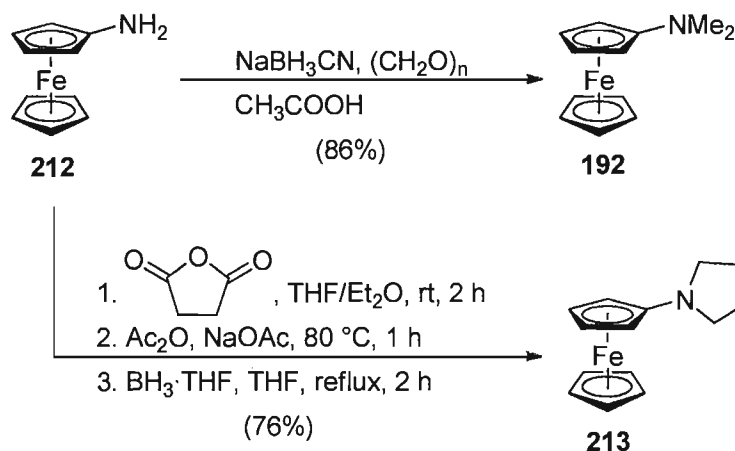
2.1 Synthesis of Aminoferrocenes.

To investigate the potential of planar chiral 2-phosphino-1-aminoferrocenes in catalysis, two different tertiary amine starting materials, *N,N*-dimethylaminoferrocene (**192**) and *N*-ferrocenyl pyrrolidine (**213**), were prepared from aminoferrocene (**212**). Aminoferrocene was prepared according to literature procedures (Scheme 42).¹¹⁷ To this end, lithioferrocene (**209**) was prepared by reacting ferrocene (**208**) with *tert*-butyllithium in THF at 0 °C. Solid lithioferrocene was isolated in 68% yield as a pyrophoric orange powder by precipitation with hexane at -78 °C and collection in a Schlenk filtration apparatus. Lithium-halogen exchange of lithioferrocene with iodine gave iodoferrocene (**210**) as a yellow-orange semi-solid in 73% yield. Copper-mediated cross coupling of iodoferrocene with phthalimide provided *N*-ferrocenyl phthalimide (**211**) in 57% yield.^{117a,b} This intermediate was recrystallized to give deep red needles and stored until needed. Hydrolysis of **211** with hydrazine gave aminoferrocene (**212**) in 98% yield, 28% overall yield from commercially available ferrocene.



Scheme 42. Aminoferrocene preparation.

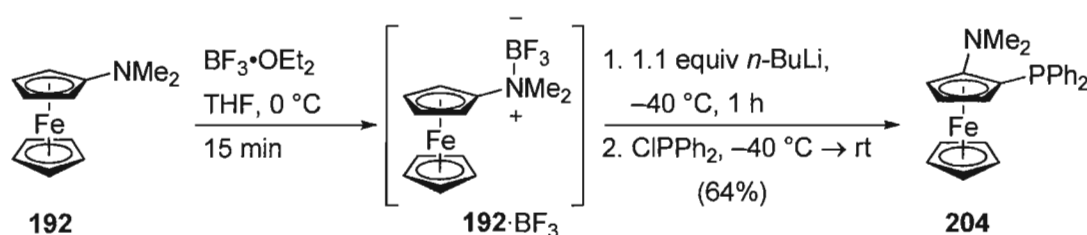
From aminoferrocene, both tertiary aminoferrocenes were prepared in good yields (Scheme 43). Reductive amination of aminoferrocene with paraformaldehyde using sodium cyanoborohydride in acetic acid was used to prepare dimethylaminoferrocene (**192**) in 86% yield. Alternatively, reaction of aminoferrocene with succinic anhydride followed by reduction with borane provided *N*-ferrocenylpyrrolidine (**213**) in 76% yield over 3 steps.



Scheme 43. Preparation of tertiary aminoferrocenes **192** and **213**.

2.2 2-Phosphino-1-aminoferrocene Ligand Synthesis.

The investigation of 2-phosphino-1-aminoferrocene ligands in catalysis was initiated with racemic 2-diphenylphosphino-1-dimethylaminoferrocene **204**. This ligand was prepared using the Metallinos BF_3 -activated lithiation method (Scheme 44).¹¹⁰ Treatment of a THF solution of dimethylaminoferrocene (**192**) with BF_3 etherate resulted in a colour change from orange to yellow with precipitation of a yellow solid, attributed to the formation of the Lewis acid-base complex **192**· BF_3 . Treatment of a stirred solution of **192**· BF_3 with *n*-BuLi at $-40\text{ }^\circ\text{C}$ resulted in a rapid colour change to orange. After 1 hour of stirring, a red-orange homogenous solution had formed, attributed to the formation of the 2-lithioferrocene species. Addition of chlorodiphenylphosphine electrophile to the intermediate carbanionic intermediate also resulted in a colour change to yellow-orange. At this point, the reaction mixture was allowed to warm from $-40\text{ }^\circ\text{C}$ to room temperature over approximately 4 hours. After workup, the product was filtered through a plug of silica and recrystallized from ether to give racemic 2-diphenylphosphino-1-dimethylaminoferrocene (**204**) as orange crystals in 64% yield.



Scheme 44. Synthesis of racemic ligand **204**.

The Metallinos group had previously shown that palladium complexes of this ligand were catalytically active in reactions such as Suzuki-Miyaura cross coupling and Buchwald-Hartwig aminations of aryl halides (Table 7, 8).¹¹¹ Moreover, crystal structures of square planar Pd(II) and Pt(II) complexes of **204** were obtained that indicated *cis*-bidentate coordination of the ligand and near orthogonal bite angles. With these results in mind, the investigation of iridium complexes of this ligand and their potential activity in hydrogenation of alkenes was carried out.

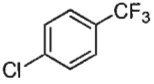
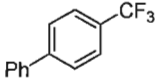
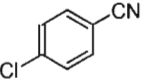
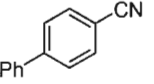
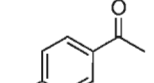
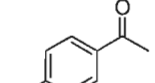
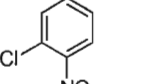
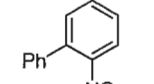
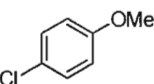
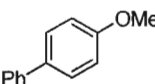
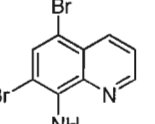
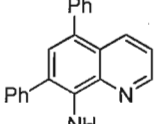
$\text{PhB(OH)}_2 \text{ (214)} + \text{ArX (215)} \xrightarrow[\text{3 equiv. CsF, dioxane, reflux}]{\text{2 mol \% Pd(OAc)}_2, \text{4 mol \% 204}}$			Ph-Ar (216)		
ArX 215	Ph-Ar 216	Yield (%)	ArX 215	Ph-Ar 216	Yield (%)
a 		94	d 		92
b 		88	e 		73
c 		70	f 		88

Table 7. Pd-catalyzed Suzuki-Miyaura cross coupling (reproduced from ref 111)

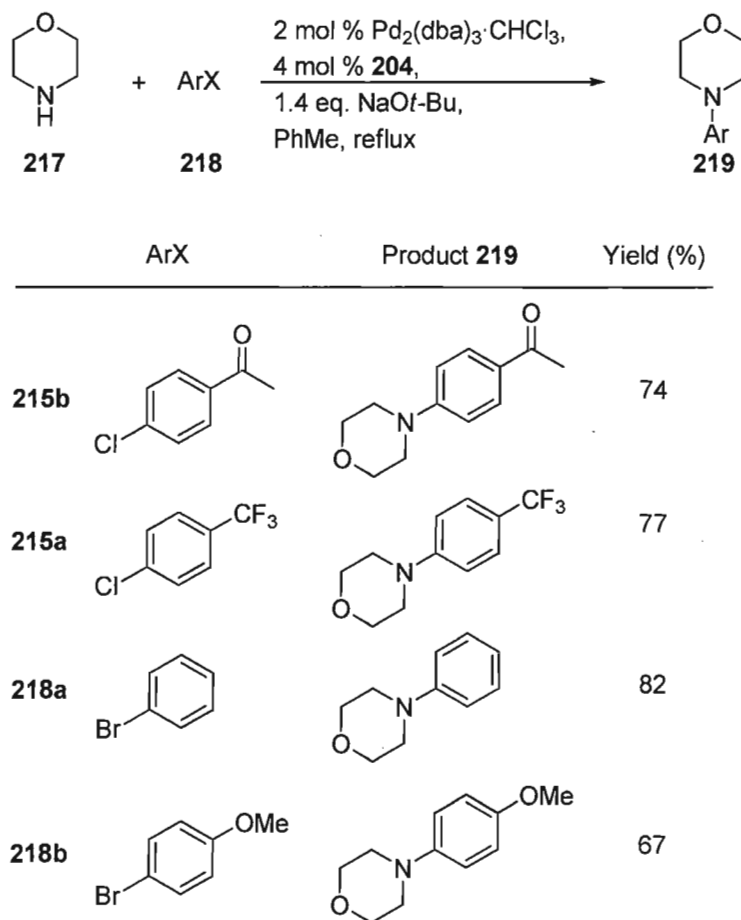
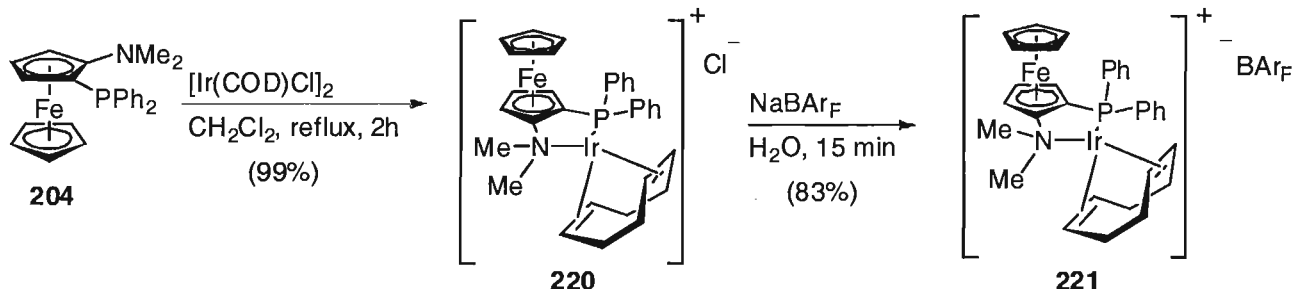


Table 8. Pd-catalyzed Buchwald-Hartwig aminations (reproduced from ref 111).

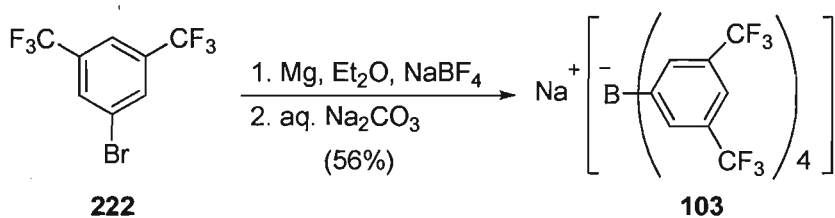
2.3 Synthesis of Iridium Complexes.

Reaction of racemic **204** with iridium cyclooctadiene chloride dimer in CH_2Cl_2 at reflux gave cationic iridium(I) complex **220**, isolated as the chloride salt in 99% yield. This complex was converted to BAr_F salt **221** by anion exchange (Scheme 45), isolated as an air stable orange solid in 83% yield. For this purpose, sodium tetrakis[3,5-bis(trifluoromethyl)phenyl] borate (NaBAr_F , **103**, Scheme 46) was prepared by Grignard reaction of 3,5-bis(trifluoromethyl)phenyl magnesium bromide with sodium

tetrafluoroborate because of its exorbitant commercial price.¹¹⁸ Complex **221** could be recrystallized as orange needles from benzene.¹¹¹



Scheme 45. Synthesis of iridium BARF complex **221** from ligand **204**.



Scheme 46. Synthesis of NaBARF .

With complex **221** in hand, bidentate coordination of the ligand to iridium was established by NMR spectroscopy. The ^{31}P NMR spectrum of the free ligand showed a peak at -20.4 ppm. Coordination of phosphorus was inferred by the downfield shift of this signal to 15.0 ppm (Figure 35). In addition, the ^1H NMR spectrum of the free ligand showed a singlet at 2.69 ppm for the two methyl groups on nitrogen. Simultaneous coordination of the phosphorus and nitrogen moieties to iridium would render the methyl groups diastereotopic giving two signals. This was observed in the ^1H NMR spectrum (Figure 36) of the complex, with aminomethyl signals at 3.13 and 2.69 ppm.

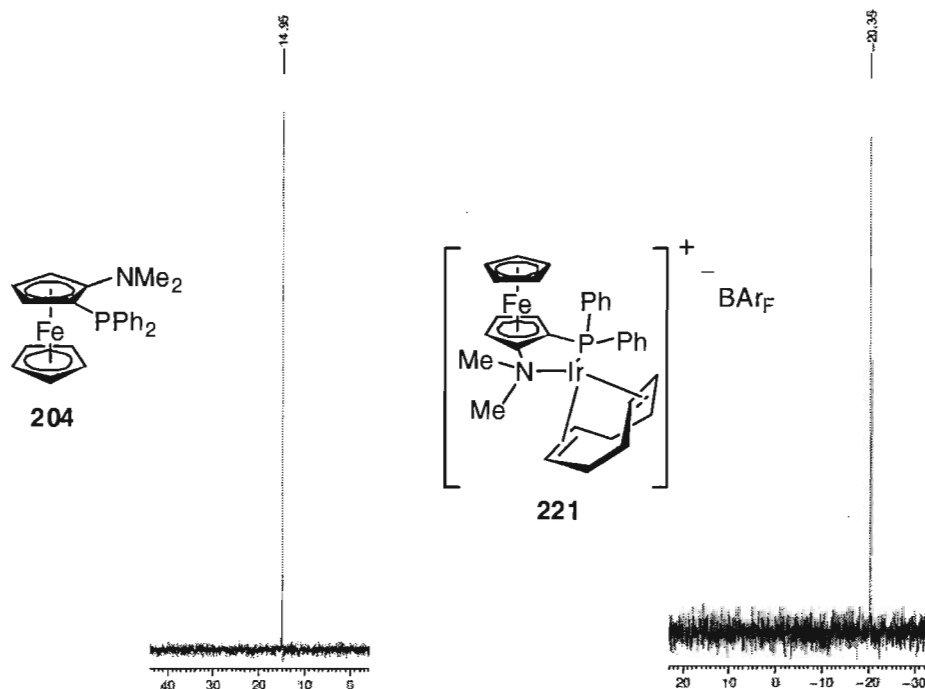


Figure 35. ^{31}P NMR spectra of the free ligand **204** and iridium complex **221**.

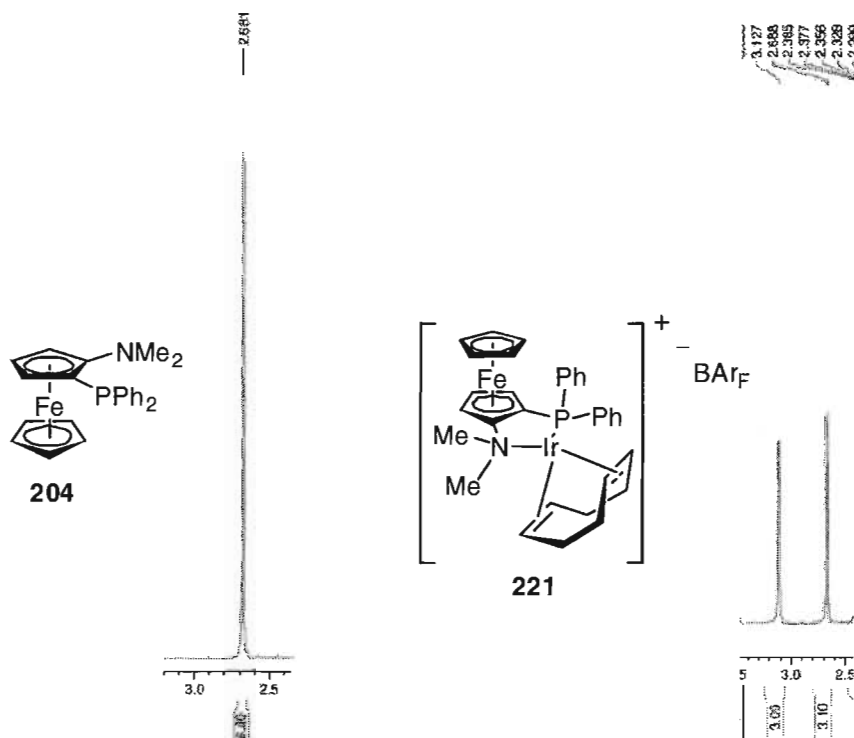


Figure 36. ^1H NMR spectra of NMe_2 group in free ligand **204** and iridium complex **221**.

Sufficient quality crystals of complex **221** were grown from benzene and an X-ray structure was obtained, clearly showing bidentate coordination of the ligand to Ir(COD) (Figure 37). The crystals packed in the triclinic space group $P\bar{1}$. The heteroatom-metal bond distances were 2.225(3) Å for N1-Ir1 and 2.2951(9) Å for P1-Ir1, resulting in a ligand bite angle (N1-Ir1-P1) of 82.84(8)°. This was slightly lower than previous Pd and Pt complexes [87.87(6)° and 88.78(5)° respectively]¹¹¹, and similar to Pfaltz's PHOX complex with ligand **50c** (N-Ir-P angle of 84.96°)⁶⁵. Unlike the Pd and Pt complexes, the iridium COD portion of the complex was bent out of the plane of the substituted Cp ring of the ligand due to the steric demands of COD. This spacial preference brought the COD ligand in close contact with the protons of the unsubstituted Cp' ring (H1'-H26B distance = 2.68(1) Å; H2'-H26B distance = 2.56(1) Å) causing a near eclipsed configuration of the cyclopentadienyl rings of the ferrocene moiety (H4-C4-C4'-H4' dihedral angle = 4.53(8)°). Similarly to Pfaltz's complex,⁶⁵ longer Ir-C distances for the C=C bond coordinated *trans* to the phosphine were observed. (Ir1-C20 2.173 Å; Ir1-C21 2.217 Å; Ir1-C24 2.148 Å; Ir1-C25 2.125 Å). In addition, the pseudoequatorial phenyl group on phosphorus (C6-C11) pointed away from the unsubstituted Cp' ring in the preferred conformation of the chelate ring. Another interesting aspect of the crystal structure is the large distance between the cation and the BAr_F counterion, as can be seen in the packing diagram (Figure 38).

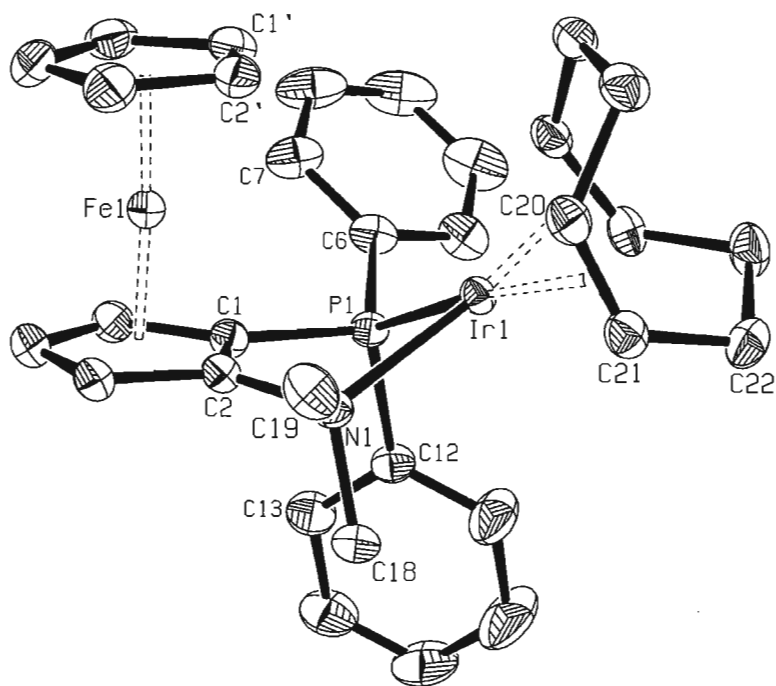


Figure 37. ORTEP plot of Ir complex **221** at 50% probability; all H atoms and the BArF₄⁻ counterion have been omitted for clarity.

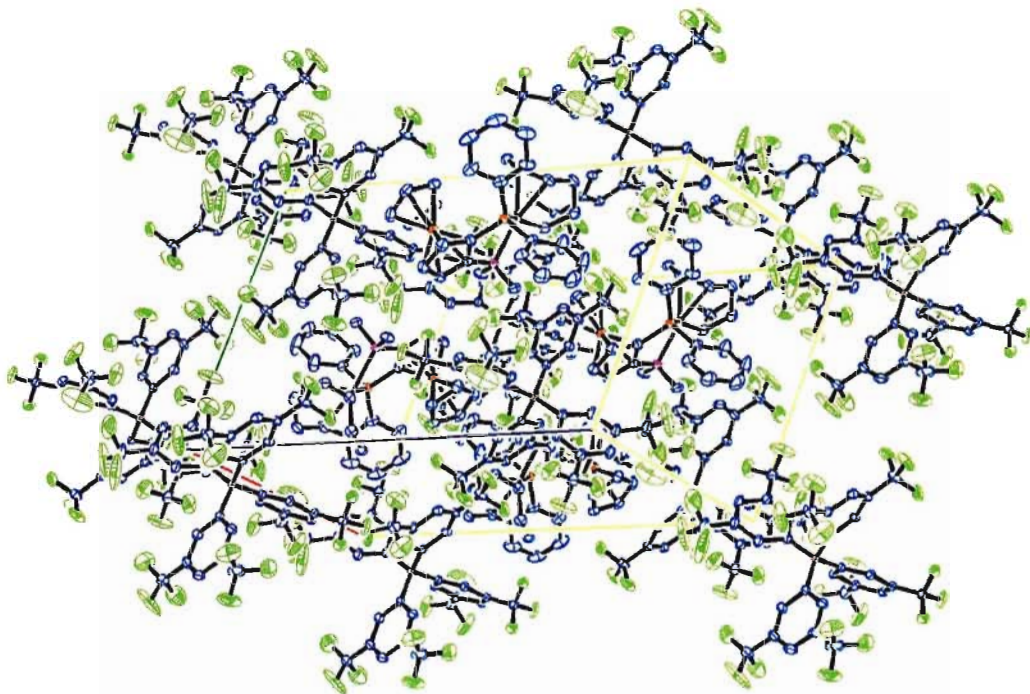
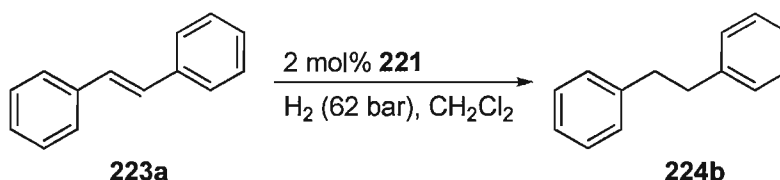


Figure 38. ORTEP plot of crystal packing of Ir complex **221** at 50% probability; all H atoms have been omitted for clarity.

2.4 Hydrogenation of Alkenes with Racemic Iridium(COD) Complex **221**.

Initial studies focused on the potential of catalyst **221** in hydrogenation of several prochiral and non-prochiral alkenes.¹¹¹ Hydrogenation of the common test alkene 1,2-diphenylethene (*trans*-stilbene, **223a**) was performed. Not surprisingly, the chloride complex (**220**) was found to be inactive in hydrogenation of this substrate, as was the complex with tetraphenylborate counterion. However, the BAr_F complex (**221**) gave full conversion of **223a** after 72 hours at 62 bar H₂ in CH₂Cl₂ at room temperature (Scheme 47), and **224a** could be isolated pure in 97% yield. A diverse array of alkenes could be hydrogenated in full conversion and with excellent isolated yields (Table 9) including 1,2-disubstituted alkenes such as α,β -unsaturated esters and ketones (**223b**, **223c**), cyclic enones such as cyclohexenone (**223d**) and maleimide (**223e**), and exocyclic alkenes (**223f**).

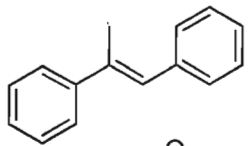
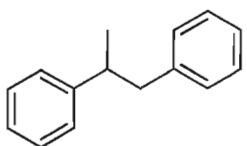
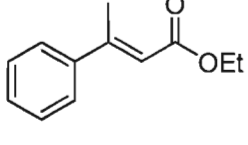
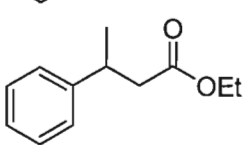
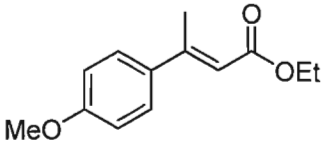
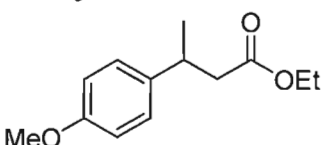
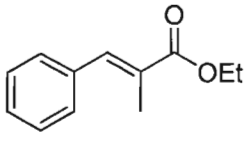
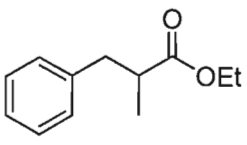
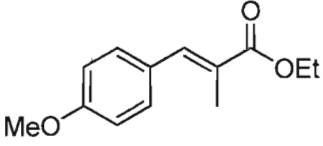
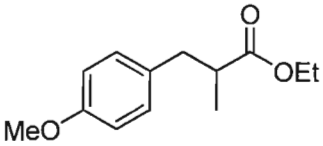
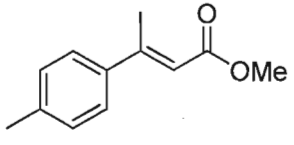
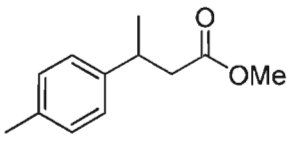
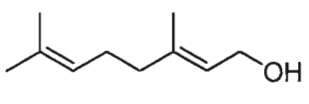
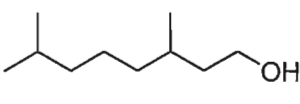
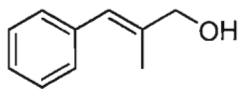
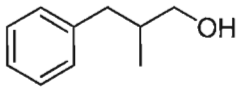
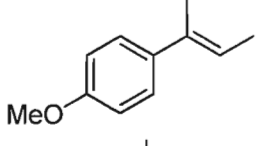
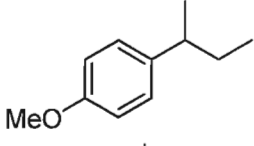
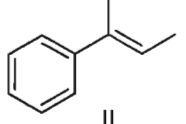
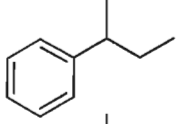
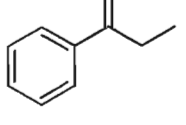
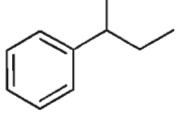


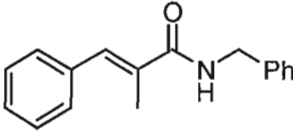
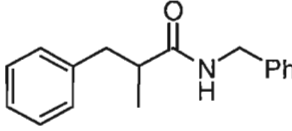
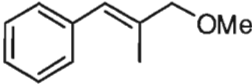
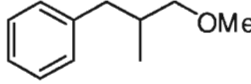
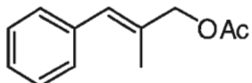
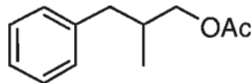
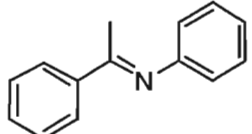
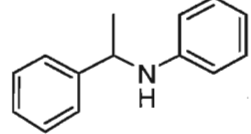
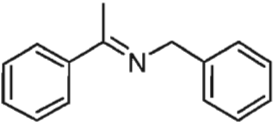
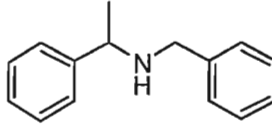
Scheme 47. Hydrogenation of stilbene.

	Alkene (223)	Product (224)	Isolated Yield
223a		224a	97 %
223b		224b	95 %
223c		224c	99 %
223d		224d	84 %
223e		224e	82 %
223f		224f	96 %

Table 9. Iridium catalyzed hydrogenation of disubstituted alkenes.

A number of prochiral trisubstituted alkenes were then investigated (Table 10), and many types of alkenes were hydrogenated in full conversion and with excellent isolated yields.¹¹¹ These included methyl stilbene (**124**), α,β -unsaturated esters (**128**, **225a-d**), allylic alcohols (**225e,f**), aryl-alkyl alkenes (**125**, **225g,h**), α,β -unsaturated amide (**225i**), allylic ether (**225j**) and acetate (**225k**), as well as imines (**225l,m**).

	Alkene		Product	Isolated Yield (%)
124		124a		99
128		128a		94
225a		226a		96
225b		226b		92
225c		226c		98
225d		226d		94
225e		226e		98
225f		226f		96
125		125a		94
225g		226g		94
225h		226h		83

225i		226i		98
225j		226j		41 ^a
225k		226k		79
225l		226l		81
225m		226m		88

^a low yield due to volatility of alkane

Table 10. Racemic Ir-catalyzed hydrogenation of prochiral alkenes.

Strongly coordinating alkenes (**227a,b**), enamines (**227c**), oximes (**227d,e,f**), cyclic dienamines (**227i**) and cyclic α,β -unsaturated esters (**227j,k**) did not show any conversion with catalyst **221** (Figure 39). From these results it can be gleaned that alkenes that are too "electron rich" are not tolerated well (for example **227a, b**, or **c**) nor are substituted cyclic alkenes (for example **227g, j**, or **k**). Additionally, some substrates that were attempted did not undergo complete hydrogenation (Figure 40). In some cases however, this reactivity could be increased by using higher pressures of H₂ and/or using additives such as NEt₃ or Hünig's base (for example, chromone **227m** and isoflavone **227n**, and the α,β -unsaturated acids **227v-x**).

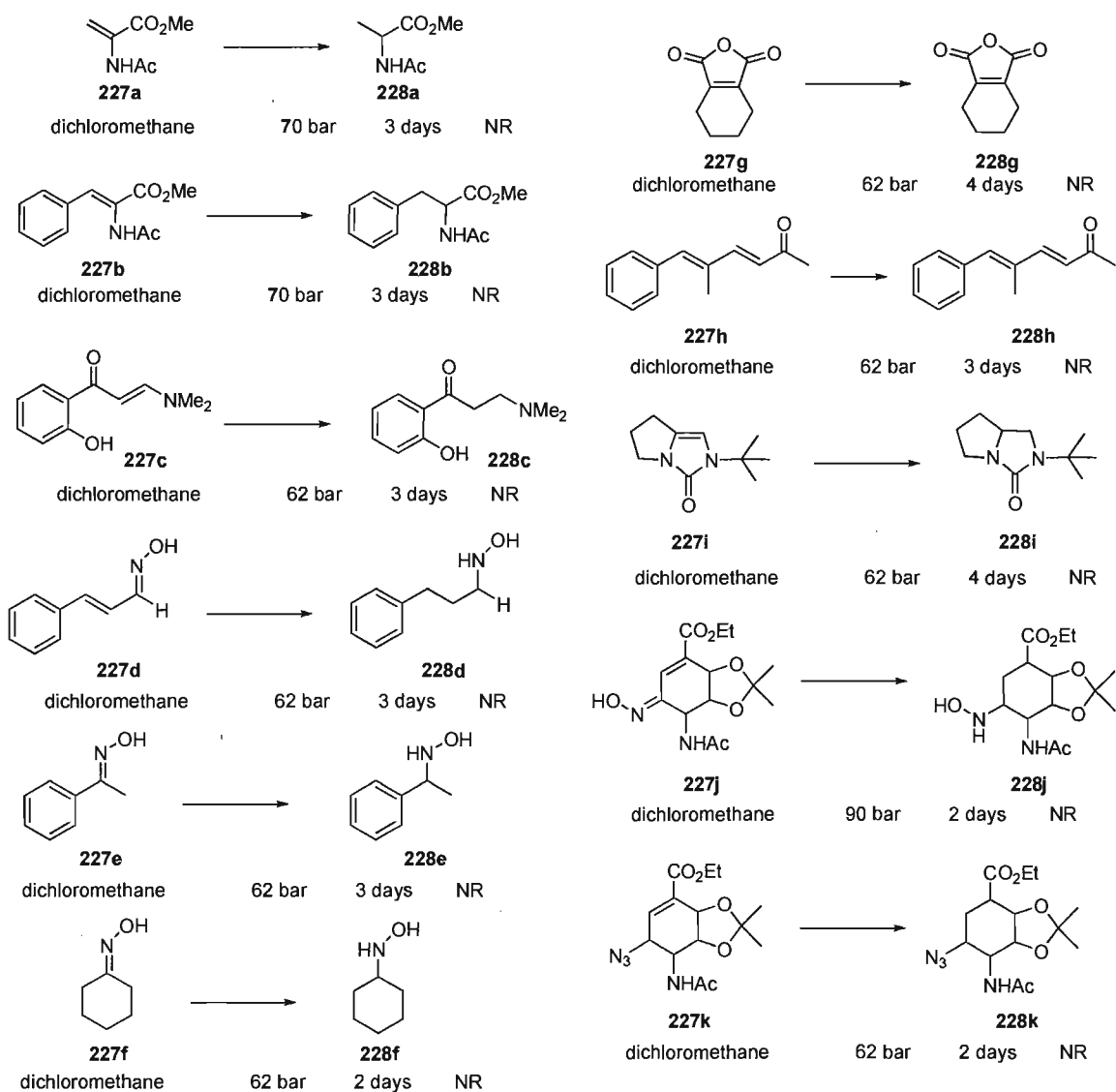


Figure 39. Attempted hydrogenation reactions with no conversion.

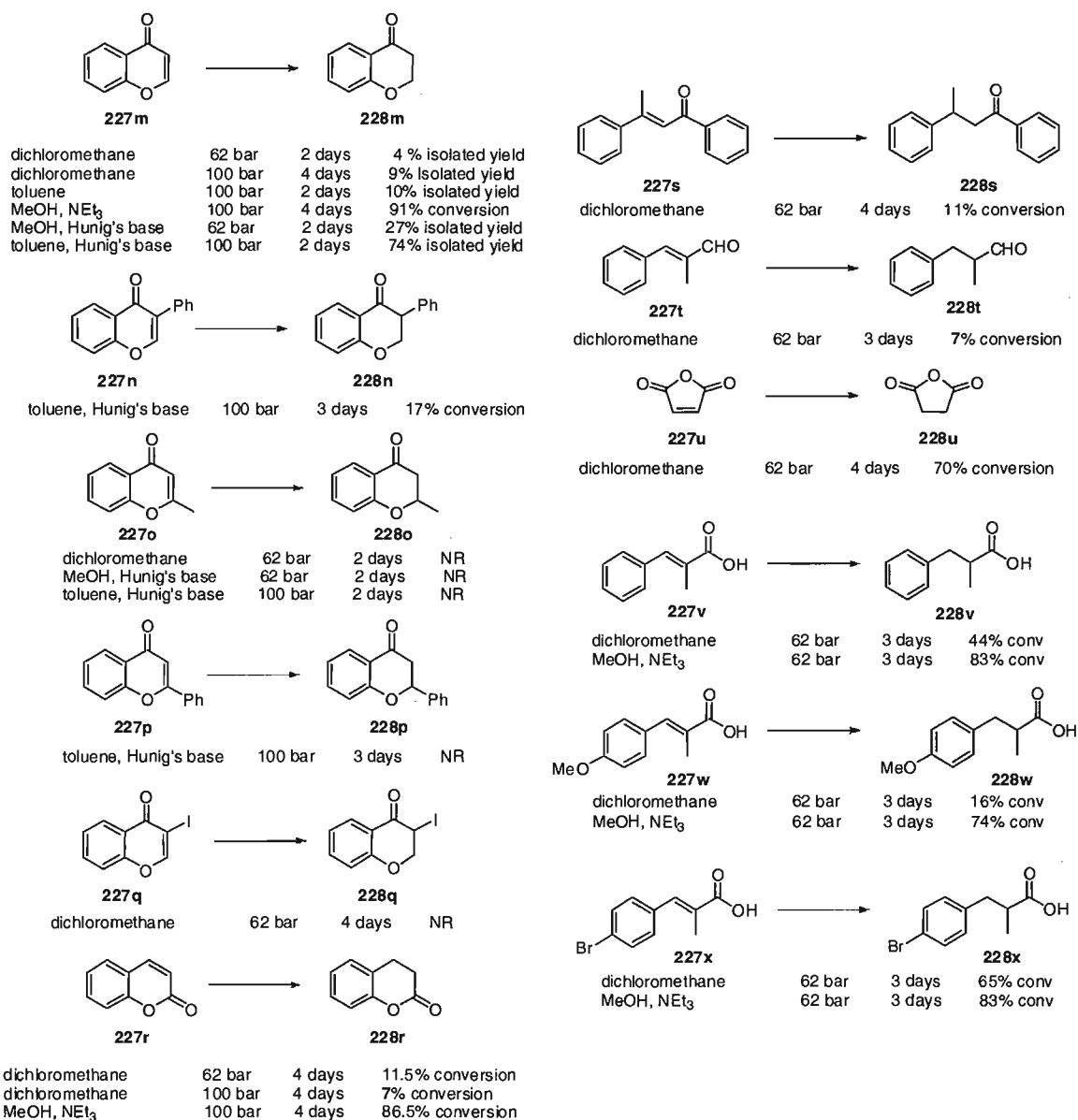
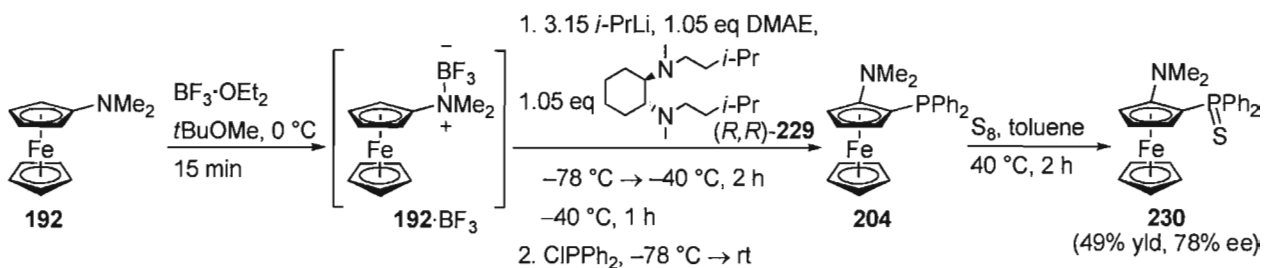


Figure 40. Attempted hydrogenation reactions with incomplete hydrogenation.

Clearly, enough substrates were hydrogenated in good yields to prompt investigation of enantioenriched versions of **221** and its congeners in asymmetric hydrogenations. The synthesis of these complexes is the topic of the next section.

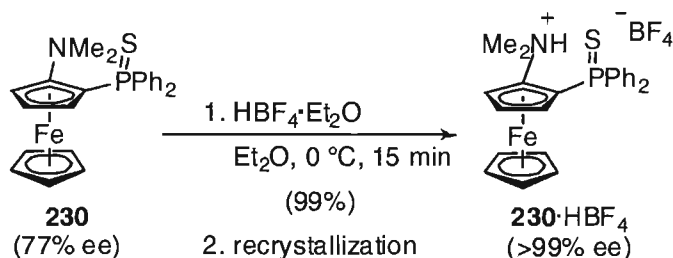
2.5 Synthesis of Enantiopure 2-Phosphino-1-aminoferrocenes and their Iridium Complexes.

Enantioenriched ligand **204** was prepared (Scheme 48) following the optimal asymmetric lithiation conditions developed by the Metallinos group.^{112,113} Specifically, a suspension of Lewis acid-base complex **192**·BF₃ in *tert*-butyl methyl ether (*t*-BuOMe) at −78 °C was treated with a pre-formed lithiating reagent prepared from 3.15 equivalents of isopropyllithium (*i*-PrLi) and 1.05 equivalents each of diamine (*R,R*)-**229** and dimethylaminoethanol (DMAE) in *t*-BuOMe at −40 °C. As observed in the non-selective reaction, slow warming of the solution from −78 °C to −40 °C over a two to three hour period resulted in the formation of a red-orange solution, which was held at −40 °C for an additional hour. Chlorodiphenylphosphine electrophile was added to the solution at −78 °C, and the whole was allowed to warm slowly to room temperature over approximately 15 hours. In order to facilitate purification as well as measurement of enantiomeric excess on chiral stationary phase HPLC, this crude mixture was treated with sulfur to produce (*S*)-2-diphenylphosphinothionyl-1-dimethylaminoferrocene **215** in 49% overall yield with 78% enantiomeric excess.



Scheme 48. Synthesis of enantioenriched (*S*)-2-diphenylphosphinothionyl-1-dimethylaminoferrocene **230**.

Sulfide **230** was treated with tetrafluoroboric acid to form the ammonium fluoroborate salt **230**·HBF₄ (Scheme 49). This salt could be recrystallized via liquid-liquid or vapour-liquid diffusion of diethyl ether into a solution of the salt in dichloromethane. After two recrystallizations, the salt was enantiopure as determined by neutralization of a small amount of the ammonium salt back to free aminophosphine sulfide with sodium bicarbonate under sonication. Notably, the melting point of the ammonium salt increased significantly after recrystallization (from 115 °C to >225 °C) and the optical rotation ($[\alpha]^{20}_{\text{D}}$) increased from -76.0 ° to -94.9 °. The enantiomeric purity of the phosphine sulfide was assayed by chiral stationary phase HPLC separation as before and found to be 99.7:0.3 er (>99% ee).



Scheme 49. Formation of ammonium tetrafluoroborate salt **230**·HBF₄.

The absolute stereochemistry of (*R,R*)-**229** derived (*S*)-**230**·HBF₄ was determined by X-ray crystallographic analysis (Figure 41) and found to corroborate the stereochemistry of lithiation as previously determined with alcohol **193** (Figure 32, Section 1.4.2). Importantly, the relative stereochemistry of (*S*)-**230**·HBF₄ was opposite to (*S,S*)-**191** derived alcohol **193** previously prepared by the Metallinos group¹¹², indicating

that the configuration the diamine ligand **229** determines the stereochemistry of the products. Crystals were obtained via vapour diffusion of diethyl ether into a solution of salt **230**·HBF₄ in dichloromethane. The salt crystallized in the orthorhombic P2₁2₁2₁ space group. The X-ray structure features an intramolecular hydrogen bond between H1a, and S1, in addition to an intermolecular hydrogen bond between H1a, and F4 of the fluoroborate counterion. The presence of these hydrogen bonds may be a critical factor in increasing the propensity of the compound to crystallize as a single enantiomer, especially as an intramolecular hydrogen bond was also observed in alcohol **193**. This observation raised the possibility that the same ammonium salt-recrystallization technique could be used to obtain other enantiopure 2-phosphino-1-aminoferrocenes.

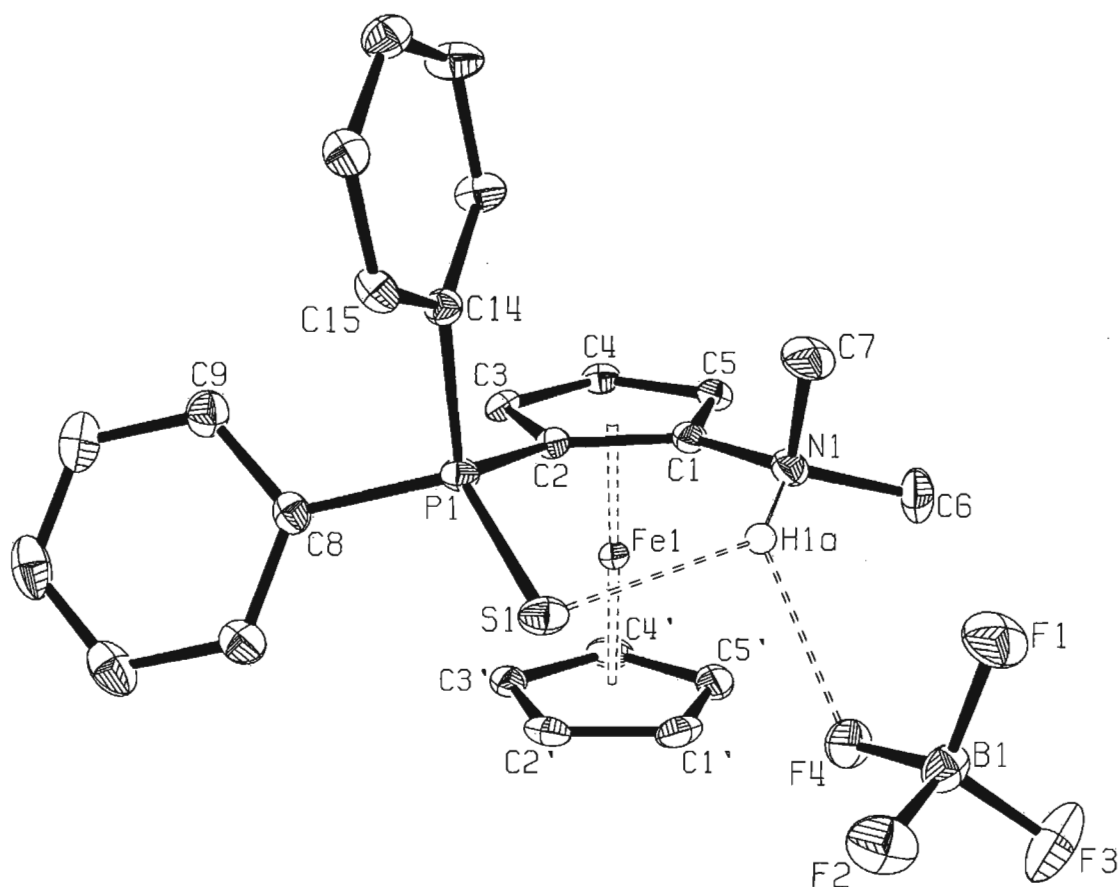
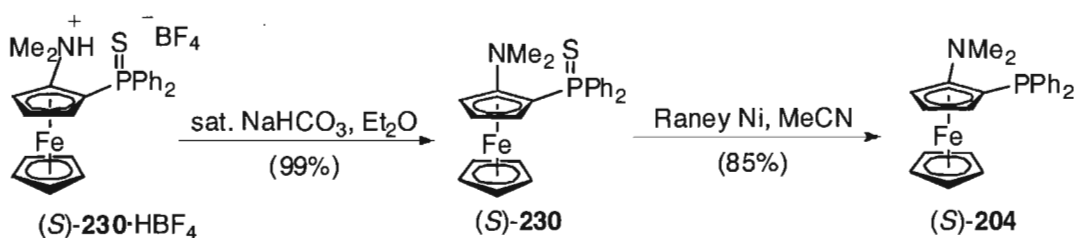


Figure 41. ORTEP plot of ammonium tetrafluoroborate salt **230**·HBF₄ at 50% probability; all H atoms except H1a are omitted for clarity.

Neutralization of (*S*)-**230**·HBF₄ with saturated NaHCO₃ and extraction into ether/ethyl acetate provided enantiopure phosphine sulfide (*S*)-**230**. This solvent system was found to be crucial for maintaining enantiopurity, as use of stronger bases such as NaOH or Na₂CO₃, or extraction with dichloromethane resulted in isolation of product with reduced enantiopurity. Enantiopure phosphine sulfide (*S*)-**230** was readily desulfurized to the free phosphine in good yield using freshly activated Raney nickel (Scheme 50). To the best of our knowledge, (*S*)-**204** is the first enantiomerically pure 2-phosphino-1-aminoferrrocene to be made.

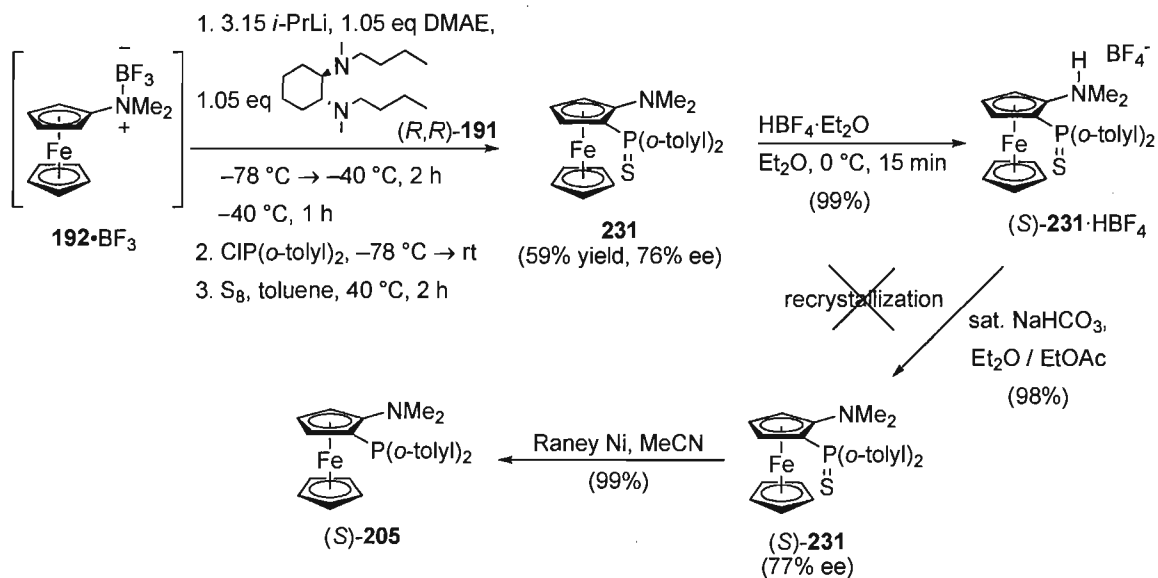


Scheme 50. Neutralization and desulfurization to enantiopure ligand (*S*)-**204**.

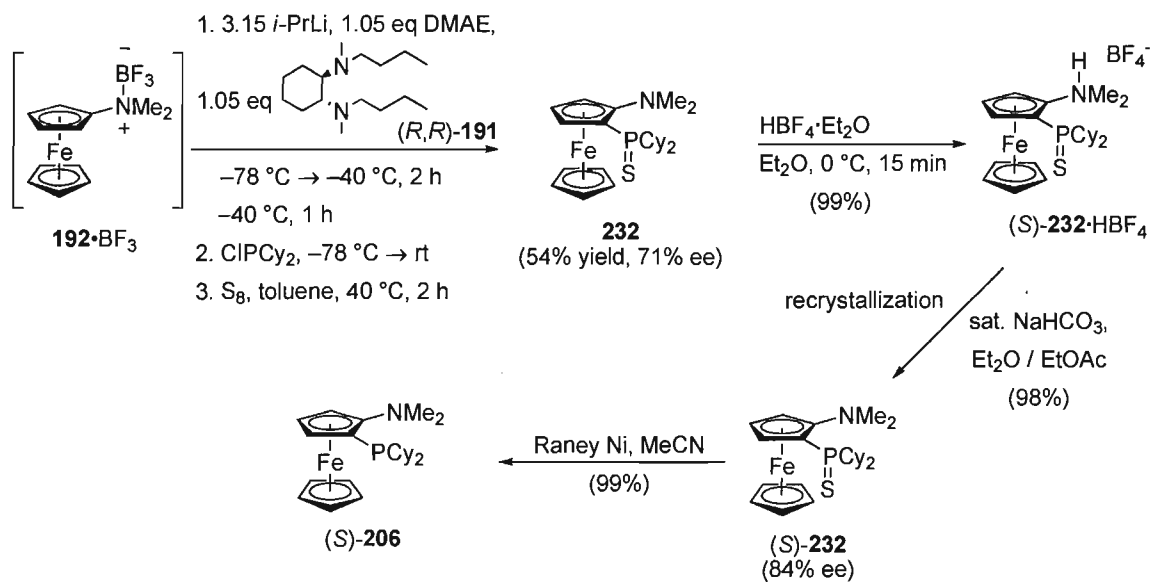
In view of the preceding results, it was expected that a similar approach could be pursued for the preparation of other aminophosphine ligands by using different chlorophosphines as electrophiles after the asymmetric lithiation step, or by starting with an alternative tertiary aminoferrocene, such as *N*-ferrocenylpyrrolidine (**213**). For the purposes of this project, a few key steric variations to the structure of **204** were pursued. As can be seen in the X-ray structure of the racemic iridium complex **221** (Figure 37), a cyclic amine (such as in **207**) is likely to have an influence on catalyst conformation, due to changes in steric demand in that spacial quadrant of the complex. The *ortho*-tolyl (**205**) or cyclohexyl (**206**) phosphine analogues of **204** would also be expected to introduce both steric and electronic differences compared to the original complex, which may have an impact on yield and enantioselectivity in asymmetric hydrogenation reactions.

Following the established procedure to prepare (*S*)-**204**, salt (*S*)-**231**·HBF₄ was prepared (Scheme 51), but unfortunately could not be recrystallized to enantiomeric purity. Nonetheless, the salt was neutralized and desulfurized to phosphine **205**. The cyclohexylphosphine derivative **206** could be prepared following the established procedure, and the ammonium salt of the phosphine sulfide (**232**·HBF₄) was enriched from 71% to 84% ee (Scheme 52). Fortunately, *N*-ferrocenyl pyrrolidine derived salt (*S*)-

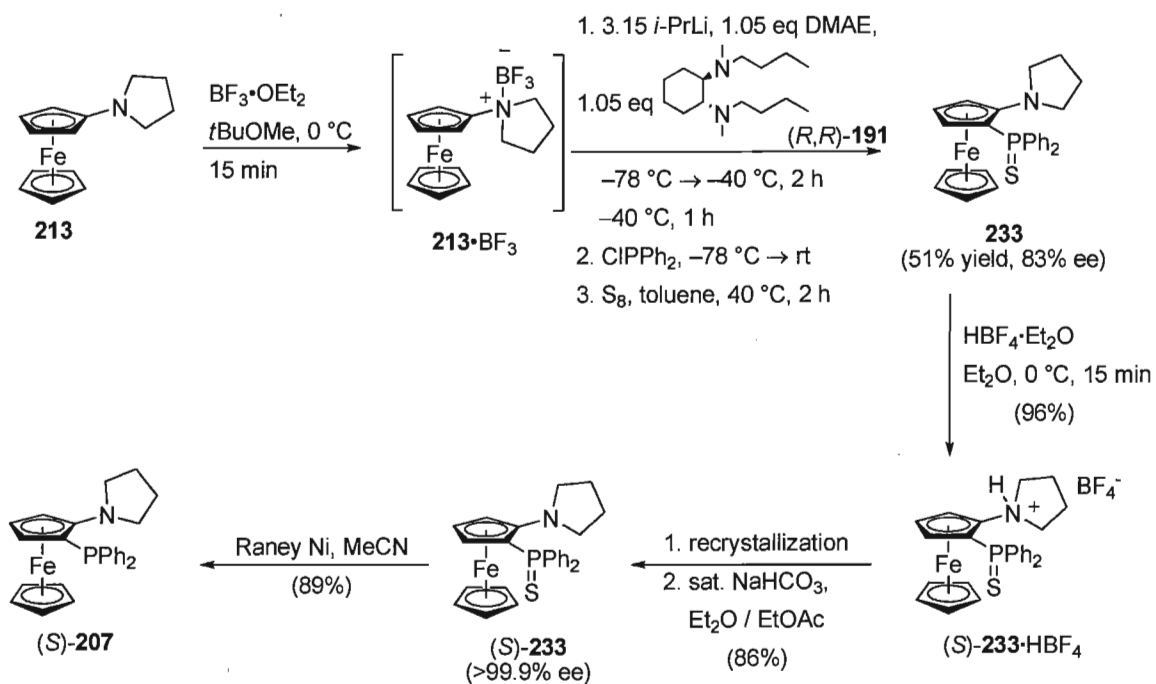
233·HBF₄ was recrystallized to enantiomeric purity, enabling isolation of homochiral (*S*)-**207** (Scheme 53).



Scheme 51. Synthesis of *ortho*-tolyl derivative **205**.



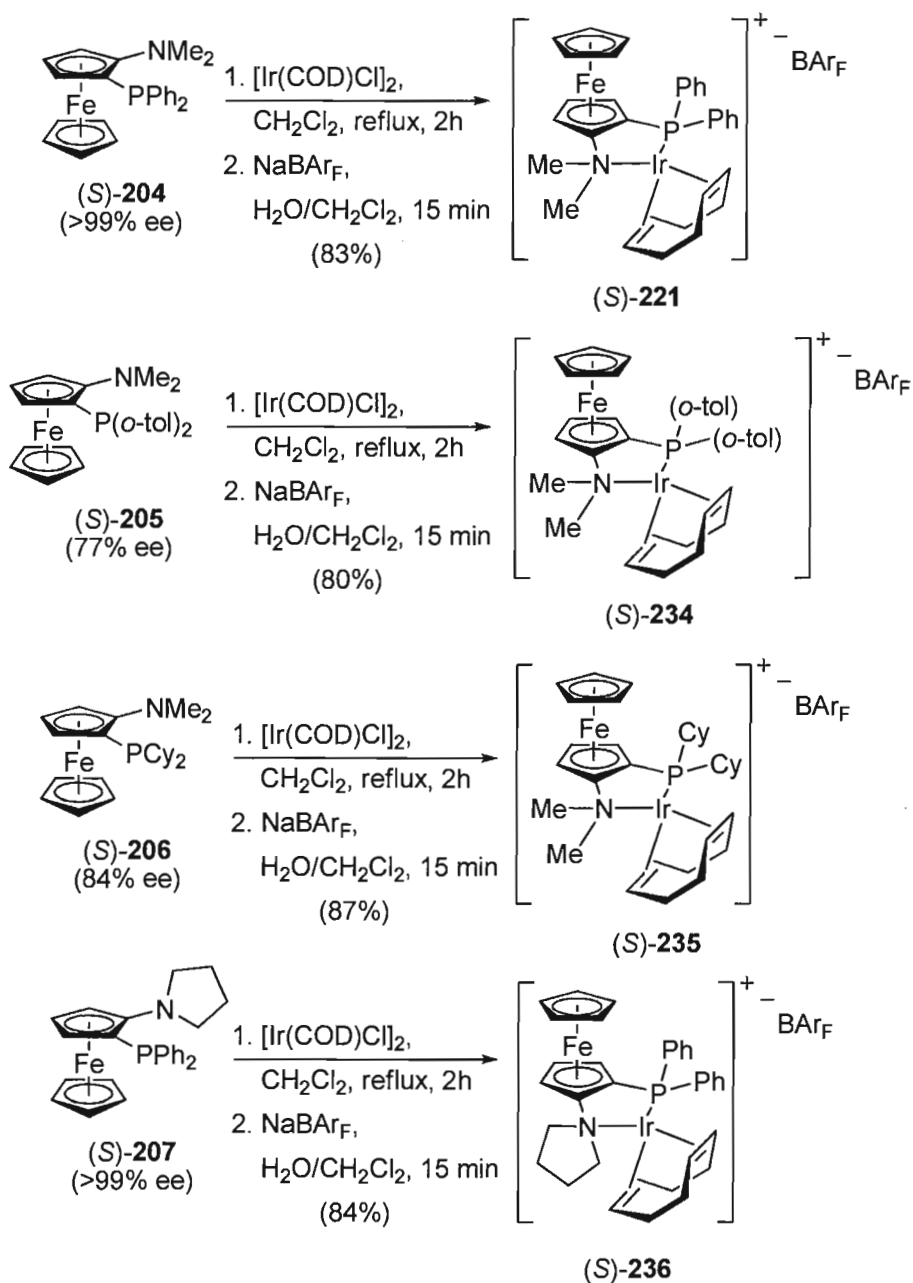
Scheme 52. Synthesis of cyclohexyl derivative **206**.



Scheme 53. Synthesis of *N*-ferrocenylpyrrolidine ligand (*S*)-**207**.

2.6 Synthesis of Enantiopure Iridium Complexes.

With enantiopure/enriched aminophosphine ligands in hand, iridium complexes (*S*)-**221**, (*S*)-**234**, (*S*)-**235**, and (*S*)-**236** were prepared in 80-87% yield following the procedure described previously (Scheme 54).



Scheme 54. Synthesis of enantioenriched cationic Ir(COD)[BAR_F] complexes (S)-**221**, (S)-**234**, (S)-**235**, and (S)-**236**.

2.7 Asymmetric Hydrogenation of Alkenes with Enantioenriched / Enantiopure Iridium(COD)[BAR_F] Complexes (*S*)-221, (*S*)-234, (*S*)-235, and (*S*)-236.

Enantioenriched / enantiopure iridium complexes were employed in asymmetric hydrogenation of several prochiral alkenes (Table 11).¹¹⁹ In contrast to most iridium catalysts currently explored which form six membered chelate rings with iridium, 2-phosphino-1-aminoferrocenes form a five membered chelate ring. In addition, the *N*-donor is an sp³ hybridized amine and both ligating heteroatoms are attached to the Cp ring. The ligands also feature only planar chirality. As a result, this is a relatively unexplored class of iridium complexes, which should provide some insight as to the potential of planar chiral 2-phosphino-1-aminoferrocenes in asymmetric catalysis.

Alkene	Product	cat (<i>S</i>)-221 (> 99 % ee)	cat (<i>S</i>)-234 (77 % ee)	cat (<i>S</i>)-235 (84 % ee)	cat (<i>S</i>)-236 (> 99 % ee)
124	(<i>R</i>)-124a	94% yld 84% ee (<i>R</i>)	99% yld 77% ee (<i>R</i>)	98% yld 49% ee (<i>R</i>)	96% yld 84% ee (<i>R</i>)
128	(<i>R</i>)-128a	97% yld 91% ee (<i>R</i>)	97% yld 76% ee (<i>R</i>)	87% yld 55% ee (<i>R</i>)	98% yld 82% ee (<i>R</i>)
225a	(<i>R</i>)-225a	99% yld 92% ee (<i>R</i>)	99% yld 74% ee (<i>R</i>)	96% yld 56% ee (<i>R</i>)	83% yld 61% ee (<i>R</i>)
225n	(<i>R</i>)-225n	96% yld 82% ee (<i>R</i>)	97% yld 72% ee (<i>R</i>)	99% yld 55% ee (<i>R</i>)	91% yld 36% ee (<i>R</i>)
225b	(<i>S</i>)-225b	88% yld 82% ee (<i>S</i>)	96% yld 21% ee (<i>S</i>)	94% yld, 49% ee (<i>S</i>)	74% conv 4% ee (<i>R</i>)
225c	(<i>S</i>)-225c	98% yld 84% ee (<i>S</i>)	93% yld 28% ee (<i>S</i>)	95% yld 55% ee (<i>S</i>)	79% conv 2% ee (<i>R</i>)
225i	(<i>S</i>)-225i	96% yld, 48% ee (<i>S</i>)	95% yld, 11% ee (<i>S</i>)	96% yld, 11% ee (<i>S</i>)	98% yld, 16% ee (<i>R</i>)
225f	(<i>R</i>)-225f	83% yld 18% ee (<i>R</i>)	95% yld 48% ee (<i>R</i>)	99% yld 23% ee (<i>R</i>)	99% yld 12% ee (<i>S</i>)
225j	(<i>R</i>)-225j	^a 61% yld 17% ee	^a 56% yld 37% ee	^a 82% yld 10% ee	^a 61% yld 2% ee

^a low yield due to volatility of alkene

Table 11. Asymmetric hydrogenation results with complexes (*S*)-221, (*S*)-234, (*S*)-235, and (*S*)-236.

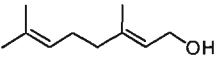
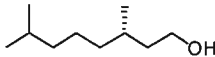
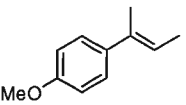
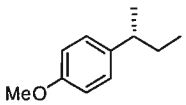
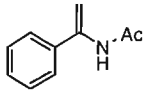
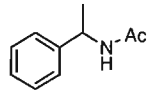
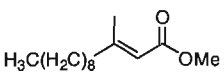
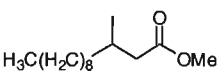
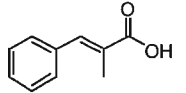
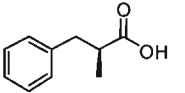
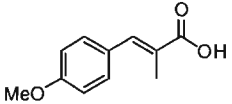
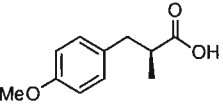
227e		(S)-228e		99% yld 43% opt pur (S)
125		(R)-125a		95% yld 26% ee (with 80% ee cat)
225o		ent-226o		97% yld, 17% ee
225p		ent-226p		97% yld, 9% opt pur
227v		(S)-228v		78% yld, 97% conv, 53% opt pur
227w		(S)-228w		91% yld, 91% conv, 60% opt pur

Table 12. Additional asymmetric hydrogenation results with complex (S)-221.

Trans-1,2-diphenylpropene (methyl stilbene, **124**) was the first substrate tested. For initial catalyst (S)-221, (*R*)-1,2-diphenylpropane ((*R*)-**124a**) was obtained in excellent yield (94%) and good enantioselectivity (84% ee). Given that **204** was the first ligand tested in the series, this was an encouraging result. Variation of solvent conditions led to a decrease in activity and selectivity in some cases. For example, using toluene provided the product in only 46% conversion and 74% ee. Chloroform (60% conversion, 81% ee) and dichloroethane (91% conversion, 77% ee) were also inferior solvents. Satisfyingly, it was found that lowering the catalyst loading 1 mol % or even 0.5 mol % was sufficient to provide full conversion while still maintaining enantioselectivity (94% yield, 81% ee with 1 mol %; and 93% yield, 85% ee with 0.5 mol %). Utilizing complex (S)-234 improved the enantioselectivity, giving (*R*)-**124a** in 77% ee (equal to the catalyst % ee),

while complex (*S*)-**236** gave similar results to **221**, with (*R*)-**124a** isolated in 84% ee. Complex (*S*)-**235** gave the poorest results with product (*R*)-**124a** produced in only 49% ee.

Electron deficient alkenes such as α,β -unsaturated esters were then explored. β -Substituted- α,β -unsaturated ester *trans*-ethyl 3-phenylbut-2-enoate (**128**) was hydrogenated to give (*R*)-ethyl 3-phenylbutanoate ((*R*)-**128a**), again in excellent isolated yield, and satisfyingly, with greater enantiomeric excess (91% ee with complex (*S*)-**221**). Excellent induction was also found with complex (*S*)-**234** giving (*R*)-**128a** in 76% ee (with 77% ee catalyst). Complex (*S*)-**236** gave lower selectivity and provided ester (*R*)-**128a** in 62% ee, and complex (*S*)-**235** was also less selective (55% ee with 84% ee catalyst). *Trans*-ethyl 3-(4-methoxyphenyl)but-2-enoate (**225a**) was converted to (*R*)-ethyl 3-(4-methoxyphenyl)butanoate ((*R*)-**226a**) in 92% enantiomeric excess with complex (*S*)-**221**, in 74% ee with complex (*S*)-**234** (at 77% ee), in 61% ee with complex (*S*)-**236**, and in 56% ee with complex (*S*)-**235** (at 84% ee). As a further example, *trans*-ethyl 3-(naphthalen-2-yl)butenoate (**227y**) was hydrogenated with isolation of (*R*)-ethyl 3-(naphthalen-2-yl)butanoate ((*R*)-**228y**) in 82% enantiomeric excess using (*S*)-**221**, and in 72% ee using (*S*)-**234** (at 77% ee).

Hydrogenation of α -substituted- α,β -unsaturated ester *trans*-ethyl 2-methyl-3-phenylacrylate (**227b**) gave (*S*)-ethyl 2-methyl-3-phenylpropanoate ((*S*)-**228b**) in 82% enantiomeric excess with (*S*)-**221**, in 21% ee with (*S*)-**234**, in 49% ee with (*S*)-**235**, and surprisingly was only hydrogenated in 74% conversion and gave the product in nearly racemic (4% ee) form favouring the opposite enantiomer (*R*) with (*S*)-**236**. Similarly, *trans*-ethyl 3-(4-methoxyphenyl)-2-methylacrylate (**227c**) was hydrogenated to give (*S*)-

ethyl 3-(4-methoxyphenyl)-2-methylpropanoate ((*S*)-**228c**) in 84% enantiomeric excess with catalyst (*S*)-**221**, in 28% ee with (*S*)-**234**, in 55% ee with (*S*)-**235**, and again was not fully hydrogenated (79% conversion) and gave nearly racemic product (2% ee favouring the (*R*) enantiomer) with (*S*)-**236**. α -Substituted- α,β -unsaturated amide *trans*-*N*-benzyl-2-methyl-3-phenylacrylamide (**227i**) is slightly more electron rich than the ester analogues, and was hydrogenated to (*S*)-*N*-benzyl-2-methyl-3-phenylpropanamide ((*S*)-**228i**) in 48% enantiomeric excess with (*S*)-**221**, and in low (~10%) selectivity with all other complexes.

Electron rich allylic alcohol geraniol (**227e**) was converted to (*S*)-3,7-dimethyloctanol ((*S*)-**228e**) in 99% isolated yield and 43% optical purity with complex (*S*)-**221**, and *trans*-2-methyl-3-phenylpropenol (**227f**) was converted to (*R*)-2-methyl-3-phenylpropanol ((*R*)-**228f**) in 18% enantiomeric excess with complex (*S*)-**221**, with slightly higher selectivity (23% ee) with (*S*)-**235** (at 84% ee), and the highest selectivity achieved with (*S*)-**234** at 48% ee (catalyst at 77% ee). Again with (*S*)-**236**, the opposite enantiomer, (*S*)-2-methyl-3-phenylpropanol, was obtained in 12% ee. Allylic ether *trans*-(3-methoxy-2-methylprop-1-enyl)benzene (**227j**), was hydrogenated with selectivities similar to allylic alcohol **227f**. Complex (*S*)-**221** provided (–)-(3-methoxy-2-methylpropyl)benzene (**228j**) in 17% ee, nearly racemic product (2% ee) was obtained using complex (*S*)-**236**, and 10% ee was achieved with (*S*)-**235** (at 84% ee). Again, the highest enantioselectivity was achieved with complex (*S*)-**234** providing (–)-**228j** in 37% ee (with catalyst at 77% ee). Electron neutral *trans*-1-(but-2-enyl)-4-methoxybenzene (**125**) was hydrogenated giving (*R*)-1-sec-butyl-4-methoxybenzene ((*R*)-**125a**) in 26% enantiomeric excess (with 80% ee catalyst (*S*)-**221**). Electron rich *N*-acyl- α -arylenamide

227z was hydrogenated in 17% ee with complex (*S*)-**221**. Purely alkyl substituted α,β -unsaturated ester, *trans*-methyl 3-methyldodecenoate (**227ab**), provided fatty acid methyl ester (–)-methyl 3-methyldodecanoate ((–)-**228ab**) in 9% optical purity showing the commonly observed trend that aryl substituted alkenes give products in higher enantioselectivity than alkyl substituted alkenes.

From the preceding results, it can be seen that initial ligand **204** has the broadest substrate scope with good to excellent enantioselectivities with a number of substrates. Complex **234** with bulkier *ortho*-tolyl groups on the phosphorus moiety of the ligand proved to be more selective for several alkenes, especially those substituted on the same carbon as the aromatic group, although unfortunately the ligand could not be recrystallized to enantiomeric purity as with ligands **204** and **207**. Complex **235** with more electron rich cyclohexyl groups on the phosphorus moiety was less selective in hydrogenation of all alkenes. Finally, complex **236** with pyrrolidine amine moiety proved to be the least selective, exhibiting lower reactivity in some cases as well, while some alkanes were obtained with opposite stereochemistry.

2.8 Proposed Mechanism of Hydrogenation.

The mechanism of hydrogenation with (*S*)-**221** starts with oxidative addition of hydrogen. Four dihydride complexes can be envisioned (Figure 42). Complexes **237a** and **237b** can be discounted as oxidative addition *trans* to phosphorus is electronically disfavoured, and complex **237c** is sterically disfavoured as the COD ligand is forced into the region of the ferrocene backbone. Thus, complex **237d** is both sterically and

electronically favoured. Hydrogenation of the COD ligand and coordination of solvent provides complexes **238c** and **238d** (Figure 42).

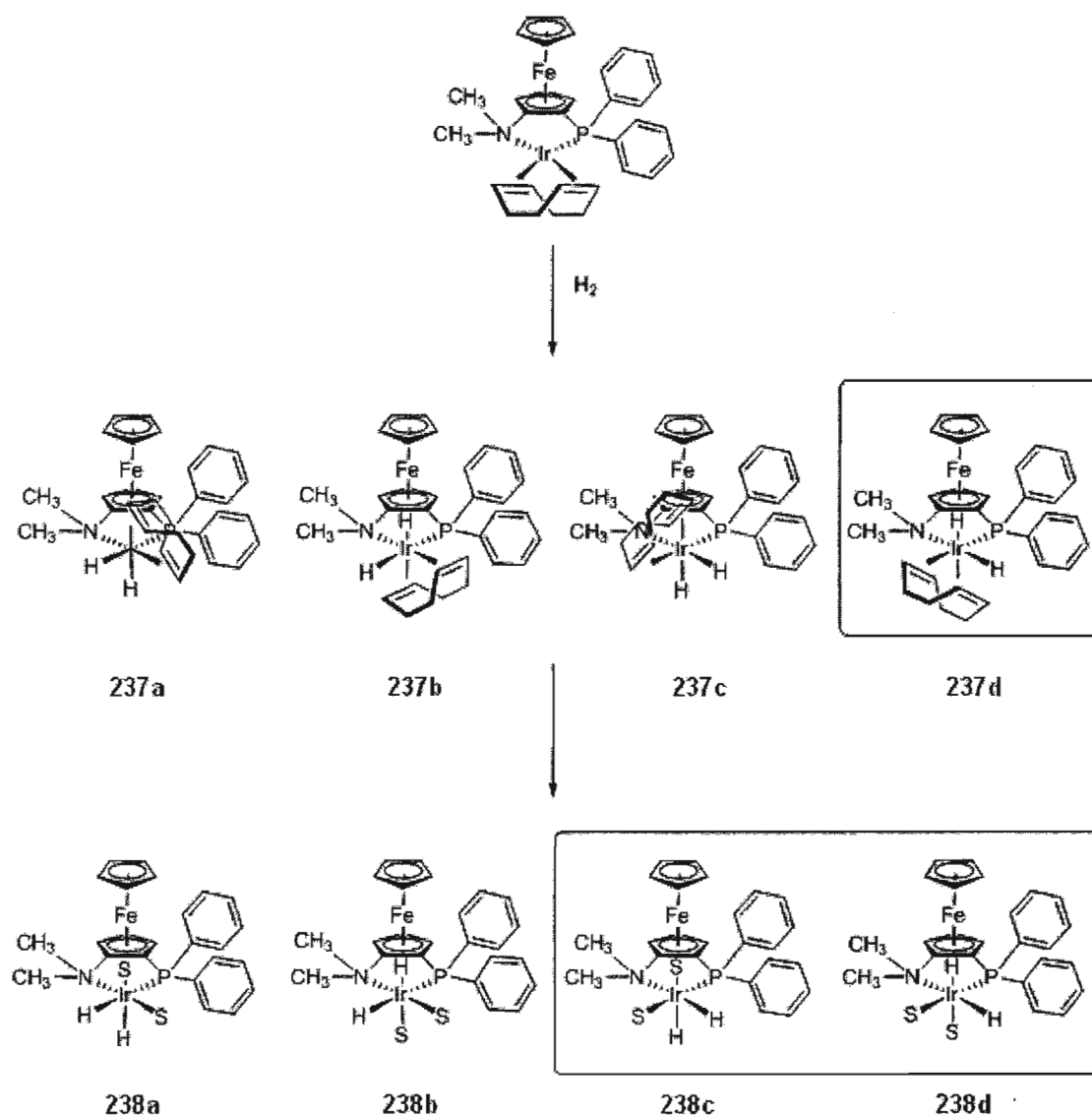


Figure 42. Formation of catalytically active Ir-dihydride solvent species.

After this species is formed, substrate alkene will coordinate *trans* to the phosphorus moiety. The orientation of coordination depends on the steric environment of

the catalyst, and influences the enantioselectivity of the reaction. As can be seen in Figure 43, placing a quadrant system over the ligand provides insight into how the alkene will bind. Coordination of a substrate alkene (such as β -methyl ethyl cinnamate) can potentially occur in four ways. Based on the quadrant system, it becomes clear that species **239a** is sterically preferred (Figure 44).

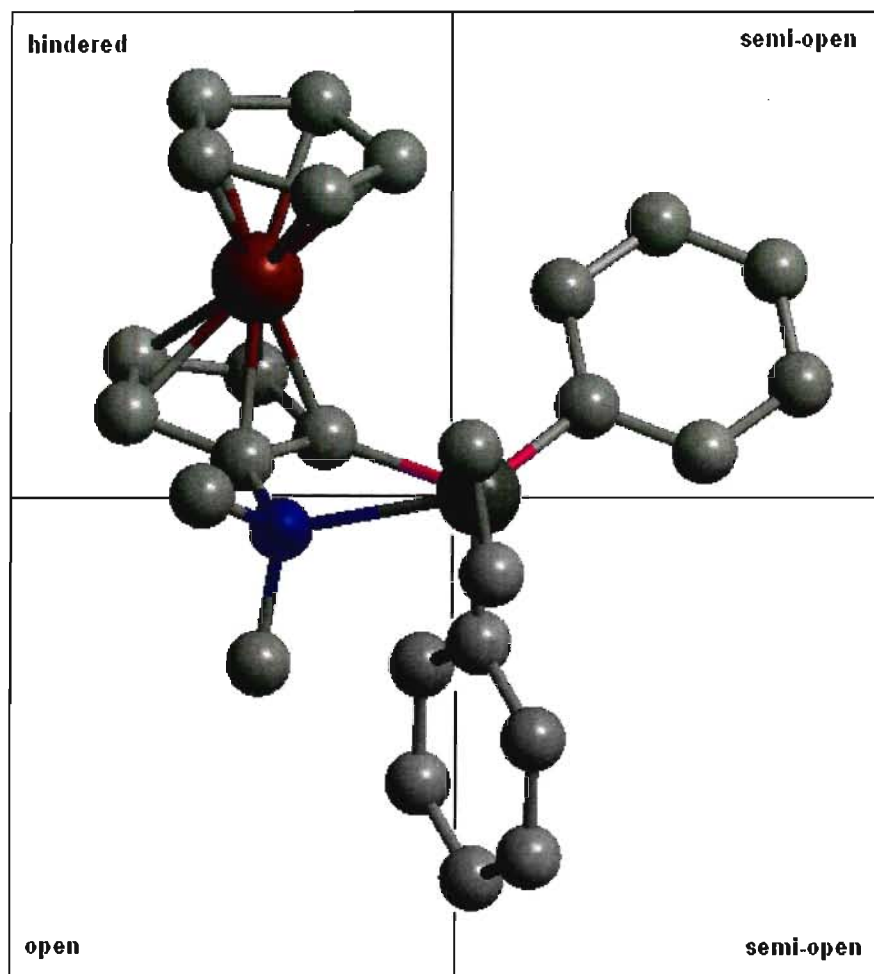


Figure 43. Quadrant system for selective binding of substrate alkene.

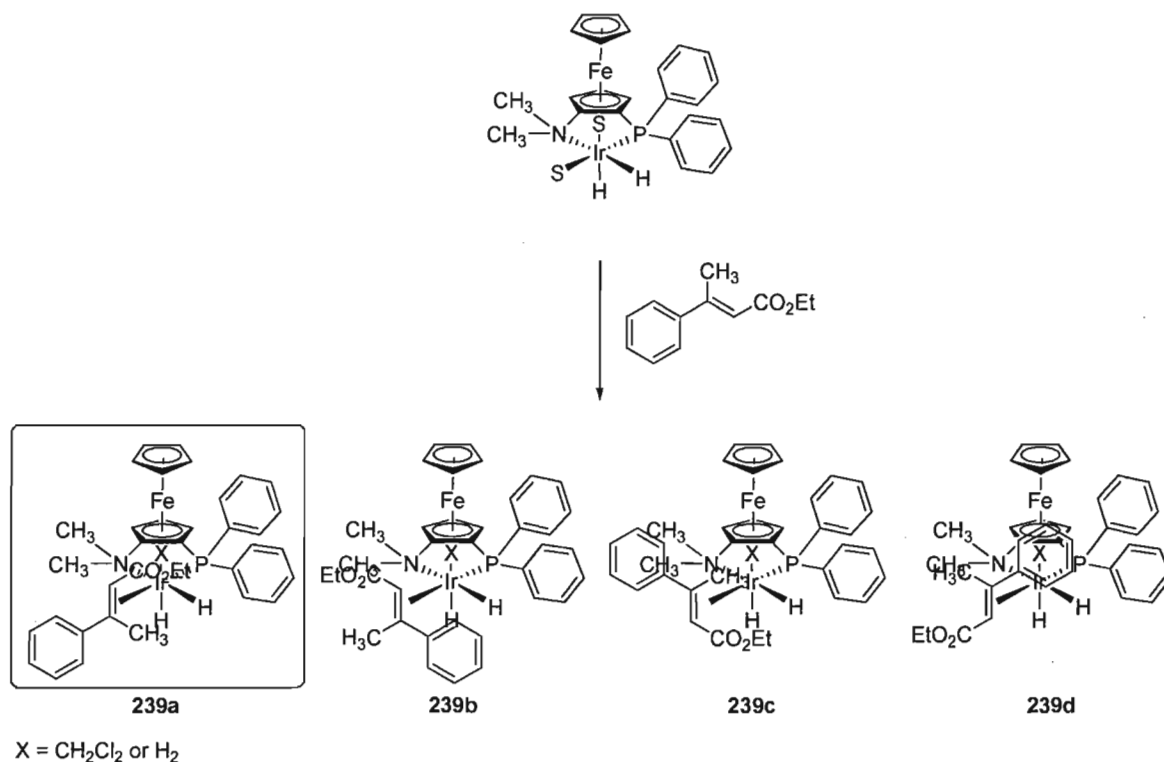


Figure 44. Alkene coordination modes for β -methyl ethyl cinnamate.

A second factor affecting the enantioselectivity of the reaction is the migratory insertion step. Following selective coordination, hydride migratory insertion can occur at either the α - or β -carbon (Figure 45). Electronically, hydride addition to the β -carbon is preferred (**240a**). In the case of β -methyl substituted cinnamate derivatives, addition to this carbon is also sterically favoured, accounting for the high levels of selectivity.

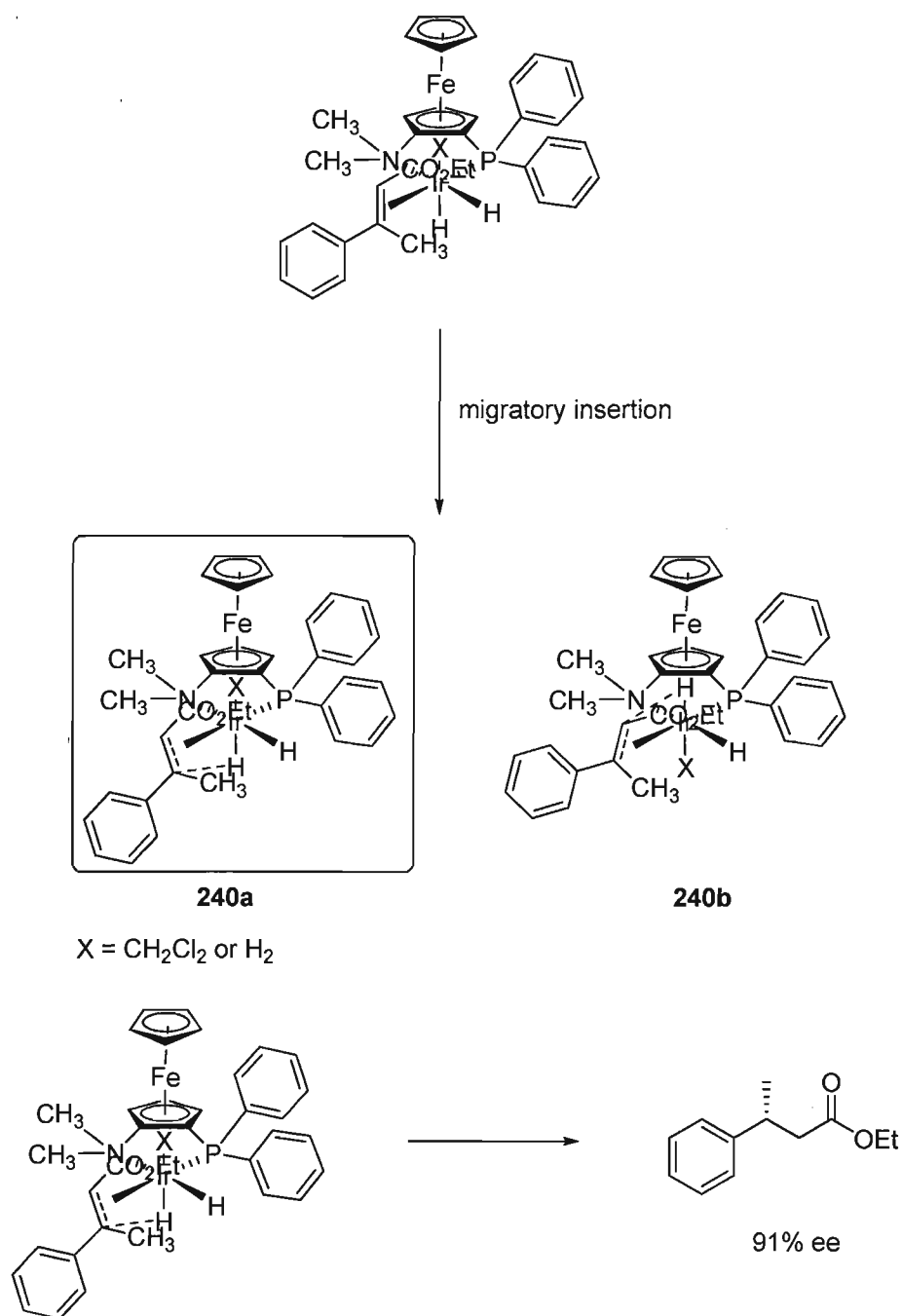


Figure 45. Migratory insertion modes for β -methyl ethyl cinnamate.

This mechanism also helps to explain the reduced enantioselectivities obtained with α -substituted α,β -unsaturated esters, in which case there are bulky groups on both ends of the alkene (i.e. making binding in one manner less preferential) (Figure 46).

Additionally, electronically favoured transfer of the hydride to the β -carbon explains why the opposite stereochemistry is obtained when compared to β -substituted cinnamate derivatives (Figure 47).

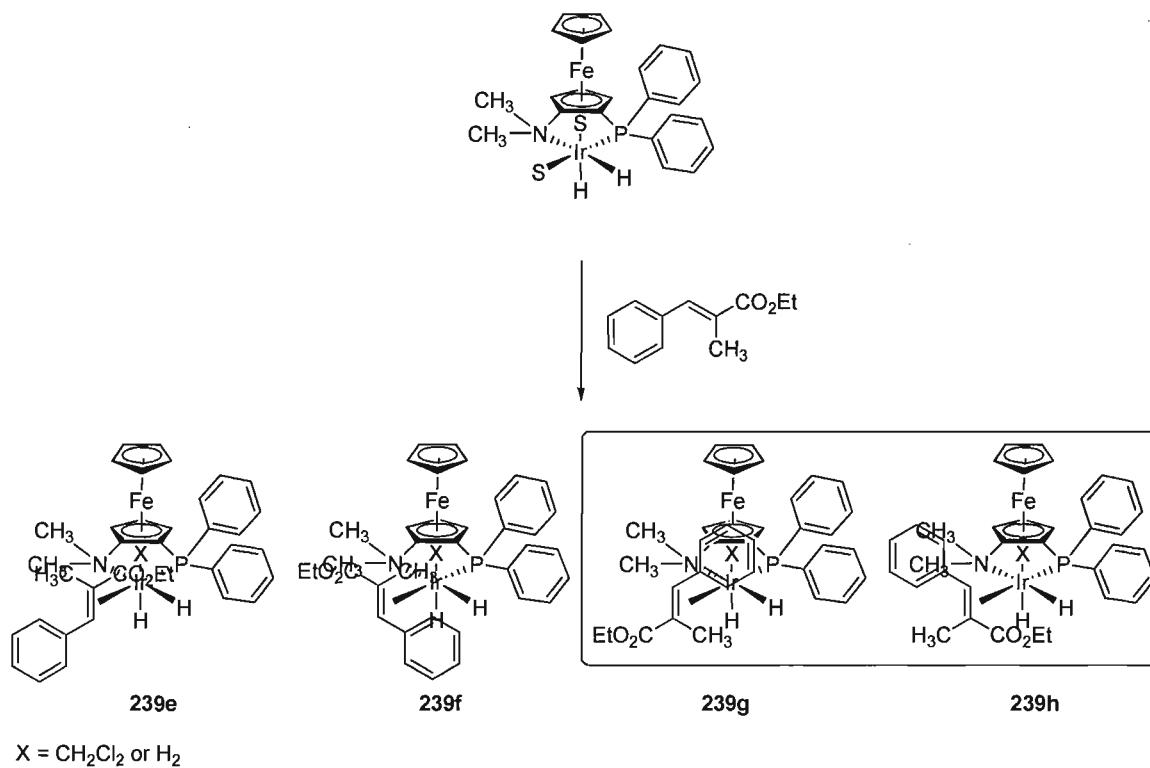


Figure 46. Alkene coordination modes for α -methyl ethyl cinnamate.

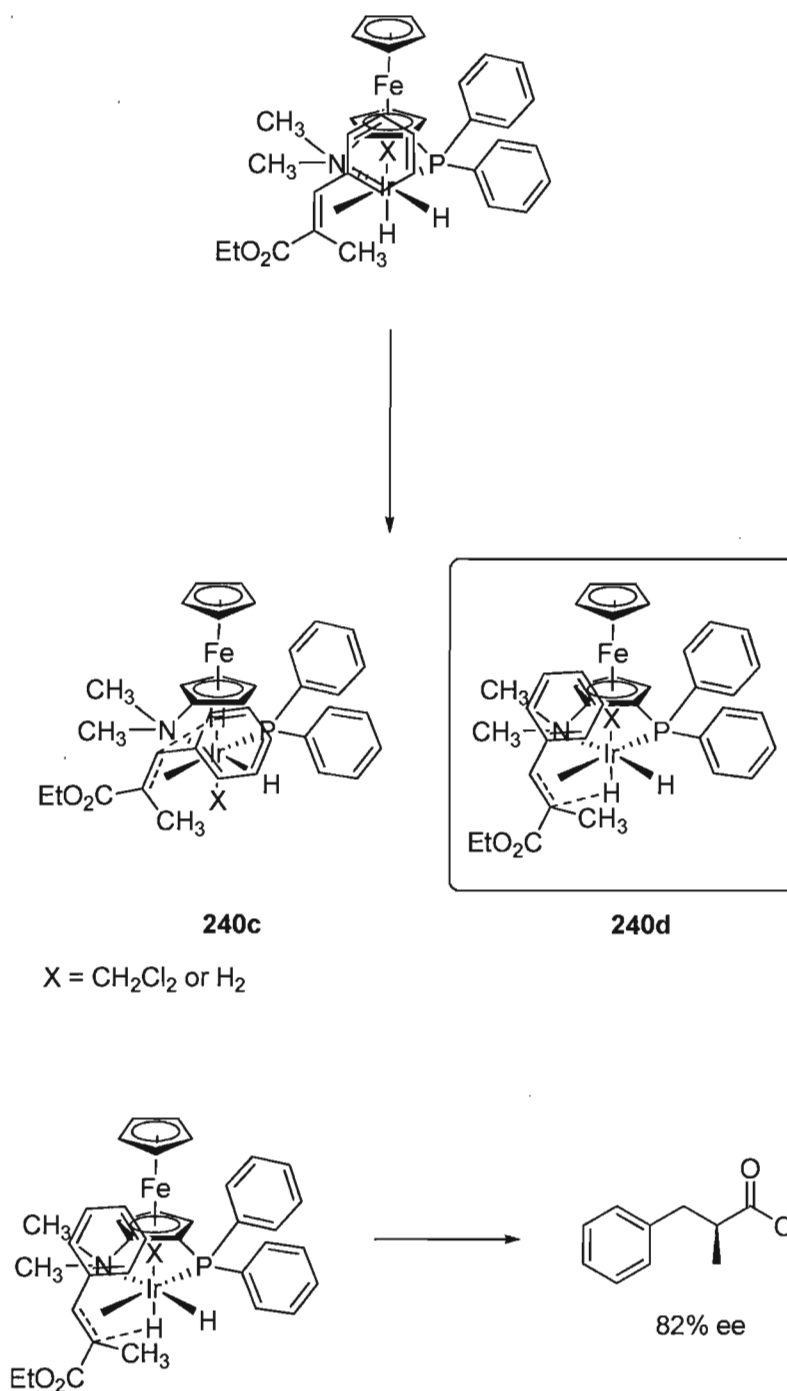


Figure 47. Migratory insertion modes for α -methyl ethyl cinnamate.

The differences in asymmetric induction between complexes **221**, **234-235** can be rationalized by the proposed mechanism. For example, the bulkier *ortho*-tolyl derivative

gives higher selectivity for methyl stilbene, and the β -substituted α,β -unsaturated esters where the increased steric bulk of the ligand makes alkene coordination more selective towards the *re*-face, but not with the α -substituted α,β -unsaturated esters because of the increased steric interaction of the aromatic portion of the alkene with the *ortho*-tolyl groups of the ligand upon alkene coordination.

Complex **236** with a pyrrolidine amine moiety has increased steric bulk at nitrogen in the complex, thus leading to less selective alkene coordination, and reduced enantioselectivity with some alkenes. This also explains why there is a reversal of stereochemistry and loss in reactivity with the α -substituted α,β -unsaturated esters compared to the other complexes.

There are still limitations of this rudimentary model, of course, especially with "electron rich" alkenes, but it does help to explain some of the obtained results, as well as being potentially useful for the rational design of new chiral ligands, especially if considering specific substrates for hydrogenation.

Chapter 3: Conclusions

Several new planar chiral and rare 2-phosphino-1-aminoferrocenes have been prepared, their coordination chemistry investigated with iridium and their applications in asymmetric hydrogenation of alkenes explored. These ligands take advantage of the planar chiral backbone of ferrocene to impart asymmetry. The initial ligand (2-diphenylphosphino-1-dimethylaminoferrocene) provided excellent asymmetric induction in the hydrogenation of several prochiral alkenes. A trend relating selectivity to alkene electronic properties was observed, with several electron poor alkenes providing high selectivities. For example, hydrogenation of β -substituted- α,β -unsaturated esters provided products in 91-92% enantiomeric excess. The α -substituted counterparts of these esters were hydrogenated with slightly lower selectivity, nevertheless good enantiomeric excesses of 82-84% were achieved. Electron neutral substituted alkenes were also hydrogenated with less selectivity, for example providing 1,2-diphenylpropane in 84% enantiomeric excess. Finally, electron rich alkenes, such as allylic alcohol 2-methyl-3-phenylpropenol, were hydrogenated with the lowest selectivity and were obtained in 17-48% enantiomeric excess.

Variation of the substituents on both the phosphorus and nitrogen donor atoms of the ligand was performed for evaluation of their effect on selectivity. Locking the dimethylamino group into a pyrrolidine ring had a detrimental effect on selectivity and reactivity in some cases. Changing the *P*-phenyl substituents to cyclohexyl groups again had a detrimental effect on selectivity, with no loss in reactivity. However, changing to *P-ortho*-tolyl groups had a positive effect on selectivity. From these results it can be

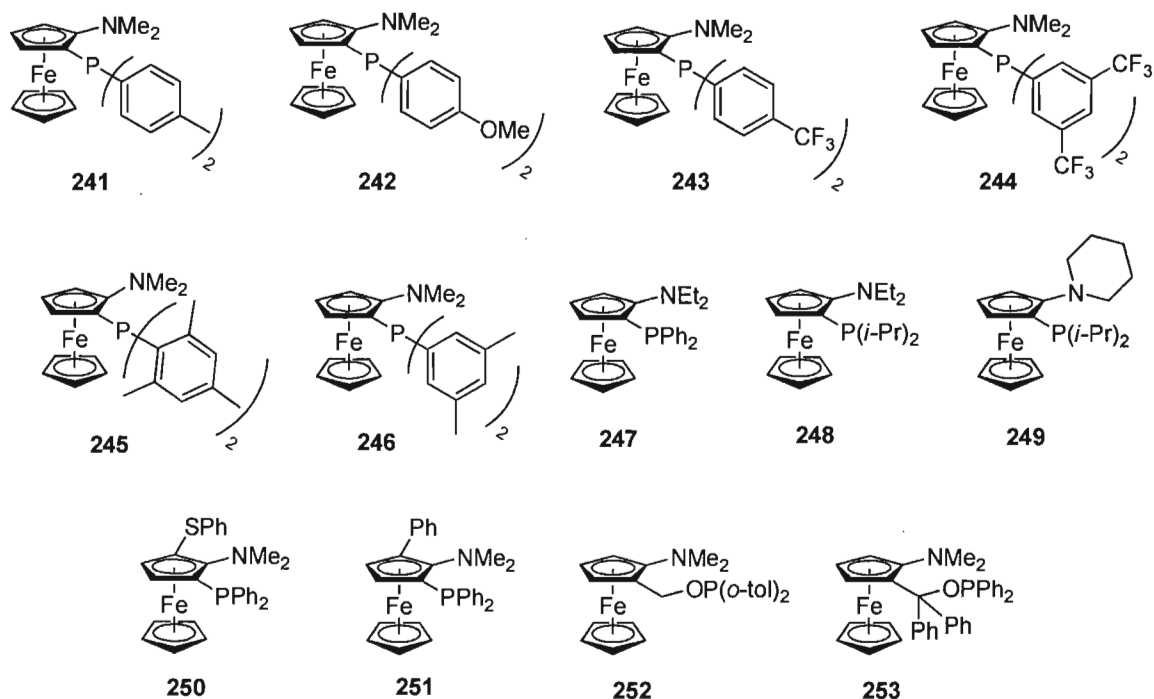
predicted that electron rich donors on phosphorus would be detrimental to selectivity, while bulkier aromatic groups could provide a way to excellent selectivities. A mechanism is proposed that helps to explain the sense and extent of chiral induction differences between ligands.

In contrast to many ligands currently used, which contain mostly imine or related sp^2 nitrogen donors, the ligands described here offer an alternative structural scaffold and warrant further investigation in asymmetric catalysis. It is clear that the prepared complexes, which exhibit 5-membered chelate rings with iridium (as opposed to a 6-membered ring which is normally seen) are viable catalysts. The results also show that the planar chirality of ferrocene is capable of inducing high levels of asymmetry during catalytic reactions, in the absence of any other elements of chirality.

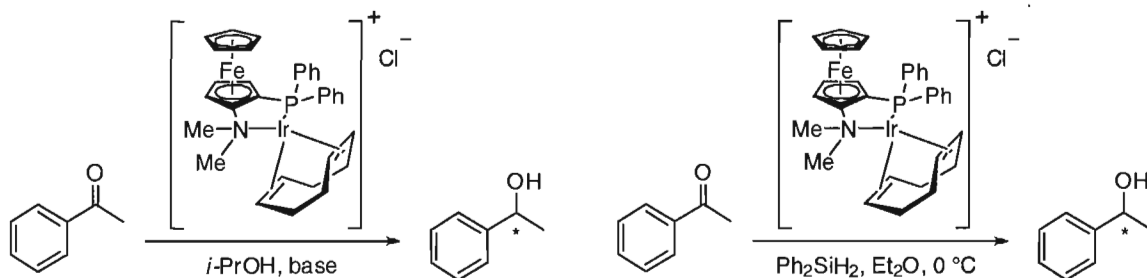
The synthetic route to these ligands is straightforward, and provides the products in good yields and enantioselectivities. Two of the four aminophosphine ligands were recrystallized to enantiomeric purity in relatively few steps. Either enantiomer of the ligands may be obtained simply by switching the configuration of the chiral diamine ligand used in the asymmetric lithiation step.

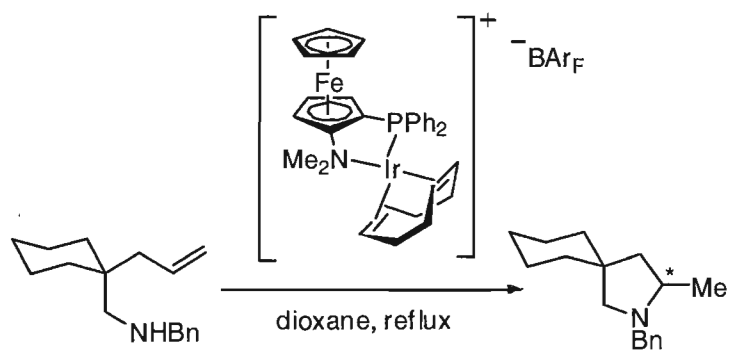
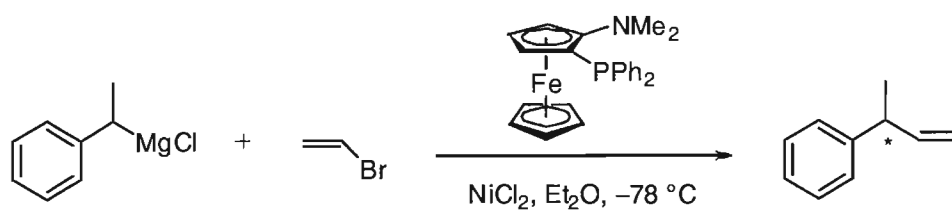
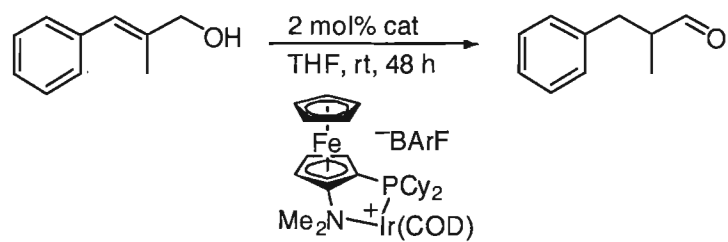
Chapter 4: Future Work

Future work will focus on two different areas – modification of the ligand structure, and use of these ligands in different catalytic reactions. Further modifications on the ligand may include variation of the phenyl substituents on phosphorus to other aromatic groups with various electronic and steric properties. It has been shown that substituent electronic effects in chiral ligands can have an impact on asymmetric induction in many catalytic reactions.¹²⁰ For example, electron donating *p*-methoxy (**242**) derivative, electron withdrawing *p*-trifluoromethyl (**243**) or 3,5-bis(trifluoromethyl) (**244**), as well as neutral *p*-tolyl (**241**) derivatives could be prepared. Bulky phosphine derivatives should also be investigated. For example, mesityl (**245**) or 3,5-xylyl (**246**) derivatives would increase the steric bulk without altering the electronic environment too much. Additionally, different groups on nitrogen should be investigated, such as diethylaminoferrocene (**247** and **248**), which increases steric bulk on nitrogen without locking the groups into a ring system. Increasing the steric bulk on nitrogen while decreasing the steric bulk on phosphorus (for example, **249**) may also provide insight into the origin of selectivity. Other routes to variation of ligand properties could involve use of an additional substituent. 1,2,3-Trisubstituted ferrocenes such as **250** or **251** can be easily prepared by the Metallinos route, and as such may lead to ligands that are more sterically and electronically desymmetrized. It would also be advantageous to investigate phosphinite derivatives such as **252** and **253**, considering the work of Pfaltz.^{76d}



Additional catalytic reactions that could be attempted would be asymmetric Ir-catalyzed transfer hydrogenation, hydrosilylation, and hydroboration with the Ir-Cl complex, as well as Ir-catalyzed allylic isomerization. This ligand system could also be utilized in Pd or Ni-catalyzed asymmetric Grignard reactions. Asymmetric hydroamination is also worth investigating with either the Ir complex, or via preparation and utilization of a Rh complex.





Chapter 5: Experimental

General procedures.

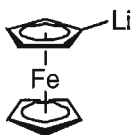
All reagents were purchased from commercial sources and used as received unless otherwise indicated. Tetrahydrofuran (THF) was dried and distilled over sodium/benzophenone ketyl under an atmosphere of nitrogen. Toluene was dried and distilled over sodium under an atmosphere of nitrogen. Dichloromethane was dried and distilled over CaH_2 under an atmosphere of nitrogen. *Tert*-butyl methyl ether (TBME) was dried and distilled over LiAlH_4 under an argon atmosphere. Dimethylaminoethanol was distilled over KOH under an argon atmosphere. Alkyl lithium reagents were titrated according to literature procedure with *N*-benzylbenzamide at $-40\text{ }^\circ\text{C}$ to a blue endpoint.¹²¹ All reactions were performed under argon in flame- or oven-dried glassware using syringe-septum cap techniques or Schlenk conditions unless otherwise indicated. Column chromatography was performed on silica gel 60 (70-230 mesh) or neutral alumina.

NMR spectra were obtained on a Bruker Advance 300 or 600 MHz instrument and are referenced to the residual proton signal of the deuterated solvent for ^1H spectra and to the carbon multiplet of the deuterated solvent for ^{13}C spectra according to published values. Pressurized reactions were performed with a Parr 4760 bomb. FT-IR spectra were obtained on an ATI Mattson Research Series spectrometer as KBr pellets for solids or on KBr discs for liquids. Mass spectra were obtained on an MSI/Kratos Concept 1S mass spectrometer. Combustion analyses were performed by Atlantic Microlab Inc., Norcross, GA. Melting points were determined on a Kofler hot-stage apparatus and are

uncorrected. X-ray data were collected on a Bruker APEX II CCD area detector equipped with a Kappa goniometer and using Mo KR graphite-monochromated radiation, $\lambda = 0.71073 \text{ \AA}$. The structure was solved by direct methods using SHELXTL software. The refinement and all further calculations were carried out using SHELXTL. The H atoms were included in calculated positions and treated as riding atoms using SHELXL default parameters. The non-H atoms were refined anisotropically using weighted full-matrix least-squares on F². A multiscan absorption correction was applied using the SADABS routine.

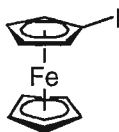
Isopropyllithium.¹²² To a dry flask under argon was added 50 mL dry pentane. Hammer-flattened lithium wire cut into chips (5.83 g, 840 mmol) was added, followed by addition of another 60 mL dry pentane. The mixture was heated to reflux, and 2-chloropropane (32 mL, 350 mmol) with *tert*-butyl methyl ether (0.42 mL, 3.5 mmol) was added dropwise to the refluxing solution over 2.5 hours. After addition was complete, the solution was allowed to cool to room temperature and precipitates allowed to settle (over 16 hours). The solution was transferred by cannula to a dry serum bottle and titrated to give a concentration of 1.85 mol/L.

Lithioferrocene (209). To a dry flask under argon was added ferrocene (20 g, 108 mmol) and dry THF (125 mL). The stirred solution was cooled to 0 °C and treated with *t*-BuLi (112 mL, 1.11 M, 124 mmol). After addition was complete, the solution was cooled to -78 °C and dry hexane (150 mL) was added causing precipitation of an orange solid. With sufficient stirring the suspension



was cannulated into a Schlenk filter, and washed with dry hexane (5 x 50 mL). The orange powder was dried under vacuum and then transferred to a Schlenk flask, affording 14.2 g of lithioferrocene (69%).

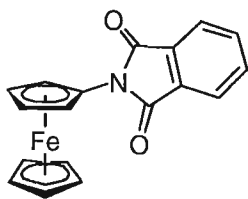
Iodoferrocene (210). To a dry flask containing lithioferrocene (14.2 g, 74 mmol) was



added dry THF (135 mL). The stirred solution was cooled to $-78\text{ }^{\circ}\text{C}$, and iodine (18.8 g, 74 mmol) was added in one portion under a stream of argon.

The solution was allowed to warm to room temperature over 2 h then diluted with ether (384 mL) and treated with saturated sodium thiosulfate. The layers were separated, the organic layer washed with water and brine, and then dried with MgSO_4 . The solution was filtered and the solvent removed *in vacuo*. The crude dark orange / yellow oil was dissolved in minimal hexanes, and passed through silica (50 mL) with hexanes. The solvent was removed *in vacuo* to yield 16.9 g (73%) of iodoferrocene as a dark orange semi-solid. ^1H NMR (300 MHz, CDCl_3) δ 4.42 (t, 1H), 4.38 (t, 1H), 4.20 (s, 5 H), 4.19 (t, 1H), 4.16 (t, 1H).

N-ferrocenyl phthalimide (211). To a dry flask containing iodoferrocene (16.9 g, 54

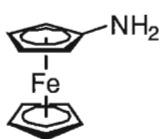


mmol) was added phthalimide (13.0 g, 88 mmol), copper oxide (3.78 g, 26 mmol), and pyridine (105 mL). The solution was heated at reflux for 48 hours, after which the pyridine was removed by

vacuum distillation. Hexane was added and the solution filtered through neutral alumina (200 mL) to remove unreacted iodoferrocene (1.38 g). Crude N-ferrocenyl phthalimide was obtained by flushing the alumina with Et_2O . The crude N-ferrocenyl phthalimide was

crystallized from absolute ethanol in two crops to yield 10.25 g (57%) of red needles. mp 161-164 °C; ^1H NMR (300 MHz, CDCl_3) δ 7.88 (m, 2H), 7.75 (m, 2H), 5.01 (t, 2 H, $J = 2.1$ Hz), 4.22 (s, 5 H), 4.20 (t, 2 H, $J = 1.8$ Hz).

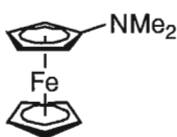
Aminoferrocene (212). Absolute EtOH (80 mL) in a dry flask was degassed for 10 min



with argon. **211** (5.5 g, 17 mmol) was added under a stream of argon, followed by hydrazine monohydride (32 mL, 7 mmol). The solution was heated to reflux for 2 hours, then cooled to room temperature, and water

was added. The solution was extracted with Et_2O until colourless. The combined organic layer was washed with water and brine, dried with Na_2SO_4 , filtered, and the solvent removed *in vacuo* to yield 3.3 g (98%) of aminoferrocene as a bright orange solid. mp 112-115 °C (sub); ^1H NMR (CDCl_3 , 300 MHz) δ 4.10 (s, 5 H), 3.99 (t, 2 H, $J = 1.8$ Hz), 3.84 (t, 2H, $J = 1.8$ Hz), 2.59 (bs, 2H).

N,N-dimethylaminoferrocene (192). To a dry flask containing aminoferrocene (2.0 g,

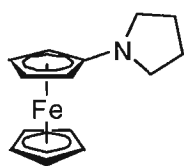


10 mmol), was added acetic acid (30 mL), paraformaldehyde (3.0 g, 10 mmol), and sodium cyanoborohydride (3.1 g, 5 mmol). The solution was stirred under argon for 18 h, after which water was added, and the

solution made basic with 6 M NaOH. Hexanes was added, the layers separated, and the aqueous layer extracted with hexanes. The combined organic layer was washed with water, brine, dried with Na_2SO_4 , filtered, and most of the solvent removed *in vacuo*. The solution was cooled to -20 °C to induce precipitation, and **192** (1.95 g, 86%) obtained as shiny orange flakes. mp 72-76 °C; ^1H NMR (300 MHz, CDCl_3) δ 4.26 (s, 5H), 3.94 (t,

2H, $J = 1.8$ Hz), 3.79 (t, 2H, $J = 1.8$ Hz), 2.59 (s, 6H); ^{13}C NMR (75.5 MHz, CDCl_3) δ 115.4, 66.8, 63.5, 55.1, 42.3.

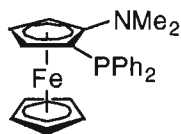
***N*-ferrocenyl pyrrolidine (213).** To a dry flask containing aminoferrocene (1.3 g, 6.5



mmol) in Et_2O (45 mL) was added a solution of succinic anhydride (0.65 g, 6.5 mmol) in THF (20 mL). The solution was allowed to stir under argon at room temperature for 3.5 h, after which solvent was removed *in vacuo*. To the crude oil was added a suspension of NaOAc (0.53 g, 6.5 mmol) in acetic anhydride (14 mL). The solution was heated at reflux for 30 min, then poured into ice cold saturated NaHCO_3 . The layers were separated, aqueous layer extracted with EtOAc until colourless. The combined organic layer was washed with water, brine, dried with Na_2SO_4 , filtered, and solvent removed *in vacuo*. Filtration of the preadsorbed crude oil through silica with 1:1 hexanes:EtOAc, followed by crystallization from 1:1 hexanes:EtOAc afforded *N*-ferrocenyl succinimide (1.45 g, 79%) as an orange solid. ^1H NMR (300 MHz, CDCl_3) δ 4.91 (t, $J = 1.8$ Hz, 2H), 4.19 (s, 5H), 4.16 (t, 2H, $J = 1.8$ Hz), 2.78 (s, 4H). To a dry flask under argon was added intermediate *N*-ferrocenyl succinimide (1.0 g, 3.5 mmol), dry THF (20 mL), and borane ($\text{BH}_3 \cdot \text{THF}$, 18 mL, 0.8 M in THF, 14.4 mmol). The solution was heated at reflux at which point a yellow precipitate formed. After refluxing for 2 h, the solution was cooled to room temperature, diluted with Et_2O , and 10 % NaOH was added until bubbling had ceased. The layers were separated, aqueous extracted with Et_2O (1 x 20 mL), combined organic washed with water (2 x 10 mL), brine, dried with Na_2SO_4 , filtered, and concentrated *in vacuo*. Filtration of the preadsorbed crude material through silica with 1:1 Et_2O :pentane afforded **213** (874 mg,

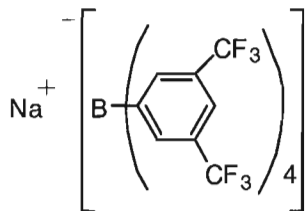
97%) as an orange yellow solid. mp 109-110 °C; ^1H NMR (300 MHz, CDCl_3) δ 4.18 (s, 5H), 3.89 (s, 2H), 3.71 (s, 2H), 2.97 (m, 4H), 1.94 (qn, 4H, $J = 3.3$ Hz).

2-diphenylphosphine-1-dimethylaminoferrocene (204). To a dry flask under argon



was added **192** (460 mg, 2.0 mmol) and dry THF (20 mL). The solution was cooled to 0 °C, treated with $\text{BF}_3 \cdot \text{OEt}_2$ (0.265 mL, 2.11 mmol) at which point a colour change from orange to yellow with precipitation of a yellow solid occurred, and allowed to stir at 0 °C for 15 min. The solution was cooled to -40 °C, treated with *n*-BuLi (1.27 mL, 2.21 mmol), and allowed to stir at -40 °C for 1 h. ClPPh_2 (440 μL , 2.41 mmol) was added at -40 °C and the solution was allowed to warm slowly to room temperature over 3.5 h, at which point the solution was diluted with Et_2O and saturated NaHCO_3 added. The layers were separated and the aqueous washed with Et_2O (1 x 10 mL). The combined organic layer was washed with water, brine, dried with Na_2SO_4 , filtered, and concentrated *in vacuo*. Filtration of the preadsorbed crude material through silica with Et_2O , followed by crystallization from Et_2O afforded **204** (534 mg, 64%) as orange needles in two crops. mp 146-148 °C; ^{31}P NMR (121.5 MHz, CDCl_3) δ -20.40; ^1H NMR (300 MHz, CDCl_3) δ 7.57-7.51 (m, 2H), 7.39-7.37 (m, 3H), 7.25 (m, 5H), 4.19 (q, 1H, $J = 1.8$ Hz), 4.12 (s, 5H), 4.08 (t, 1H, $J = 2.4$ Hz), 3.49 (t, 1H, $J = 1.5$ Hz), 2.68 (s, 6H); ^{13}C NMR (75 MHz, CDCl_3) δ 139.7 (d, $J^{13}\text{C}-^{31}\text{P} = 10.6$ Hz), 137.8 (d, $J^{13}\text{C}-^{31}\text{P} = 11.3$ Hz), 135.2 (d, $J^{13}\text{C}-^{31}\text{P} = 21.9$ Hz), 132.4 (d, $J^{13}\text{C}-^{31}\text{P} = 18.1$ Hz), 129.0, 128.0 (d), 127.8 (d), 118.9 (d, $J^{13}\text{C}-^{31}\text{P} = 18.1$ Hz), 68.6, 68.4 (d, $J^{13}\text{C}-^{31}\text{P} = 3.8$ Hz), 65.9 (d, $J^{13}\text{C}-^{31}\text{P} = 10.6$ Hz), 65.1, 60.1 (d, $J^{13}\text{C}-^{31}\text{P} = 3.0$ Hz), 45.4 (d, $J^{13}\text{C}-^{31}\text{P} = 9.1$ Hz).

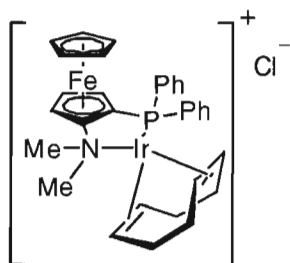
Sodium tetrakis[3,5-bis(trifluoromethyl)phenyl]borate (103). To a dry flask under



argon was added cleaned (acetone/HCl) Mg turnings (485 mg, 20 mmol), dry Et₂O (30 mL), dry NaBF₄ (338 mg, 3.1 mmol) and an iodine crystal. The solution was heated briefly to activate the Mg, and 3,5-bis(trifluoromethyl)bromobenzene (3

mL, 17.3 mmol) in Et₂O (20 mL) was added dropwise. The solution was then stirred at reflux and a colour change to dark tan / brown was observed. After 1 h, the solution was cooled to room temperature and allowed to stir for 16 h, over which a tan solid precipitated. The solution was slowly poured into a solution of Na₂CO₃ (24 g) in H₂O (100mL) and stirred for 20 min. The layers were separated, brine was added to the aqueous layer, and the aqueous layer was extracted with Et₂O (4 x 25 mL). The organic was dried with Na₂SO₄, treated with decolourizing charcoal, filtered, and concentrated *in vacuo*. The crude oil was dissolved in minimal hot CHCl₃, and product precipitated with hexanes. The solid was collected by filtration, washed with cold CHCl₃, and dried *in vacuo* to afford **103** (1.52 g, 56%) as a pale grey crystalline solid. mp >230 °C; ¹⁹F NMR (300 MHz, acetone-d₆) δ -63.3; ¹H NMR (300 MHz, acetone-d₆) δ 7.79 (t, 8H), 7.67 (s, 4H).

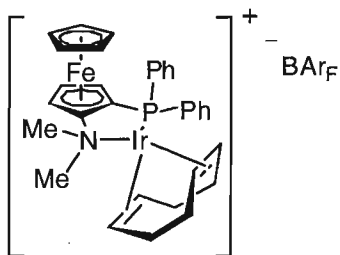
2-Diphenylphosphino-1-dimethylaminoferroceneiridium (cyclooctadiene)chloride



(220). To a dry flask under argon was added **204** (83 mg, 0.20 mmol), [Ir(COD)Cl]₂ (68 mg, 0.10 mmol), and CH₂Cl₂ (2.1 mL). The solution was stirred at reflux for 1 h and solvent removed *in vacuo* to afford **220** (150 mg, 99%) as an orange-yellow solid.

mp 122-125 °C (dec, CH₂Cl₂); IR (KBr) ν_{max} 3406, 3049, 2939, 2881, 2831, 2775, 1645, 1479, 1435, 1385, 1325, 1097, 1003, 822, 750, 696 cm⁻¹; ³¹P NMR (121.5 MHz, CDCl₃) δ 20.1; ¹H NMR (300 MHz, CDCl₃) δ 8.29 (t, 2H, *J* = 8.1 Hz), 8.01 (m, 2H), 7.48 (m, 3H), 7.38 (m, 3H), 4.33 (t, 1H, *J* = 3.9 Hz), 4.17 (t, 1H, *J* = 2.4 Hz), 3.92 (s, 5H), 3.68 (t, 1H, *J* = 1.2 Hz), 2.98 (s, 6H), 2.12 (m, 4H), 1.62 (m, 4H); FABMS [*m/z*(%)] 714 (M-Cl, 90), 712 (100); HRMS (FAB) calcd for C₃₂H₃₆NPFe¹⁹³Ir 714.1564, found 714.1500.

2-Diphenylphosphino-1-dimethylaminoferroceneiridium (cyclooctadiene) tetrakis(3,5-bis(trifluoromethyl)phenyl)borate (221).



Direct synthesis: To a dry flask containing NaBAR_F (45 mg, 0.051 mmol) was added distilled water (1 mL), CH₂Cl₂ (1 mL), and **220** (24 mg, 0.032 mmol). The solution was stirred vigorously for 15 min, layers separated, and aqueous layer extracted with CH₂Cl₂ (3 x 2 mL). The combined organic

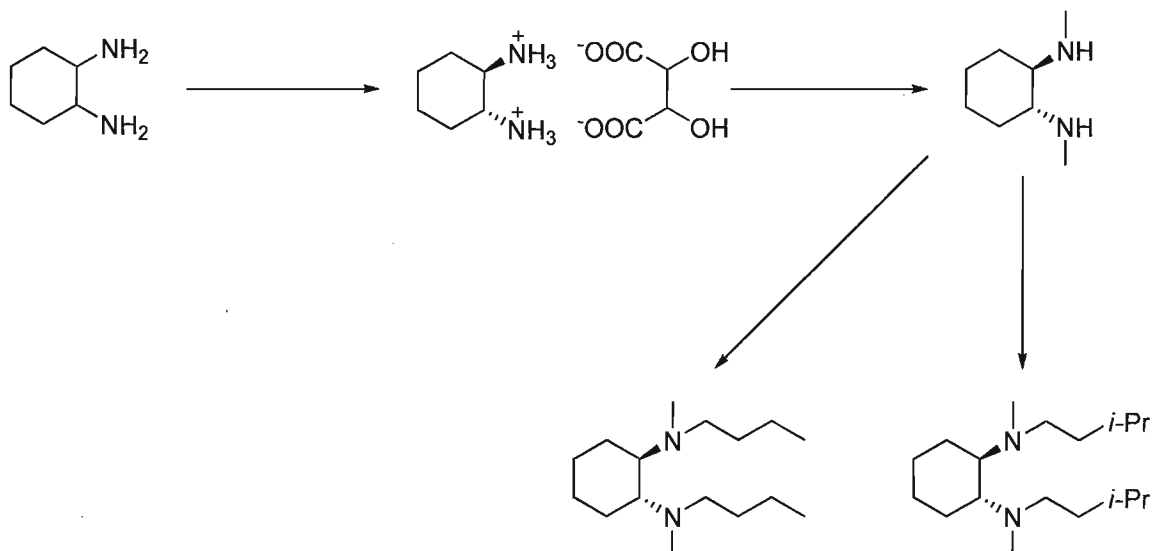
layer was washed with water (1 x 5 mL), and concentration *in vacuo*. Filtration through a plug of silica with CH₂Cl₂ provided **221** (42 mg, 83%) as a bright orange solid.

In situ synthesis: To a dry flask containing **204** (83 mg, 0.20 mmol) was added [Ir(COD)Cl]₂ (67 mg, 0.10 mmol), and CH₂Cl₂ (2.1 mL). After refluxing for 1 h, the solution was cooled to room temperature, and NaBAR_F (277 mg, 0.31 mmol) and 2.1 mL distilled water was added. After vigorous stirring for 15 min, the layers were separated, the aqueous layer extracted with CH₂Cl₂ (3 x 5 mL), and the combined organic layer washed with water (1 x 10 mL). The crude was concentrated *in vacuo*, and filtered through a plug of silica with CH₂Cl₂ to afford **221** (299 mg, 94%). mp 197-198 °C (dec,

benzene); IR(KBr) ν_{\max} 2958, 2925, 2891, 1610, 1439, 1356, 1279, 1169, 1126; ^{31}P NMR (121.5 MHz, CDCl_3) δ 14.95; ^{19}F NMR (282.4 MHz, CDCl_3) δ -62.34; ^1H NMR (300 MHz, CDCl_3) δ 7.75-7.72 (m, 2H), 7.72 (s, 8H), 7.58-7.54 (m, 4H), 7.53 (s, 4H), 7.46-7.40 (m, 4H), 5.03 (m, 1H), 4.90 (t, 1H, $J = 2.7$ Hz), 4.57 (m, 1H), 4.47 (s, 1H), 4.41 (s, 1H), 4.31 (s, 5H), 4.05 (m, 1H), 3.51 (m, 1H), 3.12 (s, 3H), 2.69 (s, 3H), 2.40-2.33 (m, 2H), 2.30-2.24 (m, 2H), 2.04 (m, 1H), 1.92-1.90 (m, 2H), 1.78-1.74 (m, 1H); ^{13}C NMR (75.5 MHz, CDCl_3) δ 161.7 (q, $J^{13}\text{C}-^{11}\text{B} = 49.8$ Hz, B-C BArF), 134.8 (2 x *ortho*-BArF), 132.6 (d, $J^{13}\text{C}-^{31}\text{P} = 51.3$ Hz, Ph-P), 132.5 (d, $J^{13}\text{C}-^{31}\text{P} = 4.5$ Hz, *meta*-Ph), 132.4 (d, *meta*-Ph), 132.1 (d, $J^{13}\text{C}-^{31}\text{P} = 1.5$ Hz, *para*-Ph), 131.7 (d, $J^{13}\text{C}-^{31}\text{P} = 1.5$ Hz, *para*-Ph), 129.6 (d, $J^{13}\text{C}-^{31}\text{P} = 10.6$ Hz, *ortho*-Ph), 129.5 (d, $J^{13}\text{C}-^{31}\text{P} = 12.1$ Hz, *ortho*-Ph), 128.9 (2 x q, $J^{13}\text{C}-^{19}\text{F} = 30.8$ Hz, *meta*-BArF), 127.4 (d, $J^{13}\text{C}-^{31}\text{P} = 60.4$ Hz, Ph-P), 124.5 (2 x q, $J^{13}\text{C}-^{19}\text{F} = 271.6$ Hz, BArF CF_3), 124.1 (d, $J^{13}\text{C}-^{31}\text{P} = 24.1$ Hz, 1-Cp-N), 117.5 (para BArF), 92.7 (d, $J^{13}\text{C}-^{31}\text{P} = 12.1$ Hz, COD alkene – *trans*-P), 91.3 (d, $J^{13}\text{C}-^{31}\text{P} = 12.1$ Hz, COD alkene – *trans*-P), 74.6 (d, $J^{13}\text{C}-^{31}\text{P} = 6.0$ Hz, 5-Cp sub), 72.0 (Cp unsub), 70.2 (d, $J^{13}\text{C}-^{31}\text{P} = 57.3$ Hz, 2-Cp-P), 65.5 (4-Cp sub), 60.7 (COD alkene – *trans*-N), 60.5 (COD alkene – *trans*-N), 58.4 (d, $J_{3\text{C}-31\text{P}} = \text{Hz}$, 3-Cp sub), 57.6 (NMe), 50.5 (NMe), 32.3 (COD), 32.2 (COD), 29.6 (COD), 29.4 (COD); FABMS [m/z , (%)] 714 (M-BArF, 100); HRMS (FAB) calcd for $\text{C}_{32}\text{H}_{36}\text{NP}^{56}\text{Fe}^{193}\text{Ir}$ 714.1564, found 714.1502. Anal. Calcd for $\text{C}_{64}\text{H}_{48}\text{BF}_{24}\text{FeNP}^{56}\text{Ir}$: C, 48.75; H, 3.07. Found: C, 48.79; H, 2.98; X-ray crystallographic analysis was performed on an orange block (0.30 x 0.26 x 0.04 mm³): $\text{C}_{64}\text{H}_{48}\text{BF}_{24}\text{FeNP}^{56}\text{Ir}$: M = 1576.86 g/mol, triclinic, $P\bar{1}$, $a = 12.7697(6)$ Å, $b = 12.8455(6)$ Å, $c = 19.8377(10)$ Å, $V = 3045.8(3)$ Å³, $\alpha = 74.724(2)^\circ$, $\beta = 76.026(3)^\circ$, $\gamma = 87.188(2)^\circ$, $Z = 2$, $D_c = 1.719$ g/cm³, $F(000) = 1556$, $T = 150(2)$ K. Data were collected on a Bruker Kappa Apex II area detector system with

graphite monochromated Mo K α radiation ($\lambda = 0.71073 \text{ \AA}$); 81694 data were collected. The structure was solved by Direct Methods (SHELXTL) and refined by full-matrix least squares on F^2 resulting in final R, R_w and GOF [for 15144 data with $F > 2\sigma(F)$] of 0.0352, 0.0985 and 1.133, respectively.

(1*R*,2*R*)-*N*¹,*N*²-diisopentyl-*N*¹,*N*²-dimethylcyclohexane-1,2-diamine (229).¹²³



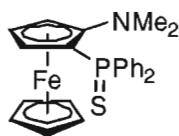
To a flask containing *L*-tartrate (12.5 g, 83.4 mmol) in distilled H₂O (45 mL) was added *trans*-1,2-cyclohexanediamine (20 mL, 184.4 mmol) dropwise over 30 min resulting in heat evolution (to ~ 40 °C) and production of a white precipitate. Glacial acetic acid (5 mL) was added dropwise over 15 min resulting in a temperature increase to 40 °C. This solution was allowed to cool to room temperature over 4 h, stirred at 0 °C for 2 h, then placed in the fridge (at 2-4 °C) for ~12 h to crystallize. White crystals were filtered, washed once with H₂O (20 mL), then with MeOH (5 x 10 mL – filtrates collected into separate receiving flasks), and dried *in vacuo* to give (*R,R*)-1,2-cyclohexanediamine tartrate salt (15.5 g, 64%). $[\alpha]_D^{20} +12.6$ (c 4.0, H₂O). To a stirred solution of the salt (15.5

g, 58.7 mmol) in toluene (75 mL) at 0 °C was simultaneously added a solution of NaOH (18.8 g, 469 mmol) in distilled H₂O (35 mL) and methylchloroformate (9.56 mL, 124 mmol). The solution was allowed to warm to room temperature, then stirred open to air. After 48 h, CHCl₃ (75 mL) was added, the solid filtered off, and washed with CHCl₃ (3 x 25 mL). H₂O (40 mL) was added to the filtrate, the layers separated, and aqueous extracted with CHCl₃ (2 x 75 mL). The combined organic phase was dried with K₂CO₃, filtered, and solvent removed *in vacuo* to give carbamate intermediate (12.82 g, 95%). To a flask containing LiAlH₄ under Ar was added dry THF (100 mL) and the suspension cooled to 0 °C, and a solution of carbamate intermediate (12.82 g, 55.7 mmol) in dry THF (125 mL) was added dropwise over 2.25 hours. The solution was allowed to warm to room temperature over 1 h then heated to reflux. After stirring at reflux for 40 h, the solution was cooled to room temperature, placed in an ice bath at 0 °C, diluted with Et₂O (100 mL), and saturated Na₂SO₄ was added dropwise until residual LiAlH₄ was quenched (~50 mL). The solution was allowed to warm to room temperature, and filtered through celite washing with 24:1 CH₂Cl₂:MeOH (2 x 75 mL). The filtrate was dried with K₂CO₃, filtered, and solvent removed *in vacuo* to provide (1*R*,2*R*)-*N*¹,*N*²-dimethylcyclohexane-1,2-diamine as a yellow oil (6.8 g, 82%). ¹H NMR (300 MHz, CDCl₃) δ 2.39 (s, 6H), 2.12 (m, 1H), 2.08 (m, 1H), 2.03-1.99 (m, 2H), 1.74-1.69 (m, 2H), 1.41 (bs, 2H), 1.26-1.18 (m, 2H), 1.00-0.89 (m, 2H); ¹³C NMR (75.5 MHz, CDCl₃) δ 63.3, 33.7, 30.9, 25.1. To a flask containing *N*¹,*N*²-dimethyl diamine (6.8 g, 47.8 mmol) in MeOH (100 mL) was added butyraldehyde (12.9 mL, 144 mmol), sodium cyanoborohydride (12.0 g, 191 mmol), and glacial acetic acid (2.75 mL, 48.1 mmol). After stirring at room temperature for 24 h, the MeOH was removed *in vacuo*, crude redissolved in Et₂O (100 mL), washed

with 10% NaOH (2 x 30 mL), H₂O (30 mL), and brine (30 mL), dried with Na₂SO₄, filtered, and solvent removed *in vacuo* to give crude diamine (12.6 g) as a yellow oil. Kugelrohr distillation (110 °C, 0.5 mmHg) provided pure diamine **229** (11.3 g, 93%) as a colourless oil. $[\alpha]_D^{20}$ -27.8 (*c* 1.0, CHCl₃); ¹H NMR (300 MHz, CDCl₃) δ 2.53-2.39 (m, 6H), 2.23 (s, 6H), 1.79-1.68 (m, 4H), 1.49-1.37 (m, 4H), 1.36-1.26 (m, 4H), 1.19-1.07 (m, 4H), 0.90 (t, 6 H, *J* = 7.2 Hz).

(1R,2R)-N¹,N²-dibutyl-N¹,N²-dimethylcyclohexane-1,2-diamine (191). To a solution of (1R, 2R)-N¹,N²-dimethylcyclohexane-1,2-diamine (1.5 g, 10.5 mmol) in MeOH (25 mL) under Ar was added isovaleraldehyde (3.4 mL, 32 mmol), sodium cyanoborohydride (2.6 g, 42 mmol), and glacial acetic acid (0.60 mL, 10.5 mmol). After stirring at room temperature for 24 h, the MeOH was removed *in vacuo*, crude redissolved in Et₂O (25 mL), washed with 10% NaOH (2 x 20 mL), H₂O (20 mL), and brine (20 mL), dried with Na₂SO₄, filtered, and solvent removed *in vacuo* to give crude diamine (3.0 g) as a yellow oil. Kugelrohr distillation (115 °C, 0.2 mmHg) provided pure diamine **191** (2.9 g, 97%) as a colourless oil. $[\alpha]_D^{20}$ -27.2 (*c* 1.0, CHCl₃); ¹H NMR (300 MHz, CDCl₃) δ 2.56-2.39 (m, 6H), 2.23 (s, 6H), 1.79-1.68 (m, 4H), 1.61-1.53 (m, 2H), 1.38-1.29 (m, 4H), 1.11-1.07 (m, 4H), 0.89 (d, 6H, *J* = 1.5 Hz), 0.87 (d, 6H, *J* = 1.5 Hz); ¹³C NMR (300 MHz, CDCl₃) δ 63.1, 52.8, 37.9, 36.9, 26.7, 26.1, 25.7, 23.2, 22.9.

2-diphenylphosphinothionyl-1-dimethylaminoferrocene (230). A solution of (*R,R*)-

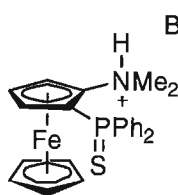


229 (390 mg, 1.38 mmol) in *t*-BuOMe (3 mL) was cooled to -40 °C, treated sequentially with *i*-PrLi (2.23 mL, 1.85 M in pentane, 4.13 mmol) and dimethylaminoethanol (124 mg, 1.39 mmol) in *t*-BuOMe (3 mL),

and stirred for 20 min at that temperature. The solution was transferred by cannula to a mixture of **192**·BF₃ at –78 °C [prepared by addition of BF₃·OEt₂ (175 µL, 1.39 mmol) to a solution of **192** (300 mg, 1.31 mmol) in *t*-BuOMe (13 mL) at 0 °C and stirring for 10 min]. The mixture was allowed to warm slowly to –40 °C over approximately 2 h and then held at that temperature for an additional hour. After cooling back to –78 °C, ClPPh₂ (600 µL, 3.27 mmol) was added and the mixture was allowed to warm slowly to room temperature. The reaction mixture was diluted with Et₂O and worked-up by addition of saturated aqueous NaHCO₃. The aqueous layer was extracted with Et₂O (3 x 15 mL) and the combined organic extract was washed with H₂O (1 x 15 mL), brine (1 x 15 mL), dried over anhydrous Na₂SO₄ and concentrated under reduced pressure *in vacuo* to afford the crude aminophosphine. To the crude material in a dry round bottom flask under argon was added sulfur powder (1.59 g, 49.6 mmol) and toluene (25 mL), and the mixture was heated at 40 °C for 2 h. After cooling to room temperature, the reaction mixture was gravity filtered to remove excess sulfur and the filtrate was pre-adsorbed on silica gel *in vacuo*. Flash column chromatography (silica gel, 9:1 pentane:Et₂O) gave **230** (285 mg, 50%) as an orange foam. $[\alpha]_D^{20} +38.5$ (*c* 1.0, CHCl₃); CSP HPLC analysis (Chiralcel OD-H; eluent: 99:1 hexane:*i*-PrOH, 1.0 mL/min) determined an 88.9:11.1 er (78% ee) [*t*_R(minor) = 6.7 min, *t*_R(major) = 7.2 min]; IR (KBr) ν_{max} 3394, 2950, 2788, 1494, 1419; ³¹P NMR (121.5 MHz, CDCl₃) δ 44.21; ¹H NMR (300 MHz, CDCl₃) δ 8.00-7.88 (m, 2H), 7.79-7.71 (m, 2H), 7.48-7.36 (m, 6H), 4.33 (s, 5H), 4.29 (s, 1H), 4.13 (s, 1H), 3.81 (s, 1H), 2.50 (s, 6H); ¹³C NMR (75.5 MHz, CDCl₃) δ 135.4 (d, $J^{13}_C-^{31}_P$ = 87.6 Hz), 133.5 (d, $J^{13}_C-^{31}_P$ = 86.8 Hz), 132.6 (d, $J^{13}_C-^{31}_P$ = 10.6 Hz), 131.8 (d, $J^{13}_C-^{31}_P$ = 10.6 Hz), 131.1 (d, $J^{13}_C-^{31}_P$ = 2.3 Hz), 130.8 (d, $J^{13}_C-^{31}_P$ = 2.3 Hz), 127.9 (d, $J^{13}_C-^{31}_P$ = 12.8 Hz), 127.9 (d,

$J^{13}\text{C}-^{31}\text{P} = 12.8 \text{ Hz}$), 117.2 (d, $J^{13}\text{C}-^{31}\text{P} = 9.1 \text{ Hz}$), 72.3 (d, $J^{13}\text{C}-^{31}\text{P} = 13.6 \text{ Hz}$), 69.9, 67.1 (d, $J^{13}\text{C}-^{31}\text{P} = 92.9 \text{ Hz}$), 65.3 (d, $J^{13}\text{C}-^{31}\text{P} = 11.3 \text{ Hz}$), 61.8 (d, $J^{13}\text{C}-^{31}\text{P} = 8.3 \text{ Hz}$), 46.0; EIMS [m/z(%)] 445 (M^+ , 100), 413 (32); HRMS (EI) calcd for $\text{C}_{24}\text{H}_{24}\text{NPS}^{56}\text{Fe}$: 445.0716; found 445.0716. Anal. Calcd for $\text{C}_{24}\text{H}_{24}\text{NPSFe}$: C, 64.73; H, 5.43. Found: C, 64.79; H, 5.44.

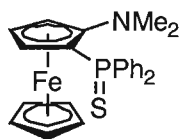
(S)-(-)-[2-(Diphenylphosphinothiyl)ferrocenyl]-1-dimethylammonium



tetrafluoroborate ((S)-230·HBF₄). A solution of aminophosphine sulfide **230** (131 mg, 0.29 mmol) in diethyl ether (13 mL) at 0 °C was treated with tetrafluoroboric acid-diethyl ether complex (50 μL , 0.38 mmol). An immediate change in color from orange to yellow was observed, and a yellow powder precipitated out of solution. The solid was collected by suction filtration, washed with cold Et_2O , and dried *in vacuo* to afford ammonium salt (S)-**230**·HBF₄ as a yellow powder (155 mg, 99%). mp 115-117°C; $[\alpha]_{\text{D}}^{20} -76.0$ (c 1.0, CHCl_3); IR (KBr) ν_{max} 3449, 3369, 3051, 2923, 1436, 1100, 1053, 751, 714 cm^{-1} ; ^{31}P NMR (121.5 MHz, CDCl_3) δ 37.7; ^1H NMR (300 MHz, CDCl_3) δ 11.03 (s, 1H), 7.94-7.87 (m, 2H), 7.68-7.55 (m, 6H), 7.52-7.50 (m, 2H), 5.52 (s, 1H), 4.73 (s, 6H), 4.31 (s, 6H), 3.63 (d, 3H, $J = 5.4 \text{ Hz}$), 2.90 (d, 3H, $J = 5.1 \text{ Hz}$); ^{13}C NMR (150.9 MHz, acetone- d_6) δ 134.4 (d, $J^{13}\text{C}-^{31}\text{P} = 87.6 \text{ Hz}$), 133.8, 133.4, 132.8 (d, $J^{13}\text{C}-^{31}\text{P} = 12.1 \text{ Hz}$), 132.0 (d, $J^{13}\text{C}-^{31}\text{P} = 10.6 \text{ Hz}$), 130.8 (d, $J^{13}\text{C}-^{31}\text{P} = 95.1 \text{ Hz}$), 130.1 (d, $J^{13}\text{C}-^{31}\text{P} = 12.1 \text{ Hz}$), 129.8 (d, $J^{13}\text{C}-^{31}\text{P} = 12.1 \text{ Hz}$), 109.1 (d, $J^{13}\text{C}-^{31}\text{P} = 37.8 \text{ Hz}$), 73.8 (d, $J^{13}\text{C}-^{31}\text{P} = 10.6 \text{ Hz}$), 73.4, 71.0 (d, $J^{13}\text{C}-^{31}\text{P} = 9.8 \text{ Hz}$), 66.3 (d, $J^{13}\text{C}-^{31}\text{P} = 93.6 \text{ Hz}$), 66.2 (d, $J^{13}\text{C}-^{31}\text{P} = 5.3 \text{ Hz}$), 50.7, 46.8; FABMS [m/z(%)] 446 (M^+ , 100), 229 (87) HRMS (FAB) calcd for $\text{C}_{24}\text{H}_{25}\text{NPS}^{56}\text{Fe}$: 446.0794; found 446.0789; Anal. Calcd for

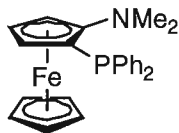
$C_{24}H_{25}NPSFeBF_4$: C, 54.07; H, 4.73. Found: C, 54.36; H, 4.75. Two recrystallizations via liquid-liquid diffusion of Et_2O into a solution of (*S*)-**230**· HBF_4 in CH_2Cl_2 rendered the salt as enantiomerically pure orange rod-shaped crystals. mp >225 °C (dec); $[\alpha]_D^{20}$ -94.9 (*c* 1.0, acetone); X-ray crystallographic analysis was performed on an orange block (0.33 x 0.23 x 0.21 mm³): $C_{24}H_{25}BF_4FeNPS$: *M* = 533.14 g/mol, orthorhombic, $P2_12_12_1$, *a* = 10.3605(13) Å, *b* = 12.6260(16) Å, *c* = 17.967(2) Å, *V* = 2350.3(5) Å³, $\alpha = \beta = \gamma = 90^\circ$, *Z* = 4, *D_c* = 1.507 g/cm³, *F*(000) = 1096, *T* = 100(2) K. Data were collected on a Bruker APEX CCD system with graphite monochromated Mo $K\alpha$ radiation (λ = 0.71073 Å); 35112 data were collected. The structure was solved by Direct Methods (SHELXTL) and refined by full-matrix least squares on *F*² resulting in final *R*, *R_w* and GOF [for 6435 data with *F* > 2σ(*F*)] of 0.0238, 0.0578 and 1.021, respectively, for solution using the *S* enantiomer model [Flack parameter = 0.000(7)].

(*S*)-(+)-2-diphenylphosphinothionyl-1-dimethylaminoferrocene ((*S*)-**230**). A flask



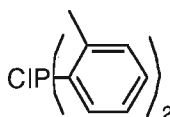
containing a biphasic suspension of recrystallized salt (*S*)-**230**· HBF_4 (140 mg, 0.26 mmol) in sat. aqueous $NaHCO_3$ and diethyl ether was sonicated for 1 min or until all the solid dissolved. The layers were separated and the aqueous phase was washed once with diethyl ether. The combined ether layer was washed with water, brine, dried over anhydrous Na_2SO_4 , filtered and concentrated *in vacuo* to give (*S*)-**230** (116 mg, 99%). mp 120-122 °C; $[\alpha]_D^{20}$ +62.4 (*c* 0.85, $CHCl_3$); CSP HPLC analysis (Chiralcel OD-H; eluent: 99:1 hexane:*i*-PrOH, 1.0 mL/min) determined a 99.7:0.3 er (>99% ee) [*t_R*(minor) 6.7 min, *t_R*(major) 7.4 min].

(S)-(-)-2-diphenylphosphino-1-dimethylaminoferrocene ((S)-204). Acetonitrile (25



mL) was added to freshly activated Ni-Al catalyst [(1.44 g, 16.8 mmol, activated by portion-wise addition to 25 mL 6 M NaOH and heating at 50 °C for 1 h, followed by washing the residue with H₂O (7 x 10 mL), MeOH (3 x 10 mL), Et₂O (2 x 10 mL) and MeCN (2 x 10 mL)] and aminophosphine sulfide **230** (150 mg, 0.34 mmol) in a round bottom flask under argon, and the mixture was heated to 60 °C for 3 h. The reaction mixture was allowed to cool to room temperature and filtered through a pad of Celite, washing with acetonitrile. Removal of the solvent afforded (S)-**204** as an orange semi-solid (118 mg, 85%) having spectroscopic data matching the racemate. $[\alpha]_D^{20} -213$ (*c* 0.81, CHCl₃).

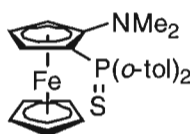
Chlorodi(ortho-tolyl)phosphine.¹²⁴ To a refluxing solution of Mg turnings (4.57 g, 188



mmol) in dry THF (25 mL) was added dropwise a solution of ortho-chlorotoluene (20 mL, 171 mmol) in dry THF (25 mL) over 1.5 hours. The solution was allowed to reflux under argon overnight (approximately 20 hours). To a solution of PCl₃ (6.75 mL, 77.2 mmol) in dry THF (150 mL) at -78 °C was added dropwise to the preformed Grignard solution. The solution was allowed to warm slowly to room temperature and then stirred at room temperature overnight (approximately 24 hours total) after which the solution was heated to reflux for 1.5 hours. At this point, a large amount of white precipitate formed. The solution was allowed to cool to room temperature, THF was removed *in vacuo*, and benzene (150 mL) was added. The mixture was filtered (to remove Mg salts), and concentrated *in vacuo*. Kugelrohr distillation (120-125 °C, 0.45 mmHg) provided the desired chlorophosphine (15.0 g, 78%) as a white solid.

^{31}P NMR (121.5 MHz, CDCl_3) δ 73.6; ^1H NMR (300 MHz, CDCl_3) δ 7.45 (q, 2H, $J = 5.1$ Hz), 7.34 (t, 2H, $J = 7.5$ Hz), 7.22 (m, 4H); 2.49 (d, 6H, $J = 2.1$ Hz) ^{13}C NMR (75.5 MHz, CDCl_3) δ 141.5 (d, $J^{13}\text{C}-^{31}\text{P} = 31.0$ Hz), 135.5 (d, $J^{13}\text{C}-^{31}\text{P} = 35.5$ Hz), 131.5 (d, $J^{13}\text{C}-^{31}\text{P} = 3.0$ Hz), 130.3, 130.3 (d, $J^{13}\text{C}-^{31}\text{P} = 3.8$ Hz), 126.5, 20.6 (d, $J^{13}\text{C}-^{31}\text{P} = 24.2$ Hz).

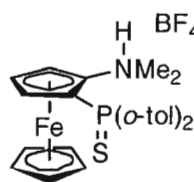
2-bis[(*ortho*-tolyl)phosphinothionyl]-1-dimethylaminoferrocene (231). A solution of



(*R,R*)-**191** (235 mg, 0.922 mmol) in *t*-BuOMe (4.5 mL) was cooled to –40 °C, treated sequentially with *i*-PrLi (1.25 mL, 2.25 M in pentane, 2.81 mmol) and dimethylaminoethanol (86 mg, 0.970 mmol) in *t*-BuOMe (4.5 mL), and stirred for 20 min at that temperature. The solution was transferred by cannula to a mixture of **192**·BF₃ at –78 °C [prepared by addition of BF₃·OEt₂ (115 μL , 0.917 mmol) to a solution of **192** (200 mg, 0.873 mmol) in *t*-BuOMe (13 mL) at 0 °C and stirring for 10 min]. The mixture was allowed to warm slowly to –40 °C over approximately 2.5 h and then held at that temperature for an additional hour. After cooling back to –78 °C, ClP(*o*-tolyl)₂ (548 mg, 2.20 mmol) in 4 mL *t*-BuOMe was added and the mixture was allowed to warm slowly to room temperature. The reaction mixture was diluted with Et₂O and worked-up by addition of saturated aqueous NaHCO₃. The aqueous layer was extracted with Et₂O (3 x 10 mL) and the combined organic extract was washed with H₂O (1 x 10 mL), brine (1 x 10 mL), dried over anhydrous Na₂SO₄ and concentrated under reduced pressure *in vacuo* to afford the crude aminophosphine. Flash column chromatography (silica gel, 9:1 hexanes:EtOAc) gave **205** (232 mg, 60%) as an orange semi-solid. ^{31}P NMR (75.5 MHz, CDCl_3) δ –39.8; ^1H NMR (300 MHz, CDCl_3) δ 7.16–6.94 (m, 8H), 4.23 (s, 1H), 4.11 (s, 6H), 3.62 (s, 1H), 2.90 (s, 3H), 2.67 (s, 6 H),

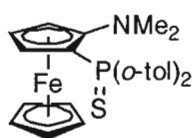
2.11 (s, 3H). To **205** (254 mg, 0.576 mmol) in a dry round bottom flask under argon was added sulfur powder (185 g, 57.6 mmol) and toluene (6 mL), and the mixture was heated at 40 °C for 2 h. After cooling to room temperature, the reaction mixture was gravity filtered to remove excess sulfur and the filtrate was pre-adsorbed on silica gel *in vacuo*. Flash column chromatography (silica gel, 9:1 hexanes:Et₂O) gave **231** (321 mg, 99%) as an orange foam. mp 60-64 °C; [α]_D²⁰ +31.7 (*c* 1.0, CHCl₃); CSP HPLC analysis (Chiralcel OD-H; eluent: 99:1 hexane:*i*-PrOH, 1.0 mL/min) determined an 88.0:12.0 er (76% ee) [*t*_R(minor) = 5.8 min, *t*_R(major) = 6.3 min]; IR (KBr) ν_{max} 3097, 3055, 2951, 2925, 2854, 2783, 1732, 1591, 1566, 1493, 1454, 1421, 1383, 1327, 1276, 1146, 1107, 1055, 1006, 819, 756, 713, 687, 647, 609, 581, 532, 474 cm⁻¹; ³¹P NMR (121.5 MHz, CDCl₃) δ 43.8; ¹H NMR (300 MHz, CDCl₃) δ 8.69-8.63 (m, 1H), 7.88-7.81 (m, 1H), 7.45-7.42 (m, 2H), 7.21-7.10 (m, 4H), 4.40 (s, 6H), 4.08 (s, 1H), 3.73 (s, 1H), 2.79 (s, 6H), 2.12 (s, 3H), 1.85 (s, 3H); ¹³C NMR (75.5 MHz, CHCl₃) δ 141.3 (d, $J^{13}\text{C}-^{31}\text{P}$ = 10.6 Hz), 140.4 (d, $J^{13}\text{C}-^{31}\text{P}$ = 8.3 Hz), 134.7 (d, $J^{13}\text{C}-^{31}\text{P}$ = 13.6 Hz), 134.2, 133.1, 132.7 (d, $J^{13}\text{C}-^{31}\text{P}$ = 12.1 Hz), 131.8 (d, $J^{13}\text{C}-^{31}\text{P}$ = 10.6 Hz), 131.5 (d, $J^{13}\text{C}-^{31}\text{P}$ = 15.1 Hz), 131.4 (d, $J^{13}\text{C}-^{31}\text{P}$ = 9.8 Hz), 130.9 (d, $J^{13}\text{C}-^{31}\text{P}$ = 3.0 Hz), 126.0 (d, $J^{13}\text{C}-^{31}\text{P}$ = 13.6 Hz), 125.5 (d, $J^{13}\text{C}-^{31}\text{P}$ = 12.8 Hz), 117.9 (d, $J^{13}\text{C}-^{31}\text{P}$ = 8.3 Hz), 72.0 (d, $J^{13}\text{C}-^{31}\text{P}$ = 13.6 Hz), 69.8, 66.0 (d, $J^{13}\text{C}-^{31}\text{P}$ = 28.7 Hz), 64.9 (d, $J^{13}\text{C}-^{31}\text{P}$ = 11.3 Hz), 64.1 (d, $J^{13}\text{C}-^{31}\text{P}$ = 8.3 Hz), 46.7, 22.5 (d, $J^{13}\text{C}-^{31}\text{P}$ = 3.8 Hz), 21.5 (d, $J^{13}\text{C}-^{31}\text{P}$ = 5.3 Hz); EIMS [*m/z*(%)] 473 (M⁺, 100), 441 (21); HRMS (EI) calcd for C₂₆H₂₈NPS⁵⁶Fe: 473.1029; found 473.1032; Anal. calcd for C₂₆H₂₈NPSFe: C, 65.97; H, 5.96. Found: C, 65.74; H, 5.97.

(S)-(-)-{2-[bis(*ortho*-tolyl)phosphino]ferrocenyl}-1-dimethylammonium



tetrafluoroborate ((S)-231**·HBF₄).** A solution of **231** (190 mg, 0.401 mmol) in Et₂O (20 mL) at 0 °C open to air was treated with HBF₄·Et₂O (66 μL, 0.485 mmol). An immediate colour change was observed with precipitation of a yellow powder. The solution was allowed to stir for 10 minutes, after which the solid was collected by suction filtration, washed with cold Et₂O, and dried *in vacuo* to afford ammonium salt (S)-**231**·HBF₄ (210 mg, 93%) as a yellow powder. mp 137-139°C; [α]_D²⁰ -46.9 (c 0.5, acetone); IR (KBr, thin film) ³¹P NMR (121.5 MHz, CDCl₃) δ 38.8; ¹H NMR (300 MHz, CDCl₃) δ 11.60 (bs, 1H), 8.84-8.79 (m, 1H), 7.62 (m, 3H), 7.46-7.42 (m, 1H), 7.26 (m, 2H), 7.05-6.97 (m, 1H), 5.59 (s, 1H), 4.78 (s, 1H), 4.28 (s, 6H), 3.66 (d, 3H, *J* = 4.8 Hz), 3.12 (d, 3H, *J* = 4.5 Hz), 2.21 (s, 3H), 1.94 (s, 3H); ¹³C NMR (75.5 MHz, acetone-d₆) δ 142.1 (d, *J*¹³C-³¹P = 10.6 Hz), 140.9 (d, *J*¹³C-³¹P = 9.1 Hz), 135.8 (d, *J*¹³C-³¹P = 15.1 Hz), 134.2 (d, *J*¹³C-³¹P = 3.0 Hz), 134.1 (d, *J*¹³C-³¹P = 55.1 Hz), 133.5 (d, *J*¹³C-³¹P = 4.5 Hz), 133.4 (2 x d), 131.6 (d, *J*¹³C-³¹P = 11.3 Hz), 128.2 (d, *J*¹³C-³¹P = 53.6 Hz), 127.6, 127.4, 109.6 (d, *J*¹³C-³¹P = 9.8 Hz), 73.6, 72.4 (d, *J*¹³C-³¹P = 9.1 Hz), 71.3 (d, *J*¹³C-³¹P = 9.8 Hz), 67.3 (d, *J*¹³C-³¹P = 67.3 Hz), 66.5 (d, *J*¹³C-³¹P = 6.8 Hz), 50.2, 47.6, 22.8 (d, *J*¹³C-³¹P = 3.0 Hz), 20.9 (d, *J*¹³C-³¹P = 6.0 Hz); FABMS [*m/z*(%)] 474 (M-BF₄, 100), 229 (94), HRMS (FAB) calcd for C₂₆H₂₉NPS⁵⁶Fe: 474.1107; found 474.1072; All attempts at enriching the salt by recrystallization were unsuccessful.

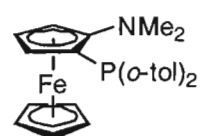
(S)-(+)-2-bis[(*ortho*-tolyl)phosphinothionyl]-1-dimethylaminoferrocene ((S)-231**).** A



flask containing a biphasic suspension of (S)-**231**·HBF₄ (190 mg, 0.34 mmol) in Et₂O (10 mL) and 1M NaHCO₃ (7 mL) was sonicated for 1

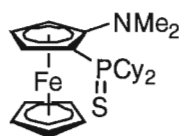
min or until all the solid dissolved. The layers were separated and the aqueous phase was extracted with diethyl ether. The combined ether layer was washed with water, brine, dried over anhydrous Na_2SO_4 , filtered and concentrated *in vacuo*, then filtered through a plug of silica with 7:3 hexanes:EtOAc to give (*S*)-**231** (113 mg, 71%) as an orange semi-solid. $[\alpha]_{\text{D}}^{20} +31.3$ (*c* 0.5, CHCl_3); CSP HPLC analysis (Chiralcel OD-H; eluent: 99:1 hexane:*i*-PrOH, 1.0 mL/min) determined an 88.4:11.6 er (77% ee) [$t_{\text{R}}(\text{minor}) = 5.6$ min, $t_{\text{R}}(\text{major}) = 6.1$ min].

(*S*)-(-)-2-bis[(*ortho*-tolyl)phosphino]-1-dimethylaminoferrocene ((*S*)-205**).**

 Acetonitrile (20 mL) was added to freshly activated Ni-Al catalyst [(814 mg, 9.51 mmol, activated by portion-wise addition to 14 mL 6 M NaOH and heating at 50 °C open to air for 1 h, followed by washing with H_2O (7 x 10 mL), MeOH (3 x 10 mL), Et_2O (2 x 10 mL) and MeCN (2 x 10 mL)] and aminophosphine sulfide **231** (90 mg, 0.19 mmol) in a round bottom flask under argon, and the mixture was heated to 60 °C for 2 h. The reaction mixture was allowed to cool to room temperature and filtered through a pad of Celite, washing with acetonitrile. Flask chromatography (silica, 9:1 hexanes: Et_2O) afforded (*S*)-**205** as an orange solid (85 mg, 99%). mp 115-118 °C; $[\alpha]_{\text{D}}^{20} -133.4$ (*c* 0.5, CHCl_3); IR (KBr) ν_{max} 3052, 2950, 1923, 2843, 2778, 1488, 1451, 1417, 1330, 1105, 1051, 1000, 813, 750, 463 cm^{-1} ; ^{31}P NMR (75.5 MHz, CDCl_3) δ -39.8; ^1H NMR (300 MHz, CDCl_3) δ 7.26-6.94 (m, 8H), 4.23 (s, 1H), 4.11 (s, 6H), 3.62 (s, 1H), 2.90 (s, 3H), 2.67 (s, 6H), 2.11 (s, 3H); ^{13}C NMR (75.5 MHz, CDCl_3) δ 143.4 (d, $J^{13}\text{C}-^{31}\text{P} = 29.4$ Hz), 140.3 (d, $J^{13}\text{C}-^{31}\text{P} = 24.2$ Hz), 139.3 (d, $J^{13}\text{C}-^{31}\text{P} = 14.3$ Hz), 136.0, 135.3 (d, $J^{13}\text{C}-^{31}\text{P} = 10.6$ Hz), 131.8, 129.8 (d, $J^{13}\text{C}-^{31}\text{P} = 11.3$ Hz), 129.7, 129.7, 129.0,

127.5, 125.4 (d, $J^{13}\text{C}-^{31}\text{P} = 15.1$ Hz), 119.0 (d, $J^{13}\text{C}-^{31}\text{P} = 18.1$ Hz), 69.0 (d, $J^{13}\text{C}-^{31}\text{P} = 3.0$ Hz), 68.4, 65.2 (d, $J^{13}\text{C}-^{31}\text{P} = 12.1$ Hz), 65.1, 61.1 (d, $J^{13}\text{C}-^{31}\text{P} = 2.3$ Hz), 45.4, 45.3, 22.1 (d, $J^{13}\text{C}-^{31}\text{P} = 24.9$ Hz), 20.8 (d, $J^{13}\text{C}-^{31}\text{P} = 19.6$ Hz); EIMS [$m/z(\%)$] 441 (100, M^+); HRMS (EI) calcd for $\text{C}_{26}\text{H}_{28}\text{NPS}^{56}\text{Fe}$: 441.1308; found 441.1311.

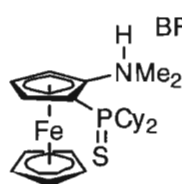
2-dicyclohexylphosphinothionyl-1-dimethylaminoferrocene (232). A solution of



(*R,R*)-**191** (233 mg, 0.916 mmol) in *t*-BuOMe (4.5 mL) was cooled to -40 °C, treated sequentially with *i*-PrLi (1.40 mL, 1.98 M in pentane, 2.76 mmol) and dimethylaminoethanol (82 mg, 0.917 mmol) in *t*-BuOMe (4.5 mL), and stirred for 15 min at that temperature. The solution was transferred by cannula to a mixture of **192**·BF₃ at -78 °C [prepared by addition of BF₃·OEt₂ (115 μ L, 0.916 mmol) to a solution of **192** (200 mg, 0.873 mmol) in *t*-BuOMe (9 mL) at 0 °C and stirring for 10 min]. The mixture was allowed to warm slowly to -40 °C over approximately 3.5 h and then held at that temperature for an additional hour. After cooling back to -78 °C, ClPCy₂ (390 μ L, 1.77 mmol) was added and the mixture was allowed to warm slowly to room temperature (over 3.5 h). The reaction mixture was diluted with Et₂O and worked-up by addition of saturated aqueous NaHCO₃. The aqueous layer was extracted with Et₂O (3 x 15 mL) and the combined organic extract was washed with H₂O (1 x 15 mL), brine (1 x 15 mL), dried over anhydrous Na₂SO₄ and concentrated under reduced pressure *in vacuo* to afford the crude aminophosphine which was filtered through a plug of silica with 90:10 hexane:Et₂O. To the crude material in a dry round bottom flask under argon was added sulfur powder (700 mg, 21.8 mmol) and toluene (15 mL), and the mixture was heated at 40 °C for 2 h. After cooling to room temperature, the reaction mixture was

gravity filtered to remove excess sulfur and the filtrate was pre-adsorbed on silica gel *in vacuo*. Flash column chromatography (silica gel, 95:5 hexane:EtOAc) gave **232** (215 mg, 54%) as an orange semi-solid. $[\alpha]_D^{20} -51.2$ (*c* 1.7, CHCl₃); CSP HPLC analysis (Chiralcel OD-H; eluent: 99:1 hexane:EtOAc, 1.0 mL/min) determined an 85.5:14.5 er (71% ee) [t_R (minor) = 8.0 min, t_R (major) = 8.5 min].

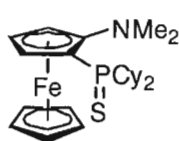
(S)-(-)-{2-[dicyclohexylphosphino]ferrocenyl}-1-dimethylammonium



tetrafluoroborate ((S)-232·HBF₄). A solution of **232** (180 mg, 0.394 mmol) in Et₂O (20 mL) at 0 °C open to air was treated with HBF₄·Et₂O (76 μL, 0.559 mmol). An immediate colour change was observed with precipitation of a yellow precipitate. The solution was allowed to stir for 10 minutes, after which the solid was collected by suction filtration, washed with cold Et₂O, and dried *in vacuo* to afford ammonium salt (S)-**232**·HBF₄ (212 mg, 99%) as a yellow powder. mp 84-89 °C; $[\alpha]_D^{20} -43.2$ (*c* 1.0, CHCl₃). Two recrystallizations via liquid-liquid diffusion of Et₂O into a solution of **232**·HBF₄ in CH₂Cl₂ provided product in 84% ee as determined by neutralization of a small portion back to the free phosphine sulfide and measurement on chiral HPLC. Further attempts at recrystallization did not increase the enantiomeric excess. mp 104-106 °C; $[\alpha]_D^{20} -51.3$ (*c* 1.0, CHCl₃); IR (KBr) ν_{max} 3037, 2933, 2856, 2652, 2564, 2423, 1450, 1217, 1176, 1110, 1053, 851, 754, 608 cm⁻¹; ³¹P NMR (121.5 MHz, CDCl₃) δ 56.7; ¹H NMR (300 MHz, CDCl₃) δ 12.01 (s, 1H), 5.45 (t, 1H, *J* = 1.2 Hz), 4.78 (q, 1H, *J* = 1.5 Hz), 4.57 (s, 5H), 4.35 (d, 1H, *J* = 2.4 Hz), 3.58 (d, 3H, *J* = 5.1 Hz), 3.11 (d, 3H, *J* = 5.1 Hz), 2.59 (m, 1H), 2.50-2.45 (m, 1H), 2.41-2.31 (m, 1H), 2.05 (m, 3H), 1.85-1.70 (m, 5H), 1.58-1.35 (m, 8H), 1.17 (m, 3H); ¹³C NMR (75.5 MHz,

CDCl₃) δ 110.9 (d, $J^{13}\text{C}-^{31}\text{P} = 7.6$ Hz), 72.5, 70.4 (d, $J^{13}\text{C}-^{31}\text{P} = 8.3$ Hz), 69.2 (d, $J^{13}\text{C}-^{31}\text{P} = 8.3$ Hz), 64.2 (d, $J^{13}\text{C}-^{31}\text{P} = 6.8$ Hz), 62.85 (d, $J^{13}\text{C}-^{31}\text{P} = 75.6$ Hz), 49.2, 48.7, 44.5 (d, $J^{13}\text{C}-^{31}\text{P} = 48.3$ Hz), 39.6 (d, $J^{13}\text{C}-^{31}\text{P} = 47.6$ Hz), 27.6 (d, $J^{13}\text{C}-^{31}\text{P} = 3.2$ Hz), 27.4, 27.2 (d, $J^{13}\text{C}-^{31}\text{P} = 6.8$ Hz), 27.1 (d, $J^{13}\text{C}-^{31}\text{P} = 3.8$ Hz), 26.3 (d, $J^{13}\text{C}-^{31}\text{P} = 8.3$ Hz), 26.2 (d, $J^{13}\text{C}-^{31}\text{P} = 5.3$ Hz), 25.9 (d, $J^{13}\text{C}-^{31}\text{P} = 6.8$ Hz), 25.8 (d, $J^{13}\text{C}-^{31}\text{P} = 6.0$ Hz), 25.7 (d, $J^{13}\text{C}-^{31}\text{P} = 3.8$ Hz), 25.3; FABMS [$m/z(\%)$] 458 (95, M^+), 229 (100), HRMS (FAB) calcd for $\text{C}_{24}\text{H}_{37}\text{NPS}^{56}\text{Fe}$: 458.1733, found 458.1732; Anal. calcd for $\text{C}_{24}\text{H}_{37}\text{NPSFeBF}_4$: C, 52.87; H, 6.84. Found: C, 52.17; H, 6.72.

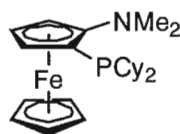
(S)-(-)-2-dicyclohexylphosphinothionyl-1-dimethylaminoferrocene ((S)-232). A flask



containing a biphasic suspension of (S)-**232**·HBF₄ (190 mg, 0.34 mmol) in Et₂O (10 mL) and 1M NaHCO₃ (5 mL) was sonicated for 1 min or until all the solid dissolved. The layers were separated and the aqueous phase was extracted with diethyl ether (2 x 10 mL). The combined ether layer was washed with water, brine, dried over anhydrous MgSO₄, filtered and concentrated *in vacuo*, then filtered through a plug of silica with 1:1 hexane:EtOAc to give (S)-**232** (89 mg, 82%) as an orange semi-solid. $[\alpha]_{\text{D}}^{20} -64.8$ (c 0.51, CHCl₃); CSP HPLC analysis (Chiralcel OD-H; eluent: 99:1 hexane:EtOAc, 1.0 mL/min) determined an 92.0:8.0 er (84% ee) [$t_{\text{R}}(\text{minor}) = 8.0$ min, $t_{\text{R}}(\text{major}) = 8.4$ min]; IR (KBr, thin film) ν_{max} 2929, 2851, 1644, 1635, 1475, 1447, 1413, 1383, 1320, 1156, 1109, 1035, 1003, 850, 821, 755, 638 cm⁻¹; ³¹P NMR (121.5 MHz, CDCl₃) δ 60.7; ¹H NMR (300 MHz, CDCl₃) δ 4.48 (q, 1H, $J = 2.7$ Hz), 4.35 (s, 5H), 4.34 (m, 1H), 4.30 (q, 1H, $J = 1.5$ Hz), 2.65 (s, 6H), 2.55 (m, 2H), 2.09 (m, 1H), 1.93 (m, 4H), 1.82-1.61 (m, 7H), 1.16 (m, 5H), 1.13 (m, 3H); ¹³C

NMR (75.5 MHz, CDCl₃) δ 116.1 (d, $J^{13}_{\text{C}-^{31}\text{P}} = 7.6$ Hz), 70.7, 70.6 (d, $J^{13}_{\text{C}-^{31}\text{P}} = 7.6$ Hz), 62.7 (d, $J^{13}_{\text{C}-^{31}\text{P}} = 62.7$ Hz), 66.6 (d, $J^{13}_{\text{C}-^{31}\text{P}} = 9.8$ Hz), 62.3 (d, $J^{13}_{\text{C}-^{31}\text{P}} = 8.3$ Hz), 43.4, 39.4 (d, $J^{13}_{\text{C}-^{31}\text{P}} = 50.6$ Hz), 37.3 (d, $J^{13}_{\text{C}-^{31}\text{P}} = 51.3$ Hz), 28.2 (d, $J^{13}_{\text{C}-^{31}\text{P}} = 2.3$ Hz), 27.4 (d, $J^{13}_{\text{C}-^{31}\text{P}} = 3.0$ Hz), 27.3, 27.1 (d, $J^{13}_{\text{C}-^{31}\text{P}} = 6.0$ Hz), 26.8 (d, $J^{13}_{\text{C}-^{31}\text{P}} = 6.0$ Hz), 26.6 (d, $J^{13}_{\text{C}-^{31}\text{P}} = 3.8$ Hz), 26.5, 26.0 (d, $J^{13}_{\text{C}-^{31}\text{P}} = 2.3$ Hz), 26.0 (d, $J^{13}_{\text{C}-^{31}\text{P}} = 3.2$ Hz), 25.9 (d, $J^{13}_{\text{C}-^{31}\text{P}} = 3.8$ Hz); EIMS [m/z(%)] 457 (100, M⁺), 308 (23), 229 (16); HRMS (FAB) calcd for C₂₄H₃₆NPS⁵⁶Fe: 457.1655, found 457.1662.

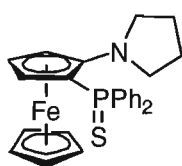
(S)-(-)-2-dicyclohexylphosphino-1-dimethylaminoferrocene ((S)-206). Acetonitrile



(15 mL) was added to freshly activated Ni-Al catalyst [(646 mg, 7.54 mmol, activated by portion-wise addition to 11 mL 6 M NaOH and heating at 50 °C open to air for 1 h, followed by washing with H₂O (7 x 10 mL), MeOH (3 x 10 mL), Et₂O (2 x 10 mL) and MeCN (2 x 10 mL)] and aminophosphine sulfide **232** (68 mg, 0.15 mmol) in a round bottom flask under argon, and the mixture was heated to 60 °C for 2 h. The reaction mixture was allowed to cool to room temperature and filtered through a pad of Celite, washing with acetonitrile. Flask chromatography (silica, 9:1 hexanes:Et₂O) afforded (S)-**206** as an orange oil (62 mg, 99%). [α]_D²⁰ -14.3 (c 0.55, CHCl₃); IR (KBr) ν_{max} 3095, 2922, 2849, 2781, 1488, 1448, 1419, 1332, 1182, 1141, 1106, 1053, 999, 813, 614 cm⁻¹; ³¹P NMR (121.5 MHz, CDCl₃) δ -11.2; ¹H NMR (300 MHz, CDCl₃) δ 4.23 (s, 5H), 4.10 (s, 1H), 4.04 (q, 1H, $J = 2.4$ Hz), 3.91 (m, 1H), 2.75 (s, 6H), 2.42 (m, 1H), 1.86 (m, 4H), 1.73-1.53 (m, 6H), 1.47-1.19 (m, 10H), 0.89-0.81 (m, 1H); ¹³C NMR (75.5 MHz, CDCl₃) δ 118.1 (d, $J^{13}_{\text{C}-^{31}\text{P}} = 13.6$ Hz), 67.9, 67.2 (d, $J^{13}_{\text{C}-^{31}\text{P}} = 3.8$ Hz), 63.9 (d, $J^{13}_{\text{C}-^{31}\text{P}} = 23.4$ Hz), 63.4, 61.3 (d, $J^{13}_{\text{C}-^{31}\text{P}} =$

2.3 Hz), 44.9, 44.8, 35.2 (d, $J^{13}_{\text{C}-^{31}\text{P}} = 14.3$ Hz), 33.8 (d, $J^{13}_{\text{C}-^{31}\text{P}} = 11.3$ Hz), 32.5, 32.2, 30.3 (d, $J^{13}_{\text{C}-^{31}\text{P}} = 14.3$ Hz), 29.7 (d, $J^{13}_{\text{C}-^{31}\text{P}} = 10.6$ Hz), 29.3 (d, $J^{13}_{\text{C}-^{31}\text{P}} = 6.8$ Hz), 27.7 (d, $J^{13}_{\text{C}-^{31}\text{P}} = 12.1$ Hz), 27.5 (d, $J^{13}_{\text{C}-^{31}\text{P}} = 6.8$ Hz), 27.5 (d, $J^{13}_{\text{C}-^{31}\text{P}} = 13.6$ Hz), 27.3 (d, $J^{13}_{\text{C}-^{31}\text{P}} = 7.6$ Hz), 26.5 (d, $J^{13}_{\text{C}-^{31}\text{P}} = 8.3$ Hz); EIMS [$m/z(\%)$] 425 (100, M^+), 342 (13), 260 (27), 138 (16); HRMS (EI) calcd for $\text{C}_{24}\text{H}_{36}\text{NP}^{56}\text{Fe}$: 425.1934; found 425.1935.

[2-(Diphenylphosphinothionyl)ferrocenyl]-1-pyrrolidine (233). A solution of (*R,R*)-



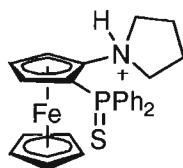
191 (315 mg, 1.24 mmol) in *t*-BuOMe (2.5 mL) was cooled to -40 °C, treated sequentially with *i*-PrLi (2.05 mL, 1.80 M in pentane, 3.69 mmol) and dimethylaminoethanol (110 mg, 1.23 mmol) in *t*-BuOMe (2.5 mL),

and stirred for 20 min at that temperature. The solution was transferred by cannula to a pre-formed mixture of **213**·BF₃ at -78 °C [prepared by addition of BF₃·OEt₂ (175 μL , 1.39 mmol) to a solution of **213** (300 mg, 1.18 mmol) in *t*-BuOMe (12 mL) at 0 °C and stirring for 10 min]. After stirring for 10 min at -78 °C, the mixture was allowed to warm slowly to -40 °C over 2 h and then held at that temperature for an additional hour. After cooling back to -78 °C, ClPPh₂ (435 μL , 1.97 mmol) was added and the mixture was allowed to warm slowly to room temperature. The reaction mixture was diluted with Et₂O and worked-up by addition of a saturated solution of aqueous NaHCO₃. The aqueous layer was extracted with Et₂O (3 x 15 mL) and the combined organic extract was washed with H₂O (1 x 15 mL), brine (1 x 15 mL), dried over anhydrous Na₂SO₄ and concentrated under reduced pressure on a rotary evaporator to afford the crude aminophosphine. To the crude mixture in a dry round bottom flask was added sulfur powder (567 mg, 18 mmol) under argon. Toluene (25 mL) was added and the reaction mixture heated at 40 °C for 2

h. The reaction mixture was gravity filtered to remove excess sulfur and pre-adsorbed on silica gel. Flash column chromatography (94:6 hexane/diethyl ether) gave (*S*)-**233** (255 mg, 43%) as an orange foam. mp 194-202 °C (dec); $[\alpha]_D^{20} +46.4$ (*c* 0.95, acetone); CSP HPLC analysis (Chiralcel OD-H; eluent: 99:1 hexane:*i*-PrOH, 1.0 mL/min) determined a 91.4:8.6 er (83% ee) [t_R (major) = 5.8 min, t_R (minor) = 7.0 min]; IR (KBr) ν_{\max} 2958, 2942, 2869, 2814, 1473, 1455, 1435, 1098, 814, 751, 710, 693, 651, 509, 434, 459 cm^{-1} ; ^{31}P NMR (121.5 MHz, CDCl_3) δ 46.45; ^1H NMR (300 MHz, CDCl_3) δ 7.86-7.79 (m, 2H), 7.76-7.69 (m, 2H), 7.47-7.36 (m, 6H), 4.42 (s, 5H), 4.13 (s, 1H), 4.03 (s, 1H), 3.46 (s, 1H), 3.18 (s, 1H), 2.84 (s, 2H), 1.73-1.66 (m, 4H); ^{13}C NMR (150.9 MHz, CDCl_3) δ 135.6 (d, $J^{13}\text{C}-^{31}\text{P} = 87.6$ Hz), 133.7 (d, $J^{13}\text{C}-^{31}\text{P} = 86.1$ Hz), 132.2 (d, $J^{13}\text{C}-^{31}\text{P} = 10.6$ Hz), 131.8 (d, $J^{13}\text{C}-^{31}\text{P} = 10.6$ Hz), 131.1 (d, $J^{13}\text{C}-^{31}\text{P} = 3.0$ Hz), 130.7 (d, $J^{13}\text{C}-^{31}\text{P} = 1.5$ Hz), 128.1 (d, $J^{13}\text{C}-^{31}\text{P} = 13.6$ Hz), 127.9 (d, $J^{13}\text{C}-^{31}\text{P} = 12.1$ Hz), 114.8 (d, $J^{13}\text{C}-^{31}\text{P} = 7.6$ Hz), 72.5 (d, $J^{13}\text{C}-^{31}\text{P} = 13.6$ Hz), 69.4, 64.6 (d, $J^{13}\text{C}-^{31}\text{P} = 12.1$ Hz), 63.7 (d, $J^{13}\text{C}-^{31}\text{P} = 92.1$ Hz), 60.8 (d, $J^{13}\text{C}-^{31}\text{P} = 9.1$ Hz), 53.2, 24.9; EIMS [m/z (%)] 471 (M^+ , 89), 467 (79), 255 (100); HRMS (EI) calcd for $\text{C}_{26}\text{H}_{26}\text{NPS}^{56}\text{Fe}$: 471.0873; found 471.0874. Anal. Calcd for $\text{C}_{26}\text{H}_{26}\text{NPS}^{56}\text{Fe}$: C, 66.25; H, 5.56. Found: C, 66.16; H, 5.51.

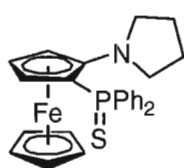
(*S*)-(-)-[2-(Diphenylphosphinothioyl)ferrocenyl]-1-pyrrolidinium tetrafluoroborate

BF_4^- ((*S*)-**233**· HBF_4). A solution of aminophosphine sulfide **233** (255 mg, 0.5084 mmol) in diethyl ether (20 mL) at 0 °C was treated with tetrafluoroboric acid-diethyl ether complex (85 μL , 0.6246 mmol). An immediate change in color from orange to yellow was observed, and a yellow powder precipitated out of solution. The solid was collected by suction filtration, washed with



cold Et₂O, and dried *in vacuo* to afford ammonium salt **233**·HBF₄ as a yellow powder (261 mg, 92%). mp 110 °C; [α]_D²⁰ -48.2 (*c* 1.0, acetone); IR (KBr) ν_{max} 3504, 3455, 3110, 3056, 2974, 2882, 2810, 2628, 2569, 2443, 2360, 1636, 1481, 1460, 1438, 1383, 1170, 1102, 1057, 998, 839, 754, 714, 694, 517, 484; ³¹P NMR (243.0 MHz, acetone-d₆) δ 38.2; ¹H NMR (600 MHz, acetone-d₆) δ 11.02 (s, 1H), 8.08-8.05 (m, 2H), 7.78-7.65 (m, 6H), 7.58 (s, 2H), 5.42 (s, 1H), 4.90 (s, 1H), 4.59 (s, 1H), 4.50 (s, 1H), 4.43 (s, 5H), 4.12 (s, 1H), 3.57 (s, 1H), 3.15 (s, 1H), 2.40 (s, 1H), 2.25 (s, 2H), 2.08 (s, 1H); ¹³C NMR (150.9 MHz, acetone-d₆) δ 134.3 (d, $J^{13}_{\text{C}-31}_{\text{P}} = 89.1$ Hz), 133.7, 133.1, 132.7 (d, $J^{13}_{\text{C}-31}_{\text{P}} = 12.1$ Hz), 131.8 (d, $J^{13}_{\text{C}-31}_{\text{P}} = 10.6$ Hz), 130.3 (d, $J^{13}_{\text{C}-31}_{\text{P}} = 89.1$ Hz), 129.8 (d, $J^{13}_{\text{C}-31}_{\text{P}} = 12.1$ Hz), 129.6 (d, $J^{13}_{\text{C}-31}_{\text{P}} = 12.1$ Hz), 105.1 (d, $J^{13}_{\text{C}-31}_{\text{P}} = 10.6$ Hz), 73.5 (d, $J^{13}_{\text{C}-31}_{\text{P}} = 9.1$ Hz), 73.1, 71.0 (d, $J^{13}_{\text{C}-31}_{\text{P}} = 9.1$ Hz), 66.3 (d, $J^{13}_{\text{C}-31}_{\text{P}} = 143.4$ Hz), 66.1 (d, $J^{13}_{\text{C}-31}_{\text{P}} = 6.0$ Hz), 62.9, 58.4, 25.2, 24.5; FABMS [*m/z*(%)] 472 (M⁺, 100), 255 (74), 134 (22) HRMS (FAB) calcd for C₂₆H₂₇NPS⁵⁶Fe: 472.0951, Found 472.0893. Recrystallization via liquid-liquid diffusion of Et₂O into a solution of (*S*)-**233**·HBF₄ in CH₂Cl₂ rendered the salt enantiomerically pure in >99% ee after two recrystallizations. mp 113-115 °C; [α]_D²⁰ -59.3 (*c* 0.99, acetone).

(*S*)-(+)-[2-(Diphenylphosphinothionyl)ferrocenyl]-1-pyrrolidine ((*S*)-**233**). A flask



containing a biphasic suspension of salt (*S*)-**233**·HBF₄ (170 mg, 0.30

mmol) in sat. aqueous NaHCO₃ and diethyl ether was sonicated for 1 min

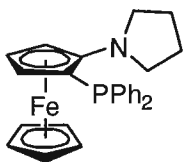
or until all the solid dissolved. The layers were separated and the aqueous

phase was washed once diethyl ether. The combined ether layer was washed with water,

brine, dried over anhydrous Na₂SO₄, filtered and concentrated *in vacuo* to give (*S*)-**233**

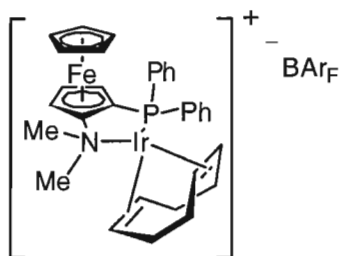
(150 mg, 98%). mp 216-218 °C; $[\alpha]_D^{20} +60.9$ (*c* 0.89, CHCl₃); CSP HPLC analysis (Chiralcel OD-H; eluent: 99:1 hexane:*i*-PrOH, 1.0 mL/min) determined a 99.98:0.02 er (>99.9% ee) [t_R (major) 5.8 min, t_R (minor) 7.0 min].

(*S*)-(-)-[2-(Diphenylphosphino)ferrocenyl]-1-pyrrolidine ((*S*)-207**).** Acetonitrile (25



mL) was added to freshly activated Ni-Al catalyst [(1.41 g, 16.4 mmol, activated by portion-wise addition to 25 mL 6 M NaOH and heating at 50 °C for 1 h, followed by washing the residue with H₂O (7 x 10 mL), MeOH (3 x 10 mL), Et₂O (2 x 10 mL) and MeCN (2 x 10 mL)] and aminophosphine sulfide (*S*)-**233** (125 mg, 0.27 mmol) in a round bottom flask under argon, and the mixture was heated to 60 °C for 3 hours. The reaction mixture was allowed to cool to room temperature and filtered through a pad of Celite, washing with acetonitrile. Removal of the solvent afforded the free aminophosphine (*S*)-**207** (91 mg, 78%) as an orange solid. mp 118-120 °C; $[\alpha]_D^{20} -137.3$ (*c* 0.75, CHCl₃); ³¹P NMR (121.5 MHz, CDCl₃) δ -16.32; ¹H NMR (300 MHz, CDCl₃) δ 7.49-7.43 (m, 2H), 7.38-7.35 (m, 3H), 7.26-7.18 (m, 5H), 4.12 (s, 5H), 4.03 (q, 1H, *J* = 1.5 Hz), 3.99 (t, 1H, *J* = 2.4 Hz), 3.26 (m, 1H), 3.20-2.12 (m, 4H), 1.90-1.81 (m, 4H); ¹³C NMR (75.5 MHz, CDCl₃) δ 139.7 (d, $J^{13}_C-^{31}_P$ = 12.1 Hz), 137.9 (d, $J^{13}_C-^{31}_P$ = 11.3 Hz), 135.3 (d, $J^{13}_C-^{31}_P$ = 21.9 Hz), 132.3 (d, $J^{13}_C-^{31}_P$ = 18.1 Hz), 128.9, 128.1 (d, $J^{13}_C-^{31}_P$ = 5.3 Hz), 128.0 (d, $J^{13}_C-^{31}_P$ = 3.8 Hz), 116.7 (d, $J^{13}_C-^{31}_P$ = 16.6 Hz), 68.0, 67.9 (d, $J^{13}_C-^{31}_P$ = 3.8 Hz), 64.7, 62.1 (d, $J^{13}_C-^{31}_P$ = 12.8 Hz), 60.2 (d, $J^{13}_C-^{31}_P$ = 3.8 Hz), 52.4, 52.3, 24.9, 24.8; EIMS [*m/z*(%)] 439 (100, M⁺); HRMS (EI) calcd for C₂₆H₂₆NP⁵⁶Fe: 439.1152; found 439.1159; Anal. Calcd for C₂₆H₂₆NP⁵⁶Fe: C, 71.08; H, 5.97. Found: C, 71.21; H, 5.92.

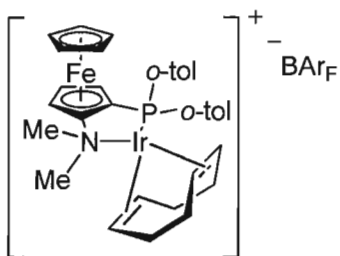
(S)-(+)-2-Diphenylphosphino-1-dimethylaminoferrocene iridium (cyclooctadiene)



tetrakis{3,5-bis(trifluoromethyl)phenyl}borate (S)-(221).

A solution of $[\text{Ir}(\text{COD})\text{Cl}]_2$ (81 mg, 0.12 mmol) and (S)-**204** (100 mg, 0.24 mmol) in dry CH_2Cl_2 (4 mL) was heated at reflux for 1 h. NaBArF_4 (322 mg, 0.36 mmol) and distilled H_2O (4 mL) were added, followed by stirring for 15 min. The layers were separated and the aqueous layer was washed with CH_2Cl_2 (3 x 5 mL). The combined organics were washed with water (1 x 5 mL), then evaporated and dried *in vacuo*. The resulting orange solid was re-dissolved in CH_2Cl_2 and filtered through a pad of silica gel with CH_2Cl_2 to afford iridium complex (S)-**221** (316 mg, 83%) having spectroscopic data matching the racemic complex. mp 168-172 °C; $[\alpha]_D^{20} +8.7$ (*c* 1.04, acetone).

(S)-(-)-2-Bis(ortho-tolyl)phosphino-1-dimethylaminoferrocene iridium



(cyclooctadiene)

tetrakis{3,5-

bis(trifluoromethyl)phenyl}borate ((S)-234). $[\text{Ir}(\text{COD})\text{Cl}]_2$

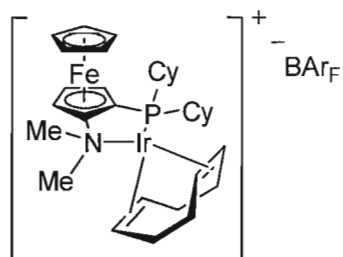
(29.6 mg, 0.044 mmol) and dry CH_2Cl_2 (2 mL) were added to a flask containing aminophosphine **205** (39 mg, 0.088 mmol) under argon. The solution was heated at reflux for 1.5 h, after which the solution was concentrated to provide (S)-(+)-2-bis(ortho-tolyl)phosphino-1-dimethylaminoferrocene iridium (cyclooctadiene) chloride (67 mg, 99%) as an orange-red solid. mp >230 °C; $[\alpha]_D^{20} -49.1$ (*c* 1.02, CHCl_3); FABMS [*m/z*(%)] 742 (M-Cl, 88), 740 (77), 630 (59), 629 (50), 628 (100), 627 (40), 626 (64), 458 (34), 457 (45), 441 (48),

229 (35), 149 (45); HRMS (FAB) calcd for $C_{34}H_{40}NP^{56}Fe^{193}Ir$ 742.1877, found 742.1831. To a flask containing chloride complex (35 mg, 0.045 mmol) was added $NaBAr_F$ (50 mg, 0.056 mmol), dry CH_2Cl_2 (1.5 mL), and deionized water (1.5 mL) under argon. The mixture was stirred for 15 minutes at room temperature over which time a colour change from orange to red occurred. The layers were separated, aqueous layer extracted with CH_2Cl_2 (3 x 1.5 mL), and the combined organic washed with deionized water (1 x 2 mL). The solvent was removed *in vacuo*, the residue taken up in CH_2Cl_2 and filtered through a plug of silica eluting with CH_2Cl_2 to give (*S*)-**234** (58 mg, 81%) as an orange solid. mp 161-163 °C; $[\alpha]_D^{20}$ -27.4 (*c* 0.50, $CHCl_3$); IR (KBr, thin film) ν_{max} 3063, 2927, 2856, 1611, 1467, 1355, 1279, 1162, 1127, 908, 888, 834, 758, 713, 682, 671 cm^{-1} ; ^{31}P NMR (121.5 MHz, acetone- d_6 , -10 °C as a 1:1 mixture of bidentate conformational isomers) δ 17.63, 12.92; ^{19}F NMR (282.4 MHz, $CDCl_3$, 22 °C) δ -62.33; 1H NMR (600 MHz, acetone- d_6 , -10 °C as a 1:1 mixture of bidentate conformational isomers) δ 9.31 (dd, 1H, $J_{H-P}^1 = 13.2$, $J_{H-H}^1 = 7.8$ Hz), 9.25 (bs, 1H), 8.57 (bs, 1H), 7.82 (s, 2 x 8H), 7.71 (bs, 1H), 7.71 (s, 2 x 4H), 7.60 (q, 2H, $J = 7.8$ Hz), 7.47 (t, 2 x 1H, $J = 7.2$ Hz), 7.45-7.37 (m, 2 x 2H), 7.33 (t, 1H, $J = 7.2$ Hz), 7.26 (bs, 1H), 7.24 (t, 1H, $J = 7.2$ Hz), 7.14 (bs, 1H), 5.66 (bs, 1H), 5.28 (bs, 1H), 5.17 (bs, 1H), 5.13 (s, 1H), 5.12 (s, 1H), 5.08 (s, 1H), 5.04 (s, 1H), 4.81 (bs, 1H), 4.80 (s, 1H), 4.63 (s, 1H), 4.57 (s, 5H), 4.30 (s, 5H), 4.14 (s, 1H), 3.87 (s, 1H), 3.72 (s, 1H), 3.50 (s, 3H), 3.47 (s, 3H), 3.46 (bs, 1H), 3.07 (s, 3H), 3.00 (s, 3H), 2.63 (bm, 2H), 2.52 (bs, 3H), 2.44-2.38 (bm, 1H), 2.36-2.29 (bm, 2H + 1H), 2.26-2.19 (bm, 2H), 2.18-2.12 (bm, 1H), 2.04 (s, 3H), 2.02 (bm, 1H), 1.99 (bs, 3H), 1.97 (bm, 1H), 1.92 (s, 3H), 1.84 (bm, 2 x 1H), 1.77-1.74 (bm, 2H), 1.54-1.52 (bm, 1H); ^{13}C NMR (150.9 MHz, acetone- d_6 , -10 °C, as a 1:1 mixture of bidentate conformational isomers) δ

162.4 (q, $J^{13}_{\text{C}-^{11}\text{B}} = 49.8$ Hz), 142.4 (d, $J^{13}_{\text{C}-^{31}\text{P}} = 9.1$ Hz), 142.2 (d, $J^{13}_{\text{C}-^{31}\text{P}} = 4.5$ Hz), 140.5 (bd, $J^{13}_{\text{C}-^{31}\text{P}} = 12.1$ Hz), 139.4 (bd, $J^{13}_{\text{C}-^{31}\text{P}} = 22.6$ Hz), 137.2 (bd, $J^{13}_{\text{C}-^{31}\text{P}} = 21.1$ Hz), 136.0 (bd, $J^{13}_{\text{C}-^{31}\text{P}} = 13.6$ Hz), 135.4, 133.6 (d, $J^{13}_{\text{C}-^{31}\text{P}} = 9.1$ Hz), 133.3 (d, $J^{13}_{\text{C}-^{31}\text{P}} = 7.5$ Hz), 133.1 (d, $J^{13}_{\text{C}-^{31}\text{P}} = 7.5$ Hz), 133.0 (d, $J^{13}_{\text{C}-^{31}\text{P}} = 1.5$ Hz), 132.7 (d, $J^{13}_{\text{C}-^{31}\text{P}} = 6.0$ Hz), 132.6 (d, $J^{13}_{\text{C}-^{31}\text{P}} = 1.5$ Hz), 132.5 (d, $J^{13}_{\text{C}-^{31}\text{P}} = 6.0$ Hz), 131.6, 130.7 (d, $J^{13}_{\text{C}-^{31}\text{P}} = 48.3$ Hz), 129.8 (qq, $J^{13}_{\text{C}-^{19}\text{F}} = 31.7, 3.0$ Hz), 128.3 (d, $J^{13}_{\text{C}-^{31}\text{P}} = 58.9$ Hz), 127.4 (d, $J^{13}_{\text{C}-^{31}\text{P}} = 15.1$ Hz), 127.2 (d, $J^{13}_{\text{C}-^{31}\text{P}} = 13.6$ Hz), 127.1 (d, $J^{13}_{\text{C}-^{31}\text{P}} = 10.6$ Hz), 126.5 (d, $J^{13}_{\text{C}-^{31}\text{P}} = 27.2$ Hz), 125.7 (d, $J^{13}_{\text{C}-^{31}\text{P}} = 24.1$ Hz), 125.2 (q, $J^{13}_{\text{C}-^{19}\text{F}} = 271.6$ Hz), 118.3 (sept, $J^{13}_{\text{C}-^{19}\text{F}} = 4.5$ Hz), 93.8 (bs), 92.1 (d, $J^{13}_{\text{C}-^{31}\text{P}} = 12.1$ Hz), 91.6 (bs), 89.1 (bs), 75.8 (bs), 74.5 (d, $J^{13}_{\text{C}-^{31}\text{P}} = 6.0$ Hz), 73.2, 72.7, 72.5 (d, $J^{13}_{\text{C}-^{31}\text{P}} = 19.6$ Hz), 71.9 (d, $J^{13}_{\text{C}-^{31}\text{P}} = 22.6$ Hz), 68.2, 65.8, 63.8 (bs), 61.8 (bs), 60.7 (d, $J^{13}_{\text{C}-^{31}\text{P}} = 10.6$ Hz), 60.2 (d, $J^{13}_{\text{C}-^{31}\text{P}} = 9.1$ Hz), 60.1 (bs), 59.1 (bs), 57.9, 57.8, 53.0, 51.1, 34.2, 33.9 (bs), 32.0 (bs), 31.5, 31.3, 31.1 (bs), 29.1 (bs), 28.4, 23.3 (2 x d, $J^{13}_{\text{C}-^{31}\text{P}} = 4.5$ Hz), 22.3 (bd, $J^{13}_{\text{C}-^{31}\text{P}} = 3.0$ Hz), 21.9 (d, $J^{13}_{\text{C}-^{31}\text{P}} = 3.0$ Hz).; FABMS [m/z (%)] 742 (62, M-BAr_F), 740 (61), 630 (54), 629 (49), 628 (100), 627 (40), 626 (65), 441 (20), 229 (26); HRMS (FAB) calcd for C₃₄H₄₀NP⁵⁶Fe¹⁹³Ir 742.1877, found 742.1915; Anal. Calcd for C₆₆H₅₂NP⁵⁶Fe¹⁹³IrBF₂₄: C, 49.39; H, 3.27. Found: C, 48.74; H, 3.25

(S)-(-)-2-Dicyclohexylphosphino-1-dimethylaminoferrocene

iridium



(cyclooctadiene)

tetrakis{3,5-

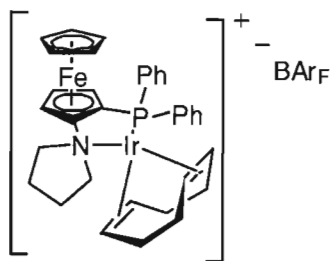
bis(trifluoromethyl)phenyl}borate ((S)-235). [Ir(COD)Cl]₂

(22.5 mg, 0.034 mmol) and dry CH₂Cl₂ (1.5 mL) were added to a flask containing aminophosphine (S)-206 (28.5 mg,

0.067 mmol) under argon. The solution was heated at reflux for 1.5 h, after which the solution was concentrated to provide (*S*)-(-)-2-dicyclohexylphosphino-1-dimethylaminoferrocene iridium (cyclooctadiene) chloride (51 mg, 99%) as an orange-rust coloured solid. mp >230 °C; $[\alpha]_D^{20}$ -25.1 (*c* 0.64, CHCl₃); FABMS [*m/z* (%)] 726 (77, M-Cl), 724 (100), 722 (67), 450 (31), 394 (31), 229 (14); HRMS (FAB) calcd for C₃₂H₄₈NP⁵⁶Fe¹⁹³Ir 726.2503, found 726.2465; Anal. Calcd for C₃₂H₄₈NP⁵⁶Fe¹⁹³IrCl: C, 50.49; H, 6.36. Found: C, 49.36; H, 5.80. To a flask containing chloride complex (25 mg, 0.033 mmol) was added NaBAR_F (36 mg, 0.041 mmol), dry CH₂Cl₂ (1.0 mL), and deionized water (1.0 mL) under argon. The mixture was stirred for 15 minutes at room temperature over which time a colour change from orange to red occurred. The layers were separated, aqueous layer extracted with CH₂Cl₂ (3 x 1.5 mL), and the combined organic washed with deionized water (1 x 2 mL). The solvent was removed *in vacuo*, the residue taken up in CH₂Cl₂ and filtered through a plug of silica eluting with CH₂Cl₂ to give (*S*)-**235** (46 mg, 88%) as a bright orange solid. mp 159-160 °C; $[\alpha]_D^{20}$ -4.21 (*c* 0.53, CHCl₃); IR (KBr) ν_{\max} 3036, 2929, 2857, 1641, 1634, 1612, 1464, 1454, 1355, 1278, 1162, 1127, 888, 839, 760, 713, 682, 670 cm⁻¹; ³¹P NMR (129.5 MHz, CDCl₃) δ 18.61; ¹⁹F NMR (282.4 MHz, CDCl₃) δ -62.32; ¹H NMR (600 MHz, CDCl₃) δ 7.71 (s, 8H), 7.53 (s, 4H), 4.90 (bm, 1H), 4.84 (t, 1H, *J* = 3.0 Hz), 4.39 (s, 6H), 4.29 (bm, 1H), 4.23 (bm, 1H), 4.13 (d, 1H, *J* = 2.4 Hz), 3.75 (bm, 1H), 3.07 (s, 3H), 2.83 (s, 3H), 2.54 (bm, 1H), 2.41-2.11 (m, 5H), 2.05-2.01 (m, 4H), 1.95 (m, 1H), 1.87-1.68 (m, 12H), 1.62-1.56 (m, 1H), 1.45-1.34 (m, 3H), 1.25-1.18 (m, 4H); ¹³C NMR (150.9 MHz, CDCl₃) δ 161.7 (q, *J*¹³C-¹¹B = 49.8 Hz, C-BAR_F), 134.8 (p-BAR_F), 128.9 (q, *J*¹³C-¹⁹F = 27.1 Hz, m-BAR_F), 125.7 (d, *J*¹³C-³¹P = 22.6 Hz, C1-Cp), 124.5 (q, *J*¹³C-¹⁹F = 273 Hz, CF₃), 117.5 (o-BAR_F),

91.8 (d, $J^{13}\text{C}-^{31}\text{P} = 10.6$ Hz, COD alkene *trans*-P), 88.8 (d, $J^{13}\text{C}-^{31}\text{P} = 12.1$ Hz, COD alkene *trans*-P), 74.8 (d, $J^{13}\text{C}-^{31}\text{P} = 4.5$ Hz, C5-Cp), 71.3 (Cp unsub), 70.1 (d, $J^{13}\text{C}-^{31}\text{P} = 45.3$ Hz, C2-Cp), 67.6 (COD alkene *trans*-N), 59.3 (COD alkene *trans*-N), 58.1 (d, $J^{13}\text{C}-^{31}\text{P} = 9.1$ Hz, C3-Cp), 57.9 (C4-Cp), 57.1 (N-CH₃), 52.3 (N-CH₃), 39.3 (d, $J^{13}\text{C}-^{31}\text{P} = 25.7$ Hz, Cy-P), 38.6, (d, $J^{13}\text{C}-^{31}\text{P} = 30.2$ Hz, Cy-P), 33.6 (d, $J^{13}\text{C}-^{31}\text{P} = 3.0$ Hz, COD-CH₂ *trans*-P), 32.0 (d, $J^{13}\text{C}-^{31}\text{P} = 3.0$ Hz, COD-CH₂ *trans*-P), 31.0 (para-Cy), 30.6 (para-Cy), 29.8 (d, $J^{13}\text{C}-^{31}\text{P} = 6.0$ Hz, meta-Cy), 29.6 (COD-CH₂ *trans*-N), 28.8 (meta-Cy), 27.9 (COD-CH₂ *trans*-N), 27.3 (d, $J^{13}\text{C}-^{31}\text{P} = 9.1$ Hz, ortho-Cy), 27.1 (d, $J^{13}\text{C}-^{31}\text{P} = 13.5$ Hz, ortho-Cy), 27.1 (d, $J^{13}\text{C}-^{31}\text{P} = 10.6$ Hz, ortho-Cy), 27.1 (meta-Cy), 27.0 (d, $J^{13}\text{C}-^{31}\text{P} = 10.6$ Hz, ortho-Cy), 25.7 (meta-Cy), 25.4 (meta-Cy); FABMS [*m/z* (%)] 726 (58, M-BAr_F), 725 (41) 724 (100), 723 (41), 722 (89), 721 (29), 720 (48), 612 (25), 610 (25), 530 (34), 528 (35), 451 (35), 450 (59), 449 (47), 448 (45), 447 (27), 406 (28), 392 (47), 345 (35), 343 (36), 330 (28), 229 (29); HRMS (FAB) calcd for C₃₂H₄₈NP⁵⁶Fe¹⁹³Ir 726.2503, found 726.2526; Anal. Calcd for C₆₄H₆₀NP⁵⁶Fe¹⁹³IrBF₂₄: C, 48.38; H, 3.81. Found: C, 45.39; H, 3.61.

(S)-(-)-2-Diphenylphosphino-1-pyrrolidinylferrocene iridium (cyclooctadiene)



tetrakis[3,5-bis(trifluoromethyl)phenyl]borate ((S)-236).

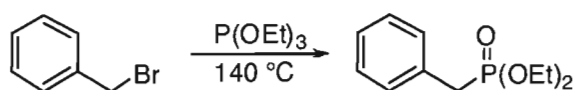
[Ir(COD)Cl]₂ (61 mg, 0.091 mmol) and dry CH₂Cl₂ (5 mL) were added to a flask containing aminophosphine **207** (80 mg, 0.182 mmol) under argon. The solution was heated at reflux

for 1.5 h, after which the solution was concentrated to provide (S)-(-)-2-diphenylphosphino-1-pyrrolidinylferrocene iridium (cyclooctadiene) chloride (138 mg, 98%) as an orange solid. mp >230 °C; [α]_D²⁰ +71.5 (c 1.0 CHCl₃); ³¹P NMR (121.5 MHz,

CDCl_3) δ 19.66; ^1H NMR (300 MHz, CDCl_3) δ 8.49 (t, 2H, $J = 7.8$ Hz), 7.93 (bs, 2H), 7.51 (s, 3H), 7.36 (s, 3H), 5.01 (bs, 1H), 4.33 (s, 1H), 4.15 (s, 1H), 3.93 (s, 5H), 3.72 (m, 2H), 7.67 (s, 1H), 2.95 (m, 2H), 2.75 (bs, 1H), 2.37 (m, 1H), 2.20-2.16 (m, 2H), 2.04 (m, 2H), 1.91 (bs, 4H), 1.91 (bs, 1H), 1.43 (m, 4H); ^{13}C NMR (121.5 MHz, CDCl_3) δ 137.6 (d, $J^{13}\text{C}-^{31}\text{P} = 10.6$ Hz), 134.0, 131.0, 129.4, 127.8 (d, $J^{13}\text{C}-^{31}\text{P} = 9.8$ Hz), 126.9 (d, $J^{13}\text{C}-^{31}\text{P} = 10.6$ Hz), 126.8, 123.6, 109.6 (d, $J^{13}\text{C}-^{31}\text{P} = 11.3$ Hz), 73.9 (d, $J^{13}\text{C}-^{31}\text{P} = 9.1$ Hz), 70.0, 68.0, 59.1, 55.7, 25.0; FABMS [m/z (%)] 740 (56, M-Cl), 738 (100), 737 (45), 736 (76), 734 (39), 630 (25), 391 (27), 149 (55); HRMS (FAB) calcd for $\text{C}_{34}\text{H}_{38}\text{NP}^{56}\text{Fe}^{193}\text{Ir}$ 740.1720, found 740.1760; Anal. Calcd for $\text{C}_{34}\text{H}_{38}\text{NP}^{56}\text{Fe}^{193}\text{IrCl}$ C, 52.68; H, 4.94. Found: C, 50.37; H, 4.77. To a flask containing chloride complex (90 mg, 0.116 mmol) was added NaBARf (129 mg, 0.145 mmol), dry CH_2Cl_2 (6 mL), and deionized water (6 mL) under argon. The mixture was stirred for 15 minutes at room temperature over which time a colour change from orange to red occurred. The layers were separated, aqueous layer extracted with CH_2Cl_2 (3 x 3 mL), and the combined organic washed with deionized water (1 x 2 mL). The solvent was removed *in vacuo*, the residue taken up in CH_2Cl_2 and filtered through a plug of silica eluting with CH_2Cl_2 to give (*S*)-**236** (158 mg, 85%) as an orange solid. mp 128-129 °C; $[\alpha]_D^{20} -140.3$ (c 0.61, CHCl_3); ^{31}P NMR (121.5 MHz, CDCl_3) δ 14.37; ^{19}F NMR (282.4 MHz, CDCl_3) δ -62.34; ^1H NMR (300 MHz, CDCl_3) δ 7.71 (s, 8 H), 7.65-7.56 (m, 5H), 7.52 (s, 4 H), 7.47-7.41 (m, 5H), 4.86 (bs, 1H), 4.84 (t, 1H, $J = 2.7$ Hz), 4.49 (s, 5H), 4.44 (s, 1H), 4.31 (s, 1H), 4.04 (bs, 1H), 3.30 (m, 1H), 3.24 (m, 2H), 2.38-2.31 (m, 1H), 2.05-1.83 (m, 7H), 1.70-1.65 (m, 2H); ^{13}C NMR (150.9 MHz, CDCl_3) δ 161.70 (q, $J^{13}\text{C}-^{11}\text{B} = 49.8$ Hz, C- BARf), 133.3 (d, $J^{13}\text{C}-^{31}\text{P} = 12.1$ Hz, *ortho*-Ph), 133.0 (d, $J^{13}\text{C}-^{31}\text{P} = 40.7$ Hz, Ph-P), 132.0 (*para*-Ph), 131.8 (d, $J^{13}\text{C}-^{31}\text{P}$

= 10.6 Hz, *ortho*-Ph), 129.7 (d, $J^{13}_{\text{C}-^{31}\text{P}} = 9.1$ Hz, *meta*-Ph), 129.2 (d, $J^{13}_{\text{C}-^{31}\text{P}} = 10.6$ Hz, *meta*-Ph), 128.9 (q, $J^{13}_{\text{C}-^{19}\text{F}} = 30.2$ Hz, *meta*-BAr_F), 128.8 (*para*-Ph) 126.5 (d, $J^{13}_{\text{C}-^{31}\text{P}} = 58.9$ Hz, Ph-P), 124.5 (q, $J^{13}_{\text{C}-^{19}\text{F}} = 273.1$ Hz, CF₃), 121.6 (d, $J^{13}_{\text{C}-^{31}\text{P}} = 22.6$ Hz, C1-Cp), 117.5 (*para*-BAr_F), 91.3 (d, $J^{13}_{\text{C}-^{31}\text{P}} = 7.5$ Hz, COD alkene *trans*-P), 90.9 (d, $J^{13}_{\text{C}-^{31}\text{P}} = 12.1$ Hz, COD alkene *trans*-P), 74.1 (d, $J^{13}_{\text{C}-^{31}\text{P}} = 6.0$ Hz, C5-Cp), 72.28 (Cp unsub), 68.8 (d, $J^{13}_{\text{C}-^{31}\text{P}} = 96.6$ Hz, C2-Cp), 66.5 (pyr CH₂ *alpha*-N), 65.9 (C4-Cp), 61.1 (d, $J^{13}_{\text{C}-^{31}\text{P}} = 9.1$ Hz, C3-Cp), 60.7 (pyr CH₂ *alpha*-N), 58.64 (COD alkene *trans*-N), 57.98 (COD alkene *trans*-N), 32.6 (COD CH₂ *trans*-P), 32.4 (d, $J^{13}_{\text{C}-^{31}\text{P}} = 4.5$ Hz, COD CH₂ *trans*-P), 29.8 (COD CH₂ *trans*-N), 28.8 (COD CH₂ *trans*-N), 24.5 (pyr CH₂), 22.2 (pyr CH₂); FABMS [*m/z* (%)] 740 (39), 739 (43), 738 (100), 737 (55), 736 (100), 735 (40), 734 (58), 732 (29), 631 (33), 630 (79), 629 (36), 628 (65), 627 (25), 626 (30), 624 (25), 472 (30), 430 (34), 426 (27), 417 (39), 388 (30), 300 (27), 208 (33), 55 (54); HRMS (FAB) calcd for C₃₄H₃₈NP⁵⁶Fe¹⁹³Ir 740.1720, found 740.1730; Anal. Calcd for C₆₆H₅₀NP⁵⁶Fe¹⁹³IrBF₂₄: C, 49.45; H, 3.14. Found: C, 46.44; H, 3.06.

Diethyl benzylphosphonate. Benzyl bromide (0.89 mL, 7.5 mmol) and triethylphosphite

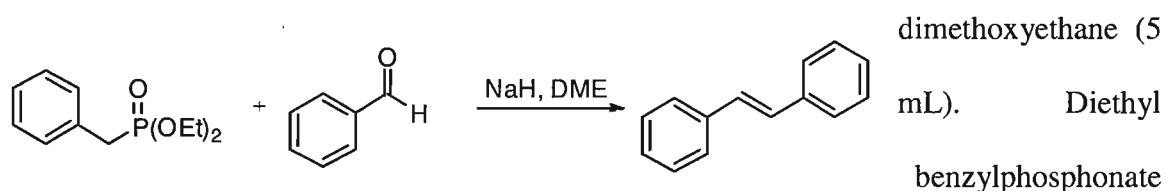


(1.74 mL, 10 mmol) were placed in a dry

round bottom flask and stirred under

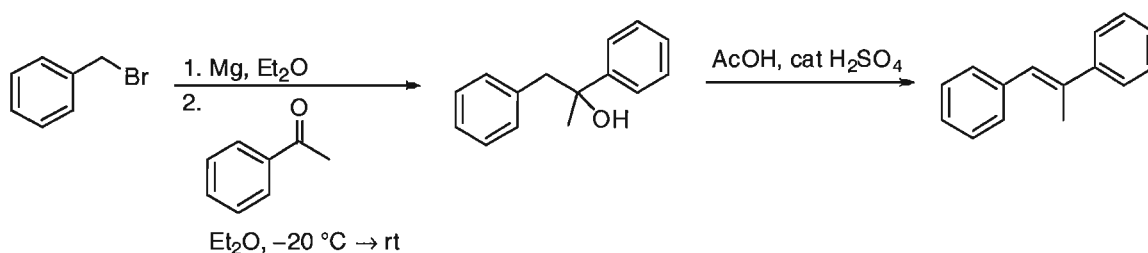
argon at 140 °C until gas evolution (bromoethane) had ceased (16 h). Excess P(OEt)₃ was removed *in vacuo* to afford product (1.5 g, 88%) as a clear, colourless oil. ³¹P NMR (121.5 MHz, CDCl₃) δ 26.4; ¹H NMR (300 MHz, CDCl₃) δ 7.31-7.29 (m, 4H), 7.26-7.21 (m, 1H), 4.0 (m, 4H), 3.13 (d, 2H, $J^1_{\text{H}-^{31}\text{P}} = 21.6$ Hz), 1.32 (t, 6H, $J = 1.8$ Hz).

1,2-diphenylethene (223a). To a dry flask was added NaH (79 mg, 3.3 mmol) and dry



(0.55 mL, 2.6 mmol) was added dropwise, followed by dropwise addition of benzaldehyde (225 μ L, 2.2 mmol), and the solution was stirred at room temperature for 16 h. Diethyl ether was added, followed by dropwise addition of water to quench excess NaH. The layers were separated and the aqueous layer extracted with Et₂O (3 x 5 mL). The combined organic layer was washed with water, brine, dried with MgSO₄, filtered, and solvent removed *in vacuo*. Recrystallization from ethanol afforded **223a** (253 mg, 64%) as shiny colourless flakes. mp 110 °C; ¹H NMR (300 MHz, CDCl₃) δ 7.52 (m, 4H), 7.37 (m, 4H), 7.27 (m, 2H), 7.12 (s, 2H); ¹³C NMR (75.5 MHz, CDCl₃) δ 128.7, 127.6, 126.5.

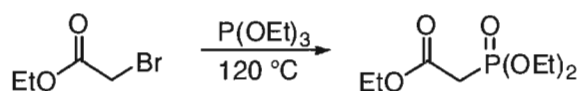
Trans-1,2-diphenylpropene (124). To a dry 3-neck flask was added cleaned Mg



turnings (1.18 g, 48 mmol, cleaned by washing with acetone / HCl and drying *in vacuo*), dry Et₂O (35 mL), and a few crystals of iodine. Distilled benzyl bromide (4.75 mL, 40 mmol) was placed in a dropping funnel with dry Et₂O (5 mL), and approximately 10% of the solution was added upon which the solution decolourized, turned cloudy grey, and started refluxing. The remainder of the solution was added dropwise over 35 minutes, and

stirred for an additional 15 min. The Grignard reagent was then cannulated into a dry flask containing distilled acetophenone (3.75 mL, 32 mmol) in Et₂O (4 mL) at –20 °C. The solution was allowed to warm slowly to room temperature, then stirred at room temperature overnight (15 hours). The reaction mixture was worked up by addition of saturated NH₄Cl solution (20 mL), extraction of the aqueous layer with Et₂O (1 x 20 mL), and washing of the combined organic layer with brine (2 x 10 mL). The organic layer was dried with Na₂SO₄, filtered, and solvent removed *in vacuo* to afford alcohol intermediate (6.57 g, 96%). Intermediate alcohol (6.5 g, 31 mmol) was added to a dry flask, followed by glacial acetic acid (10 mL), and sulfuric acid (30 µL). The mixture was stirred at reflux until consumption of starting material, neutralized with aqueous NaOH, and diluted with hexanes. The aqueous layer was extracted with hexanes (3 x 20 mL), combined organic layer washed with 1 M NaOH (1 x 10 mL), water (1 x 20 mL), and brine (1 x 10 mL). The organic phase was dried with Na₂SO₄, filtered, and solvent removed *in vacuo*. Crude product was recrystallized from absolute EtOH to give 4.2 g (71%) as shiny colourless flakes. mp 82-84 °C; ¹H NMR (300 MHz, CDCl₃) δ 7.57 (d, 2H, *J* = 1.5 Hz), 7.54-7.38 (m, 6H), 7.34-7.27 (m, 2H), 6.87 (s, 1H), 2.31 (d, 3H, *J* = 1.2 Hz); ¹³C NMR (75.5 MHz, CDCl₃) δ 129.1, 128.3, 128.2, 127.7, 126.4, 126.0, 17.5.

Triethylphosphonoacetate. Ethyl bromoacetate (5 mL, 45.2 mmol) and



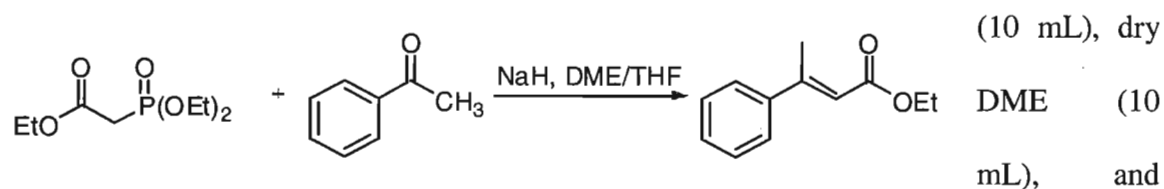
triethylphosphite (8.25 mL, 47.5 mmol)

were placed in a dry flask and stirred

under argon at 120 °C until gas evolution (bromoethane) ceased (16 hours). Excess P(OEt)₃ was removed *in vacuo* to afford product (10.1 g, 99%) as a clear, colourless oil.

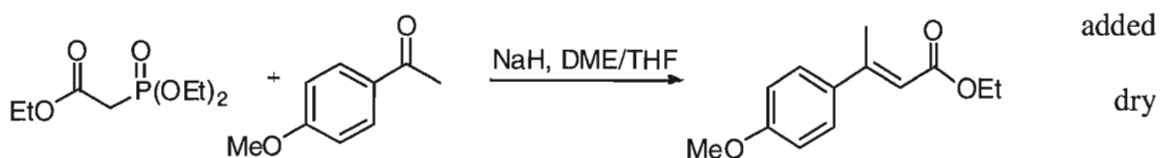
^{31}P NMR (121.5 MHz, CDCl_3) δ 19.8; ^1H NMR (300 MHz, CDCl_3) δ 4.17 (m, 6H), 2.95 (d, 2H, $J_{\text{H}-^{31}\text{P}} = 21.6$ Hz), 1.34 (t, 9 H, $J = 7.2$ Hz).

Trans-ethyl 3-phenylbut-2-enoate (128). To a dry flask under argon was added dry THF



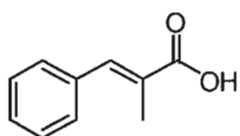
NaH (1.1 g, 27.5 mmol). Triethylphosphonoacetate (4 mL, 20.2 mmol) was added dropwise and the solution stirred at reflux for 30 min. After cooling to room temperature, a solution of acetophenone (2.14 mL, 18.3 mmol) in 10 mL 1:1 THF:DME was added dropwise. The solution was stirred at reflux until consumption of starting material was observed. The solution was diluted with Et_2O , water was added, the layers separated, and the aqueous layer extracted with Et_2O . The combined organic layer was washed with water, brine, dried with Na_2SO_4 , filtered, and concentrated *in vacuo*. Column chromatography (300 mL silica) with 20:1 hexanes:EtOAc afforded 935 mg (27%) of pure *trans* ester as a clear, colourless oil. ^1H NMR (300 MHz, CDCl_3) δ 7.50-7.27 (m, 5H), 6.13 (d, 1H, $J = 1.2$ Hz), 4.22 (q, 2H, $J = 7.2$ Hz), 2.58 (d, 3H, $J = 1.2$ Hz), 1.33 (q, 3H, $J = 7.2$ Hz); ^{13}C NMR (75.5 MHz, CDCl_3) δ 166.9, 155.5, 142.2, 128.9, 128.5, 126.3, 117.2, 59.8, 17.9, 14.3.

Trans-ethyl 3-(4-methoxyphenyl)but-2-enoate (225a). To a dry flask under argon was



THF (10 mL), dry DME (10 mL), and NaH (1.10 g, 27.5 mmol). Triethylphosphonoacetate (4.0 mL, 20.2 mmol) was added dropwise and the solution stirred at reflux for 30 min. After cooling to room temperature, a solution of 4-methoxyacetophenone (2.75 mL, 18.3 mmol) in 10 mL 1:1 THF:DME was added dropwise. The solution was stirred at reflux until consumption of starting material was observed. The solution was diluted with Et₂O, water was added, the layers separated, and the aqueous layer extracted with Et₂O. The combined organic layer was washed with water, brine, dried with Na₂SO₄, filtered, and concentrated *in vacuo*. Column chromatography (300 mL silica) with 9:1 hexanes:EtOAc afforded 867 mg (22%) of pure *trans* ester as a clear, colourless oil. ¹H NMR (300 MHz, CDCl₃) δ 7.46 (d, 2H, *J* = 9.0 Hz), 6.89 (d, 2H, *J* = 9.0 Hz), 6.11 (d, 1H, *J* = 1.2 Hz), 4.21 (q, 2H, *J* = 7.2 Hz), 3.83 (s, 3H), 2.56 (d, 3H, *J* = 1.2 Hz), 1.31 (t, 3H, *J* = 7.2 Hz); ¹³C NMR (75.5 MHz, CDCl₃) δ 167.1, 160.4, 154.9, 134.3, 127.7, 115.3, 113.8, 59.7, 55.3, 17.64, 14.4.

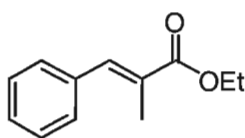
***Trans*-2-methyl-3-phenyl-acrylic acid (227v).** Triethylamine (16.2 mL, 116 mmol), propionic anhydride (15 mL, 116 mmol), and benzaldehyde (1.7 mL,



16.7 mmol) were combined in a dry flask under argon, heated at reflux for 80 h. After cooling to room temperature, the mixture was poured into 1 M H₂SO₄ (100 mL), then left to sit for 2 days at which point the crystalline solid was filtered, dissolved in CHCl₃ and extracted with 5% aqueous NaHCO₃. The combined aqueous layer was acidified with 1M H₂SO₄ at which point a white precipitate formed. The mixture was extracted with CHCl₃ (3 x 30 mL), the combined organic phase washed with water (1 x 20 mL), brine (1 x 20 mL) and dried with Na₂SO₄. Concentration

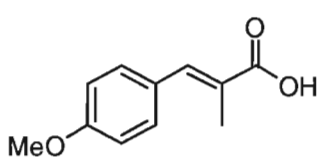
gave **227v** (1.88 g, 69%) as an off white solid. ^1H NMR (300 MHz, CDCl_3) δ 11.89 (bs, 1H), 7.86 (s, 1H), 7.45-7.36 (m, 5H), 2.17 (s, 3H).

Trans-ethyl 2-methyl-3-phenylacrylate (225b). **227v** (1.0 g, 6.2 mmol) was combined



with absolute EtOH (31 mL) and H_2SO_4 in a dry round bottom flask under argon. The mixture was heated to reflux overnight (19 h) then cooled to room temperature, and neutralized by addition of saturated aqueous NaHCO_3 . The solution was extracted with CH_2Cl_2 (3 x 20 mL), followed by washing with water, brine, and drying with MgSO_4 . Removal of the solvent *in vacuo* afforded crude product which was purified by Kugelrohr distillation (90-92 $^\circ\text{C}$ 0.2 mmHg) to give **225b** (1.1 g, 97%) as a colourless oil. ^1H NMR (300 MHz, CDCl_3) δ 7.69 (d, 1H, $J = 0.9$ Hz), 7.40 (d, 3H, $J = 4.2$ Hz), 7.36-7.26 (m, 2H), 4.28 (q, 2H, $J = 6.9$ Hz), 2.12 (d, 3H, $J = 1.5$ Hz), 1.36 (t, 3H, $J = 6.9$ Hz); ^{13}C NMR (75.5 MHz, CDCl_3) δ 168.9, 141.4, 138.6, 136.0, 129.6, 128.3, 128.2, 60.8, 14.3, 14.0.

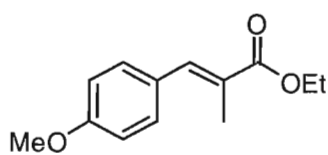
Trans-3-(4-methoxy-phenyl)-2-methyl-acrylic acid (227w). Triethylamine (16.2 mL,



116.2 mmol), propionic anhydride (15 mL, 116.4 mmol), and *p*-methoxybenzaldehyde (2.0 mL, 16.4 mmol) were combined in a dry flask under argon and heated at reflux for 80 h. After cooling to room temperature, the mixture was poured into 1 M H_2SO_4 (100 mL), then left to sit for 2 days at which point the crystalline solid was filtered, dissolved in CHCl_3 and extracted with 5% aqueous NaHCO_3 . The combined aqueous layer was acidified with 1M H_2SO_4 at which point a white precipitate formed. The mixture was extracted with CHCl_3

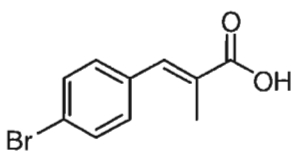
(3 x 30 mL), the combined organic phase washed with water (1 x 20 mL), brine (1 x 20 mL) and dried with Na₂SO₄. Concentration gave **227w** (992 mg, 31%) as an off white solid. ¹H NMR (300 MHz, CDCl₃) δ 11.93 (bs, 1H), 7.80 (s, 1H), 7.43 (d, 2H, *J* = 8.7 Hz), 6.95 (d, 2H, *J* = 8.7 Hz), 3.85 (s, 3H), 2.17 (s, 3H).

Trans-ethyl 3-(4-methoxyphenyl)-2-methylacrylate (225c). **227w** (192 mg, 1.57



mmol) was combined with absolute EtOH (5 mL) and H₂SO₄ (40 μL) in a dry round bottom flask under argon. The mixture was heated to reflux overnight (19 h) then cooled to room temperature, and neutralized by addition of saturated aqueous NaHCO₃. The solution was extracted with CH₂Cl₂ (3 x 20 mL), followed by washing with water, brine, and drying with MgSO₄. Removal of the solvent *in vacuo* afforded crude product which was purified by Kugelrohr distillation (90-92 °C 0.2 mmHg) to give **225c** (208 g, 95%) as a colourless oil. ¹H NMR (300 MHz, CDCl₃) δ 7.64 (s, 1H), 7.38 (d, 2H, *J* = 8.7 Hz), 6.93 (d, 2H, *J* = 9.0 Hz), 2.26 (q, 2H, *J* = 7.2 Hz), 3.84 (s, 3H), 2.13 (d, 3H, *J* = 1.2 Hz), 1.35 (t, 3H, *J* = 6.9 Hz); ¹³C NMR (75.5 MHz, CDCl₃) δ 168.9, 138.3, 131.4, 128.5, 113.8, 60.7, 55.3, 14.4, 14.1.

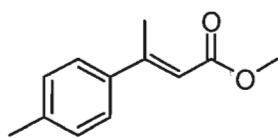
Trans-3-(4-bromo-phenyl)-2-methyl-acrylic acid (227x). Triethylamine (16.2 mL, 116



mmol), propionic anhydride (15 mL, 116 mmol), and 4-bromobenzaldehyde (3.07 mL, 16.6 mmol) were combined in a dry flask under argon, heated at reflux for 80 h. After cooling to room temperature, the mixture was poured into 1 M H₂SO₄ (100 mL), then left to sit for 2

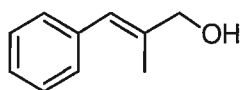
days at which point the crystalline solid was filtered, dissolved in CHCl_3 and extracted with 5% aqueous NaHCO_3 . The combined aqueous layer was acidified with 1M H_2SO_4 at which point a white precipitate formed. The mixture was extracted with CHCl_3 (3 x 30 mL), the combined organic phase washed with water (1 x 20 mL), brine (1 x 20 mL) and dried with Na_2SO_4 . Concentration gave the carboxylic acid as an off white solid (2.99 g, 75%). ^1H NMR (300 MHz, CDCl_3) δ 11.71 (bs, 1H), 7.74 (s, 1H), 7.55 (d, 2H, $J = 8.4$ Hz), 7.30 (d, 2H, $J = 8.4$ Hz), 2.12 (s, 3H).

***Trans*-methyl 3-*p*-tolylbut-2-enoate (225d).** To a suspension of NaH (325 mg, 8.13



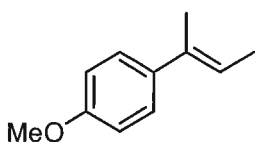
mmol) in DME (15 mL) was added dropwise trimethylphosphonoacetate (1.15 mL, 7.96 mmol), followed by dropwise addition of a solution of *p*-methyl acetophenone (1.05 mL, 7.86 mmol) in DME (5 mL). The solution was allowed to stir at room temperature overnight (approximately 14 h). Et_2O and water were added, layers separated, and the aqueous layer extracted with Et_2O . The combined organic layer was washed with brine, dried with MgSO_4 , filtered, and concentrated. The mixture of *cis* and *trans* alkene, as well as unreacted starting material was purified by flash chromatography (silica 150 mL, 95:5 hexane:MeOH) to give 201 mg of pure *trans* alkene (13%), 155 mg mixed *cis* and *trans* alkene, and 516 mg unreacted starting material. ^1H NMR (300 MHz, CDCl_3) δ 7.39 (d, 2H, $J = 8.4$ Hz), 7.18 (d, 2H, $J = 8.1$ Hz), 6.14 (d, 1H, $J = 1.2$ Hz), 3.75 (s, 3H), 2.57 (d, 3H, $J = 1.2$ Hz), 2.37 (s, 3H).

Trans-2-methyl-3-phenylpropenol (225f). To a flask containing α -methyl *trans*



cinnamaldehyde (2 mL, 14.3 mmol) in 95% EtOH (30 mL) at 0 °C was added sodium borohydride (650 mg, 17.2 mmol). The solution was stirred for 30 min, then saturated NH₄Cl (7.5 mL) and H₂O (7.5 mL) were added, followed by further stirring for 1 h. The EtOH was removed *in vacuo*, and the aqueous layer was extracted with Et₂O (3 x 10 mL). The combined organic layer was washed with brine (1 x 10 mL), dried with MgSO₄, filtered, and concentrated *in vacuo* to give **225f** (2.1 g, 97%) as a clear, colourless oil. ¹H NMR (300 MHz, CDCl₃) δ 7.37-7.20 (m, 6H), 6.53 (bs, 1H), 4.20 (bs, 2H), 1.91 (s, 3H).

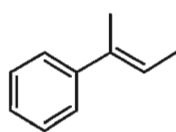
Trans-1-(butenyl)-4-methoxybenzene (125). To a solution of PPh₃ (5.25 g, 20 mmol) in



dry THF (15 mL) at 0 °C was added ethyl iodide (1.60 mL, 20 mmol). The solution was stirred for 5 minutes then the ice bath was then removed and the solution stirred at room temperature for 20 h. The mixture was filtered, washed with THF, and the solid dried *in vacuo* to give the phosphonium salt (4.23 g, 51%). The solid was dissolved in dry THF (25 mL), cooled to 0 °C, and treated slowly with *n*-BuLi (5.14 mL, 10.1 mmol, 1.97 M in hexane). The solution was allowed to stir for a further 10 minutes then was treated with a solution of *p*-methoxyacetophenone (1.52 mL, 10.1 mmol) in dry THF (12 mL). The solution was allowed to warm slowly to room temperature over 24 h over which time the solution went from deep red to light orange with precipitate formed. After treatment with saturated aqueous NH₄Cl (20 mL) the solution went colourless and more precipitate formed.

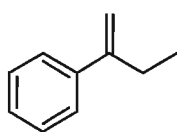
CH₂Cl₂ (40 mL) was added and the layers separated. The aqueous layer was extracted with EtOAc (2 x 20 mL), the combined organic washed with brine (40 mL), and dried with MgSO₄. Flash chromatography (silica, CH₂Cl₂) provided a colourless oil as a 3:1 *trans:cis* mixture (1.12 mg, 68%). ¹H NMR (300 MHz, CDCl₃) δ 7.31 (m, 2H), 6.88-6.83 (m, 2H), 5.79 (qq, 1H, *J* = 6.9, 1.2 Hz), 3.81 (s, 3H), 2.01 (s, 3H), 1.79 (dd, 3H, 6.9, 0.9).

Trans-butenylbenzene (225g). Mg turnings (740 mg, 30.8 mmol) and dry Et₂O (5 mL)



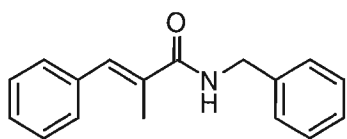
were added to a dry round bottom flask under argon and activated with a crystal of iodine. MeI (1.75 mL, 28.1 mmol) in dry Et₂O (10 mL) was added dropwise. After addition was complete, the reaction mixture was heated to reflux for 30 min. Propiophenone (3.4 mL, 25.6 mmol) in dry Et₂O (10 mL) was then added dropwise to the solution at reflux. After addition was complete, the reaction mixture was heated at reflux for a further 3 h. After cooling to 0 °C, 10 % HCl (50 mL) was added. The layers were separated, and the aqueous extracted with Et₂O. The crude was concentrated then treated with a mixture of glacial acetic acid (3.4 mL) and H₂SO₄ (0.5 mL), and the mixture heated at 60 °C for 15 minutes. The mixture was extracted with Et₂O followed by washing with 1M NaHCO₃, brine, and drying with MgSO₄. Flash chromatography (silica, 9:1 hexanes:EtOAc) gave **225g** (755 mg, 22%) as a clear colourless oil. ¹H NMR (300 MHz, CDCl₃) δ 7.38-7.25 (m, 5H), 5.95 (q, 1H, *J* = 6.9 Hz), 2.10 (s, 3H), 1.87 (d, 3H, *J* = 6.6 Hz).

But-1-en-2-ylbenzene (225h). To a solution of PPh₃ (5.25 g, 20 mmol) in dry THF (15



mL) at 0 °C was added MeI (1.25 mL, 20.1 mmol). The ice bath was then removed and the solution stirred at room temperature for 1 h over which time copious amounts of white solid formed. After 1 h the mixture was filtered, washing with THF, and the solid dried *in vacuo* to give the phosphonium salt (7.56 g, 94 %). The solid was dissolved in dry THF (25 mL), cooled to 0 °C, and treated with *n*-BuLi (9.5 mL, 18.7 mmol, 1.97 M in hexane) at which point the solution went from a white slurry to a clear red solution (formation of CH₂=PPh₃ ylide). The solution was allowed to stir for a further 10 minutes then was treated with a solution of propiophenone (2.49 mL, 18.7 mmol) in dry THF (10 mL). The solution was allowed to warm slowly to room temperature over 24 h over which time the solution became light orange and precipitate formed. After treatment with 1M HCl (20 mL) the solution went colourless and more precipitate formed. EtOAc (40 mL) was added and the layers separated. The aqueous layer was extracted with EtOAc (2 x 20 mL), the combined organic washed with brine (40 mL), and dried with MgSO₄. Flash chromatography (silica, hexanes) provided **225h** (742 mg, 28%) as a colourless oil. ¹H NMR (300 MHz, CDCl₃) δ 7.47 (d, 2H, *J* = 1.8 Hz), 7.46-7.35 (m, 3H), 5.42 (s, 1H), 5.20 (d, 1H, *J* = 1.2 Hz), 2.65 (q, 2H, *J* = 7.2 Hz), 1.24 (t, 3H, *J* = 7.5 Hz).

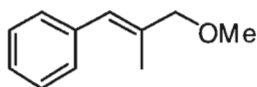
Trans-N-benzyl-2-methyl-3-phenylacrylamide (225i). **227v** (162 mg, 1.0 mmol) was



dissolved in SOCl₂ (2 mL) and heated to reflux under argon for 1 h. Removal of excess SOCl₂ *in vacuo* provided a yellow oil which was taken up in dry CH₂Cl₂ and cooled to 0 °C. To this solution was

dropwise added benzylamine (220 μL , 2 mmol) and NEt_3 (560 μL , 4 mmol) forming a cloudy orange-brown solution. The solution was stirred at 0 $^\circ\text{C}$ for 30 min, then at room temperature for 2 h. The solution was quenched with saturated aqueous NH_4Cl , EtOAc added, and the layers separated. The aqueous layer was extracted with EtOAc and the crude product dissolved in CH_2Cl_2 , and washed with 1M NaHCO_3 (3 x 10 mL). The organic layer was washed with water, brine, and dried with MgSO_4 . Flash chromatography (silica, 9:1 hexanes:EtOAc) afforded amide **225i** (165 mg, 66%) as an off white solid. ^1H NMR (300 MHz, CDCl_3) δ 7.40-7.29 (m, 11H), 6.16 (bs, 1H), 4.58 (d, 2H, $J = 5.7$ Hz), 2.12 (d, 3H, $J = 0.9$ Hz).

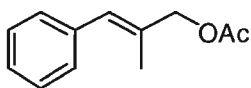
Trans-(3-methoxy-2-methylprop-1-enyl)benzene (225j). A solution of **225f** (1.0 mL,



6.75 mmol) in dry THF (7 mL) was added dropwise to a stirred suspension of NaH (450 mg, 11.25 mmol) in dry THF (15 mL) at

0 $^\circ\text{C}$ under argon. Once addition was complete, MeI (615 μL , 9.86 mmol) was added dropwise. The reaction mixture was allowed to warm to room temperature and stirred for 24 h. 4M NaOH (10 mL) was added and the solution stirred overnight (16 h). The mixture was diluted with Et_2O , layers separated, and the aqueous layer extracted with Et_2O (3 x 10 mL). The combined organic phase was washed with water, brine, and dried with MgSO_4 . Flash chromatography (silica, 8:2 hexanes:EtOAc) provided a clear oil (1.08 g, 99%). ^1H NMR (300 MHz, CDCl_3) δ 7.37-7.20 (m, 5H), 6.51 (s, 1H), 3.98 (s, 2H), 3.38 (s, 3H), 1.89 (d, 3H, $J = 1.2$ Hz); ^{13}C NMR (75.5 MHz, CDCl_3) δ 137.5, 135.1, 128.9, 128.1, 126.9, 126.4, 78.7, 57.8, 15.4.

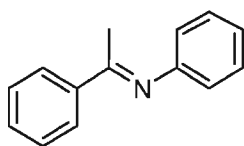
Trans-2-methyl-3-phenylallyl acetate (225k). Pyridine (3 mL, 33.75 mmol) and acetic



anhydride (3 mL, 33.75 mmol) were added to a solution of allylic alcohol **225f** and stirred at room temperature under argon for 24 h.

Water (5 mL) was added, the layers separated and the aqueous layer extracted with CH₂Cl₂ (3 x 10 mL). The combined organic phase was washed with 1M NaHCO₃, water, and brine, dried with MgSO₄ and volatiles removed *in vacuo*. Flash chromatography (silica, 8:2 hexanes:EtOAc) provided a clear oil (1.18 g, 92%). ¹H NMR (300 MHz, CDCl₃) δ 7.37-7.21 (m, 5 H), 6.54 (s, 1H), 4.64 (s, 2H), 2.13 (s, 3H), 1.91 (d, 3H, *J* = 1.2 Hz); ¹³C NMR (75.5 MHz, CDCl₃) δ 170.9, 132.7, 128.9, 128.2, 128.1, 126.8, 70.2, 21.0, 15.5.

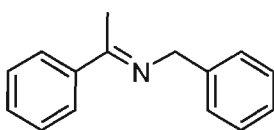
Trans-N-(1-phenylethylidene)aniline (225l). Acetophenone (1.0 mL, 8.55 mmol), and



aniline (940 μL, 10.32 mmol) in toluene (60 mL) were stirred in the presence of molecular sieves (5 Å) at reflux for 12 h. The mixture was filtered through celite and volatiles removed *in vacuo* and

recrystallized from pentane (499 mg, 30%). mp 39-40 °C; ¹H NMR (300 MHz, CDCl₃) δ 8.00-7.97 (m, 2H), 7.47-7.38 (m, 3H), 7.36 (t, 2H, *J* = 7.8 Hz), 7.09 (m, 1H), 6.80 (m, 2H), 2.24 (s, 3H).

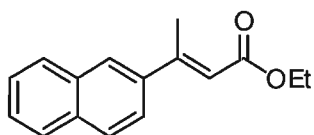
Trans-1-phenyl-N-(1-phenylethylidene)methanamine (225m). Acetophenone (590 μL,



5.05 mmol), benzyl amine (550 μL, 5.04 mmol), and *p*-toluene sulfonic acid (11 mg, 0.06 mmol) in benzene (10 mL) were heated to reflux with a Dean-Stark trap for 10 h. Na₂CO₃ was added and

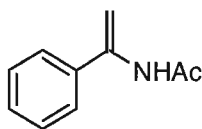
the mixture passed through celite with benzene and volatiles removed *in vacuo* to give a 16:1 mixture of *trans* and *cis* imines (646 mg, 61%). ^1H NMR (300 MHz, CDCl_3) δ 7.91-7.88 (m, 2H), 7.45-7.33 (m, 8H), 4.75 (s, 2H), 2.35 (s, 3H).

***Trans*-ethyl 3-(naphthalen-2-yl)but-2-enoate (225n).** A suspension of NaH (500 mg,



12.5 mmol) in DME (15 mL) was treated with a solution of triethylphosphonoacetate (1.82 mL, 9.17 mmol) in DME (6 mL) and the mixture stirred for 15 min. A solution of 2'-acetonaphthone (1.42 mL, 8.3 mmol) in DME (6 mL) was added, and the solution stirred at room temperature under argon for 15 h. Water (20 mL) and Et_2O (20 mL) were added, the aqueous layer extracted with Et_2O (3 x 20 mL), and the combined organic layer washed with water (1 x 20 mL), brine (1 x 20 mL) and dried with MgSO_4 . Flash chromatography (silica 200 mL, 95:5 hexanes:EtOAc) provided *trans* alkene as a clear oil which was purified by Kogelrorh distillation (130 °C, 0.125 mmHg) yielding 600 mg (30%). ^1H NMR (300 MHz, CDCl_3) δ 7.96 (s, 1H), 7.95-7.82 (m, 3H), 7.62 (dd, 1H, J = 8.7, 1.8 Hz), 7.53-7.49 (m, 2H), 6.29 (d, 1H, J = 1.2 Hz), 4.25 (q, 2H, J = 7.2 Hz), 2.69 (d, 3H, J = 7.2 Hz).

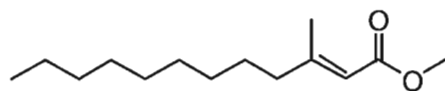
***N*-(1-phenylvinyl)acetamide (225o).** Acetophenone (3 mL, 25.7 mmol), hydroxylamine



hydrochloride (3.8 g, 54.7 mmol), pyridine (4 mL, 49.7 mmol) were combined in EtOH (40 mL) and heated at reflux for 5 h. The solution was cooled to 0 °C and water (40 mL) was added. The precipitate was collected and washed with ice cold water. The solid was dissolved in EtOAc, dried with MgSO_4 , and

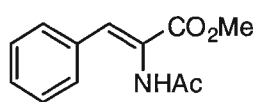
volatiles removed *in vacuo* to provide intermediate oxime (2.94 g, 85%). The intermediate oxime (2.5 g, 18.5 mmol) was dissolved in toluene, and acetic anhydride (5.25 mL, 55.6 mmol), acetic acid (3.2 mL, 55.9 mmol), iron powder (2.17 g, 38.9 mmol), and three drops of TMSCl were added. The solution was heated at 70 °C for 5 h after which the mixture was filtered through celite eluting with toluene. The organic layer was washed with 2M NaOH (2 x 20 mL), water, brine, and dried with MgSO₄. The volatiles were removed and the residue columned with 95:5 CH₂Cl₂:EtOAc giving **225o** (1.8 g, 60%) as a tan solid. ¹H NMR (300 MHz, CDCl₃) δ 7.41-7.36 (m, 5 H), 6.76 (bs, 1H), 5.89 (s, 1H), 5.09 (s, 1H), 2.15 (s, 3H).

Trans-methyl 3-methyldodecenoate (225p). To a suspension of NaH (325 mg, 8.13



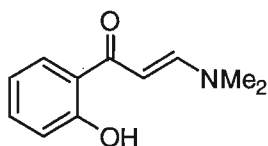
mmol) in DME (15 mL) was added dropwise trimethylphosphonoacetate (1.15 mL, 7.96 mmol), followed by dropwise addition of a solution of 2-undecanone (1.63 mL, 7.86 mmol) in DME (5 mL). The solution was allowed to stir at room temperature overnight (approximately 14 h). Et₂O and water were added, layers separated, and the aqueous layer extracted with Et₂O. The combined organic layer was washed with brine, dried with MgSO₄, filtered, and concentrated. The mixture of *cis* and *trans* alkene, as well as unreacted starting material was purified by flash chromatography (silica 150 mL, 95:5 hexane:MeOH) to give 116 mg of pure *trans* alkene (7%), and 448 mg mixed *cis* and *trans* alkene (25%). ¹H NMR (300 MHz, CDCl₃) δ 5.66 (m, 1H), 3.68 (s, 3H), 2.15 (s, 3H), 1.48 (m, 2H), 1.27 (m, 14 H), 0.88 (t, 3H, *J* = 6.9 Hz).

Methyl 2-acetamido-3-phenylacrylate (227b). To a vial containing phenyl iodide (72.4



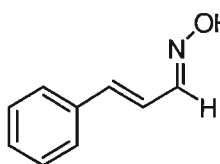
mg, 0.355 mmol) were added methyl 2-acetamidoacrylate (76 mg, 0.531 mmol), Pd(OAc)₂ (2.4 mg, 0.011 mmol), Me₄NBr (61 mg, 0.396 mmol), NaHCO₃ (80.5 mg, 0.958 mmol), and DMF (5 mL). The mixture was flushed with argon and heated at 85 °C for 36 h. Water was added, and the solution extracted with hexane. The combined organic layer was washed with water, brine, and dried with Na₂SO₄. Removal of the solvent *in vacuo*, followed by flash chromatography (silica, 6:4 EtOAc:hexanes) of the preadsorbed crude mixture provided **227b** (58 mg, 75%) as beige crystals. ¹H NMR (300 MHz, CDCl₃) δ 7.45-7.35 (m, 6 H), 3.86 (s, 3H), 2.15 (s, 3H), 1.25 (bs, 1H).

3-(dimethylamino)-1-(2-hydroxyphenyl)prop-2-en-1-one (227c). 2'-hydroxy-1-



acetophenone (2 mL, 16.6 mmol) and 1,1-diethoxy-*N,N*-dimethylmethanamine (4.3 mL, 25.1 mmol) were combined together under argon and heated at 85 °C for 3 h. The crude was recrystallized from EtOAc to give yellow-lime green needles (2.34 g, 74%). mp 140-142 °C; ¹H NMR (300 MHz, CDCl₃) δ 13.92 (s, 1H), 7.89 (d, 1H, *J* = 12.0 Hz), 7.69 (dd, 1H, *J* = 8.1, 1.5 Hz), 7.35 (dt, 1H, *J* = 8.7, 1.5 Hz), 6.94 (dd, 1H, *J* = 8.4, 0.9 Hz), 6.82 (dt, 1H, *J* = 8.1, 0.9 Hz), 5.79 (d, 1H, *J* = 12.3 Hz), 3.20 (s, 3H), 2.98 (s, 3H).

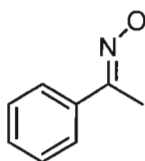
Cinnamaldehyde oxime (227d). To a solution of hydroxylamine hydrochloride (415 mg,



5.97 mmol) in absolute EtOH (10 mL) was added cinnamaldehyde (500 μL, 3.97 mmol) and pyridine (0.5 mL) and the solution was

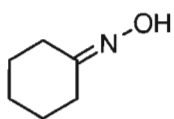
heated to reflux for 2 h. The EtOH was removed *in vacuo*, water (5 mL) was added and the solution stirred at 0 °C overnight. The solid that formed was collected by vacuum filtration, washing with H₂O, and recrystallized from absolute EtOH to give the oxime (375 mg, 64%) as pale yellow crystals.

Acetophenone oxime (227e). To a solution of hydroxylamine hydrochloride (450 mg,



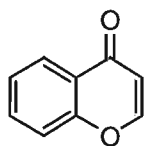
6.48 mmol) in absolute EtOH (10 mL) was added acetophenone (500 μ L, 4.29 mmol) and pyridine (0.5 mL) and the solution was heated to reflux for 2 h. The EtOH was removed *in vacuo*, water (5 mL) was added and the solution stirred at 0 °C overnight. The solid that formed was collected by vacuum filtration, washing with H₂O, and recrystallized from absolute EtOH to give the oxime (356 mg, 61%) as pale yellow crystals. mp 56-58 °C; ¹H NMR (300 MHz, CDCl₃) δ 8.14 (s, 1H), 7.65-7.62 (m, 2H), 7.40-7.39 (m 3H), 2.30 (s, 3H).

Cyclohexane oxime (227f). Cyclohexanone (500 μ L, 4.82 mmol), hydroxylamine



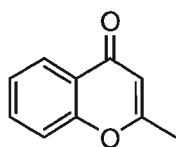
hydrochloride (402.5 mg, 5.79 mmol), and NaOH (258 mg, 6.45 mmol) were combined in a mortar and pestle and ground for 10 min, and then every 5 min for a further 10 min. The mixture was then washed with water, filtered, and then purified via hot filtration with petroleum ether to give the oxime as off-white crystals. mp 78-80 °C. ¹H NMR (300 MHz, CDCl₃) δ 8.07 (s, 1H), 2.50 (t, 2H, *J* = 6.0 Hz), 2.21 (t, 2H, *J* = 5.7 Hz), 1.69-1.61 (m, 6H).

Chromenone (227m). To a solution of 2'-hydroxyacetophenone (2 mL, 16.6 mmol) in



methyl formate (15 mL, 243 mmol) was added sodium (1.55 g, 67.4 mmol) in pieces. The addition resulted in the formation of copious amounts of off white precipitate. The solution was then heated to reflux, leading to the formation of more precipitate. More methyl formate (15 mL) was added and the solution heated at reflux for 1.5 h. The solution was cooled to room temperature and 20 g of crushed ice was added, resulting in a clear dark yellow-brown solution. The solution was extracted with Et₂O (4 x 25 mL), the combined organic phase washed with water, brine, and dried with Na₂SO₄. Volatiles were removed *in vacuo* providing intermediate aldehyde (1.80 g, 66%) as a tan precipitate. mp 93-96 °C. To a solution of intermediate aldehyde (1.0 g, 6.09 mmol) in H₂SO₄ (3 mL) was added cold water slowly until precipitate formed (20 mL). The solid was collected by suction filtration, washing with ice cold water, dried and recrystallized from petroleum ether to provide **227m** (850 mg, 96%) as a tan solid. mp 51-52 °C; ¹H NMR (300 MHz, CDCl₃) δ 8.21 (dd, 1H, *J* = 8.1, 1.5 Hz), 7.86 (d, 1H, *J* = 6.0 Hz), 7.71-7.65 (m, 1H), 7.48-7.39 (m, 2H), 6.34 (d, 1H, *J* = 6.0 Hz).

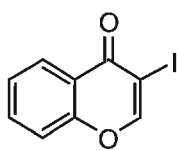
2-methylchromen-4-one (227o). To a solution of 2'-hydroxyacetophenone (2.0 mL, 16.6



mmol) in EtOAc (20 mL) was slowly added sodium (1.6 g, 69.6 mmol) in pieces over approximately 1.5 h over which time the solution turned a dark brown colour and became viscous with precipitate. After addition was complete, the solution was heated to reflux for 2 h after which the solution was a viscous tan-brown colour. Once cool, crushed ice (20 g) was added slowly and the

solution turned a dark brown colour with off white precipitate. After stirring for 25 min in an ice bath, the precipitate was collected by suction filtration, washing with petroleum ether. The precipitate was washed with 40% acetic acid (20 mL), filtered again, and solid washed with petroleum ether to give **227o** (600 mg, 20%) as an off-white solid. mp 92-95 °C; ^1H NMR (300 MHz, CDCl_3) δ 8.12 (dd, 1H, $J = 7.8, 1.5$ Hz), 7.59 (m, 1H), 7.37-7.29 (m, 2H), 6.12 (s, 1H), 2.33 (s, 3H); ^{13}C NMR (75.5 MHz, CDCl_3) δ 178.2, 166.2, 156.5, 133.5, 125.6, 124.9, 123.6, 117.8, 110.6, 20.6.

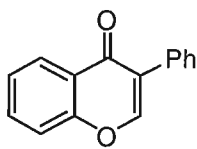
3-iodochromen-4-one (227q). A solution of **227c** (1.0 g, 5.23 mmol) and I_2 (2.0 g, 7.88



mmol) in chloroform (100 mL) was stirred open to air for 4 h. The solution was then washed with saturated aqueous $\text{Na}_2\text{S}_2\text{O}_3$ (100 mL).

The aqueous layer was extracted once with CHCl_3 (50 mL), and the combined organic layer was dried with Na_2SO_4 . Flash chromatography (silica, 70:30 hexane:EtOAc) provided **227q** (977 mg, 69%) as a tan solid. mp 94-97 °C; ^1H NMR (300 MHz, CDCl_3) δ 8.26 (s, 1H), 8.19 (dd, 1H, $J = 7.8, 1.2$ Hz), 7.68 (m, 1H), 7.41 (m, 2H).

3-phenylchromen-4-one (227n). To a solution of **227q** (300 mg, 1.10 mmol) in benzene



(44 mL) were added Na_2CO_3 (2.2 mL, 2M, 4.40 mmol), $\text{Pd}(\text{PPh}_3)_4$

(63.6 mg, 0.055 mmol), and a solution of phenylboronic acid (536.8

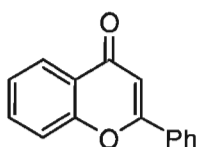
mg, 4.40 mmol) in EtOH (10 mL). The solution was heated to reflux for

18 h, after which time 30 % H_2O_2 (2.2 mL) was added and the solution stirred for 1 h.

The mixture was poured into 100 mL ice water, followed by extraction with CH_2Cl_2 . The combined organic layer was washed with water, brine, and dried with Na_2SO_4 . Flash

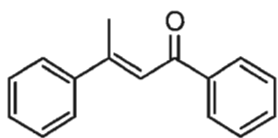
chromatography (silica, benzene) provided **227n** (208 mg, 85%) as a beige solid. ^1H NMR (300 MHz, CDCl_3) δ 8.33 (dd, 1H, $J = 7.8, 1.2$ Hz), 8.03 (s, 1H), 7.69 (m, 1H), 7.58 (m, 2H), 7.44 (m, 5H); ^{13}C NMR (75.5 MHz, CDCl_3) δ 176.2, 156.2, 153.0, 133.6, 131.8, 129.9, 128.5, 128.2, 126.4, 125.4, 125.2, 124.6, 118.0.

2-phenylchromen-4-one (227p). To a solution of 2'-hydroxyacetophenone (2.0 mL, 16.6

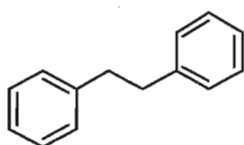


mmol) and benzaldehyde (1.65 mL, 16.6 mmol) in absolute EtOH (50 mL) was added NaOH (2.08 g, 52.0 mmol) at which point the colour changed to yellow and precipitate formed. After stirring at room temperature overnight, the solution was neutralized with HCl, the EtOH removed *in vacuo*, and the solution extracted with Et₂O. The combined organic layer was washed with brine, dried with Na₂SO₄, and the crude mixture purified by flash chromatography (silica, 90:10 hexane:EtOAc) and recrystallized from MeOH to give intermediate alkene (2.09 g, 53 %). ^1H NMR (300 MHz, CDCl_3) δ 12.81 (s, 1H), 7.96-7.91 (m, 2H), 7.70-7.65 (m, 3H), 7.51 (m, 1H), 7.46-7.44 (m, 3H), 7.04 (dd, 1H, $J = 8.4, 0.9$ Hz), 6.98-6.93 (m, 1H). To a solution of the intermediate (1.80 g, 7.54 mmol) in DMSO (15 mL) was added I₂ (192.8 mg, 0.760 mmol) and the solution heated at reflux for 2 h. After the solution was cooled to room temperature, saturated sodium thiosulfate (30 mL) was added and the solution extracted with CH₂Cl₂/hexanes. Flash chromatography (silica, 75:25 hexanes:EtOAc) provided **227p** (1.51 g, 90%) as an off-white solid. mp 96-97 °C; ^1H NMR (300 MHz, CDCl_3) δ 8.24 (dd, 1H), 7.94 (m, 2H), 7.71 (m, 1H), 7.59-7.51 (m, 4H), 7.43 (m, 1H), 6.84 (s, 1H).

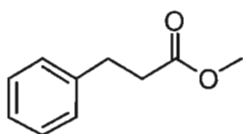
1,3-diphenylbut-2-en-1-one (227s). A mixture of acetophenone (3.0 mL, 25.7 mmol), acetic acid (2.2 mL, 34.9 mmol), and ammonium acetate (1.19g, 15.4 mmol) in toluene were heated to reflux in a Dean-Stark trap at reflux overnight (12 h). The mixture was transferred to a separator funnel and the organic washed once with water (10 mL). The organic phase was dried with Na₂SO₄ and solvent removed *in vacuo*. The mixture was Kugelrohr distilled to provide two fractions – acetophenone (65 °C, 0.35 mmHg, 1.52 g) and **227s** (150-160 °C, 0.35 mmHg, 599 mg, 21%) as a yellow oil.



1,2-diphenylethane (226a). A solution of *trans*-stilbene **225a** (50 mg, 0.28 mmol) and iridium catalyst **221** (8.8 mg, 0.0056 mmol, 2.0 mol %) in CH₂Cl₂ (3 mL) in a vial under argon was sealed in an autoclave. The autoclave was evacuated and back-filled with hydrogen three times, pressurized to 62 bar, and allowed to stir for 48 h. The reaction mixture was passed through a silica plug with Et₂O and solvent was removed *in vacuo* to give **226a** (49.6 mg, 97%) as a colourless solid. mp 48-50 °C (Lit.¹²⁵ mp 47-49 °C); ¹H NMR (300 MHz, CDCl₃) δ 7.39-7.25 (m, 10H), 3.01 (s, 4H); ¹³C NMR (75.5 MHz, CDCl₃) δ 141.9, 128.6, 128.5, 126.0, 38.1.



Methyl 3-phenylpropanoate (226b). A solution of methyl *trans* cinnamate (49 mg, 0.30 mmol) and iridium catalyst **221** (9.8 mg, 0.0062 mmol, 2.0 mol %) in CH₂Cl₂ (3 mL) in a vial under argon was sealed in an autoclave. The autoclave was evacuated and back-filled with hydrogen three times, pressurized to



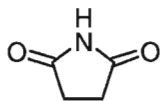
62 bar, and allowed to stir for 48 h. The reaction mixture was passed through a silica plug with Et₂O and solvent was removed *in vacuo* to give **226b** (47.6 mg, 95%) as a clear oil. ¹H NMR (300 MHz, CDCl₃) δ 7.33-7.19 (m, 5H), 3.68 (s, 3H), 2.97 (t, 2H, *J* = 8.1 Hz), 2.65 (t, 2H, *J* = 7.8 Hz); ¹³C NMR (75.5 MHz, CDCl₃) δ 173.4, 140.6, 128.6, 128.4, 126.4, 51.7, 35.8, 31.0.

1,3-diphenylpropan-1-one (226c). A solution of chalcone (50 mg, 0.24 mmol) and iridium catalyst **221** (7.4 mg, 0.0047 mmol, 2.0 mol %) in CH₂Cl₂ (3 mL) in a vial under argon was sealed in an autoclave. The autoclave was evacuated and back-filled with hydrogen three times, pressurized to 62 bar, and allowed to stir for 96 h. The reaction mixture was passed through a silica plug with Et₂O and solvent was removed *in vacuo* to give **226c** (50 mg, 99%) as a pale yellow solid. mp 69-70 °C (Lit.¹²⁶ 70-72 °C); ¹H NMR (300 MHz, CDCl₃) δ 7.98 (d, 2H, *J* = 7.2 Hz), 7.6-7.2 (m, 8H), 3.33 (t, 2H, *J* = 7.8 Hz), 3.10 (t, 2H, *J* = 7.2 Hz); ¹³C NMR (75.5 MHz, CDCl₃) δ 199.3, 141.4, 136.9, 133.2, 128.7, 128.6, 128.5, 128.1, 126.2, 40.5, 30.2.

Cyclohexanone (226d). A solution of cyclohexenone (30 μL, 0.31 mmol) and iridium catalyst **221** (9.8 mg, 0.0062 mmol, 2.0 mol %) in CH₂Cl₂ (3 mL) in a vial under argon was sealed in an autoclave. The autoclave was evacuated and back-filled with hydrogen three times, pressurized to 62 bar, and allowed to stir for 48 h. The reaction mixture was passed through a silica plug with Et₂O and solvent was removed *in vacuo* to give **226d** (26 mg, 84%) as a slightly volatile clear oil. ¹H NMR

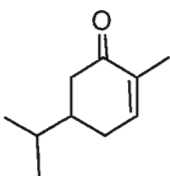
(300 MHz, CDCl₃) δ 2.31 (t, 2H, J = 6.9 Hz), 1.85-1.81 (m, 2H), 1.70-1.69 (m, 1H); ¹³C NMR (75.5 MHz, CDCl₃) δ 212.2, 40.1, 35.6, 27.1, 25.1.

Pyrrolidine-2,5-dione (226e). A solution of maleimide (32 mg, 0.33 mmol) and iridium



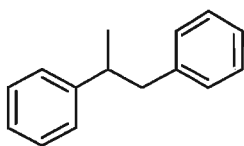
catalyst **221** (10.4 mg, 0.0066 mmol, 2.0 mol %) in CH₂Cl₂ (3 mL) in a vial under argon was sealed in an autoclave. The autoclave was evacuated and back-filled with hydrogen three times, pressurized to 62 bar, and allowed to stir for 96 hours. The reaction mixture was passed through a silica plug with Et₂O and solvent was removed *in vacuo* to give **225e** (27 mg, 82%) as an off white solid. mp 125-127 °C (Lit.¹²⁷ 125-127 °C); ¹H NMR (300 MHz, acetone-d₆) δ 2.68 (s, 4H), 9.88 (bs, 1H); ¹³C NMR (75.5 MHz, acetone-d₆) δ 178.9, 30.2.

5-isopropyl-2-methylcyclohex-2-enone (226f). A solution of carvone (45 μ L, 0.29



mmol) and iridium catalyst **221** (8.0 mg, 0.0051 mmol, 1.8 mol %) in CH₂Cl₂ (3 mL) in a vial under argon was sealed in an autoclave. The autoclave was evacuated and back-filled with hydrogen three times, pressurized to 62 bar, and allowed to stir for 48 h. The reaction mixture was passed through a silica plug with Et₂O and solvent was removed *in vacuo* to give **226f** (43 mg, 96%) as a clear oil. ¹H NMR (300 MHz, CDCl₃) δ 6.72-6.69 (m, 1H), 2.53-2.47 (m, 1H), 2.37-2.27 (m, 1H), 2.13-1.99 (m, 2H), 1.85-1.78 (m, 1H), 1.73-1.72 (m, 3H), 1.54 (qn, 1H, J = 6.6 Hz), 0.87 (dd, 6H, J = 6.9 Hz, 0.9 Hz); ¹³C NMR (75.5 MHz, CDCl₃) δ 200.7, 145.4, 135.4, 42.1, 32.1, 30.0, 19.6, 16.0.

1,2-diphenylpropane (124a). A solution of methyl stilbene **124** (40 mg, 0.21 mmol) and



iridium catalyst **221** (6.4 mg, 0.0041 mmol, 2.0 mol %) in CH₂Cl₂ (3 mL) in a vial under argon was sealed in an autoclave. The autoclave

was evacuated and back-filled with hydrogen three times,

pressurized to 62 bar, and allowed to stir for 24 h. The reaction mixture was passed

through a silica plug with Et₂O and solvent was removed *in vacuo* to give **124a** (35 mg,

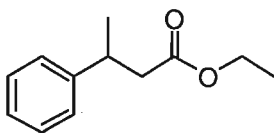
86%) as a clear oil. ¹H NMR (300 MHz, CDCl₃) δ 7.35-7.12 (m, 10H), 3.10-2.98 (m,

2H), 2.88-2.79 (m, 1H), 1.30 (d, 3H, *J* = 6.9 Hz); ¹³C NMR (75.5 MHz, CDCl₃) δ 147.1,

140.9, 129.3, 128.4, 128.2, 127.2, 126.1, 126.0, 45.1, 42.0, 21.3.

Ethyl 3-phenylbutanoate (128a). A solution of ethyl 3-phenylbut-2-enoate **128** (54 mg,

0.28 mmol) and iridium catalyst **221** (9.0 mg, 0.0057 mmol, 2.0



mol %) in CH₂Cl₂ (3 mL) in a vial under argon was sealed in an

autoclave. The autoclave was evacuated and back-filled with

hydrogen three times, pressurized to 62 bar, and allowed to stir for 48 h. The reaction

mixture was passed through a silica plug with Et₂O and solvent was removed *in vacuo* to

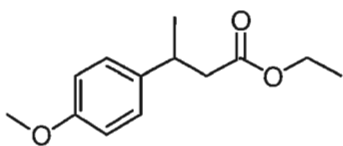
give **128a** (52 mg, 94%) as a clear oil. ¹H NMR (300 MHz, CDCl₃) δ 7.34-7.18 (m, 5H),

4.10 (q, 2H, *J* = 7.2 Hz), 3.28 (sx, 1H, *J* = 7.2 Hz), 2.67-2.51 (m, 2H), 1.32 (d, 3H, *J* =

6.9Hz), 1.19 (t, 3H, *J* = 6.9 Hz); ¹³C NMR (75.5 MHz, CDCl₃) δ 172.5, 145.9, 128.6,

126.9, 126.5, 60.3, 43.1, 60.3, 43.1, 36.6, 21.9, 14.3.

Ethyl 3-(4-methoxyphenyl)butanoate (226a). A solution of ethyl 3-(4-

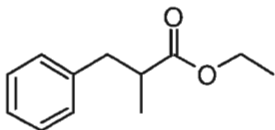


methoxyphenyl)but-2-enoate **225a** (60 mg, 0.27 mmol) and iridium catalyst **221** (8.7 mg, 0.0055 mmol, 2.0 mol %) in

CH₂Cl₂ (3 mL) in a vial under argon was sealed in an

autoclave. The autoclave was evacuated and back-filled with hydrogen three times, pressurized to 62 bar, and allowed to stir for 48 h. The reaction mixture was passed through a silica plug with Et₂O and solvent was removed *in vacuo* to give **226a** (59 mg, 96%) as a clear oil. ¹H NMR (300 MHz, CDCl₃) δ 7.14 (d, 2H, *J* = 8.7 Hz), 6.84 (d, 2H, *J* = 6.9 Hz), 4.07 (q, 2H, *J* = 7.2 Hz), 3.78 (s, 3H), 3.23 (sx, 1H, *J* = 7.2 Hz), 2.61-2.47 (m, 2H), 1.28 (d, 3H, *J* = 6.9 Hz), 1.19 (t, 3H, *J* = 7.2 Hz); ¹³C NMR (75.5 MHz, CDCl₃) δ 172.6, 158.2, 138.0, 127.8, 113.9, 60.3, 55.4, 43.4, 35.9, 22.1, 14.3.

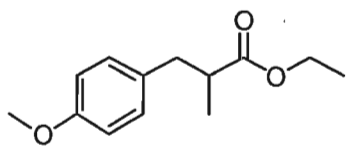
Ethyl 2-methyl-3-phenylpropanoate (226b). A solution of *trans*-ethyl 2-methyl-3-phenylacrylate **225b** (31 mg, 0.16 mmol) and iridium catalyst **221**



(5.1 mg, 0.0032 mmol, 2.0 mol %) in CH₂Cl₂ (1.6 mL) in a vial under argon was sealed in an autoclave. The autoclave was

evacuated and back-filled with hydrogen three times, pressurized to 62 bar, and allowed to stir for 72 h at room temperature. The solvent was removed *in vacuo*, crude passed through a silica plug with 9:1 hexanes:EtOAc, and solvent removed *in vacuo* to give **226b** (28 mg, 92%) as a clear oil. ¹H NMR (300 MHz, CDCl₃) δ 7.31-7.16 (m, 5H), 4.09 (q, 2H, *J* = 6.9 Hz), 3.08-2.98 (m, 1H), 2.79-2.64 (m, 2H), 1.21 (d, 3H, *J* = 7.2 Hz), 1.16 (d, 3H, *J* = 6.3 Hz); ¹³C NMR (75.5 MHz, CDCl₃) δ 176.1, 139.4, 128.9, 128.3, 126.2, 60.2, 41.4, 39.7, 16.7, 14.1.

Ethyl 3-(4-methoxyphenyl)-2-methylpropanoate (226c). A solution of *trans*-ethyl 3-(4-

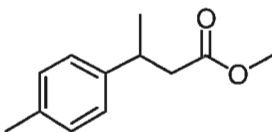


methoxyphenyl)-2-methylacrylate **225c** (31 mg, 0.14 mmol)

and iridium catalyst **221** (4.4 mg, 0.0028 mmol, 2.0 mol %)

in CH₂Cl₂ (1.4 mL) in a vial under argon was sealed in an autoclave. The autoclave was evacuated and back-filled with hydrogen three times, pressurized to 62 bar, and allowed to stir for 72 h at room temperature. The solvent was removed *in vacuo*, crude passed through a silica plug with 9:1 hexanes:EtOAc, and solvent removed *in vacuo* to give **226c** (30 mg, 96%) as a clear oil. ¹H NMR (300 MHz, CDCl₃) δ 7.08 (d, 2H, *J* = 8.7 Hz), 6.81 (d, 2H, *J* = 8.7 Hz), 4.09 (q, 2H, *J* = 7.2 Hz), 3.78 (s, 3H), 3.01-2.90 (m, 1H), 2.73-2.57 (m, 2H), 1.19 (t, 3H, *J* = 7.2 Hz), 1.13 (d, 3H, *J* = 6.6 Hz); ¹³C NMR (75.5 MHz, CDCl₃) δ 176.2, 158.1, 131.4, 129.9, 113.7, 60.2, 55.2, 41.7, 38.8, 16.7, 14.2.

Methyl 3-*p*-tolylbutanoate (226d). A solution of *trans*-methyl 3-*p*-tolylbutenoate **225d**



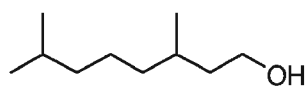
(53 mg, 0.28 mmol) and iridium catalyst **221** (8.8 mg, 0.0056

mmol, 2.0 mol %) in CH₂Cl₂ (3 mL) in a vial under argon was

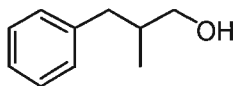
sealed in an autoclave. The autoclave was evacuated and back-

filled with hydrogen three times, pressurized to 62 bar, and allowed to stir for 72 h at room temperature. The solvent was removed *in vacuo*, crude passed through a silica plug with Et₂O, and solvent removed *in vacuo* to give **226d** (51 mg, 94%) as a clear oil. ¹H NMR (300 MHz, CDCl₃) δ 7.13 (s, 4H), 3.64 (s, 3H), 3.29 (sx, 1H, *J* = 6.9 Hz), 2.60 (dq, 2H, *J* = Hz, Hz), 2.34 (s, 3H), 1.32 (d, 3H, *J* = 6.9 Hz); ¹³C NMR (75.5 MHz, CDCl₃) δ 172.8, 142.7, 135.8, 129.1, 126.5, 51.4, 42.8, 36.0, 21.8, 20.9.

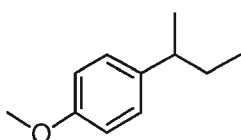
3,7-dimethyloctan-1-ol (226e). A solution of geraniol (52 μ L, 0.29 mmol) and iridium catalyst **221** (9.0 mg, 0.0057 mmol, 2.0 mol %) in CH_2Cl_2 (3 mL) in a vial under argon was sealed in an autoclave. The autoclave was evacuated and back-filled with hydrogen three times, pressurized to 62 bar, and allowed to stir for 72 h. The reaction mixture was passed through a silica plug with Et_2O and solvent was removed *in vacuo* to give **226e** (47 mg, 98%) as a clear oil. ^1H NMR (300 MHz, CDCl_3) δ 3.68 (m, 2H), 1.61-1.17 (m, 10H), 0.9 (3 s, 9H); ^{13}C NMR (75.5 MHz, CDCl_3) δ 61.4, 30.1, 39.4, 37.5, 29.7, 28.1, 24.8, 22.8, 22.7, 19.8.



2-methyl-3-phenylpropan-1-ol (226f). A solution of *trans*-2-methyl-3-phenylpropenol **225f** (34.2 mg, 0.23 mmol) and iridium catalyst **221** (7.3 mg, 0.0046 mmol, 2.0 mol %) in dry CH_2Cl_2 (2.4 mL) in a vial under argon was sealed in an autoclave. The autoclave was evacuated and back-filled with hydrogen three times, pressurized to 62 bar, and allowed to stir for 72 h at room temperature. The solvent was removed *in vacuo*, crude passed through a silica plug with 9:1 hexanes: EtOAc , and solvent was removed *in vacuo* to afford **226f** (33 mg, 96%) as a clear oil. ^1H NMR (300 MHz, CDCl_3) δ 7.31-7.17 (m, 5H), 3.51 (oct, 2H), 2.76 (dd, 1H), 2.43 (dd, 1H), 1.95 (oct, 1H), 1.47 (bs, 1H), 0.94 (d, 3H); ^{13}C NMR (75.5 MHz, CDCl_3) δ 140.6, 129.1, 128.2, 125.8, 67.6, 39.6, 37.7, 16.4.

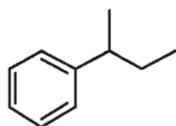


1-sec-butyl-4-methoxybenzene (125a). A solution of 1-(butenyl)-4-methoxybenzene **125** (54 mg, 0.33 mmol) and iridium catalyst **221** (10.1mg, 0.0064 mmol, 2.0 mol %) in CH_2Cl_2 (3 mL) in a vial under argon was sealed



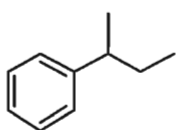
in an autoclave. The autoclave was evacuated and back-filled with hydrogen three times, pressurized to 62 bar, and allowed to stir for 72 h at room temperature. The solvent was removed *in vacuo*, crude passed through a silica plug with Et₂O, and solvent removed *in vacuo* to give **125a** (51 mg, 94%) as a clear oil. ¹H NMR (300 MHz, CDCl₃) δ 7.12 (d, 2H, *J* = 8.7 Hz), 6.87 (d, 2H, *J* = 8.7 Hz), 3.82 (s, 3H), 2.58 (sx, 1H, *J* = 6.9 Hz), 1.57 (qnt, 2H, *J* = 7.5 Hz), 1.24 (d, 3H, *J* = 6.9 Hz), 0.85 (t, 3H, *J* = 7.5 Hz).

sec-butylbenzene (226g). A solution of but-2-en-2-ylbenzene **225g** (40 mg, 0.31 mmol)



and iridium catalyst **221** (9.8 mg, 0.0062 mmol, 2.0 mol %) in CH₂Cl₂ (3 mL) in a vial under argon was sealed in an autoclave. The autoclave was evacuated and back-filled with hydrogen three times, pressurized to 62 bar, and allowed to stir for 72 h at room temperature. The solvent was removed *in vacuo* (over ice), crude passed through a silica plug with Et₂O, and solvent removed *in vacuo* (over ice) to give **226g** (38 mg, 93%) as a volatile clear oil. ¹H NMR (300 MHz, CDCl₃) δ 7.35-7.19 (m, 5H), 2.64 (sx, 1H, *J* = 6.9 Hz), 1.70-1.58 (m, 2H), 1.30 (d, 3H, *J* = 6.9 Hz), 0.88 (t, 3H, *J* = 7.5 Hz).

sec-butylbenzene (226h). A solution of but-1-en-2-ylbenzene **225h** (39 mg, 0.30 mmol)



and iridium catalyst **221** (9.3 mg, 0.0059 mmol, 2.0 mol %) in CH₂Cl₂ (3 mL) in a vial under argon was sealed in an autoclave. The autoclave was evacuated and back-filled with hydrogen three times, pressurized to 62 bar, and allowed to stir for 72 h at room temperature. The solvent was removed *in vacuo* (over ice), crude passed through a silica plug with Et₂O, and solvent removed *in vacuo*

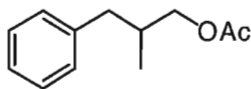
(over ice) to afford the title compound (33 mg, 83%) as a volatile clear oil, with spectroscopic data matching **226g**.

N-benzyl-2-methyl-3-phenylpropanamide (226i). A solution of *trans*-*N*-benzyl-2-methyl-3-phenylacrylamide **225i** (30 mg, 0.12 mmol) and iridium catalyst **221** (3.7 mg, 0.0023 mmol, 2.0 mol %) in dry CH₂Cl₂ (1.2 mL) in a vial under argon was sealed in an autoclave. The autoclave was evacuated and back-filled with hydrogen three times, pressurized to 62 bar, and allowed to stir for 72 h at room temperature. The solvent was removed *in vacuo*, crude passed through a silica plug with 9:1 hexanes:EtOAc, and solvent was removed *in vacuo* to give **226i** (29 mg, 98%) as a pale yellow oil. ¹H NMR (300 MHz, CDCl₃) δ 7.24-7.16 (m, 9H), 7.04-7.01 (m, 2H), 5.66 (bs, 1H), 4.32 (dd, 2H), 2.98 (dd, 1H), 2.70 (dd, 1H), 2.47 (sx, 1H), 1.23 (d, 3H); ¹³C NMR (75.5 MHz, CDCl₃) δ 175.3, 139.8, 138.1, 128.5, 128.4, 127.5, 127.2, 126.2, 43.9, 43.3, 40.5, 17.8.

3-Methoxy-2-methyl-propyl)-benzene (226j). A solution of *trans*-(3-methoxy-2-methyl-propenyl)-benzene **225j** (32.9 mg, 0.20 mmol) and iridium catalyst **221** (6.4 mg, 0.0041 mmol, 2.0 mol %) in dry CH₂Cl₂ (2.1 mL) in a vial under argon was sealed in an autoclave. The autoclave was evacuated and back-filled with hydrogen three times, pressurized to 62 bar, and allowed to stir for 72 h at room temperature. The solvent was removed *in vacuo*, crude passed through a silica plug with 9:1 hexanes:EtOAc, and solvent was removed *in vacuo* (over ice) to afford **226j** (14 mg, 41%) as a volatile clear oil. ¹H NMR (300 MHz, CDCl₃) δ 7.31-7.16 (m,

5H), 3.35 (s, 3H), 3.27-3.17 (m, 2H), 2.78 (dd, 1H, $J = 13.2, 6.0$ Hz), 2.41 (dd, 1H, $J = 13.5, 8.1$ Hz), 2.11-1.96 (m, 1H), 0.90 (d, 3H, $J = 6.6$ Hz); ^{13}C NMR (75.5 MHz, CDCl_3) δ 140.7, 129.2, 128.1, 125.7, 58.7, 39.9, 35.4, 16.7.

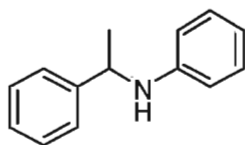
2-methyl-3-phenylpropyl acetate (226k). A solution of 2-methyl-3-phenylallyl acetate



225k (34.6 mg, 0.182 mmol) and iridium catalyst **221** (5.7 mg, 0.0036 mmol) in CH_2Cl_2 (1.9 mL) in a vial under argon was sealed

in an autoclave. The autoclave was evacuated and back-filled with hydrogen three times, pressurized to 62 bar, and allowed to stir for 72 h at room temperature. The solvent was removed *in vacuo*, crude passed through a silica plug with 9:1 hexanes:EtOAc, and solvent removed *in vacuo* (over ice) to afford **211k** (27.6 mg, 79%) as a volatile clear oil. ^1H NMR (300 MHz, CDCl_3) δ 7.31-7.15 (m, 5H), 3.95 (m, 2H), 2.74 (dd, 1H, $J = 13.5, 6.3$ Hz), 2.46 (dd, 1H, $J = 13.5, 7.8$ Hz), 2.16-2.09 (m, 1H), 2.07 (3H), 0.93 (d, 3H, $J = 6.6$ Hz).

***N*-(1-phenylethyl)aniline (226l).** A solution of *N*-(1-phenylethylidene)aniline **225l** (50

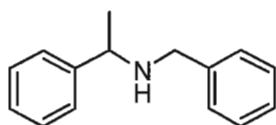


mg, 0.26 mmol) and iridium catalyst **221** (7.8 mg, 0.0050 mmol, 1.9 mol %) in CH_2Cl_2 (3 mL) in a vial under argon was sealed in an autoclave. The autoclave was evacuated and back-filled with

hydrogen three times, pressurized to 62 bar, and allowed to stir for 72 h. The reaction mixture was passed through a silica plug with Et_2O and solvent was removed *in vacuo* to give **226l** (41 mg, 81%) as a pale yellow oil. ^1H NMR (300 MHz, CDCl_3) δ 7.4-7.3 (m, 4H), 7.3-7.25 (m, 2H), 7.15 (t, 2H, $J = 7.5$ Hz), 6.7 (t, 1H, $J = 7.5$ Hz), 5.55 (d, 2H, $J =$

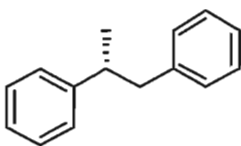
7.8 Hz), 4.53 (q, 1H, $J = 6.6$ Hz), 4.07 (bs, 1H), 1.56 (d, 3H, $J = 6.6$ Hz); ^{13}C NMR (75.5 MHz, CDCl_3) δ 147.4, 145.4, 129.3, 128.8, 127.0, 126.0, 117.4, 113.4, 53.6, 25.2.

***N*-benzyl-1-phenylethanamine (226m).** A solution of 1-phenyl-*N*-(1-



phenylethylidene)methanamine **225m** (50 mg, 0.24 mmol) and iridium catalyst **221** (7.5 mg, 0.0048 mmol, 2.0 mol %) in CH_2Cl_2 (3 mL) in a vial under argon was sealed in an autoclave. The autoclave was evacuated and back-filled with hydrogen three times, pressurized to 62 bar, and allowed to stir for 72 h. The reaction mixture was passed through a silica plug with Et_2O and solvent was removed *in vacuo* to give **226m** (45 mg, 88%) as a pale yellow oil. ^1H NMR (300 MHz, CDCl_3) δ 7.35-7.27 (m, 10H), 3.85 (q, 1H, $J = 6.6$ Hz), 3.66 (q, 2H, $J = 22.2$ Hz), 1.59 (bs, 1H), 1.39 (d, 3H, $J = 6.6$ Hz); ^{13}C NMR (75.5 MHz, CDCl_3) δ 145.7, 140.8, 128.6, 128.5, 128.3, 127.0, 126.95, 126.8, 57.6, 51.8, 24.7.

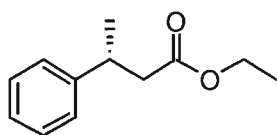
(*R*)-(-)-1,2-diphenylpropane [(*R*)-124a]. A solution of *trans*-methyl stilbene **124** (30



mg, 0.15 mmol) and iridium catalyst (*S*)-**221** (4.9 mg, 0.0031 mmol, 2.0 mol %) in CH_2Cl_2 (3 mL) in a vial under argon was sealed in an autoclave. The autoclave was evacuated and back-filled with hydrogen three times, pressurized to 62 bar, and allowed to stir for 72 h at room temperature. The solvent was removed *in vacuo*, crude passed through a silica plug with 9:1 hexanes: EtOAc , and solvent removed *in vacuo* to afford the title compound (30 mg, 94%) as a colourless oil. $[\alpha]_{\text{D}}^{20} -48.3$ (c 0.86 CHCl_3); [Lit.¹²⁸ $[\alpha]_{\text{D}}^{20} -73.7$ (c 1.0, CHCl_3)] Chiral GC analysis (Chirasil DEX-CB; 100 $^\circ\text{C}$ for 5 min, 0.5 $^\circ\text{C}/\text{min}$ increase to

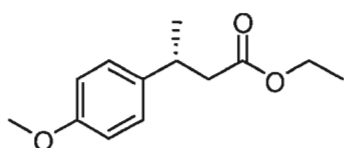
140 °C, hold at 140 °C for 5 min, 2 °C/min increase to 180 °C, hold at 180 °C for 10 min) determined an enantiomeric ratio (er) of 91.8:8.2 (84% ee) [t_R (major) = 64.32 min, t_R (minor) 64.61 = min]; ^1H NMR (300 MHz, CDCl_3) δ 7.37-7.30 (m, 3H), 7.24-7.20 (m, 2H), 7.14 (d, 2H, J = 7.2 Hz), 3.13-2.98 (m, 2H), 2.82 (q, 1H, J = 7.8 Hz), 1.31 (d, 3H, J = 6.6 Hz); ^{13}C NMR (75.5 MHz, CDCl_3) δ 147.0, 140.8, 129.1, 128.3, 128.1, 127.0, 126.0, 125.8, 45.0, 41.8, 21.1.

(R)-(-)-Ethyl 3-phenylbutanoate [(R)-128a]. A solution of *trans*-ethyl 3-phenylbut-2-



enoate **128** (57 mg, 0.29 mmol) and iridium catalyst (*S*)-**221** (9.4 mg, 0.0060 mmol, 2.0 mol %) in CH_2Cl_2 (3 mL) in a vial under argon was sealed in an autoclave. The autoclave was evacuated and back-filled with hydrogen three times, pressurized to 62 bar, and allowed to stir for 72 h at room temperature. The solvent was removed *in vacuo*, crude passed through a silica plug with 9:1 hexanes:EtOAc, and solvent removed *in vacuo* to afford the title compound (54 mg, 94%) as a colourless oil. $[\alpha]_D^{20}$ -23.5 (c 0.94 CHCl_3) [Lit.¹²⁹ $[\alpha]_D^{20}$ -24.7 (c 1.12, CHCl_3)]; CSP HPLC analysis (Chiralcel OB-H; eluent: 99.5:0.5 hexane:*i*-PrOH, 0.5 mL/min) determined an enantiomeric ratio (er) of 95.4:4.6 (91% ee) [t_R (major) 11.99 min, t_R (minor) 14.09 min]; ^1H NMR (300 MHz, CDCl_3) δ 7.33-7.17 (m, 5H), 4.08 (q, 2H, J = 6.9 Hz), 3.35-3.23 (sx, 1H, J = 7.2 Hz), 2.66-2.50 (m, 2H), 1.31 (d, 3H, J = 6.9 Hz), 1.19 (t, 3H, J = 6.9 Hz); ^{13}C NMR (75.5 MHz, CDCl_3) δ 172.4, 145.7, 128.4, 126.7, 126.3, 60.2, 43.0, 36.5, 21.8, 14.1.

(R)-(-)-Ethyl 3-(4-methoxyphenyl)butanoate [(R)-226a]. A solution of *trans*-ethyl 3-



(4-methoxyphenyl)but-2-enoate **225a** (58 mg, 0.26 mmol)

and iridium catalyst (*S*)-**221** (8.4 mg, 0.0053 mmol, 2.0 mol

%) in dry CH₂Cl₂ (3 mL) in a vial under argon was sealed in

an autoclave. The autoclave was evacuated and back-filled with hydrogen three times,

pressurized to 62 bar, and allowed to stir for 72 h at room temperature. The solvent was

removed *in vacuo*, crude passed through a silica plug with 9:1 hexanes:EtOAc, and

solvent was removed *in vacuo* to afford the title compound (58 mg, 99%) as a colourless

oil. $[\alpha]_D^{20}$ -26.7 (*c* 0.996, CHCl₃); CSP HPLC analysis¹³⁰ (Chiralcel OB-H; eluent:

99.5:0.5 hexane:*i*-PrOH, 0.5 mL/min) determined an enantiomeric ratio (er) of 96.1:3.9

(92% ee) [*t*_R(major) 21.73 min, *t*_R(minor) 28.91 min]; ¹H NMR (300 MHz, CDCl₃) δ 7.14

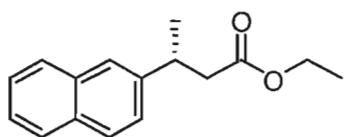
(d, 2H, *J* = 8.4 Hz), 6.84 (d, 2H, *J* = 8.7 Hz), 4.07 (q, 2H, *J* = 6.9 Hz), 3.78 (s, 3H), 3.24

(sx, 1H, *J* = 7.2 Hz), 2.61-2.46 (m, 2H), 1.27 (d, 3H, *J* = 6.9 Hz), 1.18 (t, 3H, *J* = 7.2 Hz);

¹³C NMR (75.5 MHz, CDCl₃) δ 172.4, 158.0, 137.8, 131.4, 127.6, 113.8, 60.1, 55.1, 43.2,

35.7, 21.9, 14.1.

(R)-(-)-Ethyl 3-(naphthalen-2-yl)-butanoate [(R)-226n]. A solution of *trans*-ethyl 3-



(naphthalen-2-yl)-but-2-enoate **225n** (26.6 mg, 0.11 mmol)

and iridium catalyst (*S*)-**221** (3.5 mg, 0.0022 mmol, 2.0 mol

%) in CH₂Cl₂ (1.1 mL) in a vial under argon was sealed in

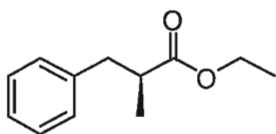
an autoclave. The autoclave was evacuated and back-filled with hydrogen three times,

pressurized to 62 bar, and allowed to stir for 80 h at room temperature. The solvent was

removed *in vacuo*, crude passed through a silica plug with 9:1 hexanes:EtOAc, and

solvent removed *in vacuo* to afford the title compound (25.6 mg, 96%) as a colourless oil. $[\alpha]_D^{20}$ -26.0 (*c* 0.97; CHCl₃); CSP HPLC analysis (Chiralcel OD-H; eluent: 99.5:0.5 hexane:*i*-PrOH, 1.0 mL/min) determined an enantiomeric ratio (er) of 91.1:8.9 (82% ee) [*t*_R(major) 25.7 min, *t*_R(minor) 20.4 min]; ¹H NMR (300 MHz, CDCl₃) δ 7.82 (d, 3H, *J* = 8.4 Hz), 7.69 (s, 1H), 7.51-7.39 (m, 3H), 4.11 (q, 2H, *J* = 7.2 Hz), 3.50 (sx, 1H, *J* = 7.5 Hz), 2.81-2.62 (m, 2H), 1.42 (d, 3H, *J* = 6.9 Hz), 1.19 (t, 3H, *J* = 7.2 Hz); ¹³C NMR (75.5 MHz, CDCl₃) δ 172.3, 143.1, 135.5, 132.3, 128.1, 127.6, 127.5, 125.9, 125.4, 125.3, 124.9, 60.2, 42.8, 42.6, 36.6, 21.7, 14.1.

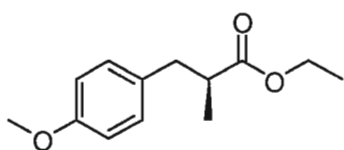
(*S*)-(+)-Ethyl 2-methyl-3-phenylpropanoate [(*S*)-226b**].** A solution of *trans*-ethyl 2-



methoxy-3-phenylacrylate **225b** (34 mg, 0.18 mmol) and iridium catalyst (*S*)-**221** (5.7 mg, 0.0036 mmol, 2.0 mol %) in CH₂Cl₂ (1.8 mL) in a vial under argon was sealed in an autoclave. The

autoclave was evacuated and back-filled with hydrogen three times, pressurized to 62 bar, and allowed to stir for 72 h at room temperature. The solvent was removed *in vacuo*, crude passed through a silica plug with 9:1 hexanes:EtOAc, and solvent removed *in vacuo* to afford the title compound (30 mg, 88%) as a colourless oil. $[\alpha]_D^{20}$ +28.4 (*c* 1.0, CHCl₃); CSP HPLC analysis⁷³ (Chiralcel OB-H; eluent: 99.5:0.5 hexane:*i*-PrOH, 1.0 mL/min) determined an enantiomeric ratio (er) of 91.1:8.9 (82% ee) [*t*_R(major) 10.1 min, *t*_R(minor) 8.5 min]; ¹H NMR (300 MHz, CDCl₃) δ 7.31-7.16 (m, 5H), 4.09 (q, 2H, *J* = 6.9 Hz), 3.08-2.98 (m, 1H), 2.79-2.64 (m, 2H), 1.21 (d, 3H, *J* = 7.2 Hz), 1.16 (d, 3H, *J* = 6.3 Hz); ¹³C NMR (75.5 MHz, CDCl₃) δ 176.1, 139.4, 128.9, 128.3, 126.2, 60.2, 41.4, 39.7, 16.7, 14.1.

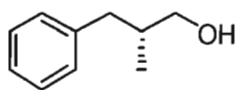
(S)-(+)-Ethyl 3-(4-methoxyphenyl)-2-methylpropanoate [(S)-226c]. A solution of



trans-ethyl 3-(4-methoxyphenyl)-2-methylacrylate **225c** (30 mg, 0.14 mmol) and iridium catalyst (*S*)-**221** (4.5 mg, 0.0029 mmol, 2.0 mol %) in CH₂Cl₂ (1.4 mL) in a vial under argon

was sealed in an autoclave. The autoclave was evacuated and back-filled with hydrogen three times, pressurized to 62 bar, and allowed to stir for 72 h at room temperature. The solvent was removed *in vacuo*, crude passed through a silica plug with 9:1 hexanes:EtOAc, and solvent removed *in vacuo* to afford the title compound (30 mg, 96%) as a colourless oil. $[\alpha]_D^{20} +24.5$ (*c* 1.25, CHCl₃); CSP HPLC analysis⁷³ (Chiralcel OB-H; eluent: 99.5:0.5 hexane:*i*-PrOH, 0.5 mL/min) determined an enantiomeric ratio (er) of 92.0:8.0 (84% ee) [*t*_R(major) 20.9 min, *t*_R(minor) 19.1 min]; ¹H NMR (300 MHz, CDCl₃) δ 7.08 (d, 2H, *J* = 8.7 Hz), 6.81 (d, 2H, *J* = 8.7 Hz), 4.09 (q, 2H, *J* = 7.2 Hz), 3.78 (s, 3H), 3.01-2.90 (m, 1H), 2.73-2.57 (m, 2H), 1.19 (t, 3H, *J* = 7.2 Hz), 1.13 (d, 3H, *J* = 6.6 Hz); ¹³C NMR (75.5 MHz, CDCl₃) δ 176.2, 158.1, 131.4, 129.9, 113.7, 60.2, 55.2, 41.7, 38.8, 16.7, 14.2.

(R)-(+)-2-methyl-3-phenylpropan-1-ol [(R)-226f]. A solution of *trans*-2-methyl-3-

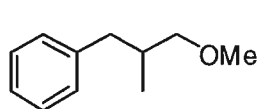


phenylpropenol **225f** (37.5 mg, 0.25 mmol) and iridium catalyst (*S*)-**221** (8.0 mg, 0.0051 mmol, 2.0 mol %) in dry CH₂Cl₂ (2.5 mL) in a

vial under argon was sealed in an autoclave. The autoclave was evacuated and back-filled with hydrogen three times, pressurized to 62 bar, and allowed to stir for 72 h at room temperature. The solvent was removed *in vacuo*, crude passed through a silica plug with 9:1 hexanes:EtOAc, and solvent was removed *in vacuo* to afford the title compound (37

mg, 98%). $[\alpha]_D^{20} +1.36$ (*c* 1.06, CHCl₃) [Lit.¹³³ $[\alpha]_D^{20} -11.1$ (*c* 0.86, CHCl₃) for (*S*)-enantiomer]; CSP HPLC analysis (Chiralcel OD-H; eluent: 95:5 hexane:*i*-PrOH, 1.0 mL/min, 254 nm) determined an enantiomeric ratio (er) of 58.8:41.2 (18% ee) [*t_R*(major) 10.52 min, *t_R*(minor) 8.73 min]; ¹H NMR (300 MHz, CDCl₃) δ 7.31-7.17 (m, 5H), 3.51 (oct, 2H), 2.76 (dd, 1H), 2.43 (dd, 1H), 1.95 (oct, 1H), 1.47 (bs, 1H), 0.94 (d, 3H); ¹³C NMR (75.5 MHz, CDCl₃) δ 140.6, 129.1, 128.2, 125.8, 67.6, 39.6, 37.7, 16.4.

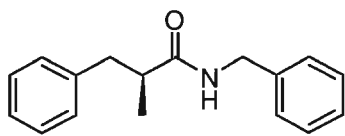
(-)-3-Methoxy-2-methyl-propyl)-benzene [(-)-226j]. A solution of *trans*-(3-methoxy-



2-methyl-propenyl)-benzene **225j** (30.5 mg, 0.19 mmol) and iridium catalyst (*S*)-**221** (5.9 mg, 0.0037 mmol, 2.0 mol %) in dry

CH₂Cl₂ (1.9 mL) in a vial under argon was sealed in an autoclave. The autoclave was evacuated and back-filled with hydrogen three times, pressurized to 62 bar, and allowed to stir for 72 h at room temperature. The solvent was removed *in vacuo*, crude passed through a silica plug with 9:1 hexanes:EtOAc, and solvent was removed *in vacuo* to afford the title compound (19 mg, 61%) as a clear volatile oil. $[\alpha]_D^{20} -1.24$ (*c* 0.38, CHCl₃); CSP HPLC analysis (Chiralcel OD-H; eluent: 99:1 hexane:*i*-PrOH, 1.0 mL/min, 254 nm) determined an enantiomeric ratio (er) of 58.45:41.55 (17 % ee) [*t_R*(major) 5.67 min, *t_R*(minor) 4.48 min]; ¹H NMR (300 MHz, CDCl₃) δ 7.31-7.16 (m, 5H), 3.35 (s, 3H), 3.27-3.17 (m, 2H), 2.78 (dd, 1H, *J* = 13.2, 6.0 Hz), 2.41 (dd, 1H, *J* = 13.5, 8.1 Hz), 2.11-1.96 (m, 1H), 0.90 (d, 3H, *J* = 6.6 Hz); ¹³C NMR (75.5 MHz, CDCl₃) δ 140.7, 129.2, 128.1, 125.7, 58.7, 39.9, 35.4, 16.7.

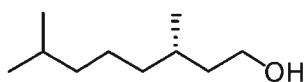
(S)-(+)-N-benzyl-2-methyl-3-phenylpropanamide [(S)-226i]. A solution of *trans*-N-



benzyl-2-methyl-3-phenylacrylamide **225i** (30 mg, 0.12 mmol) and iridium catalyst (*S*)-**221** (3.8 mg, 0.0024 mmol, 2.0 mol %) in dry CH₂Cl₂ (1.2 mL) in a vial under argon

was sealed in an autoclave. The autoclave was evacuated and back-filled with hydrogen three times, pressurized to 62 bar, and allowed to stir for 72 h at room temperature. The solvent was removed *in vacuo*, crude passed through a silica plug with 9:1 hexane:EtOAc, and solvent was removed *in vacuo* to afford the title compound (29 mg, 96%). [α]_D²⁰ +23.2 (*c* 0.93, CHCl₃) [Lit.¹³¹ [α]_D²⁰ +52.3 (*c*, 1.2 CHCl₃)]; CSP HPLC analysis (Chiralcel OB-H; eluent: 99:1 hexane:*i*-PrOH, 1.0 mL/min) determined an enantiomeric ratio (er) of 73.8:26.2 (48% ee) [*t*_R(major) 26.5 min, *t*_R(minor) 30.0 min]; ¹H NMR (300 MHz, CDCl₃) δ 7.24-7.16 (m, 9H), 7.04-7.01 (m, 2H), 5.66 (bs, 1H), 4.32 (dd, 2H), 2.98 (dd, 1H), 2.70 (dd, 1H), 2.47 (sx, 1H), 1.23 (d, 3H); ¹³C NMR (75.5 MHz, CDCl₃) δ 175.3, 139.8, 138.1, 128.5, 128.4, 127.5, 127.2, 126.2, 43.9, 43.3, 40.5, 17.8.

(S)-(-)-3,7-dimethyloctan-1-ol [(S)-226e]. A solution of geraniol (46.5 mg, 0.30 mmol)

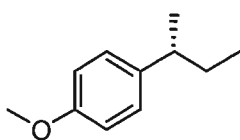


and iridium catalyst (*S*)-**221** (9.5mg, 0.0060 mmol, 2.0 mol %) in CH₂Cl₂ (3 mL) in a vial under argon was sealed in an

autoclave. The autoclave was evacuated and back-filled with hydrogen three times, pressurized to 62 bar, and allowed to stir for 24 hours. The solvent was removed *in vacuo*, crude passed through a silica plug with 9:1 hexane:EtOAc, and solvent removed *in vacuo* to afford the title compound (47 mg, 99%) as a colourless oil. [α]_D²⁰ -2.05 (*c* 0.5, CHCl₃) {Lit.¹³² [α]_D²⁰ -4.8 (*c* 0.5 CHCl₃)} ¹H NMR (300 MHz, CDCl₃) δ 3.71-7.59

(m, 2H), 1.71 (bs, 1H), 1.64-1.09 (m, 10H), 0.86 (3 x d, 9H); ^{13}C NMR (75.5 MHz, CDCl_3) δ 61.1, 39.9, 39.2, 37.3, 29.5, 27.9, 24.6, 22.6, 22.5, 19.6.

(R)-(+)-1-sec-butyl-4-methoxybenzene [(R)-125a]. A solution of *trans*-1-(butenyl)-4-



methoxybenzene **125** (51 mg, 0.32 mmol) and iridium catalyst (*S*)-

221 (9.9mg, 0.0063 mmol, 2.0 mol %) in CH_2Cl_2 (3 mL) in a vial

under argon was sealed in an autoclave. The autoclave was

evacuated and back-filled with hydrogen three times, pressurized to 62 bar, and allowed

to stir for 72 h at room temperature. The solvent was removed *in vacuo*, crude passed

through a silica plug with Et_2O , and solvent removed *in vacuo* to afford the title

compound (49 mg, 95%) as a clear oil. $[\alpha]_D^{20}$ +8.2 (*c* 0.15, CHCl_3); CSP HPLC analysis

(Chiralcel OD-H; eluent: 99.9:0.1 hexane:*i*-PrOH, 0.4 mL/min) determined an

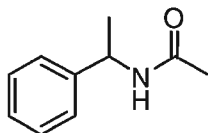
enantiomeric ratio (er) of 63.2:36.8 (26% ee) [t_R (major) 18.94 min, t_R (minor) 20.87 min];

^1H NMR (300 MHz, CDCl_3) δ 7.12 (d, 2H, J = 8.7 Hz), 6.87 (d, 2H, J = 8.7 Hz), 3.82 (s,

3H), 2.58 (sx, 1H, J = 6.9 Hz), 1.57 (qnt, 2H, J = 7.5 Hz), 1.24 (d, 3H, J = 6.9 Hz), 0.85

(t, 3H, J = 7.5 Hz).

ent-N-(1-Phenyl-ethyl)-acetamide (ent-226o). A solution of *N*-(1-phenyl-vinyl)-



acetamide **225o** (46.5 mg, 0.29 mmol) and iridium catalyst (*S*)-**221**

(9.0 mg, 0.0057 mmol) in dry CH_2Cl_2 (3 mL) in a vial under argon

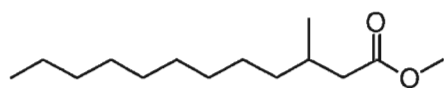
was sealed in an autoclave. The autoclave was evacuated and back-filled with hydrogen

three times, pressurized to 62 bar, and allowed to stir for 72 h at room temperature. The

solvent was removed *in vacuo*, crude passed through a plug of silica with 7:3

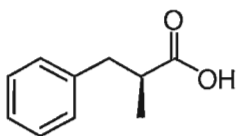
hexane:EtOAc, and solvent removed *in vacuo* to afford the title compound (56 mg, 97%) as a clear oil. CSP HPLC analysis (Chiralcel OD-H; eluent: 90:10 hexane:*i*-PrOH, 1.0 mL/min, 254 nm) determined an enantiomeric ratio (er) of 58.6:41.4 (17% ee) [t_R (major) 23.20 min, t_R (minor) 26.90 min]; ^1H NMR (300 MHz, CDCl_3) δ 7.28-7.20 (m, 5H), 6.15 (bd, 1H, $J = 4.5$ Hz), 5.04 (qnt, 1H, $J = 7.2$ Hz), 1.94 (s, 3H), 1.42 (d, 3H, $J = 6.9$ Hz).

(-)-methyl 3-methyldodecanoate [(-)-226p]. A solution of *trans*-methyl 3-



methyldodecanoate **225p** (61 mg, 0.27 mmol) and iridium catalyst (*S*)-**221** (8.5 mg, 0.0054 mmol, 2.0 mol%) in dry CH_2Cl_2 (3 mL) in a vial under argon was sealed in an autoclave. The autoclave was evacuated and back-filled with hydrogen three times, pressurized to 62 bar, and allowed to stir for 72 h at room temperature. The solvent was removed *in vacuo*, crude passed through a silica plug with 9:1 hexanes:EtOAc, and solvent was removed *in vacuo* to afford the title compound (29 mg, 96%) as a colourless oil. $[\alpha]_D^{20}$ -0.44 (c 1.0, CHCl_3) {Lit.¹³⁴ $[\alpha]_D^{20}$ +5.13 (c 1.0 CHCl_3)}; ^1H NMR (300 MHz, CDCl_3) δ 3.64 (s, 3H), 2.29 (dd, 1H), 2.08 (dd, 1H), 1.95-1.90 (m, 1H), 1.24 (s, 16H), 0.91 (d, 3H), 0.88 (t, 3H); ^{13}C NMR (75.5 MHz, CDCl_3) δ 173.7, 51.2, 41.6, 36.7, 31.9, 30.3, 29.7, 29.6, 29.6, 29.3, 26.9, 22.6, 19.7, 14.1.

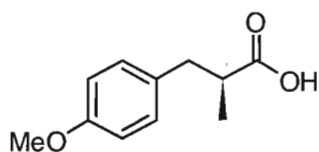
(*S*)-2-Methyl-3-phenyl-propionic acid [(*S*)-228v]. A solution of *trans*-2-methyl-3-



phenyl-acrylic acid **227v** (38.5 mg, 0.24 mmol), iridium catalyst (*S*)-**221** (7.5 mg, 0.0048 mmol, 2.0 mol %), and triethylamine (33 μL , 0.24 mmol) in dry MeOH (2.4 mL) in a vial under argon was sealed

in an autoclave. The autoclave was evacuated and back-filled with hydrogen three times, pressurized to 62 bar, and allowed to stir for 72 h at room temperature. The solvent was removed *in vacuo*, crude passed through a silica plug with 8:2 hexanes:EtOAc, and solvent removed *in vacuo* to afford the title compound (31 mg, 78%) as a colourless oil. $[\alpha]_D^{20} +15.9$ (*c* 1.0, CHCl₃) {Lit.¹³⁵ $[\alpha]_D^{20} +30.2$ (*c* 0.82, CHCl₃)}; ¹H NMR (300 MHz, CDCl₃) δ 11.68 (bs, 1H), 7.34-7.20 (m, 5H), 3.10 (dd, 1H, *J* = 12.9, 6.0 Hz), 2.80-2.66 (m, 2H), 1.20 (d, 3H, *J* = 6.9 Hz).

(*S*)-3-(4-Methoxy-phenyl)-2-methyl-propionic acid [(*S*)-228w]. A solution of *trans*-3-



(4-methoxy-phenyl)-2-methyl-acrylic acid **227w** (39.5 mg, 0.21 mmol), iridium catalyst (*S*)-**221** (6.5 mg, 0.0041 mmol, 2.0 mol %), and triethylamine (29 μ L, 0.21 mmol) in dry MeOH (2.1 mL) in a vial under argon was sealed in an autoclave. The autoclave was evacuated and back-filled with hydrogen three times, pressurized to 62 bar, and allowed to stir for 72 h at room temperature. The solvent was removed *in vacuo*, crude passed through a silica plug with 8:2 hexanes:EtOAc, and solvent removed *in vacuo* to afford the title compound (36 mg, 91%) as a colourless oil. $[\alpha]_D^{20} +18.5$ (*c* 0.81, CHCl₃) {Lit.¹³⁵ $[\alpha]_D^{20} +31.0$ (*c* 0.51, acetone)}; ¹H NMR (300 MHz, CDCl₃) δ 11.38 (bs, 1H), 7.11 (d, 2H, *J* = 8.4 Hz), 6.84 (d, 2H, *J* = 8.4 Hz), 3.79 (s, 3H), 3.02 (dd, 1H, *J* = 13.2, 6.0 Hz), 2.79-2.60 (m, 2H), 1.18 (d, 3H, *J* = 6.9 Hz).

Chapter 6: References

1. *Catalysis in Asymmetric Synthesis*; Caprio, V.; Williams J., Eds.; Wiley: Chichester, 2004.
2. Ohkuma, T.; Kitamura, M.; Noyori, R. Ligand Design for Catalytic Asymmetric Reduction. In *New Frontiers in Asymmetric Catalysis*; Mikami, K.; Lautens, M., Eds.; John Wiley & Sons, Inc.: Hoboken, NJ, 2007, pp 1-33.
3. *Homogeneous Catalysis: Understanding the Art*; van Leeuwen, P.W.N.M., Ed.; Kluwer Academic Publishers: Dordrecht, Netherlands, 2004.
4. *Inorganic Chemistry*; Housecroft, C.E.; Sharpe A.G., Eds.; Pearson Education Limited: Essex, 2005.
5. *Advanced Inorganic Chemistry*; Cotton, F. A.; Wilkinson, G.; Murillo, C.A.; Bochmann, M., Eds.; Wiley Interscience: New York, 1999.
6. Werner, A. Z. *Anorg. Allgem. Chem.* **1893**, 3, 267.
7. Chernyaev, I.I. *Ann. Inst. Platine (USSR)* **1926**, 4, 243.
8. Crabtree, R.H. *The Organometallic Chemistry of the Transition Metals*; John Wiley & Sons: Hoboken, NJ, 2009.
9. (a) Coe, B.J.; Glenwright, S.J. *Coord. Chem. Rev.* **2000**, 203, 5; (b) Anderson, K.M.; Orpen, A.G. *Chem. Comm.* **2001**, 2682.
10. Hartley, F.R. *Chem. Soc. Rev.* **1973**, 2, 163.
11. Humphries, A.C.; Pfaltz, A. Enantioselective Catalysis using Sterically and Electronically Unsymmetrical Ligands. / Hoveyda, A.N. Asymmetric Catalysis in Target-Oriented Synthesis. In *Stimulating Concepts in Chemistry*; Vogtle, F.;

- Stoddard, J.F.; Shibasaki, M., Eds.; Wiley-VCH Verlag GmbH: Weinheim, 2000, pp 89-103 / 145-160.
12. Pfaltz, A.; Drury III, W.J. *Proc. Natl. Acad. Sci.* **2004**, *101*, 5723.
 13. Anderson, J.C.; Cubbon, R.J.; Harling, J.D. *Tetrahedron: Asymmetry* **2001**, *12*, 923.
 14. (a) Guiry, P.; Saunders, C. *Adv. Synth. Catal.* **2004**, *346*, 497; (b) Kostas, I.D. *Curr. Org. Synth.* **2008**, *5*, 227.
 15. Hayashi, T.; Yamamoto, K.; Kumada, M. *Tetrahedron Lett.* **1974**, *49-50*, 4405.
 16. Hayashi, T.; Fukushima, M.; Konishi, M.; Kumada, M. *Tetrahedron Lett.* **1980**, *21*, 79.
 17. Hayashi, T.; Konishi, M.; Fukushima, M.; Mise, T.; Kagotani, M.; Tajika, M.; Kumada, M. *J. Am. Chem. Soc.* **1982**, *104*, 180.
 18. Jedlicka, B.; Kratky, C.; Weissensteiner, W.; Widhalma, M. *J. Chem. Soc. Chem. Comm.* **1993**, 1329.
 19. Wang, Y.; Guo, H.; Ding, K. *Tetrahedron: Asymmetry* **2000**, *11*, 4153.
 20. Guiry, P.J.; Hennessey, A.J.; Cahill, J.P. *Top. Catal.* **1997**, *4*, 311.
 21. Cahill, J.P.; Guiry, P.J. *Tetrahedron: Asymmetry* **1998**, *9*, 4301.
 22. Wang, Y.; Ji, B.M.; Ding, K.L. *Chinese J. Chem.* **2002**, *20*, 1300.
 23. Jin, M.J.; Jung, J.A.; Kim, S.H. *Tetrahedron Lett.* **1999**, *40*, 5197.
 24. Lee, E.K.; Kim, S.H.; Jung, B.H.; Ahn, W.S.; Kim, G.J. *Tetrahedron Lett.* **2003**, *44*, 1971.
 25. Kohara, T.; Hashimoto, Y.; Saigo, K. *Synlett* **2000**, *4*, 517.
 26. Fukuda, T.; Takehara, A.; Iwao, M. *Tetrahedron Asymmetry* **2001**, *12*, 279.

27. Hayashi, T.; Hayashi, C.; Uozumi, Y. *Tetrahedron: Asymmetry* **1995**, *6*, 2503.
28. Gommermann, N.; Knochel, P. *Chem. Eur. J.* **2006**, *12*, 4380.
29. Kloetzing, R.J.; Knochel, P. *Tetrahedron: Asymmetry* **2006**, *17*, 116.
30. Saitoh, A.; Achiwa, K.; Tanaka, K.; Morimoto, T. *J. Org. Chem.*, **2000**, *65*, 4227.
31. Hu, X.; Chen, H.; Hu, X.; Dai, H.; Bai, C.; Wang, J.; Zheng, Z. *Tetrahedron Lett.* **2002**, *43*, 9179.
32. von Matt, P.; Pfaltz, A. *Angew. Chem. Int. Ed.* **1993**, *32*, 566.
33. Sprinz, J.; Helmchen, G. *Tetrahedron Lett.* **1993**, *34*, 1769.
34. Dawson, G.J.; Frost, C.G.; Williams, J.M.J. *Tetrahedron Lett.* **1993**, *34*, 3149.
35. Loiseleur, O.; Hayashi, M.; Keenan, M.; Schmees, N.; Pfaltz, A. *J. Organomet. Chem.* **1999**, *576*, 16.
36. Hirio, K.; Watanabe, K. *Tetrahedron: Asymmetry* **2002**, *13*, 1841.
37. Nishibayashi, Y.; Uemura, S. *Synlett* **1995**, 79.
38. Richards, C.J.; Damalidis, T.; Hibbs, D.E.; Hursthouse, M.B. *Synlett* **1995**, 74.
39. Sammakia, T.; Latham, H.A.; Schaad, D.R. *J. Org. Chem.* **1995**, *60*, 10.
40. Sutcliffe, O.B.; Bryce, M.R. *Tetrahedron Asymmetry* **2003**, *14*, 2297.
41. Nishibayashi, Y.; Takei, I.; Uemura, S.; Hidai, M. *Organometallics* **1999**, *18*, 2291.
42. (a) Takei, I.; Nishibayashi, Y.; Arikawa, Y.; Uemura, Y.; Hidai, M. *Organometallics* **1999**, *18*, 2271; (b) Nishibayashi, Y.; Segawa, K.; Takada, H.; Ohe, H.; Uemura, S. *Chem. Comm.* **1996**, 847.
43. Hennessy, A.J.; Malone, Y.M.; Guiry, P.J. *Tetrahedron Lett.* **1999**, *40*, 9163.

44. Selvakumar, K.; Valentini, M.; Wörle, M.; and Pregosin, P.S. *Organometallics* **1999**, *18*, 1207.
45. Valla, C.; Pfaltz, A. *Chimica Oggi* **2004**, *4*.
46. Pfaltz, A. *Angew. Chem. Int. Ed.* **2001**, *40*, 4445.
47. Jones, G.; Richards, C.J. *Tetrahedron Lett.* **2001**, *42*, 5553.
48. Xu, G.; Gilbertson, S.R. *Tetrahedron Lett.* **2002**, *43*, 2811.
49. Noyori, R. *Asymmetric Catalysis in Organic Synthesis*. John Wiley & Sons, Inc., New York, NY, USA, **1994**.
50. Osborn, J. A.; Jardine, F. H.; Young, J. F.; Wilkinson, G. *Chem. Soc. A.* **1966**, 171.
51. Knowles, W.S. *Acc. Chem. Res.* **1983**, *16*, 106.
52. Knowles, W.S. *Angew. Chem. Int. Ed.* **2002**, *41*, 1999.
53. (a) Blaser, H-U.; Spindler, F. *Top. Catal.* **1997**, *4*, 275; (b) Spindler, F.; Pugin, B.; Blaser, H-U. *Angew. Chem. Int. Ed.* **1990**, *29*, 558.
54. Cui, X.; Burgess, K. *Chem. Rev.* **2005**, *105*, 3272.
55. Crabtree, R.H.; Felkin, H.; Morris, G.E. *J. Organomet. Chem.* **1977**, *141*, 205.
56. Crabtree, R. *Acc. Chem. Res.* **1979**, *12*, 331.
57. Suggs, J.W.; Cox, S.D.; Crabtree, R.H.; Quirk, J.M. *Tetrahedron Lett.* **1981**, *22*, 303.
58. Voelter, W.; Djerassi, C. *Chem. Ber.* **1968**, *101*, 58.
59. For reviews on iridium catalyzed hydrogenation see: (a) Valla, C.; Pfaltz, A. *Chimica Oggi* **2004**, *4*; (b) Pfaltz, A. *Angew. Chem. Int. Ed.* **2001**, *40*, 4445; Cui, X.; Burgess, K. *Chem. Rev.* **2005**, *105*, 3272; (c) Lightfoot, A.; Schnider, P.;

- Pfaltz, A. *Angew. Chem. Int. Ed.* **1998**, *37*, 2897; (d) Smidt, S.P.; Zimmermann, N.; Studer, M.; Pfaltz, A. *Chem. Eur. J.* **2004**, *10*, 4685; (e) Mazet, C.; Smidt, S.P.; (f) Meuwly, M.; Pfaltz, A. *J. Am. Chem. Soc.* **2004**, *126*, 14176; (g) Roseblade, S.J.; Pfaltz, A. *C.R. Chimie* **2007**, *10*, 178; (h) Källström, K.; Munslow, I.; Andersson, P.G. *Chem. Eur. J.* **2006**, *12*, 3194; (i) Roseblade, S.J.; Pfaltz, A. *Acc. Chem. Res.* **2007**, *40*, 1402; (j) Church, T.L.; Andersson, P.G. *Coord. Chem. Rev.* **2008**, *252*, 513.
60. Lightfoot, A.; Schnider, P.; Pfaltz, A. *Angew. Chem. Int. Ed.* **1998**, *37*, 2897.
61. Smidt, S.P.; Zimmermann, N.; Studer, M.; Pfaltz, A. *Chem. Eur. J.* **2004**, *10*, 4685.
62. Wüstenberg, B. and Pfaltz, A. *Adv. Synth. Catal.* **2008**, *350*, 174.
63. (a) Crabtree, R.H.; Uriate, R.J. *Inorg. Chem.* **1983**, *22*, 4152; (b) Crabtree, R.H.; Morehouse, S.M. *Inorg. Chem.* **1982**, *21*, 4210; (c) Crabtree, R.H.; Felkin, H.; Fillebeen-Khan, T.; Morris, G.E. *J. Organomet. Chem.* **1979**, *168*, 183.
64. Church, T.L.; Andersson, P.G. *Coord. Chem. Rev.* **2008**, *252*, 513.
65. Mazet, C.; Smidt, S.P.; Meuwly, M.; Pfaltz, A. *J. Am. Chem. Soc.* **2004**, *126*, 14176.
66. Roseblade, S.J.; Pfaltz, A. *C. R. Chimie* **2007**, *10*, 178.
67. Brandt, P.; Hedberg, C.; and Andersson, P.G. *Chem. Eur. J.* **2003**, *9*, 339.
68. Crabtree, R.H. and Morris, G.E. *J. Organomet. Chem.* **1977**, *135*, 395.
69. Gridnev, I.D.; Imamoto, T. *Acc. Chem. Res.* **2004**, *37*, 633.
70. Crabtree, R.H.; Felkin, H.; Khan, T.; Morris, G.E. *J. Organomet. Chem.* **1978**, *144*, C15.

71. Källström, K.; Munslow, I.; Andersson, P.G. *Chem. Eur. J.* **2006**, *12*, 3194.
72. Fan, Y.; Cui, X.; Burgess, K.; Hall, M.B. *J. Am. Chem. Soc.* **2004**, *126*, 16688.
73. Hedberg, C.; Källström, K.; Brandt, P.; Hansen, L.K.; Andersson, P.G. *J. Am. Chem. Soc.* **2006**, *128*, 2995.
74. Church, T.L.; Andersson, P.G. *Coord. Chem. Rev.* **2008**, *252*, 513.
75. For applications of Ir-catalyzed hydrogenation see: (a) Hedberg, C.; Kallstrom, K.; Brandt, P.; Hansen, L.K.; Andersson, P.G. *J. Am. Chem. Soc.* **2006**, *128*, 2295; (b) Lu, S.M.; Bolm, C. *Angew. Chem. Int. Ed.* **2008**, *47*, 8920; Li, S.; Zhu, S.F.; (c) Xie, J.H.; Song, S.; Zhang, C.M.; Zhou, Q.L. *J. Am. Chem. Soc.* **2010**, *132*, 1172; (d) Lu, S.M.; Han, X.W.; Zhou, Y.G.. *Adv. Synth. Catal.* **2004**, *346*, 909; (e) Knowles, W.S. *Angew. Chem. Int. Ed.* **2002**, *41*, 1999; (f) Blankenstein, J.; Pfaltz, A. *Angew. Chem. Int. Ed.* **2001**, *40*, 4445; (g) Cheemala, M.N.; Knochel, P. *Org. Lett.* **2007**, *9*, 3089.
76. (a) Blackmond, D.G.; Lightfoot, A.; Pfaltz, A.; Rosner, T.; Schnider, P.; Zimmermann, N. *Chirality*, **2000**, *12*, 442; (b) Schrems, M.G.; Pfaltz, A. *Chem. Comm.* **2009**, 6210; (c) Li, X.; Li, Q.; Wu, X.; Gao, Y.; Xu, D.; Kong, L. *Tetrahedron: Asymmetry* **2007**, *18*, 629; (d) Smidt, S.P.; Menges, F.; Pfaltz, A. *Org. Lett.* **2004**, *6*, 2023.
77. McIntyre, S.; Hormann, E.; Menges, F.; Smidt, S.P.; Pfaltz, A. *Adv. Syth. Catal.* **2005**, *347*, 282.
78. Bell, S.; Wustenberg, B.; Kaiser, S.; Menges, F.; Netscher, T.; Pfaltz, A. *Science* **2006**, *311*, 642.
79. Schrems, M.G.; Neumann, E.; Pfaltz, A. *Angew. Chem. Int. Ed.* **2007**, *46*, 8274

80. Tolstoy, P.; Engman, M.; Paptchikhine, A.; Bergquist, J.; Church, T.L.; Leung, A.W.M.; Andersson, P.G. *J. Am. Chem. Soc.* **2009**, *131*, 8855.
81. Engman, M.; Cheruku, P.; Tolstoy, P.; Bergquist, J.; Volker, S.F.; Andersson, P.G. *Adv. Synth. Catal.* **2009**, *351*, 375.
82. Lu, S.M.; Han, X.W.; Zhou, Y.G. *Adv. Synth. Catal.* **2004**, *346*, 909.
83. Baeza, A.; Pfaltz, A. *Chem. Eur. J.* **2010**, *16*, 2036.
84. Valla, C.; Baeza, A.; Menges, F.; Pfaltz, A. *Synlett* **2008**, *20*, 3167.
85. (a) Lu, W.J.; Chen, Y.W.; Hou, X.L. *Angew. Chem. Int. Ed.* **2008**, *47*, 10133; (b) Lu, S.M.; Bolm, C. *Angew. Chem. Int. Ed.* **2008**, *47*, 8920.
86. Lu, W.J.; Hou, X.L. *Adv. Synth. Catal.* **2009**, *351*, 1224.
87. (a) Li, S.; Zhu, S.F.; Zhang, C.M.; Song, S.; Zhou, Q.L. *J. Am. Chem. Soc.* **2008**, *130*, 8584; (b) Li, S.; Zhu, S.F.; Xie, J.H.; Song, S.; Zhang, C.M.; Zhou, Q.L. *J. Am. Chem. Soc.* **2010**, *132*, 1172.
88. Lightfoot, A.; Schnider, P.; Pfaltz, A. *Angew. Chem. Int. Ed.* **1998**, *37*, 2897
89. Bell, S.; Wüstenberg, B.; Kaiser, S.; Menges, F.; Netscher, T.; Pfaltz, A. *Science* **2006**, *311*, 642.
90. Bianco, G.G.; Ferraz, H.M.C.; Costa, A.M.; Costa-Lotufo, L.V.; Pessoa, C.; de Moraes, M.O.; Schrems, M.G.; Pfaltz, A.; Silva Jr., L.F. *J. Org. Chem.* **2009**, *74*, 2561.
91. For additional synthetic applications of Ir-catalyzed asymmetric hydrogenation see: Schrems, M.G.; Pfaltz, A. *Chem. Comm.* **2009**, 6210; Han, Z.; Wang, Z.; Zhang, X.; Ding, K. *Angew. Chem. Int. Ed.* **2009**, *48*, 5345; Yoshinari, T.;

- Ohmori, K.; Schrems, M.G.; Pfaltz, A.; Suzuki, K. *Angew. Chem. Int. Ed.* **2010**, *49*, 881.
92. (a) *Chiral Ferrocenes in Asymmetric Catalysis: Synthesis and Applications*; Dai, L.-X.; Hou, X.-L., Eds.; Wiley-VCH Verlag GmbH & Co. KGaA: Weinheim, Germany, 2010; (b) *Ferrocenes: Homogeneous Catalysis, Organic Synthesis, and Materials Science*; Togni, A.; Hayashi, T., Eds.; VCH Verlag GmbH: Weinheim, Germany, 1995; (c) *Ferrocenes: Ligands, Materials, and Biomolecules*; Stěpnička, P., Ed.; John Wiley & Sons Ltd.: Chichester, England, 2008.
93. Deng, W.-P.; Snieckus, V.; Metallinos, C. Stereoselective Synthesis of Planar Chiral Ferrocenes. In *Chiral Ferrocenes in Asymmetric Catalysis: Synthesis and Applications*; Dai, L.-X.; Hou, X.-L., Eds.; Wiley-VCH Verlag GmbH & Co. KGaA: Weinheim, Germany, 2010, pp 15-53.
94. (a) Yamazaki, Y.; Hosono, K. *Biotech. Lett.* **1989**, *11*, 679; (b) Izumi, T.; Murakami, S.; Kasahara, A. *Soc. Chem. Ind. (London)* **1990**, *3*, 79; (c) Izumi, T.; Tamura, F.; Sasaki, K. *Bull. Chem. Soc. Jpn.* **1992**, *65*, 2784; (d) Izumi, T.; Hino, T.; Ishihara, A. *J. Chem. Tech. Biotech.* **1993**, *56*, 45; (e) Lambusta, D.; Nicolosi, G.; Patti, A.; Piattelli, M. *Tetrahedron Lett.* **1996**, *37*, 127; (f) Patti, A.; Lambusta, D.; Piattelli, M.; Nicolosi, G. *Tetrahedron: Asymmetry* **1998**, *9*, 3073.
95. (a) Bueno, A.; Rosol, M.; Garcia, J.; Moyano, A. *Adv. Synth. Catal.* **2006**, *348*, 2590; (b) Ogasawara, M.; Watanabe, S.; Fan, L.; Nakajima, K.; Takahashi, T. *Organometallics* **2006**, *25*, 5201; (c) Ogasawara, M.; Watanabe, S.; Nakajima, K.; Takahashi, T. *Pure Appl. Chem.* **2008**, *60*, 1109.
96. Snieckus, V. *Chem. Rev.* **1990**, *90*, 879.

97. Marquarding, D.; Klusacek, H.; Gokel, G.; Hoffmann, P.; Ugi, I. *J. Am. Chem. Soc.* **1970**, 92, 5389.
98. Togni, A.; Breutel, C.; Schnyder, A.; Spindler, F.; Landert, H.; Tijani, A. *J. Am. Chem. Soc.* **1994**, 116, 4062.
99. Boaz, N.W.; Ponasik, Jr., J.A.; Large, S.E. *Tetrahedron Asymmetry* **2005**, 16, 2063.
100. (a) ref 38; (b) Sammakia, T.; Latham, H.A.; Schaad, D.R. *J. Org. Chem.* **1995**, 60, 10; (c) Nishibayashi, Y.; Uemura, S. *Synlett* **1995**, 79.
101. Sutcliffe, O.B.; Bryce, M.R. *Tetrahedron: Asymmetry* **2003**, 14, 2297.
102. Richards, C.J.; Mulvaney, A.W. *Tetrahedron Asymmetry* **1996**, 7, 1419.
103. Rebiere, F.; Riant, O.; Ricard, L.; Kagan, H.B. *Angew. Chem. Int. Ed.* **1993**, 32, 568.
104. Priego, J.; Mancheño, O.G.; Cabrera, S.; Carretero, J.C. *J. Org. Chem.* **2002**, 67, 1346.
105. Bertogg, A.; Camponovo, F.; Togni, A. *Eur. J. Inorg. Chem.* **2005**, 3.
106. (a) Riant, O.; Samuel, O.; Kagan, H.B. *J. Am. Chem. Soc.* **1993**, 115, 5835; (b) Riant, O.; Samuel, O.; Flessner, T.; Taudien, S.; Kagan, H.B. *J. Org. Chem.* **1997**, 62, 6733; (c) Bertogg, A.; Camponovo, F.; Togni, A. *Eur. J. Inorg. Chem.* **2005**, 347.
107. Nishibayashi, Y.; Arikawa, Y.; Ohe, K.; Uemura, S. *J. Org. Chem.* **1996**, 61, 1172.

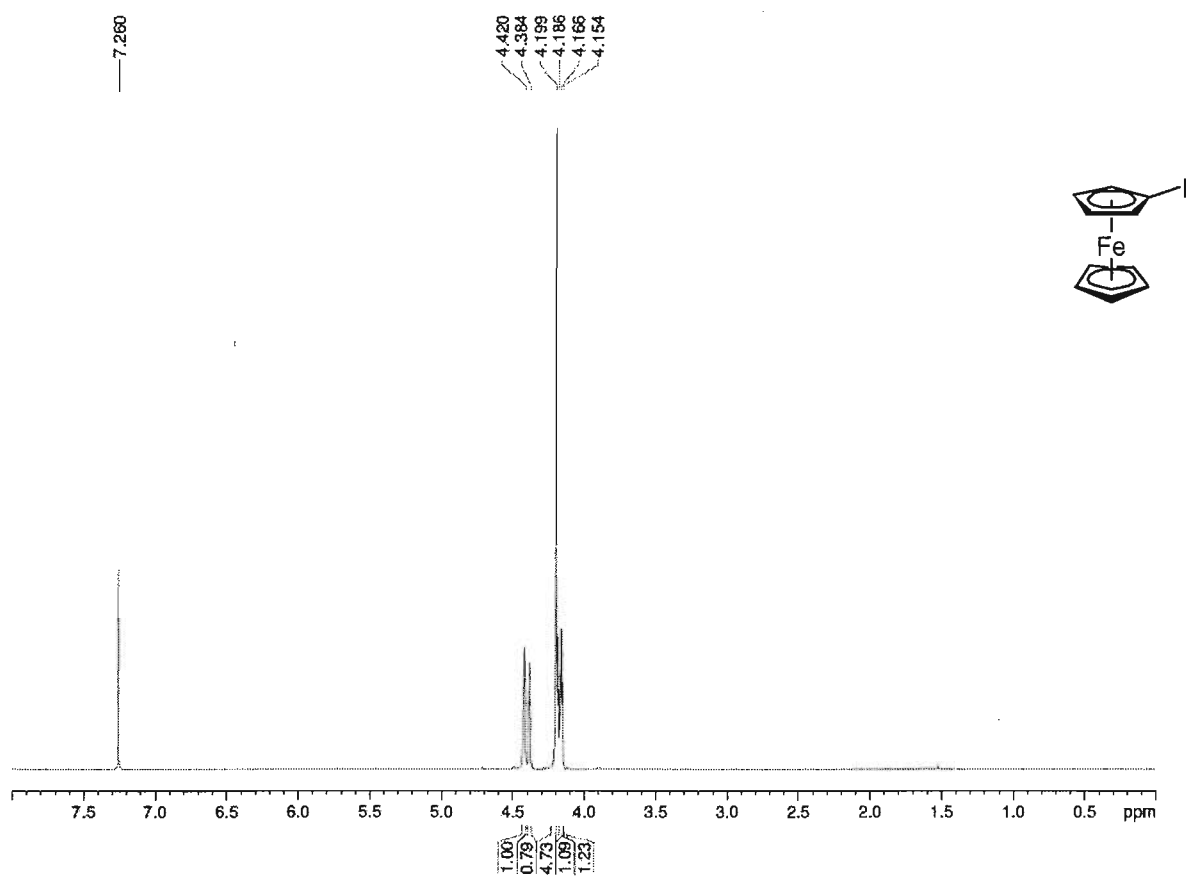
108. (a) Tsukazaki, M.; Tinkl, M.; Roglans, A.; Chapell, B.J.; Taylor, N.J.; Snieckus, V. *J. Am. Chem. Soc.* **1996**, *118*, 685; (b) Metallinos, C.; Szillat, H.; Taylor, N.J.; Snieckus, V. *Adv. Synth. Catal.* **2003**, *345*, 370.
109. Price, D.; Simpkins, N.S. *Tetrahedron Lett.* **1995**, *36*, 6135.
110. Metallinos, C.; Zaifman, J.; Dodge, L. *Org. Lett.*, **2008**, *10*, 3527.
111. Metallinos, C.; Zaifman, J.; Van Belle, L.; Dodge, L.; Pilkington, M. *Organometallics* **2009**, *28*, 4534.
112. Metallinos, C.; Zaifman, J.; Dudding, T.; Van Belle, L.; Taban, K., *Adv. Synth. Catal.* **2010**, *352*, 1967.
113. Zaifman, J. Ph.D. Thesis, Brock University, 2010.
114. For reviews on ferrocene ligands see: ref 92; (a) Balavoine, G.G.A.; Daran, J.C.; Iftime, G.; Manoury, E.; and Moreau-Bossuet, C. *J. Organomet. Chem.* **1998**, *567*, 191; (b) Richards, C.J.; Locke, A.J. *Tetrahedron: Asymmetry* **1998**, *9*, 2377; (c) Dai, L.X.; Tu, T.; You, S.L.; Deng, W.P.; Hou, X.L. *Acc. Chem. Res.* **2003**, *36*, 659; (d) Atkinson, R.C.J.; Gibson, V.C.; Long, N.J. *Chem. Soc. Rev.* **2004**, *33*, 313; (e) Arrayás, R.G.; Adrio, J.; Carretero, J.C. *Angew. Chem. Int. Ed.* **2006**, *45*, 7674.
115. Boaz, N.W.; Large, S.E.; Ponasik, Jr., J.A.; Moore, M.K.; Barnette, T.; Nottingham, W.D. *Org. Process Res. Dev.* **2005**, *9*, 472.
116. Naud, F.; Malan, C.; Spindler, F.; Rüggeberg, C.; Schmidt, A.T.; Blaser, H.U. *Adv. Synth. Catal.* **2006**, *348*, 47.
117. (a) Sato, M.; Ebine, S.; Akabori, S. *Synthesis*. **1981**, 472; (b) Bildstein, B.; Malaun, M.; Kopacka, H.; Wurst, K.; Mitterböck, M.; Ongania, K-H.; Opromolla,

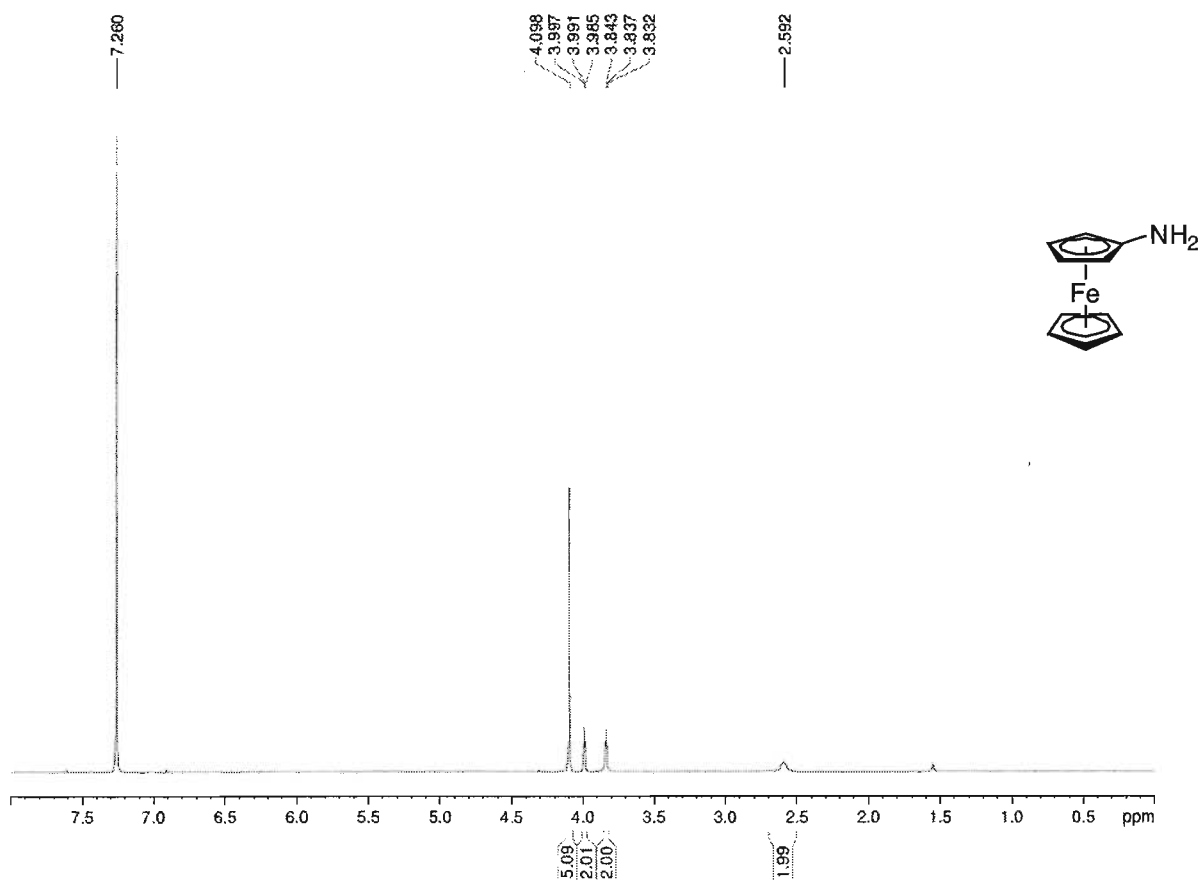
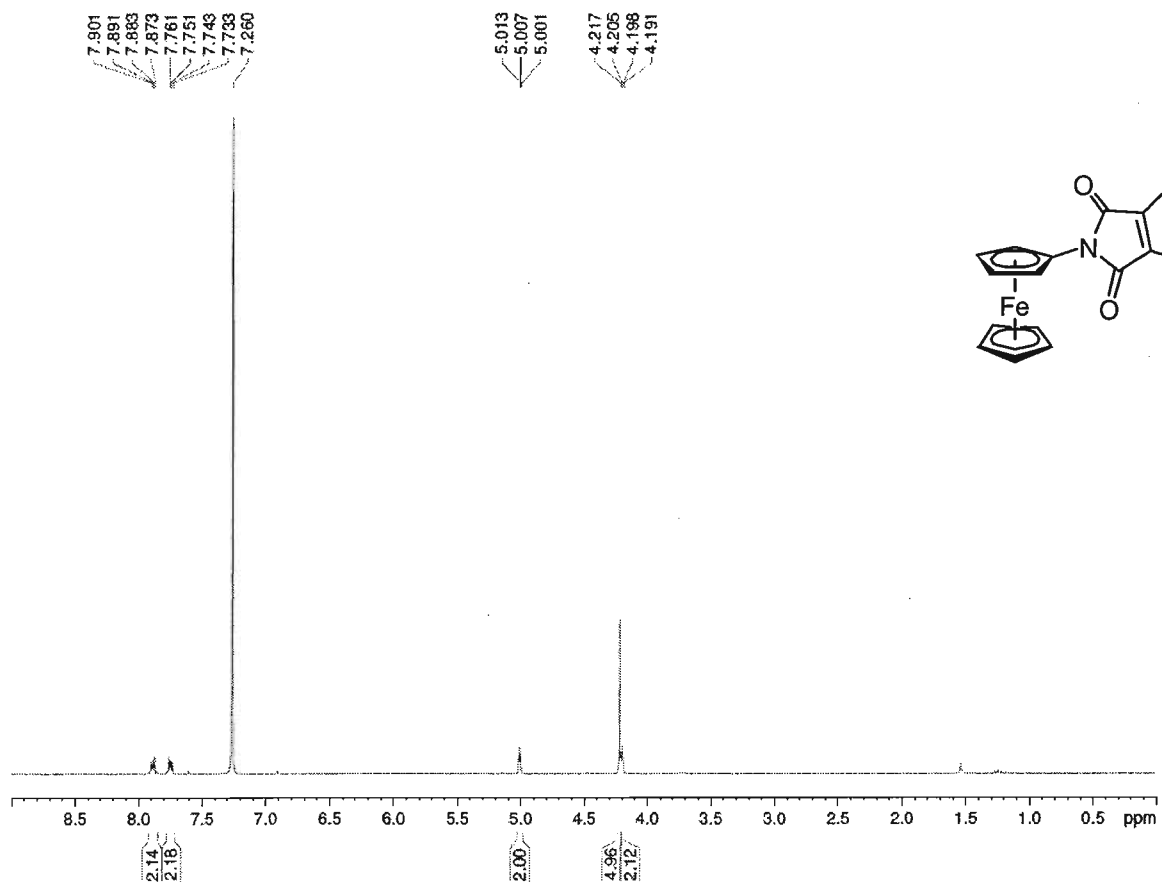
- G.; Zanello, P. *Organometallics* **1999**, *18*, 4325; (c) van Leusen, D.; Hessen, B. *Organometallics* **2001**, *20*, 224.
118. (a) Brookhart, M.; Grant, B.; Volpe, Jr., A.F. *Organometallics* **1992**, *11*, 3920; (b) Reger, D.L.; Little, C.A.; Lamba, J.J.S.; Brown, K.J. *Inorg. Synth.* **2004**, *34*, 5; (c) Nishida, H.; Takada, N.; Yoshimura, M. *Bull. Chem. Soc. Jpn.* **1984**, *57*, 2600; (d) Yakelis, N.A.; Bergman, R.G. *Organometallics* **2005**, *24*, 3579; (e) Smith, C.R.; Zhang, A.; Mans, D.J.; RajanBabu, T.V. *Org. Synth.* **2008**, *85*, 248.
119. Metallinos, C.; Van Belle, L. *J. Organomet. Chem.*, in press.
120. (a) Flanagan, S.P.; Guiry, P.J. *J. Organomet. Chem.* **2006**, *691*, 2125; (b) Schnyder, A.; Togni, A.; Wiesli, U. *Organometallics* **1997**, *16*, 255.
121. Burchat, A.F.; Chong, J.M.; Nielsen, N. *J. Organomet. Chem.* **1997**, *542*, 281.
122. Morrison, R.C.; Hall, R.W.; Schwinderman, J.A.; Kamienski, C.W.; Engel, J.F. **1992**, EP 0 525 881 A1.
123. (a) Stead, D.; O'Brien, P.; Sanderson, A. *Org. Lett.* **2008**, *10*, 1409; (b) Kizirian, J.C.; Caille, J.C.; Alexakis, A. *Tetrahedron Lett.* **203**, *44*, 8893; (c) Kizirian, J.C.; Cabello, N.; Pinchard, L.; Caille, J.C.; Alexakis, A. *Tetrahedron* **2005**, *61*, 8939.
124. Clark, P.; Mulraney, B.J. *J. Organomet. Chem.* **1981**, *217*, 51.
125. Black, P.J.; Edwards, M.G.; Williams, J.M.J. *Eur. J. Org. Chem.* **2006**, *19*, 4367.
126. Fox, D.J.; Pedersen, D.S.; Warren, S. *Org. Biomol. Chem.* **2006**, *4*, 3102.
127. Taherpour, A.A.; Mansuri, H.R. *Turk. J. Chem.* **2005**, *29*, 317.
128. Ruano, J.L.G.; Aranda, M.T.; Puente, M. *Tetrahedron* **2005**, *61*, 10099.

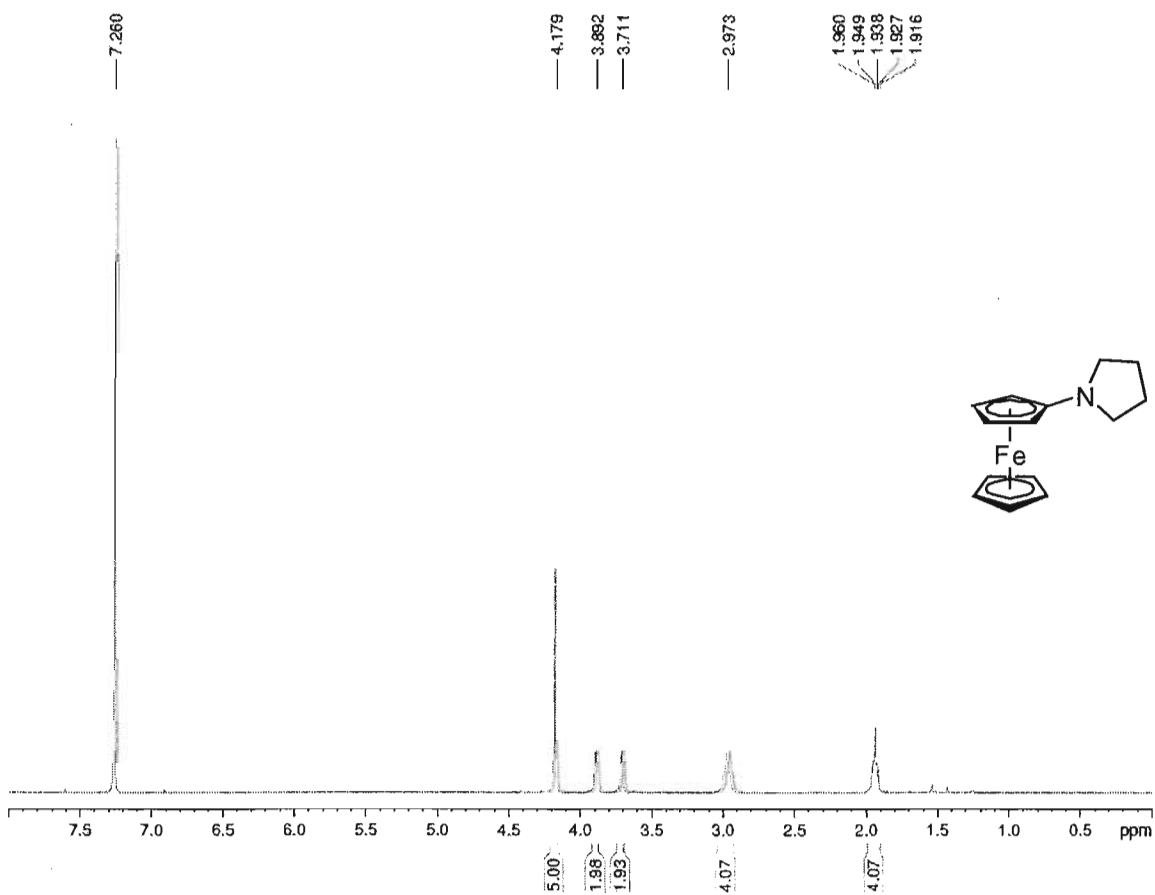
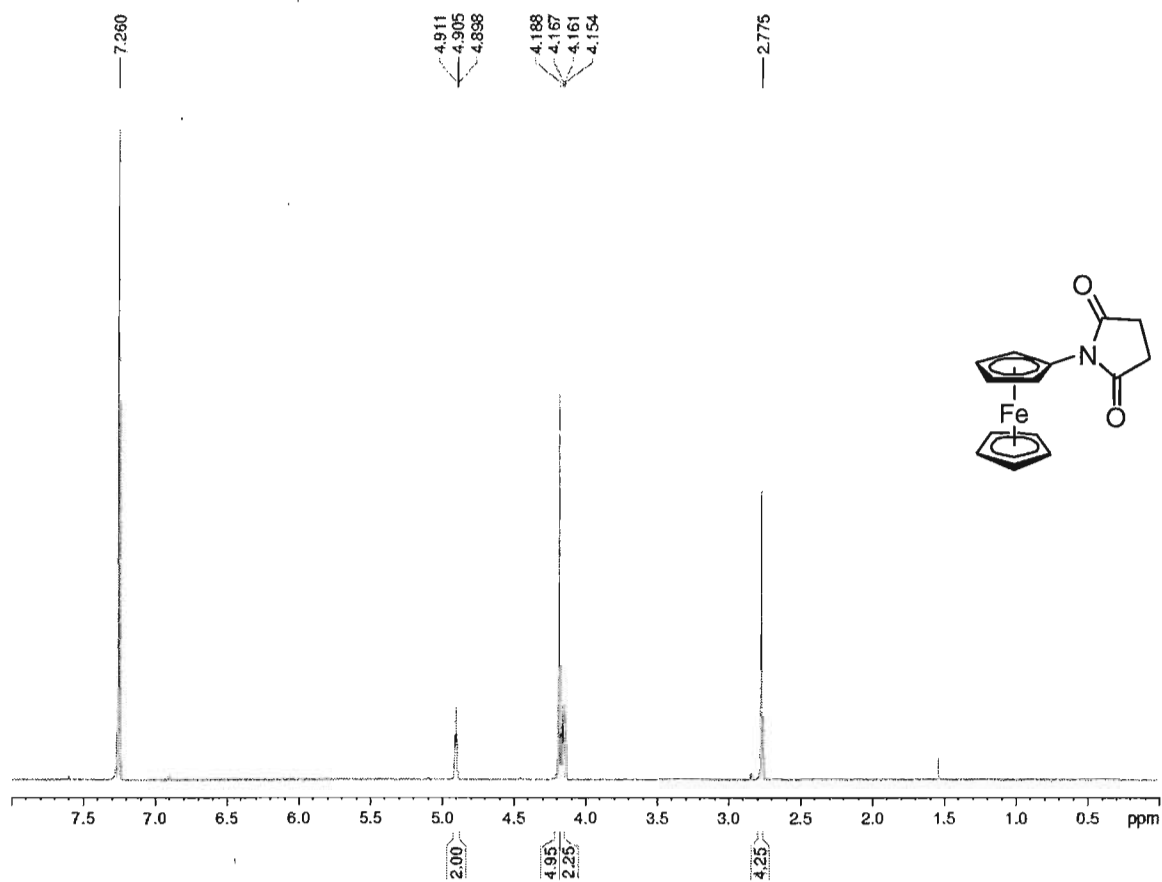
129. Kanazawa, Y.; Tsuchiya, Y.; Kobayashi, K.; Shiomi, T.; Itoh, J.; Kikuchi, M.; Yamamoto, Y.; Nishiyama, H. *Chem. Eur. J.* **2005**, *12*, 63.
130. Schrems, M.; Pfaltz, A. *Chem. Comm.* **2009**, 6210.
131. Davies, S.G. and Dixon, D.J. *J. Chem. Soc. Perkin Trans. 1* **2002**, *16*, 1869.
132. Tietze, L.F.; Schiemann, K.; Wegner, C.; Wulff, C. *Chem. Eur. J.* **1996**, *2*, 1164.
133. Ahn, K.Y.; Lim, A.; Lee, S. *Tetrahedron: Asymmetry* **1993**, *4*, 2435.
134. Christensen, P.K.; Gehe, R.A. *Acta Chemica Scandinavica*, **1965**, *19*, 1153.
135. Li, S.; Zhu, S.F.; Zhang, C.M.; Song, S.; Zhou, Q.L. *J. Am. Chem. Soc.* **2008**, *130*, 8584.

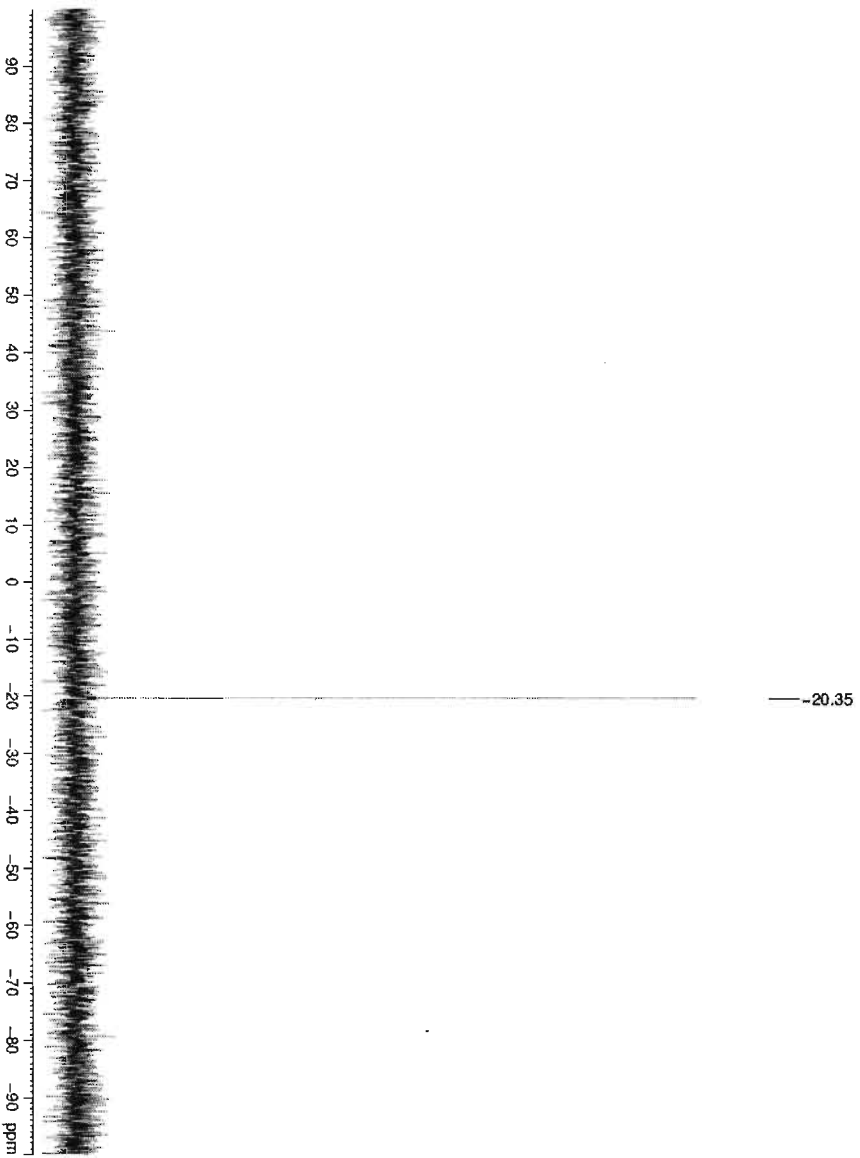
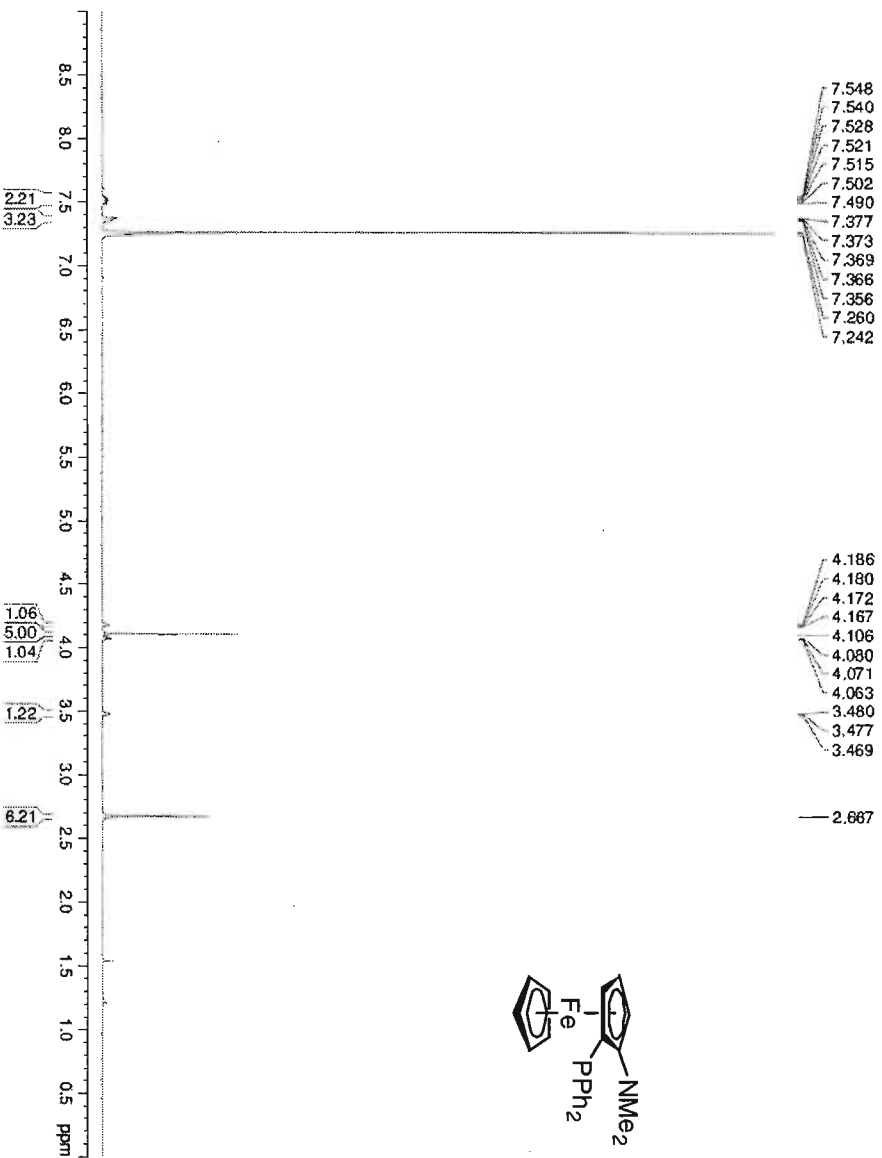
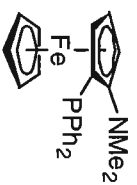
Chapter 7: Appendices

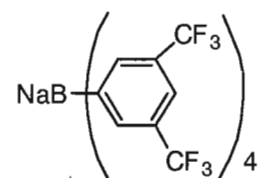
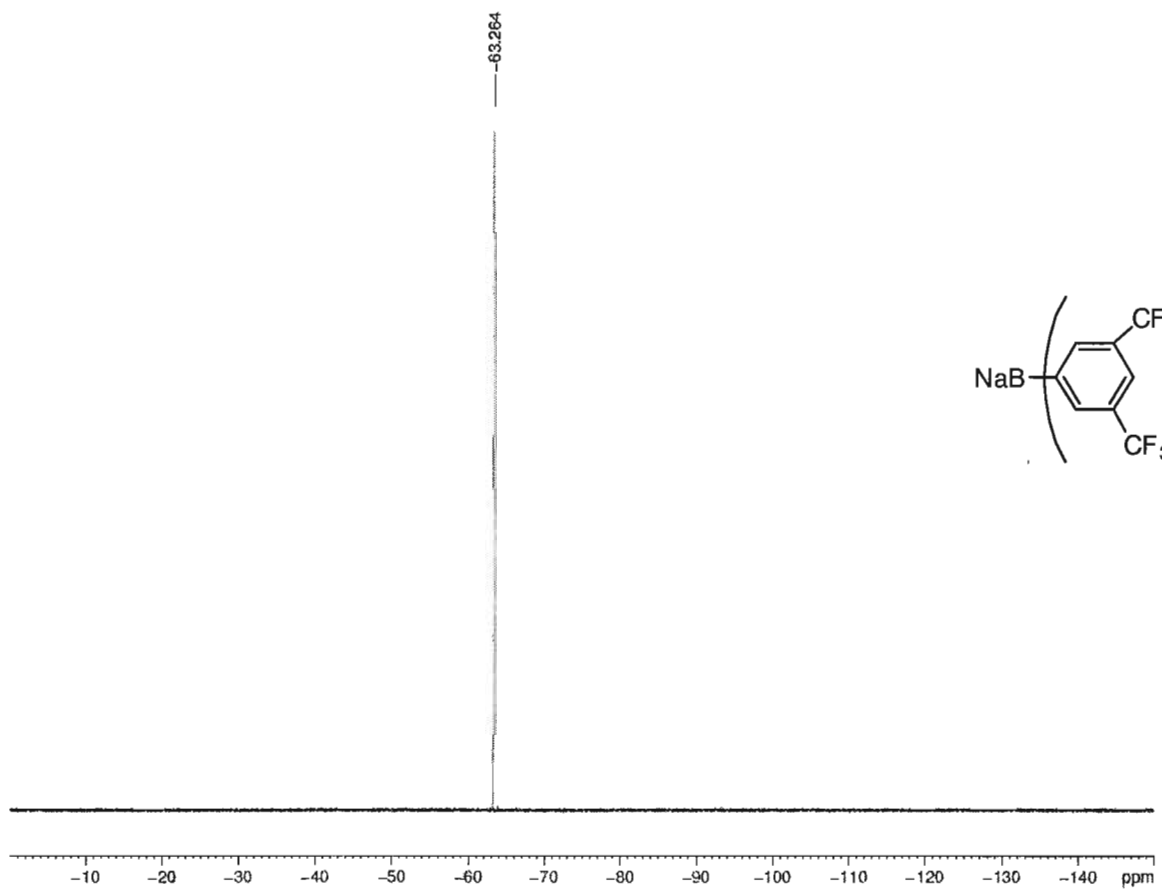
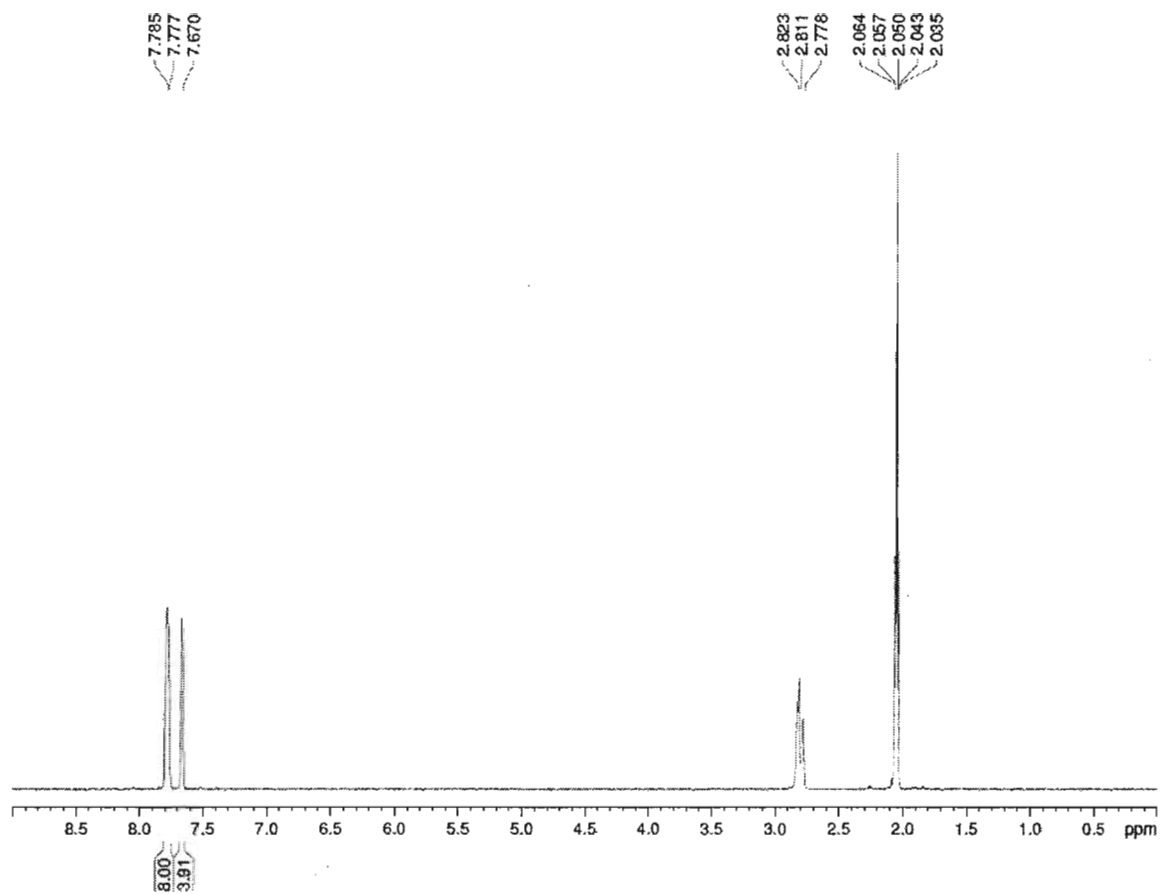
7.1 Appendix 1 – NMR data.

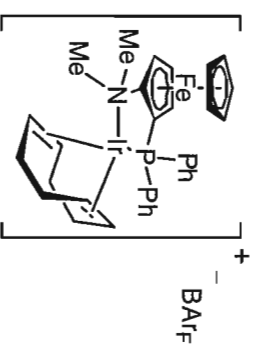






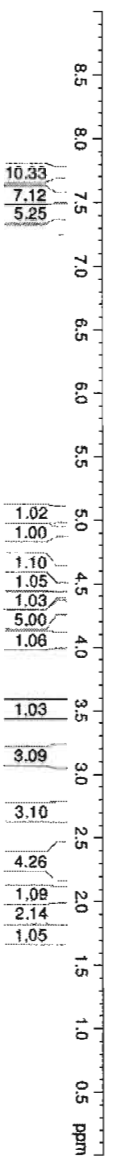




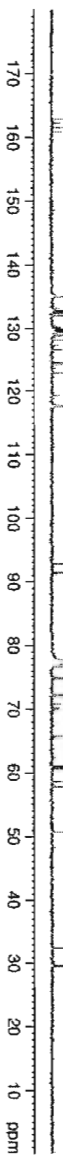


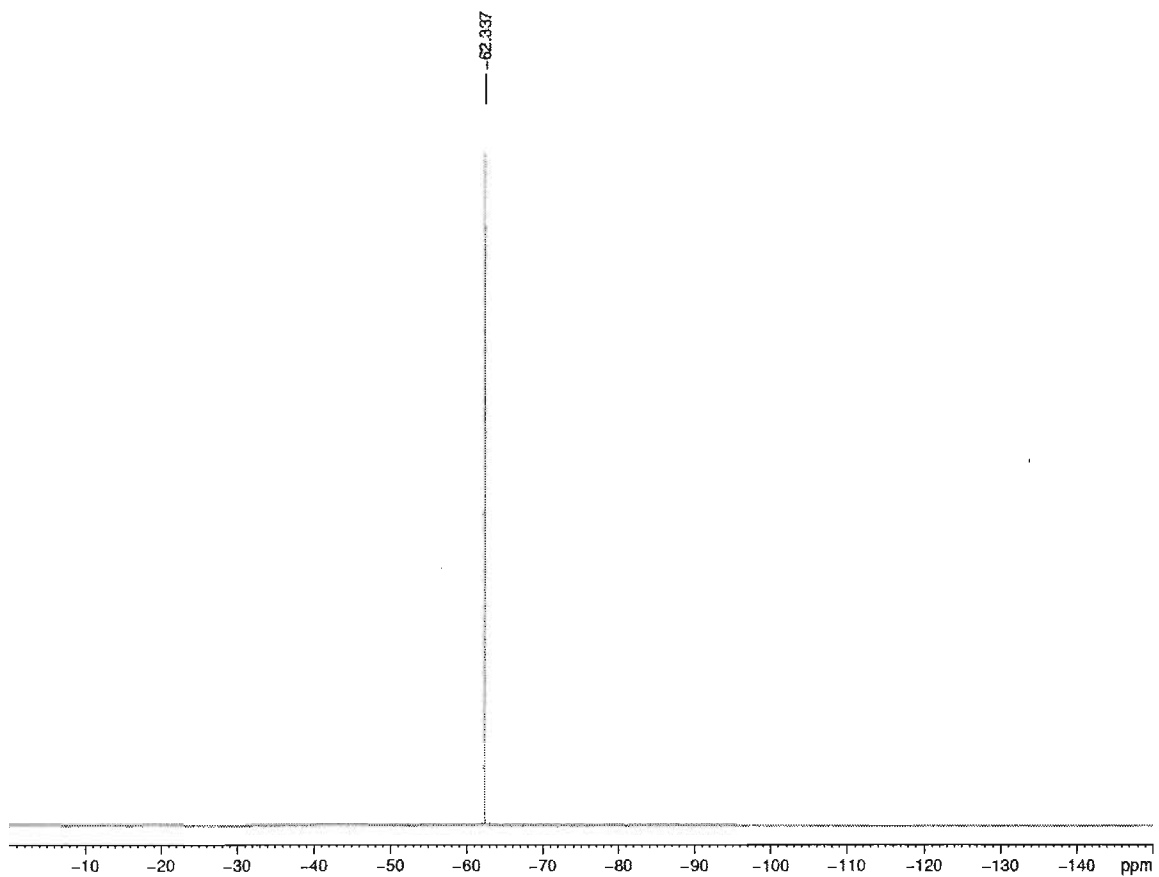
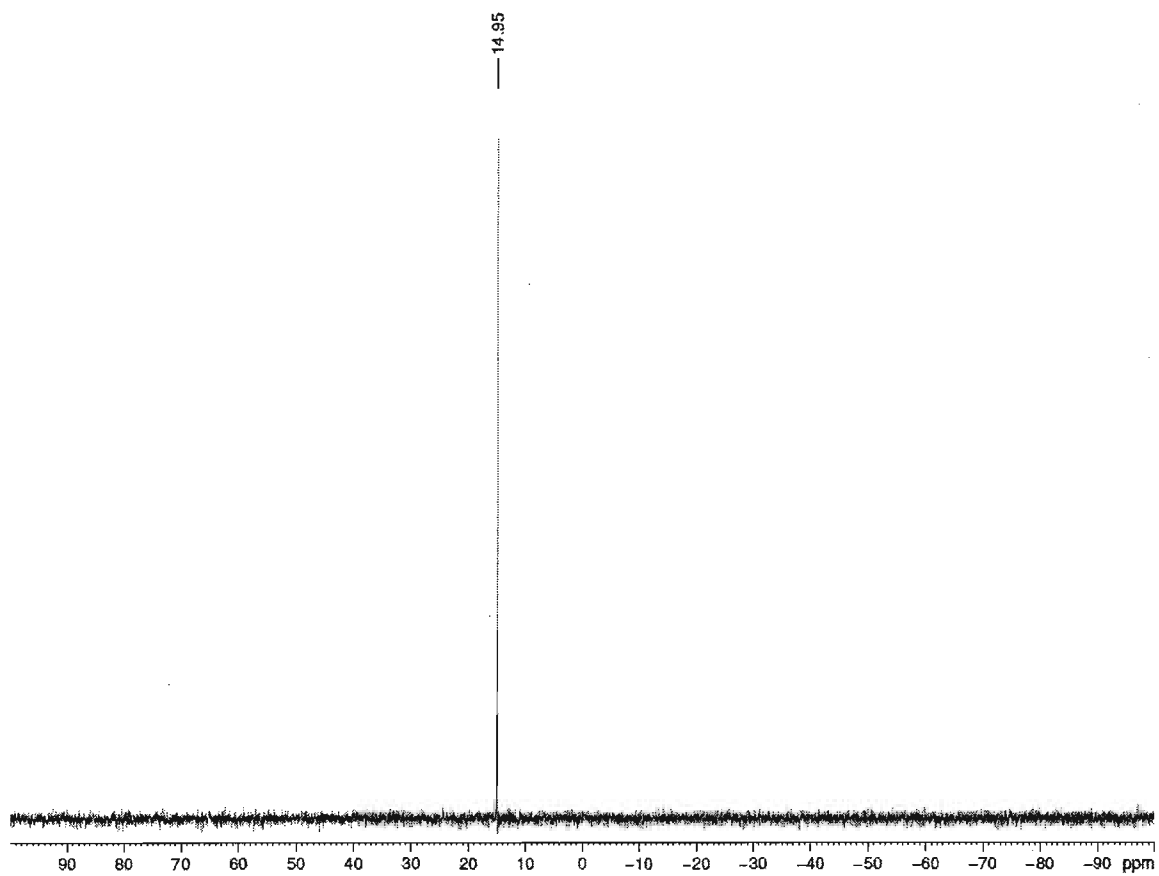
7.717
7.551
7.526
7.453
7.421
7.260

5.038
5.025
4.909
4.900
4.891
4.579
4.568
4.555
4.467
4.408
4.313
4.078
4.065
4.054
4.043
4.031
3.520
3.506
3.127
2.688
2.385
2.377
2.356
2.326
2.299
2.281
2.264
2.239
2.078
2.065
2.048
2.019
2.007
1.925
1.894
1.776
1.760
1.749
1.732



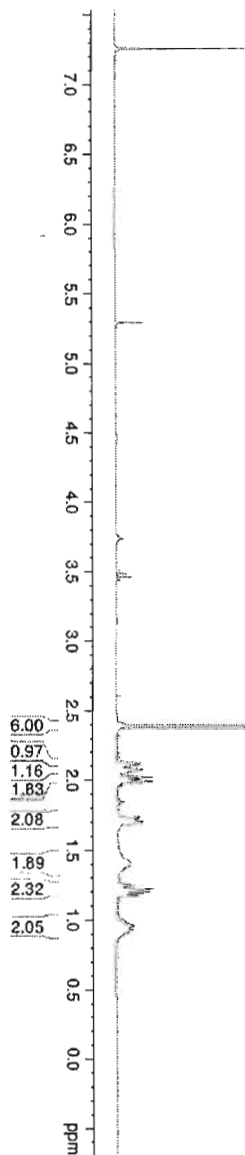
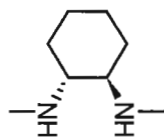
162.19
161.53
160.86
134.95
133.09
132.75
132.60
132.41
132.27
132.24
131.92
131.90
130.12
129.86
129.71
129.52
129.38
129.24
128.85
128.41
128.01
127.20
126.50
124.49
124.19
122.89
119.28
117.63
92.90
92.74
91.47
91.31
77.58
77.16
76.74
74.85
74.77
72.17
70.79
70.03
65.67
60.96
60.65
58.61
58.49
57.76
50.65
32.44
32.40
29.73
29.54





7.260

2.389
2.123
2.113
2.087
2.078
2.031
2.023
2.011
2.005
1.993
1.738
1.729
1.717
1.706
1.699
1.690
1.406
1.282
1.254
1.224
1.212
1.202
1.190
1.185
1.179
0.997
0.989
0.964
0.957
0.931
0.922
0.890



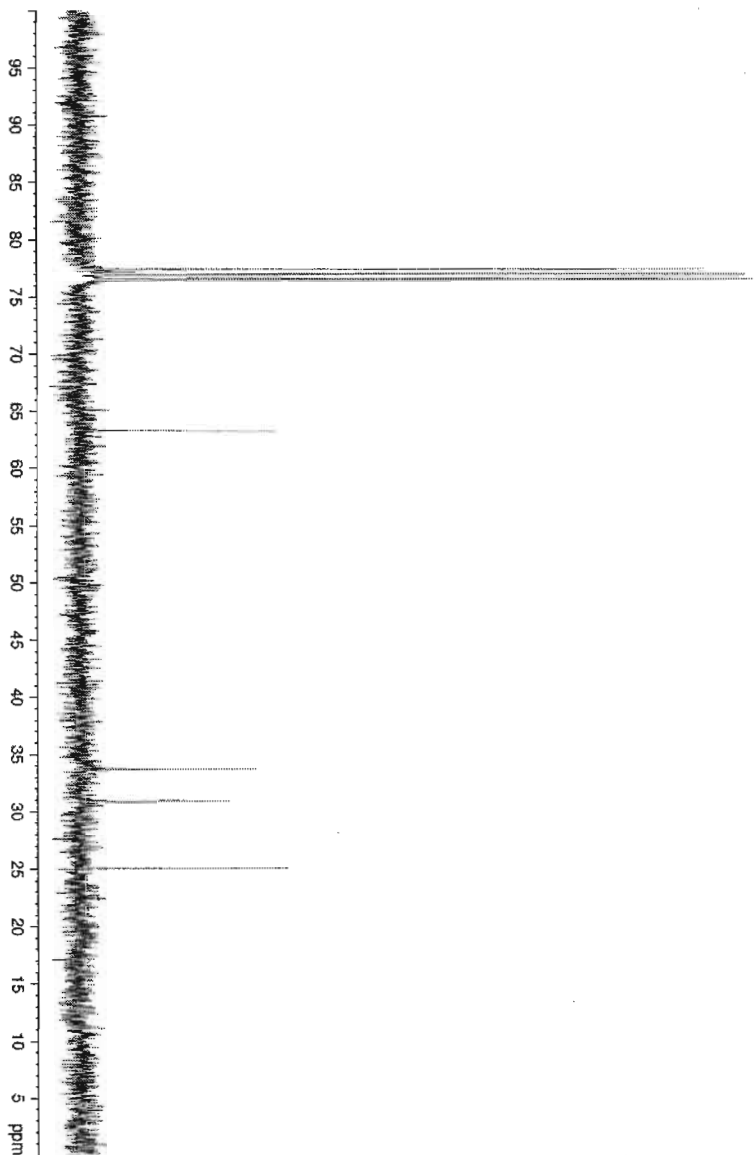
77.43
77.01
76.58

63.33

33.73

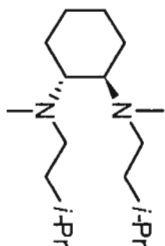
30.92

25.06



7.260

2.561
2.542
2.522
2.498
2.491
2.471
2.445
2.427
2.405
2.392
2.226
1.785
1.776
1.745
1.707
1.699
1.689
1.678
1.614
1.592
1.569
1.547
1.525
1.381
1.360
1.351
1.339
1.329
1.316
1.309
1.286
1.227
1.203
1.180
1.140
1.107
1.081
1.074
0.895
0.890
0.873
0.868



7.5
7.0
6.5
6.0
5.5
5.0
4.5
4.0
3.5
3.0
2.5
2.0
1.5
1.0
0.5
0.0
-0.5
-1.0
ppm

6.47
6.00
4.52
2.21
4.41
3.89
13.35

77.58
77.16
76.74

63.07

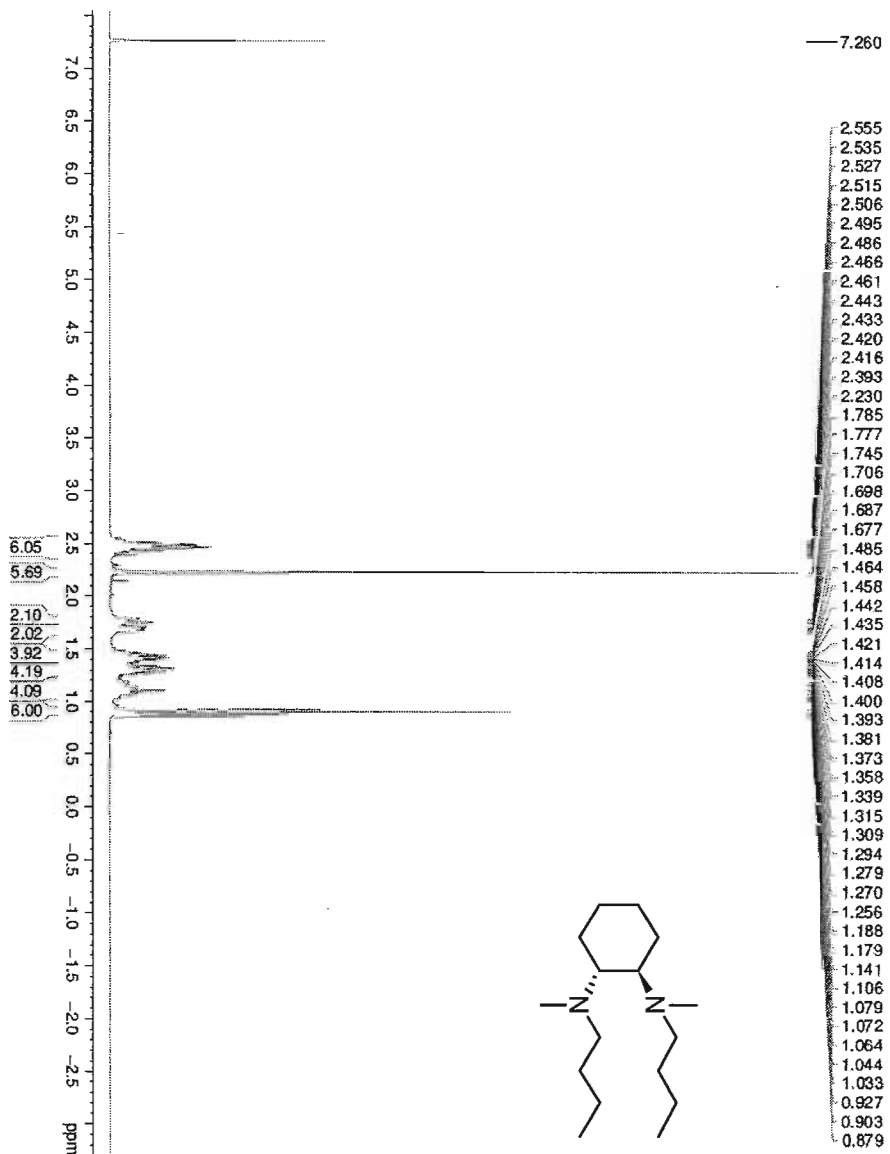
52.78

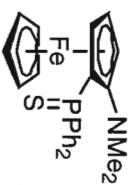
37.85
36.91

26.68
26.07
25.67
23.17
22.91

95
90
85
80
75
70
65
60
55
50
45
40
35
30
25
20
15
10
5
ppm

7.260

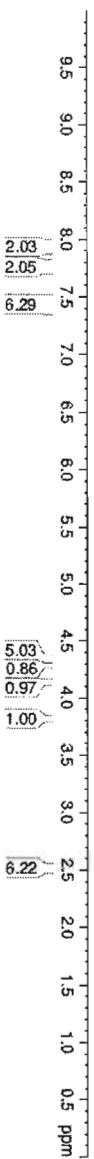




7.960
7.938
7.932
7.915
7.893
7.789
7.785
7.764
7.758
7.741
7.719
7.713
7.463
7.451
7.442
7.426
7.420
7.406
7.396
7.260

4.324
4.146
4.138
4.133
4.124
3.822
3.813
3.808

2.496

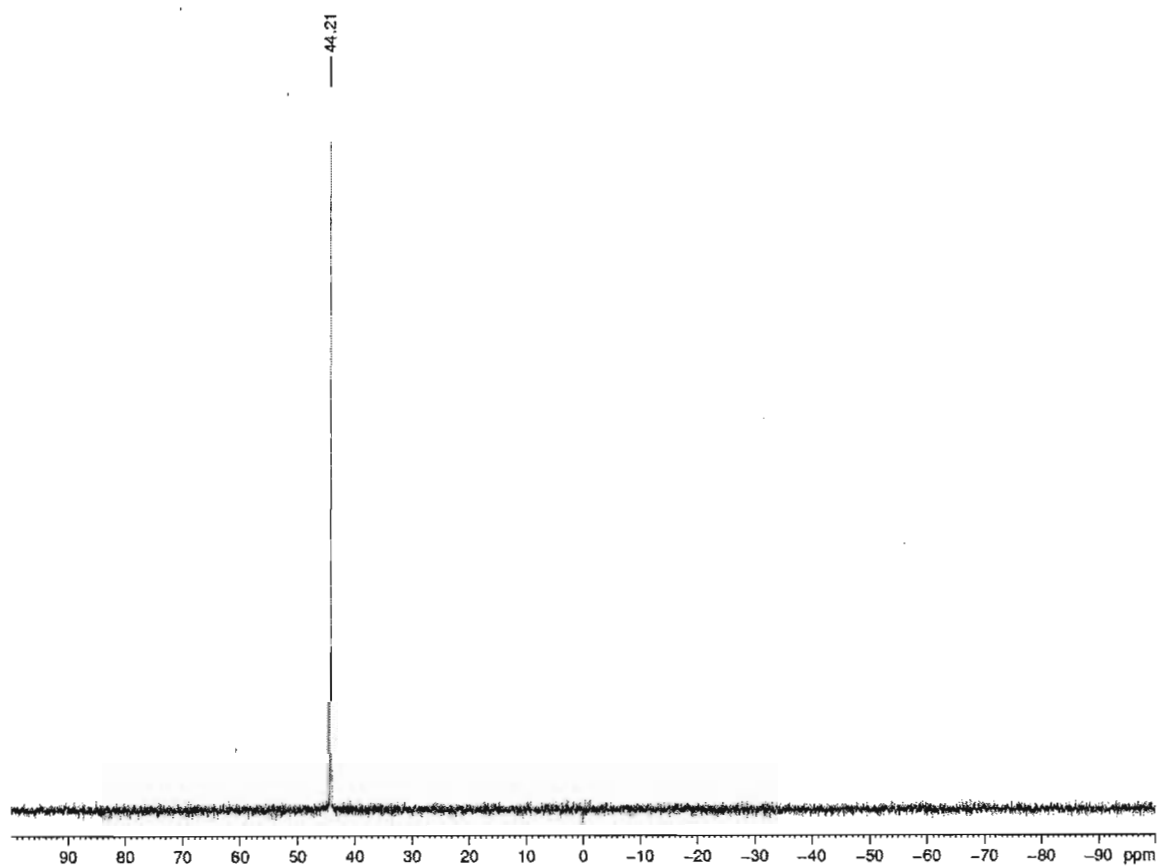


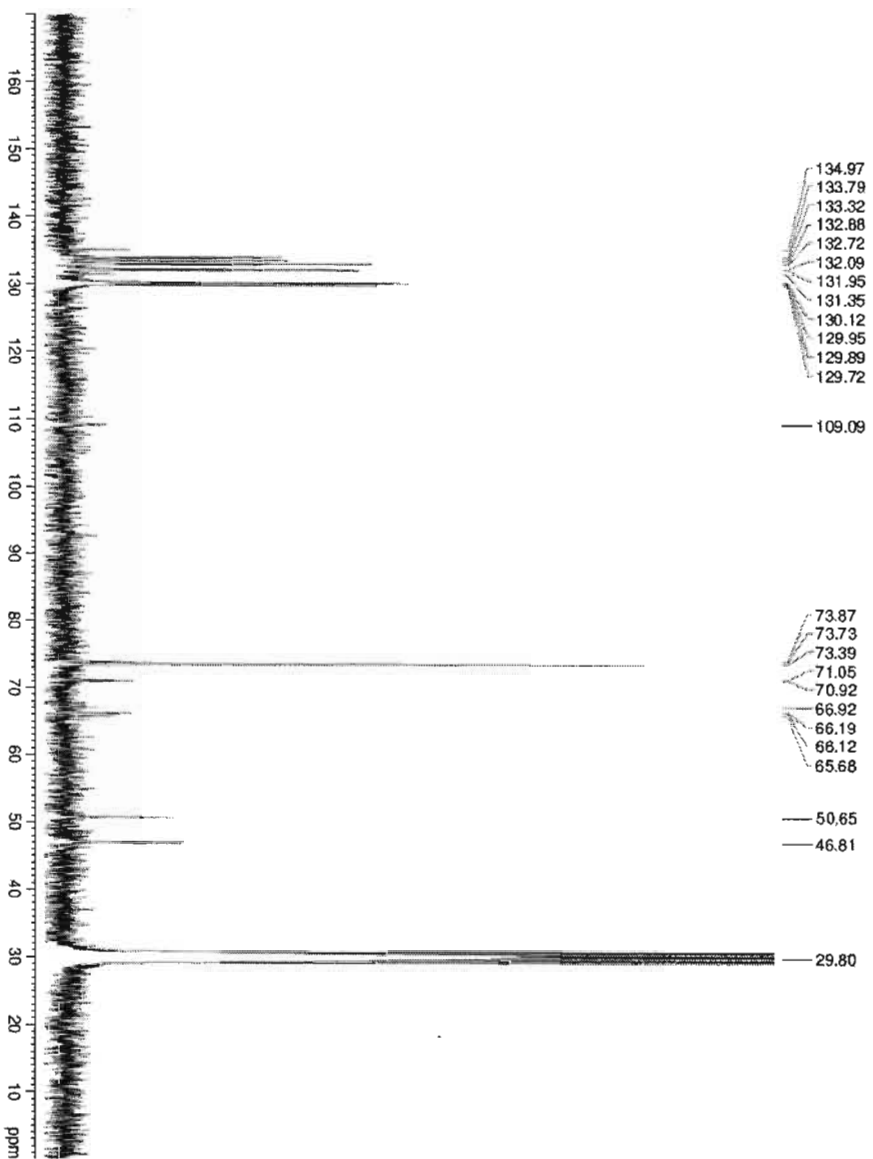
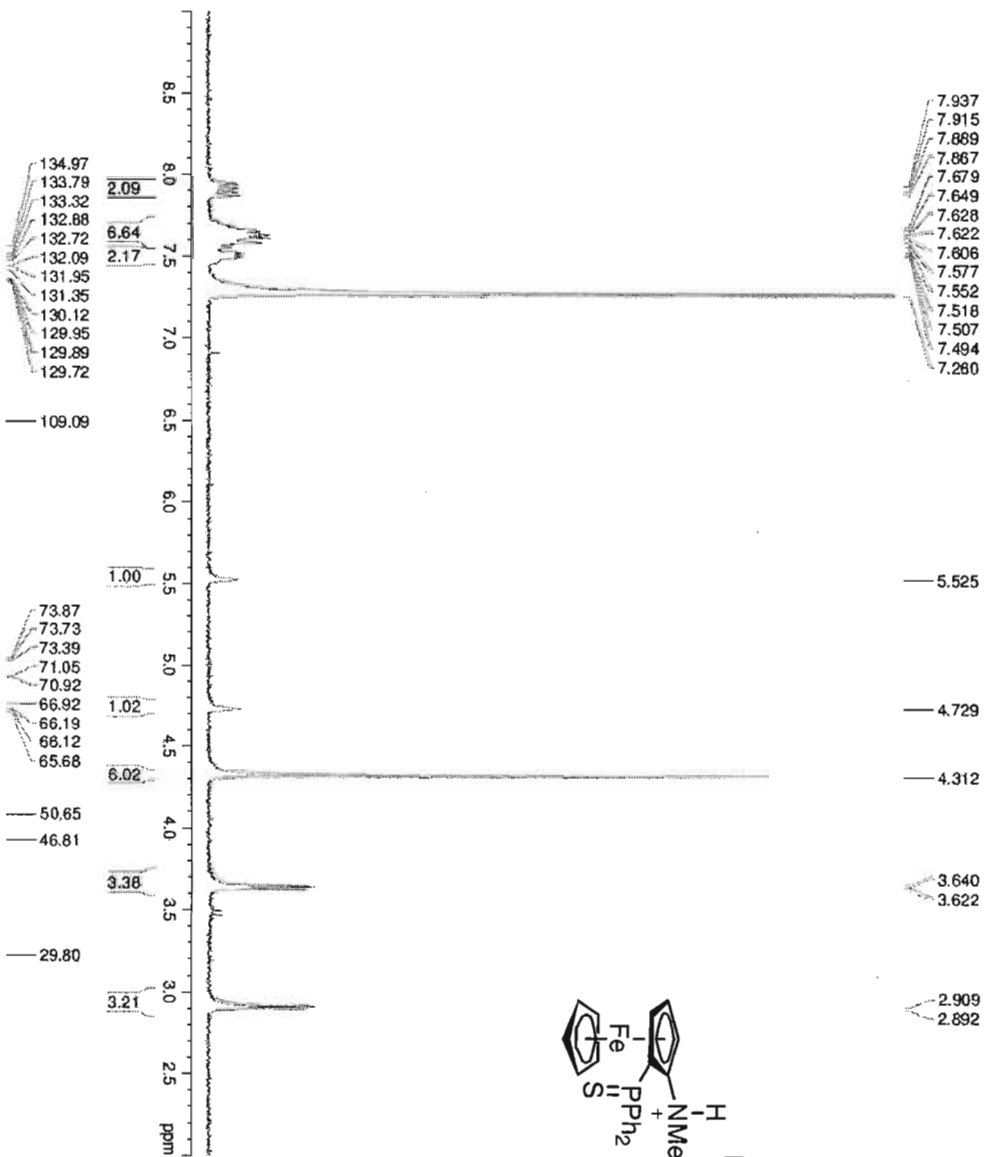
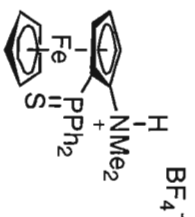
135.90
134.74
134.06
132.91
132.58
132.44
131.81
131.67
131.08
130.78
127.94
127.77

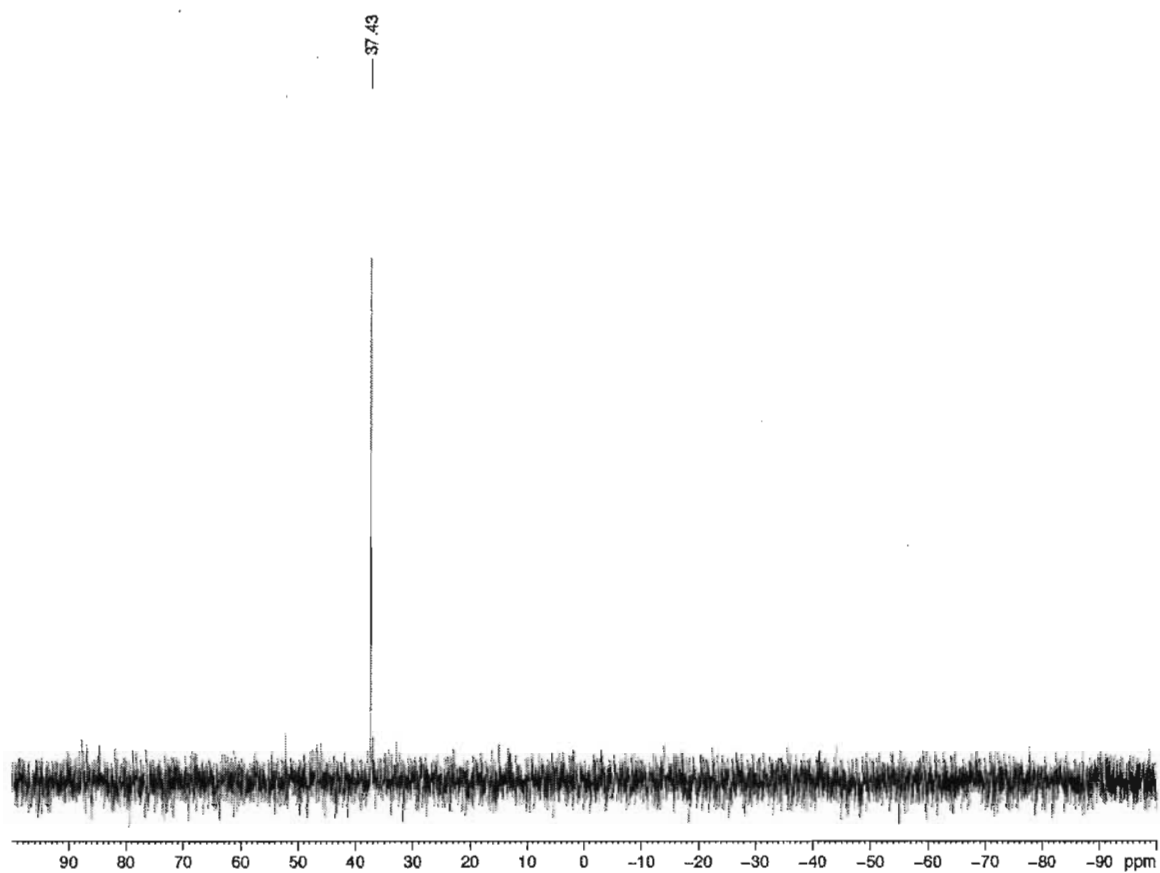
77.42
77.00
76.58
72.36
72.18
69.92
67.68
66.46
65.44
65.30
61.68

46.00





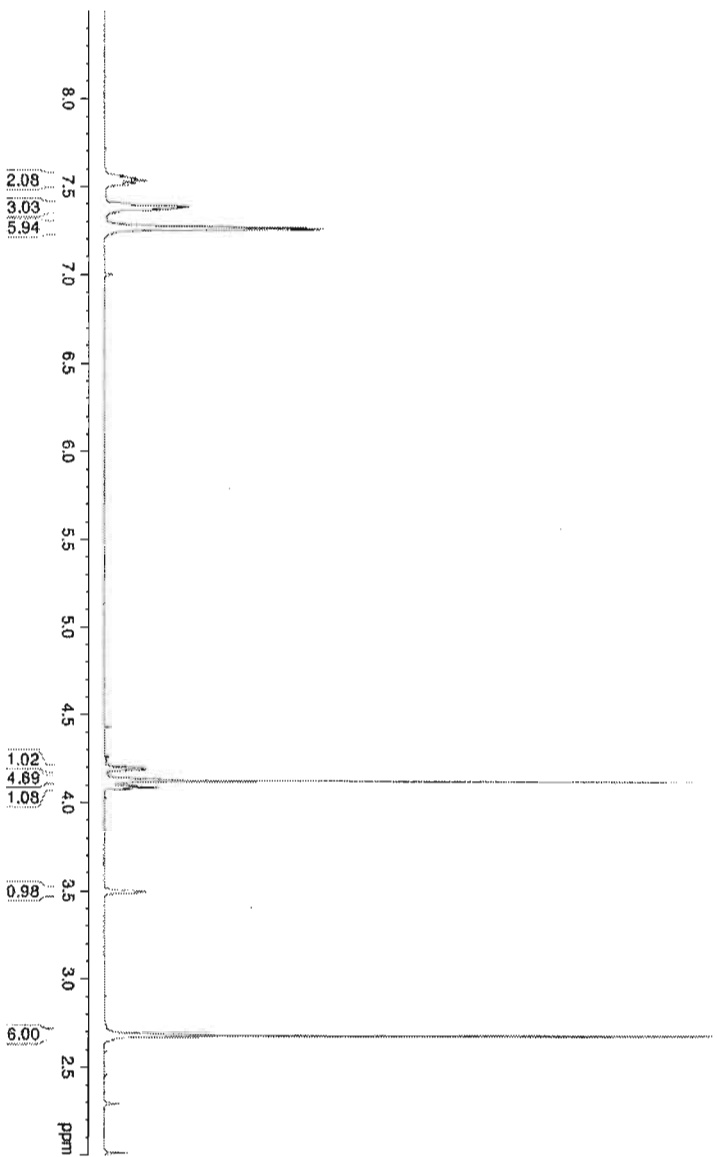




7.566
7.559
7.547
7.540
7.534
7.521
7.509
7.388
7.384
7.379
7.367
7.267
7.260
7.256

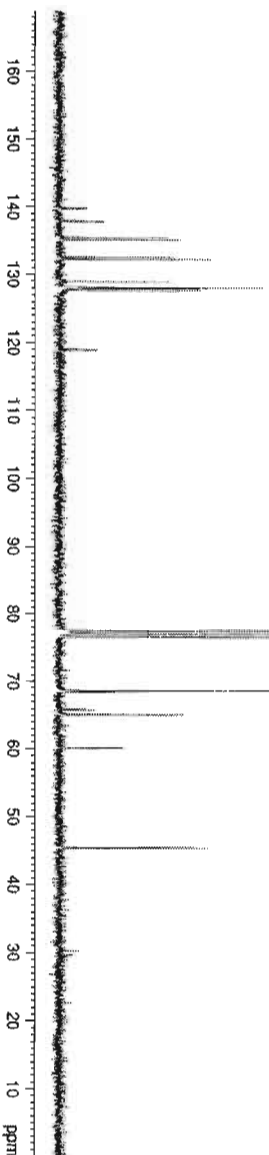
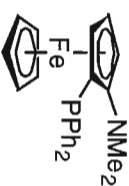
4.200
4.194
4.187
4.181
4.123
4.094
4.085
4.077
3.499
3.494
3.491

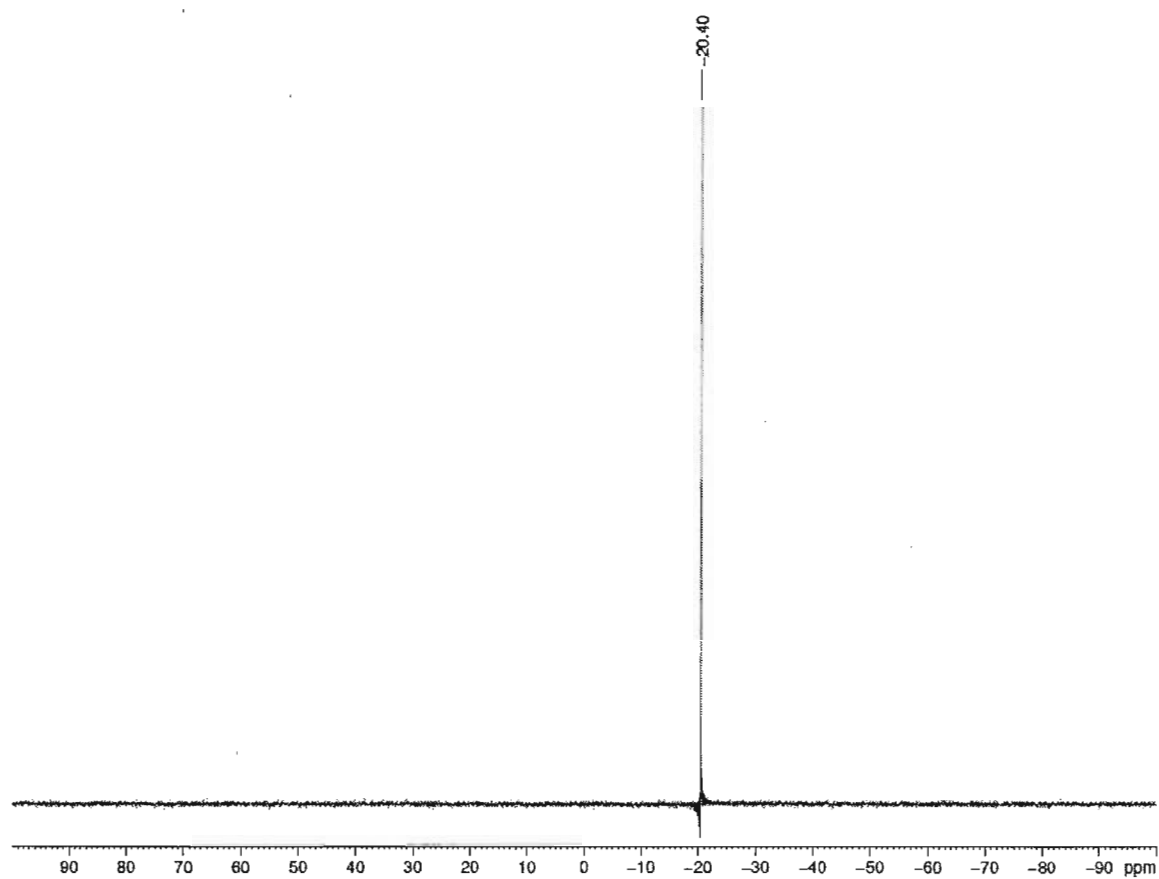
2.681



139.79
139.65
137.92
137.77
135.38
135.09
132.49
132.25
128.98
128.07
128.00
127.91
127.72
119.02
118.78

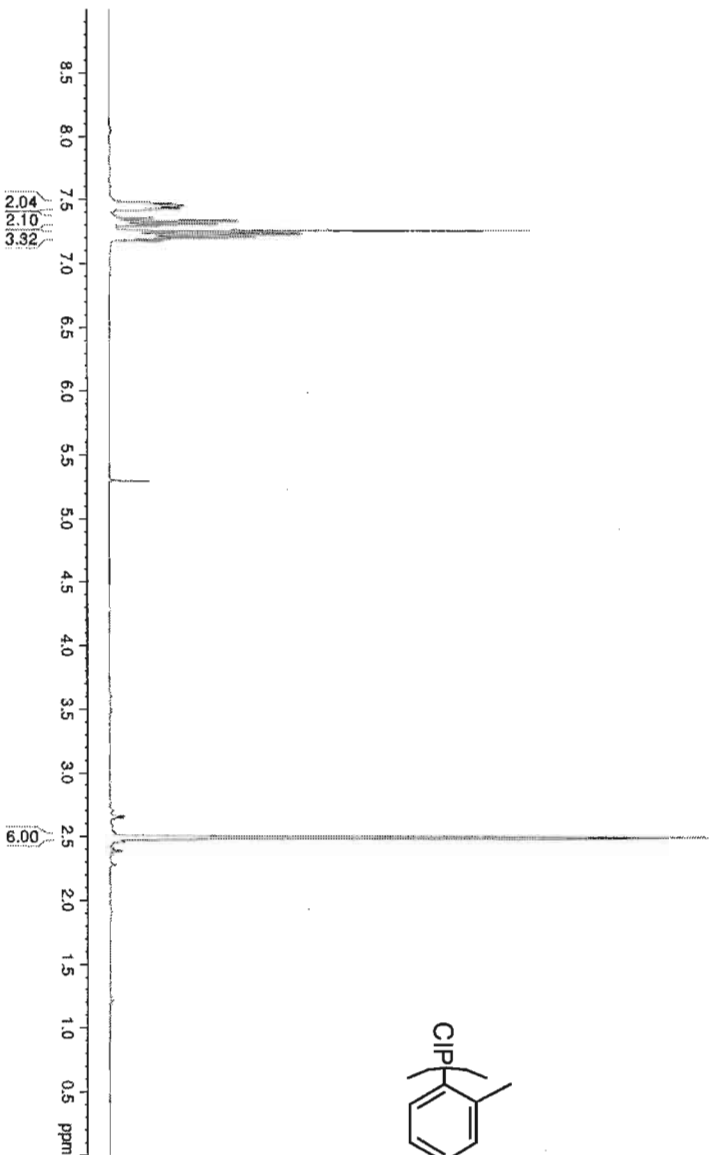
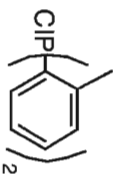
77.42
77.00
76.58
68.62
68.49
68.44
65.94
65.60
65.12
60.13
60.09
45.50
45.38





7.475
7.458
7.451
7.437
7.363
7.339
7.314
7.260
7.237
7.215
7.192

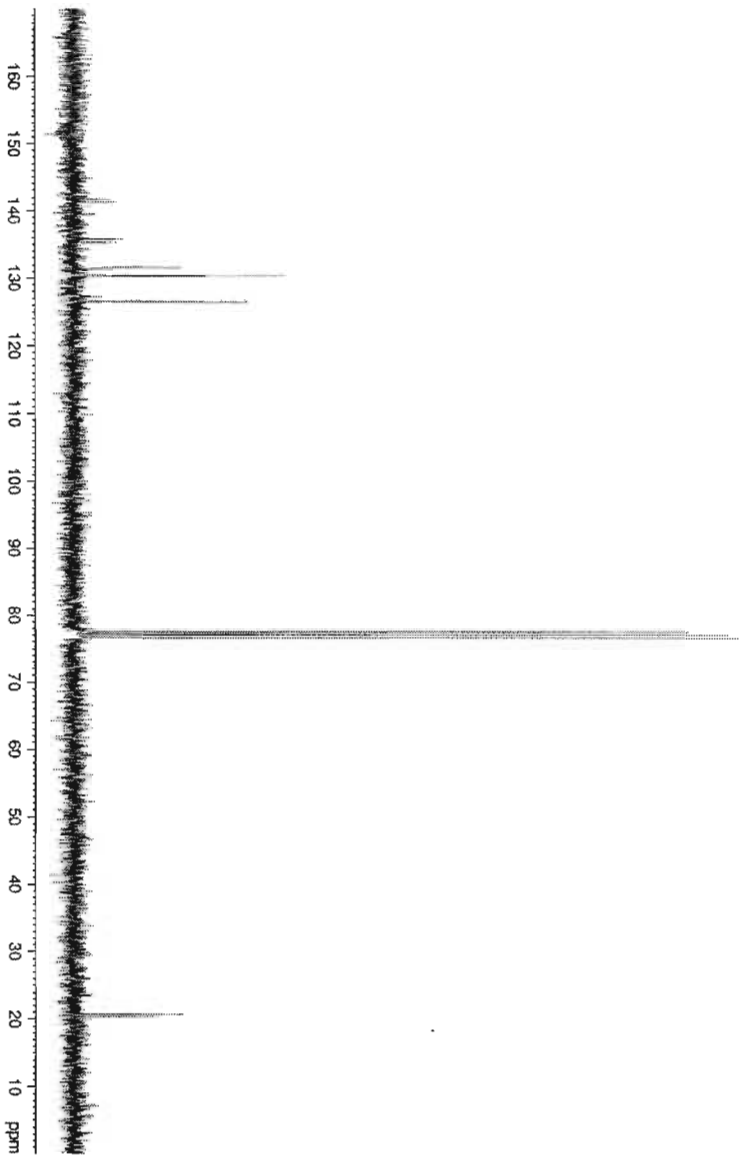
2.495
2.488

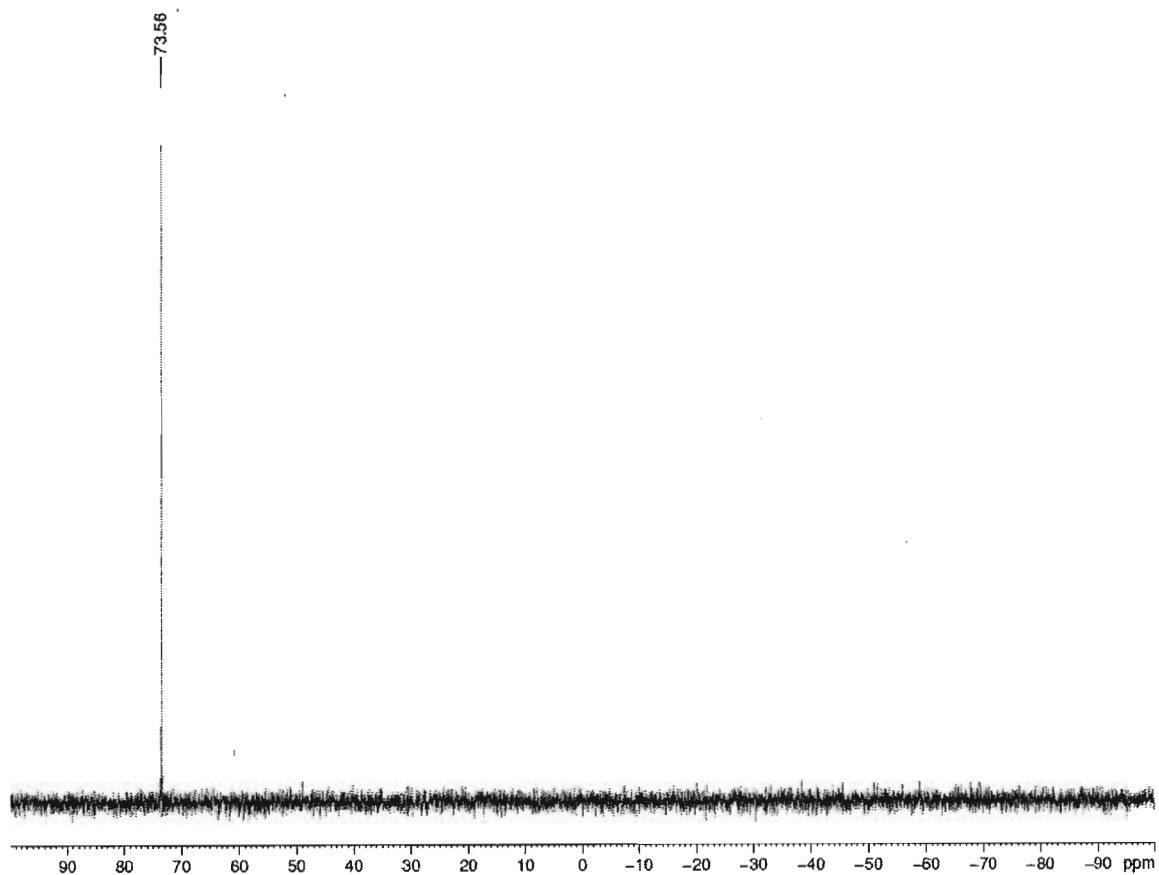


141.71
141.30
135.78
135.31
131.56
131.52
130.38
130.36
130.31
126.48

77.44
77.02
76.59

20.72
20.40





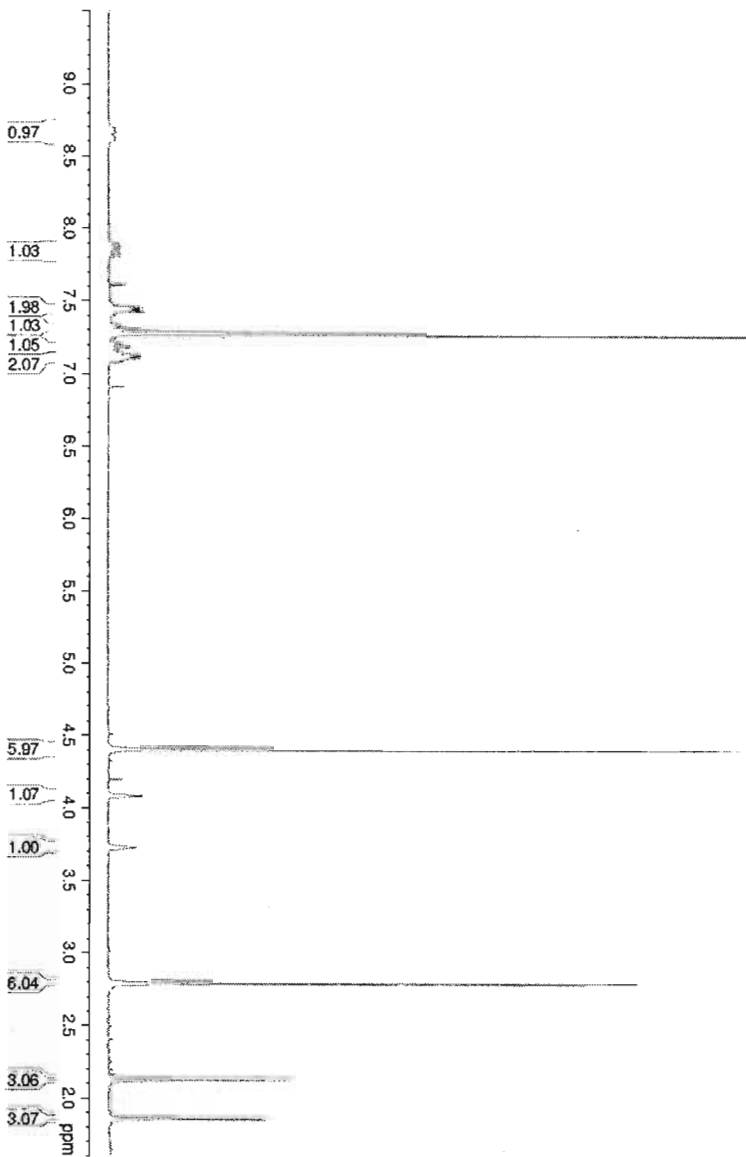
8.691
8.661
8.631
8.605
7.880
7.854
7.828
7.803
7.451
7.445
7.439
7.432
7.428
7.421
7.328
7.323
7.318
7.303
7.298
7.293
7.260
7.200
7.175
7.151
7.133
7.117
7.104
7.079

4.396
4.090
4.086
4.082
4.077
4.073
4.069
3.738
3.732
3.727
3.723
3.718
3.713

2.789

2.119

1.852

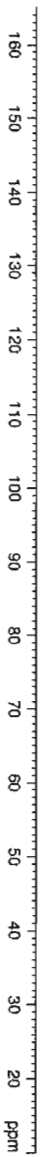
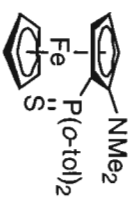


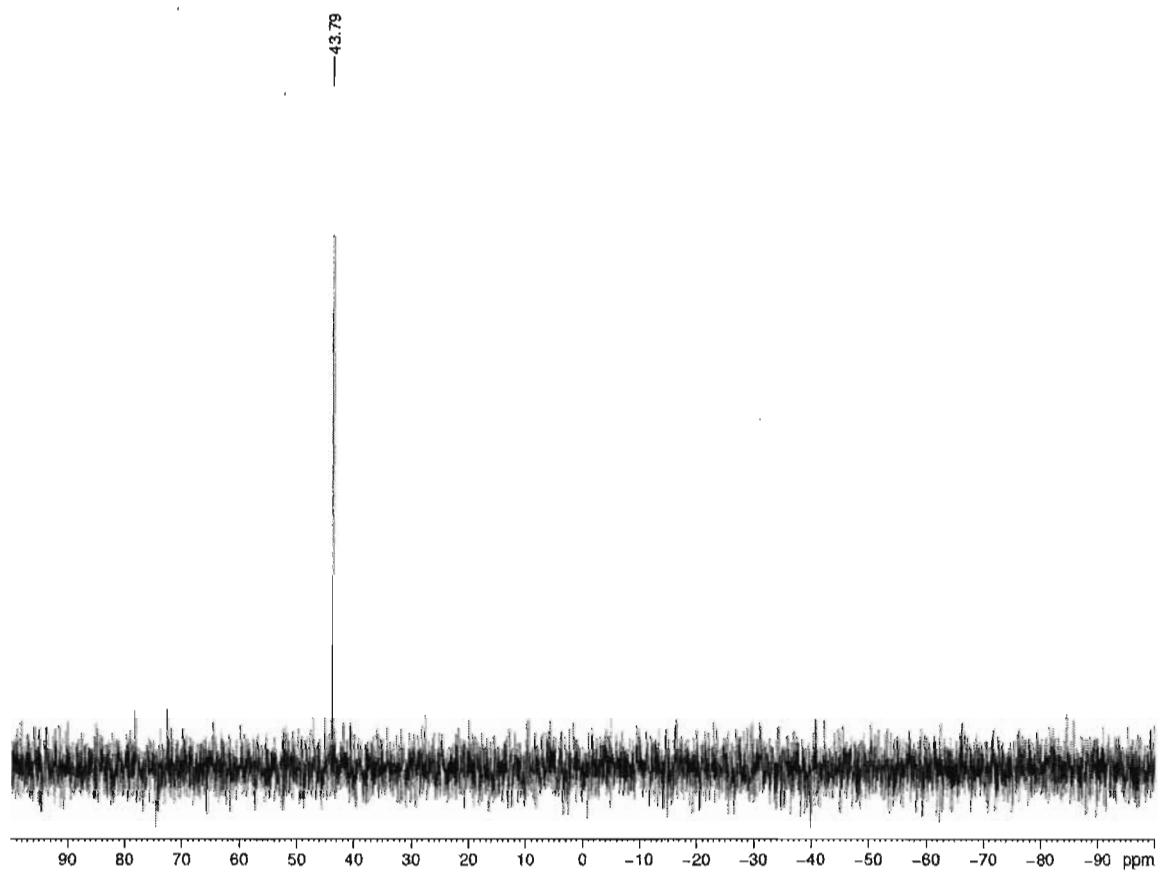
141.37
141.23
140.54
140.43
134.82
134.64
134.22
133.09
132.79
132.63
131.85
131.71
131.59
131.52
131.39
130.88
130.64
126.11
125.93
125.59
125.42
117.92
117.81

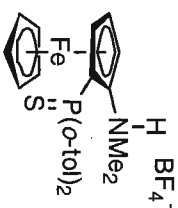
77.43
77.01
76.58
72.07
71.89
69.82
66.21
65.83
65.00
64.85
64.19
64.08

46.67

22.56
22.51
21.49
21.42







11.599

8.837
8.790

7.817
7.460
7.436
7.412
7.260
7.051
7.027
7.001
6.974

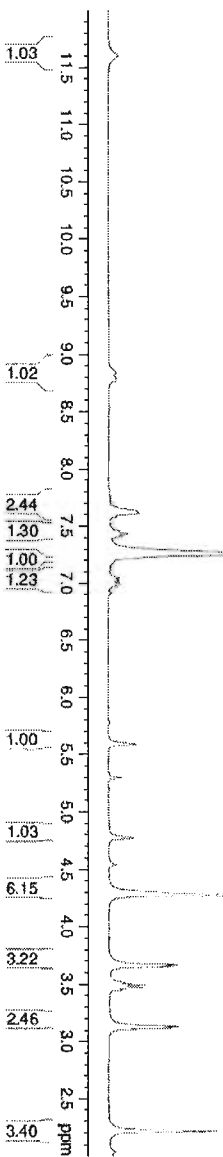
5.590

4.776

4.277

3.666
3.650
3.515
3.493
3.470
3.448
3.134
3.119

2.214

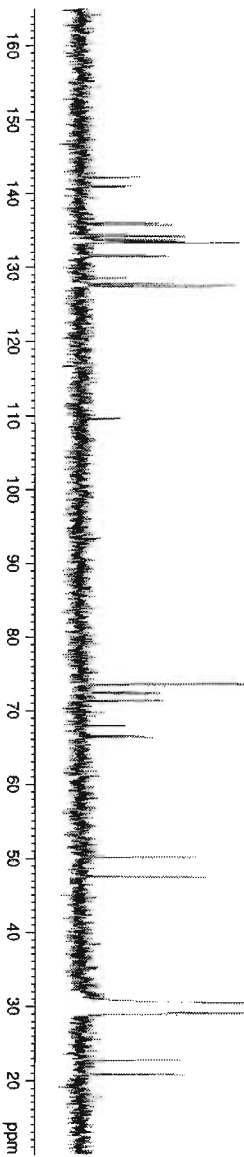


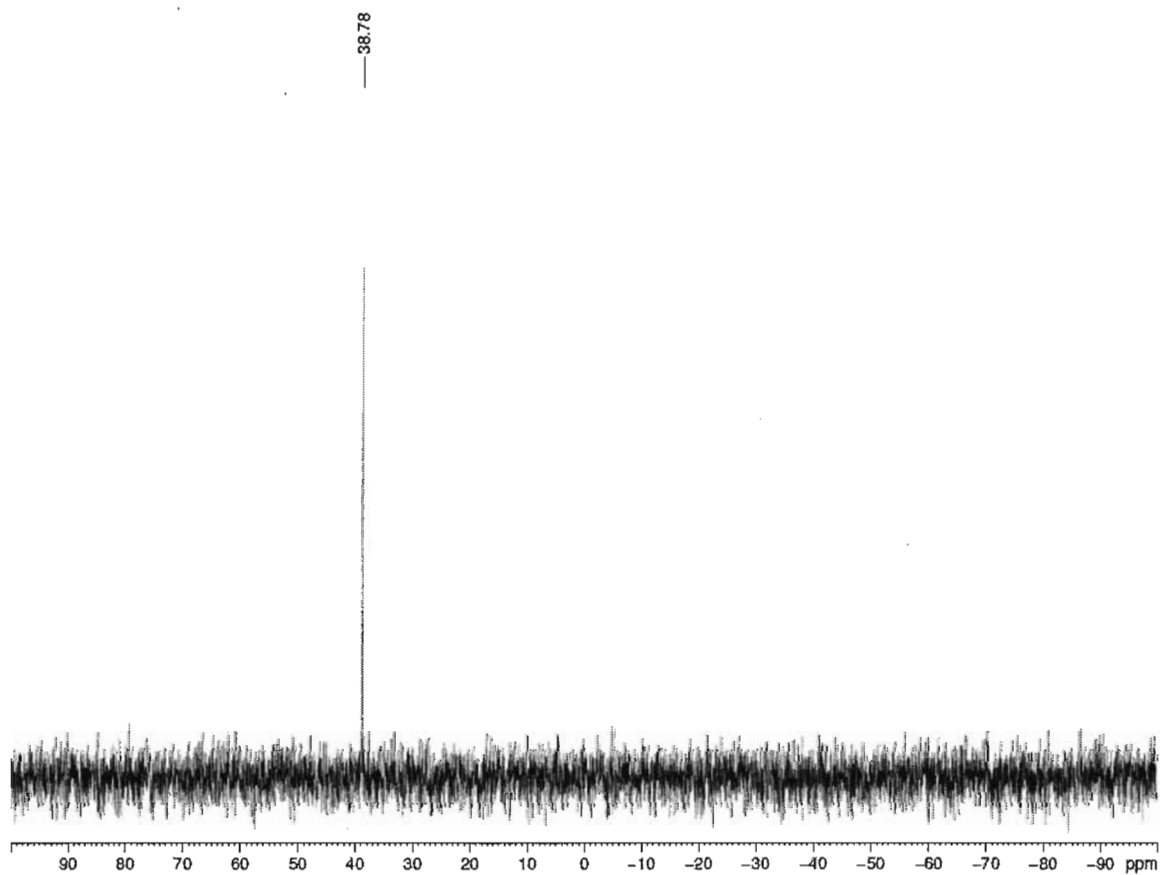
142.16
142.02
141.00
140.88
135.94
135.74
134.44
134.20
134.16
133.71
133.57
133.51
133.39
133.36
131.64
131.49
128.52
127.81
127.61
127.44
109.66
109.53

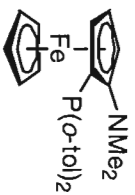
73.57
72.49
72.37
71.38
71.25
69.78
69.22
67.92
66.67
66.50
66.41

50.19
47.56

29.84
22.81
22.77
20.92
20.84







7.261
7.155
7.135
7.130
7.111
7.106
7.090
7.066
7.045
7.035
7.030
7.024
6.999
6.978
6.965
6.955
6.949
6.941

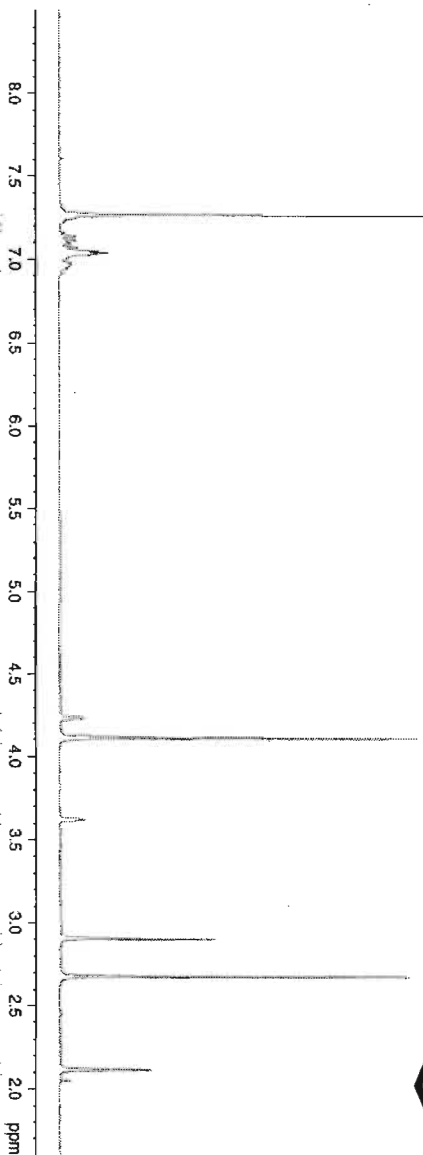
4.236
4.230
4.227
4.223
4.217
4.107

3.620

2.900

2.672

2.115
2.111

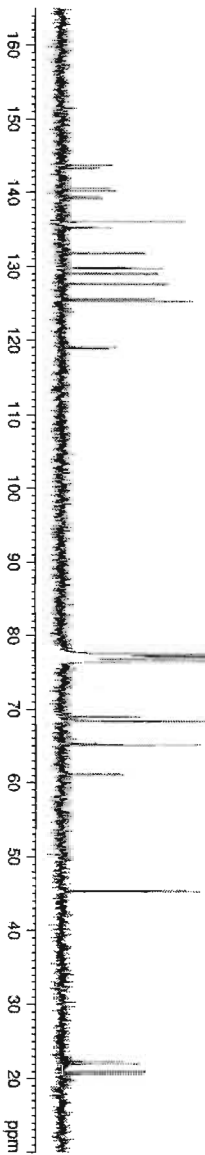


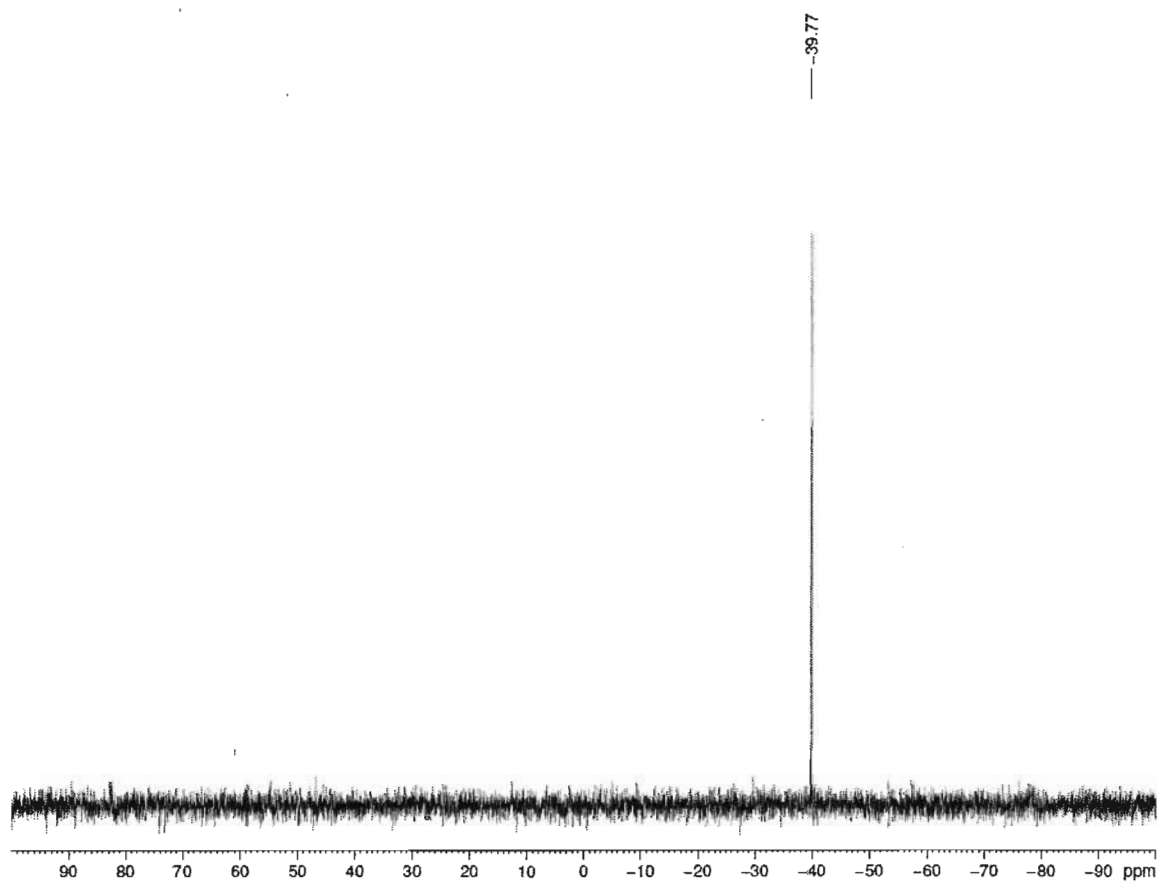
143.62
143.23
140.51
140.19
139.39
139.20
136.00
135.28
135.14
131.77
129.81
129.72
129.66
129.01
127.54
125.54
125.34
119.10
118.86

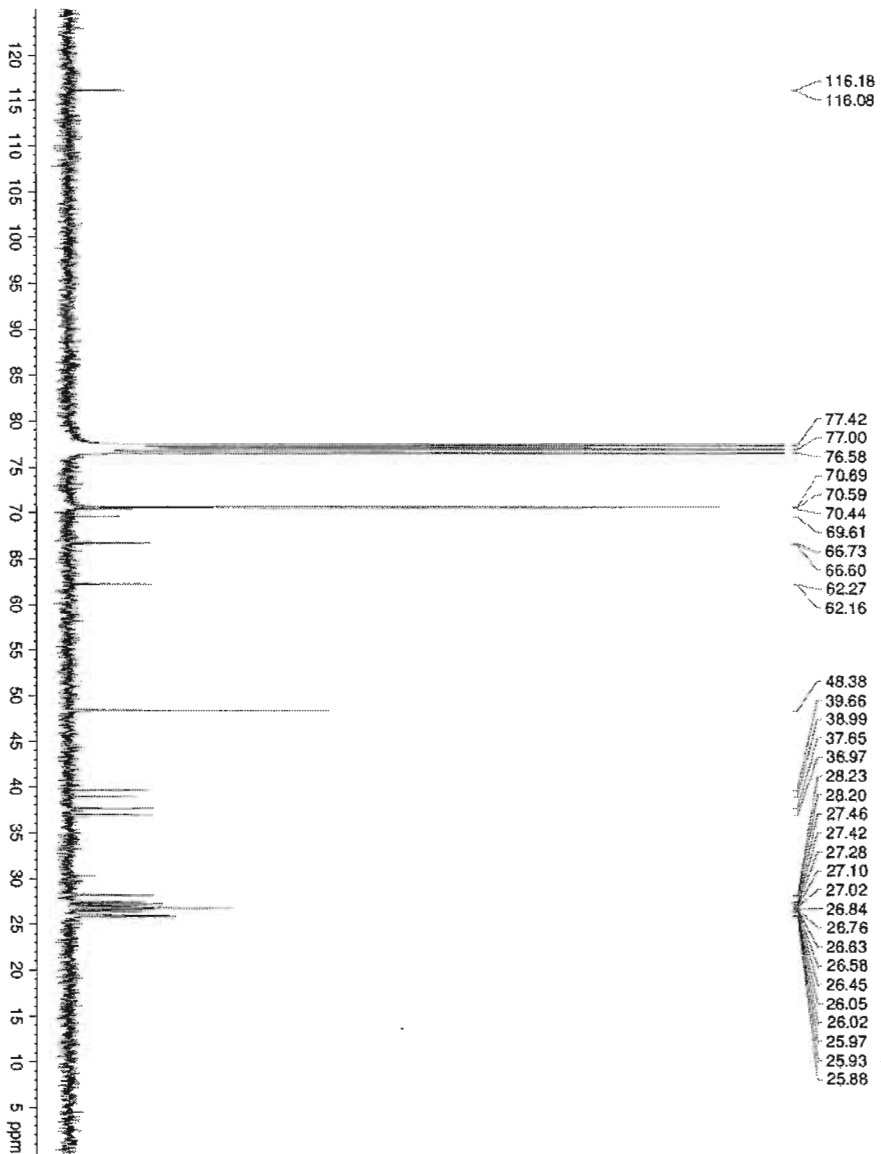
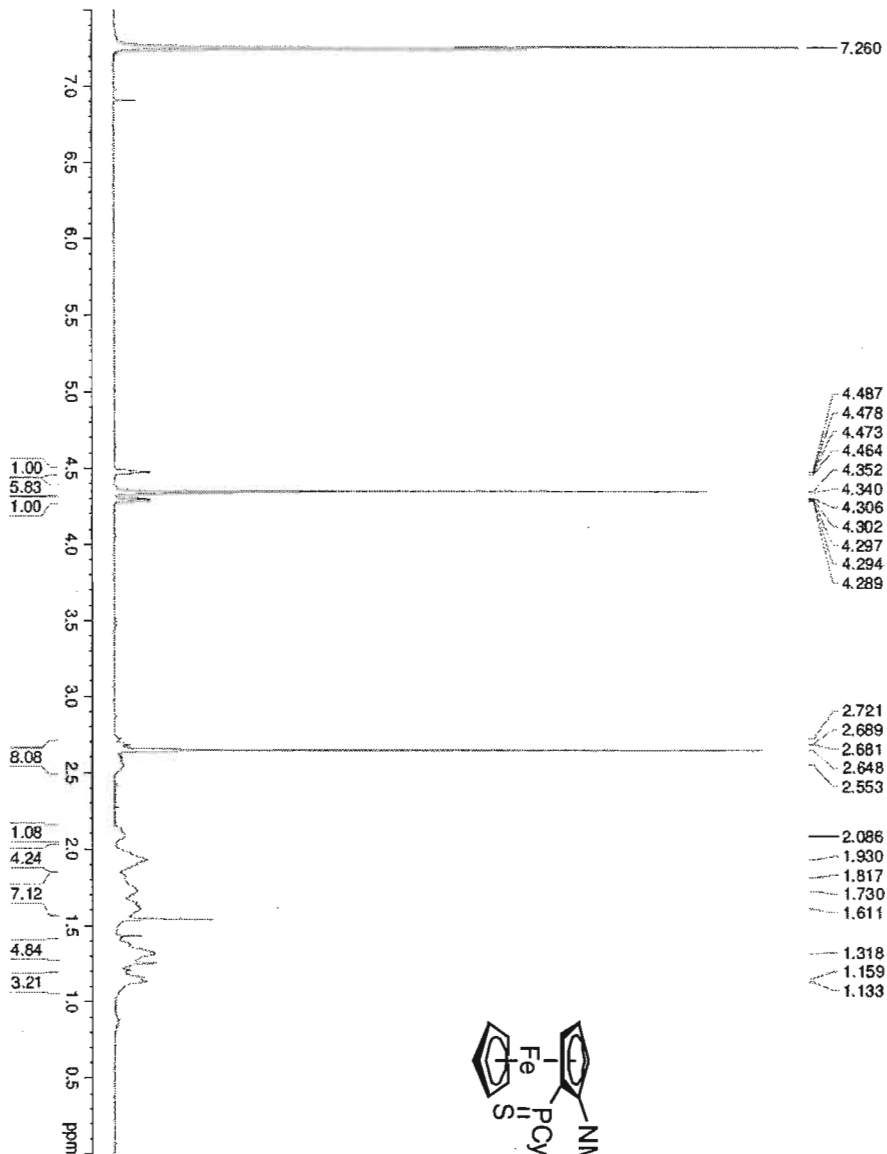
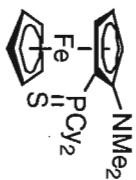
77.42
77.00
76.58
69.00
68.96
68.38
65.33
65.17
65.13
61.16
61.13

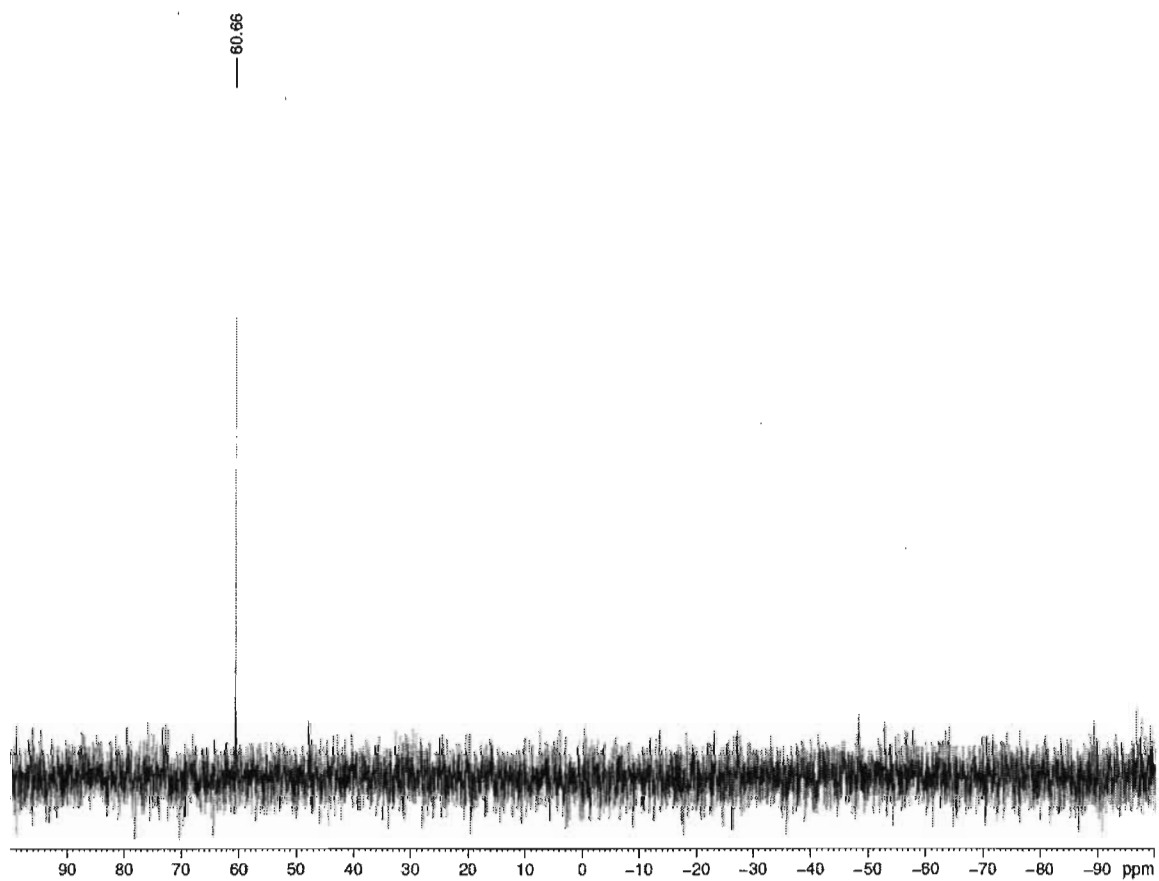
45.38
45.26

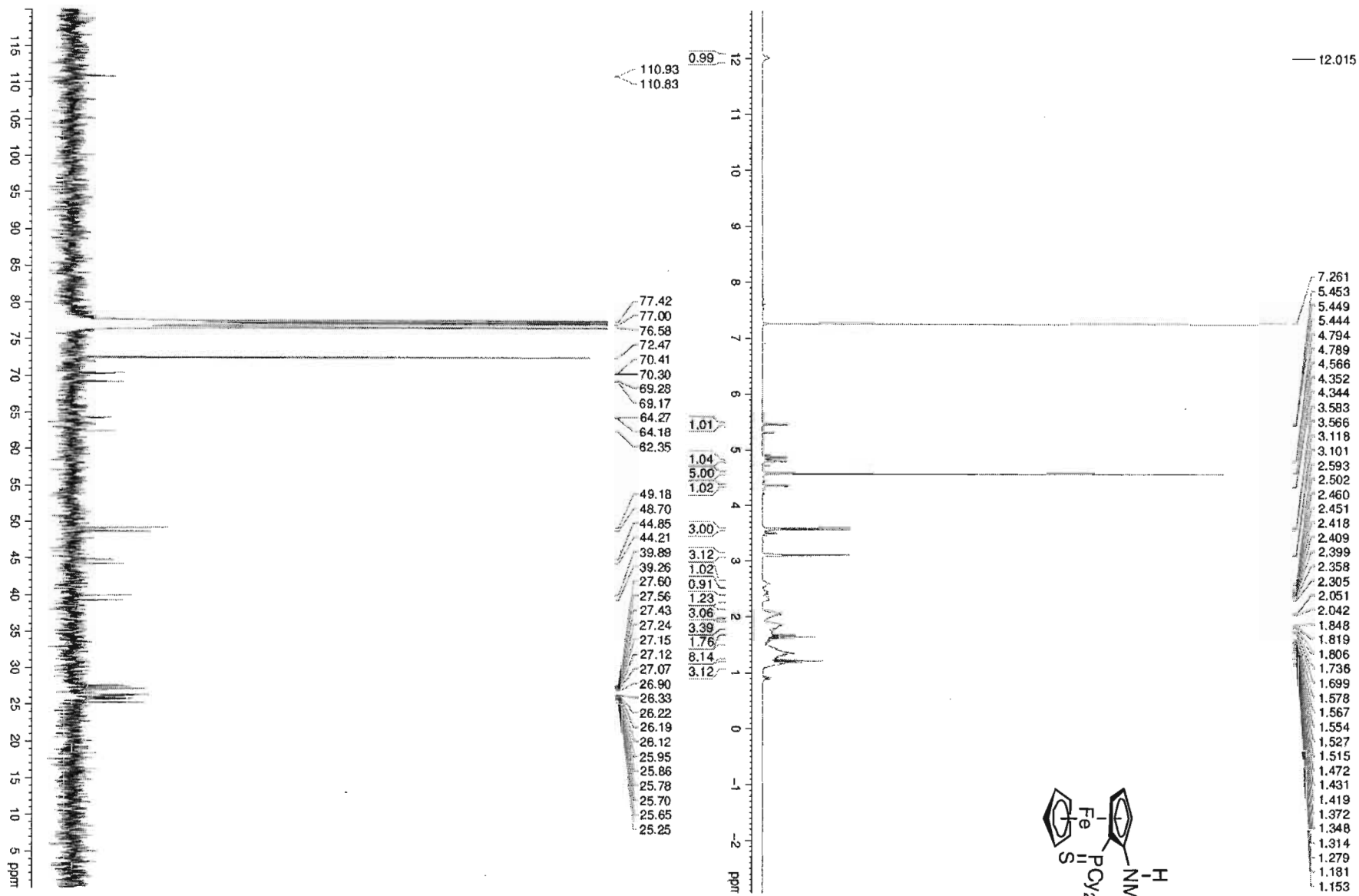
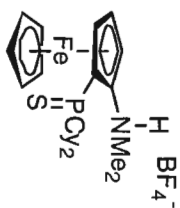
22.30
21.97
20.92
20.66

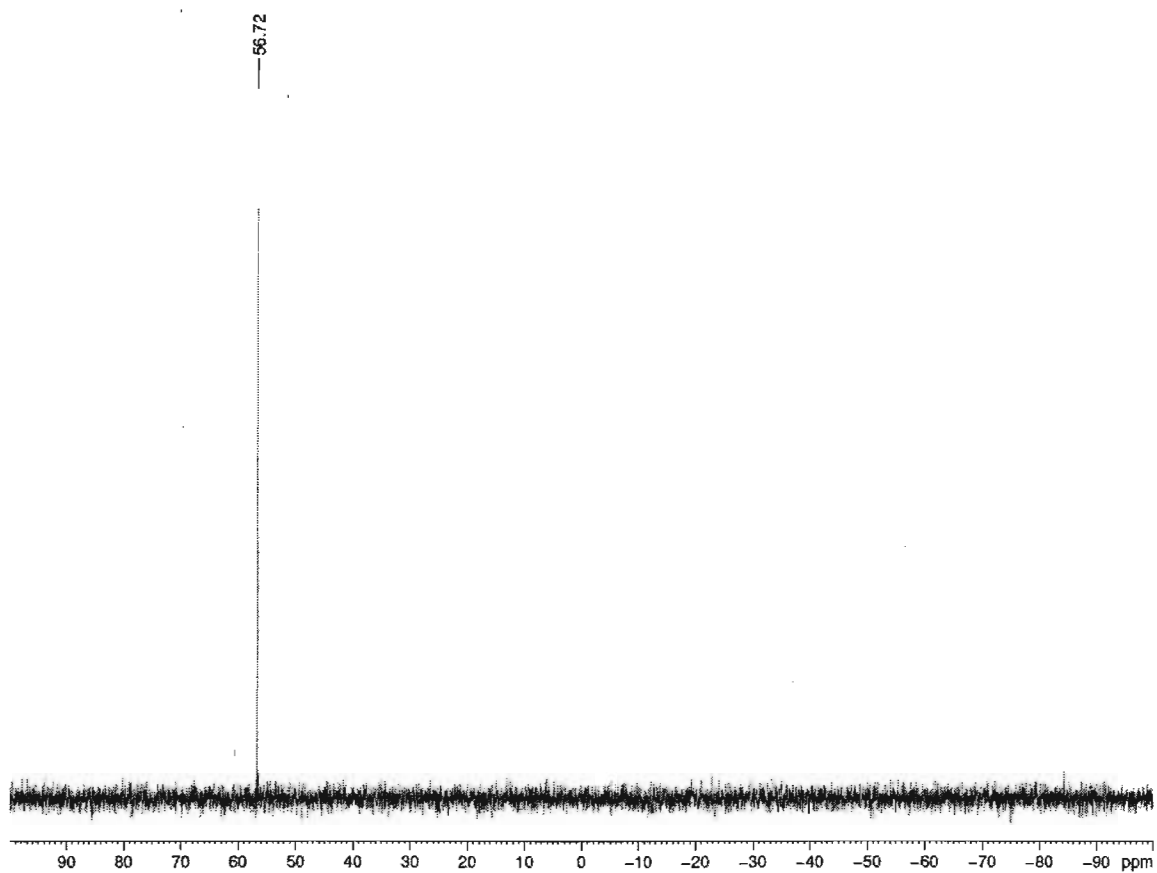






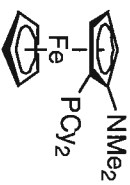






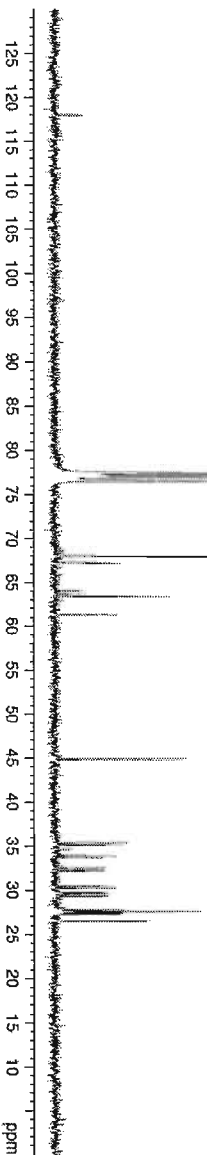
7.260

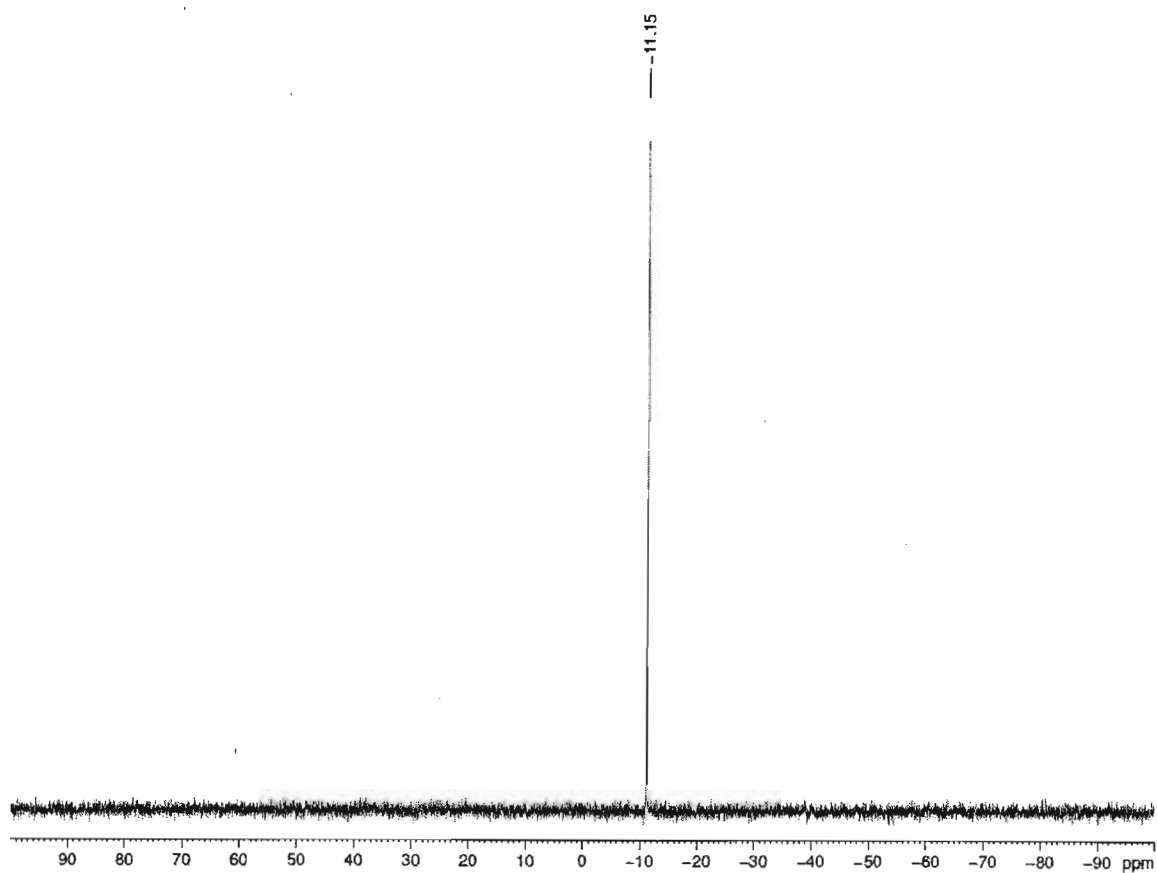
4.233
4.096
4.092
4.044
4.036
4.028
3.905
3.900
2.748
2.430
2.396
1.879
1.852
1.731
1.686
1.646
1.623
1.611
1.584
1.588
1.544
1.533
1.469
1.432
1.421
1.385
1.338
1.308
1.256
1.209
1.185
1.170
1.130
1.090



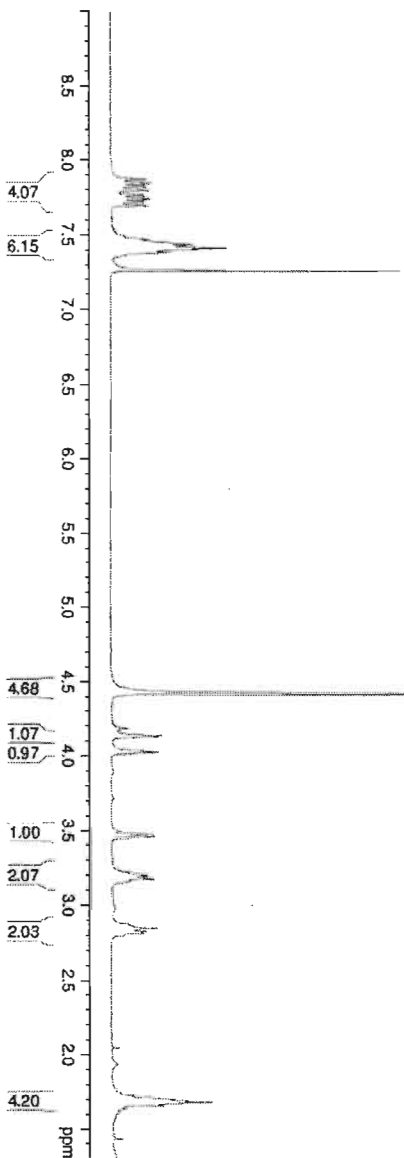
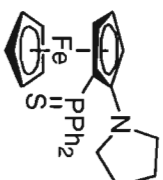
118.14
117.96

77.42
77.00
76.58
67.92
67.23
67.18
64.02
63.71
63.40
61.31
61.28
44.94
44.78
35.30
35.11
33.83
33.68
32.46
32.21
30.41
30.22
29.72
29.58
29.39
29.30
27.75
27.59
27.50
27.41
27.37
27.27
26.54
26.43

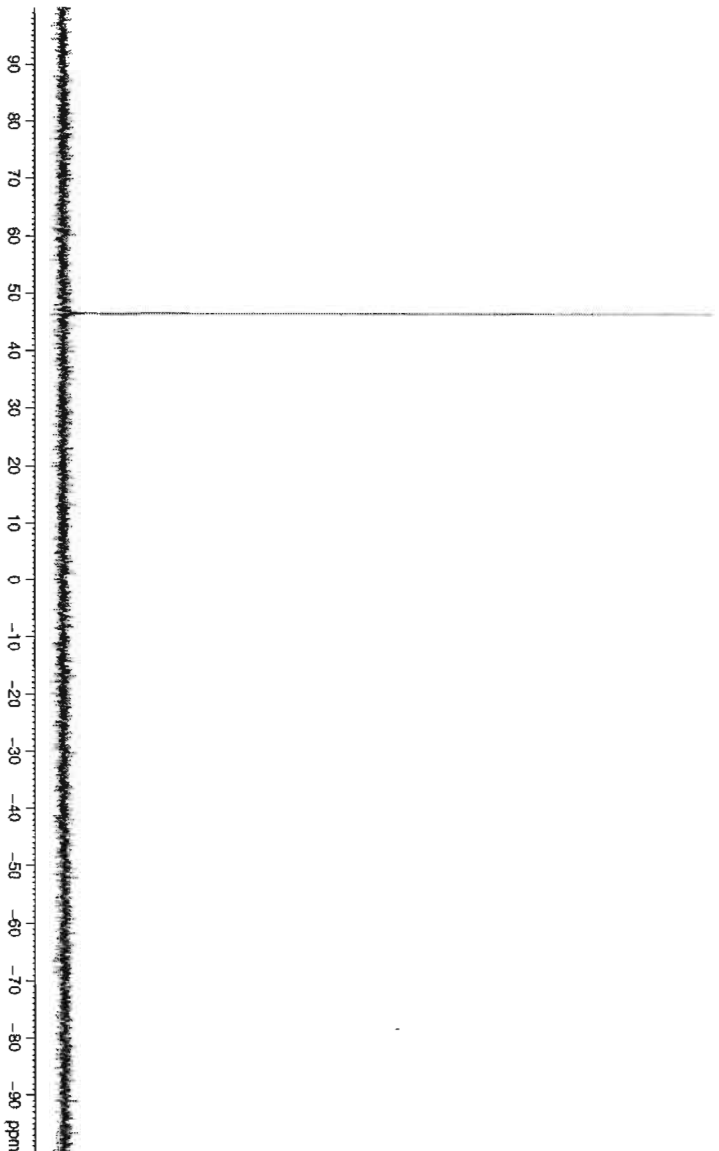


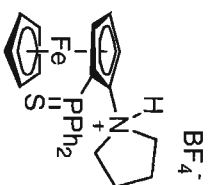


7.865
7.861
7.839
7.834
7.820
7.816
7.794
7.789
7.763
7.759
7.738
7.732
7.719
7.715
7.693
7.688
7.483
7.470
7.463
7.453
7.447
7.440
7.435
7.425
7.418
7.411
7.401
7.395
7.385
7.377
7.364
7.356
7.260
4.416
4.142
4.136
4.129
4.122
4.036
4.027
4.023
3.471
3.462
3.457
3.447
3.221
3.203
3.192
3.173
3.158
3.149
2.872
2.848
2.826
2.818
1.723
1.698
1.689
1.682
1.659



— 46.45





11.009

8.069
8.057
8.048
8.036
7.769
7.763
7.723
7.696
7.683
7.661
7.636
7.557

5.409

4.886

4.577

4.488

4.419

4.109

3.555

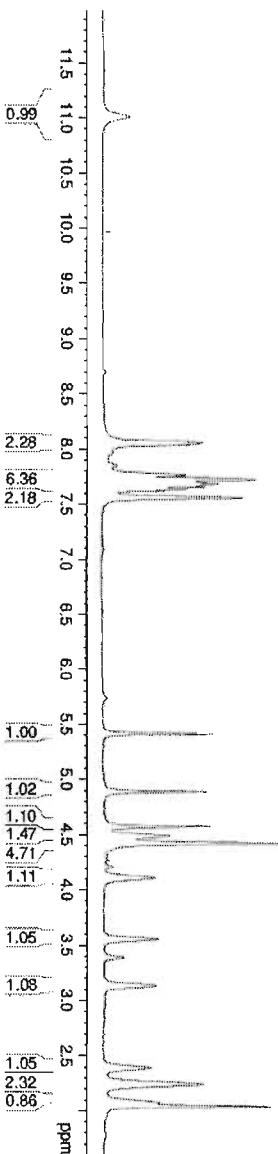
3.135

2.394

2.244

2.074

2.040

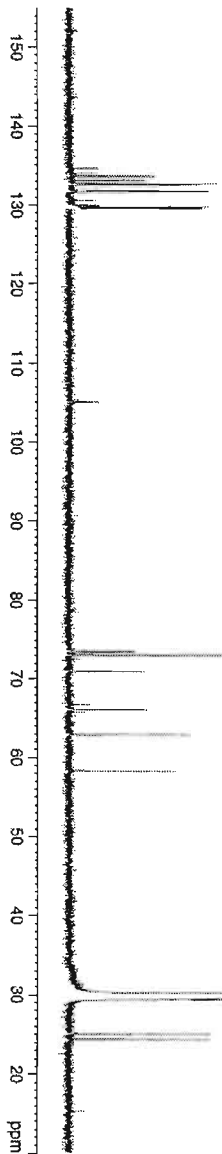


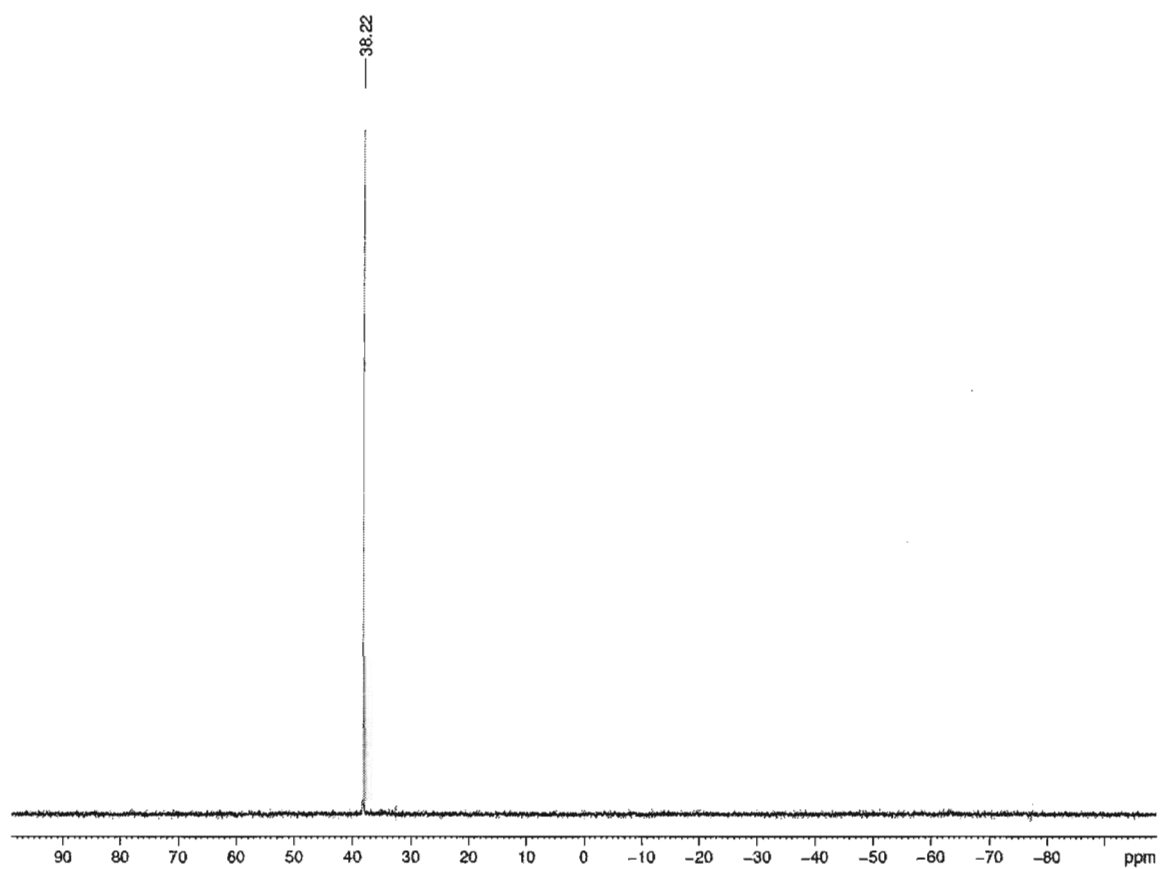
134.59
134.00
133.63
133.10
132.69
132.61
131.79
131.72
130.57
129.98
129.84
129.76
129.65
129.57

105.07
105.00

73.51
73.45
73.08
70.99
70.93
66.76
66.11
66.07
62.88
58.33

29.80
25.12
24.45



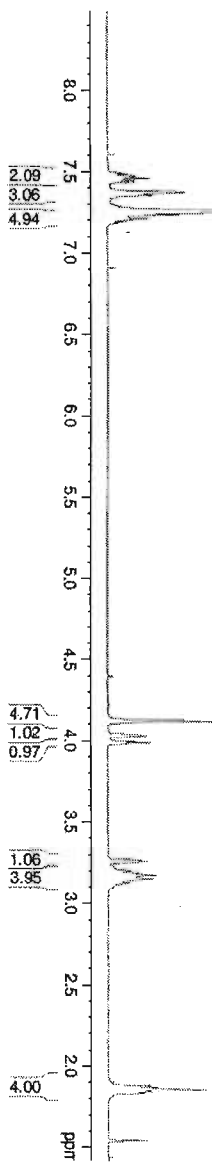
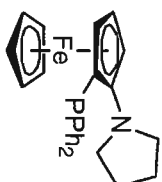


7.492
7.484
7.472
7.467
7.459
7.447
7.434
7.375
7.370
7.353
7.260
7.251
7.235
7.213
7.203
7.188
7.181

4.120
4.027
4.022
3.995
3.987
3.979

3.258
3.197
3.182
3.173
3.149
3.124
3.096

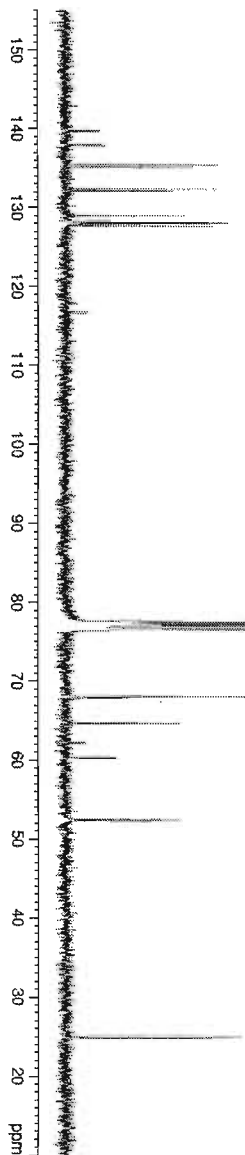
1.900
1.878
1.867
1.844
1.835
1.813

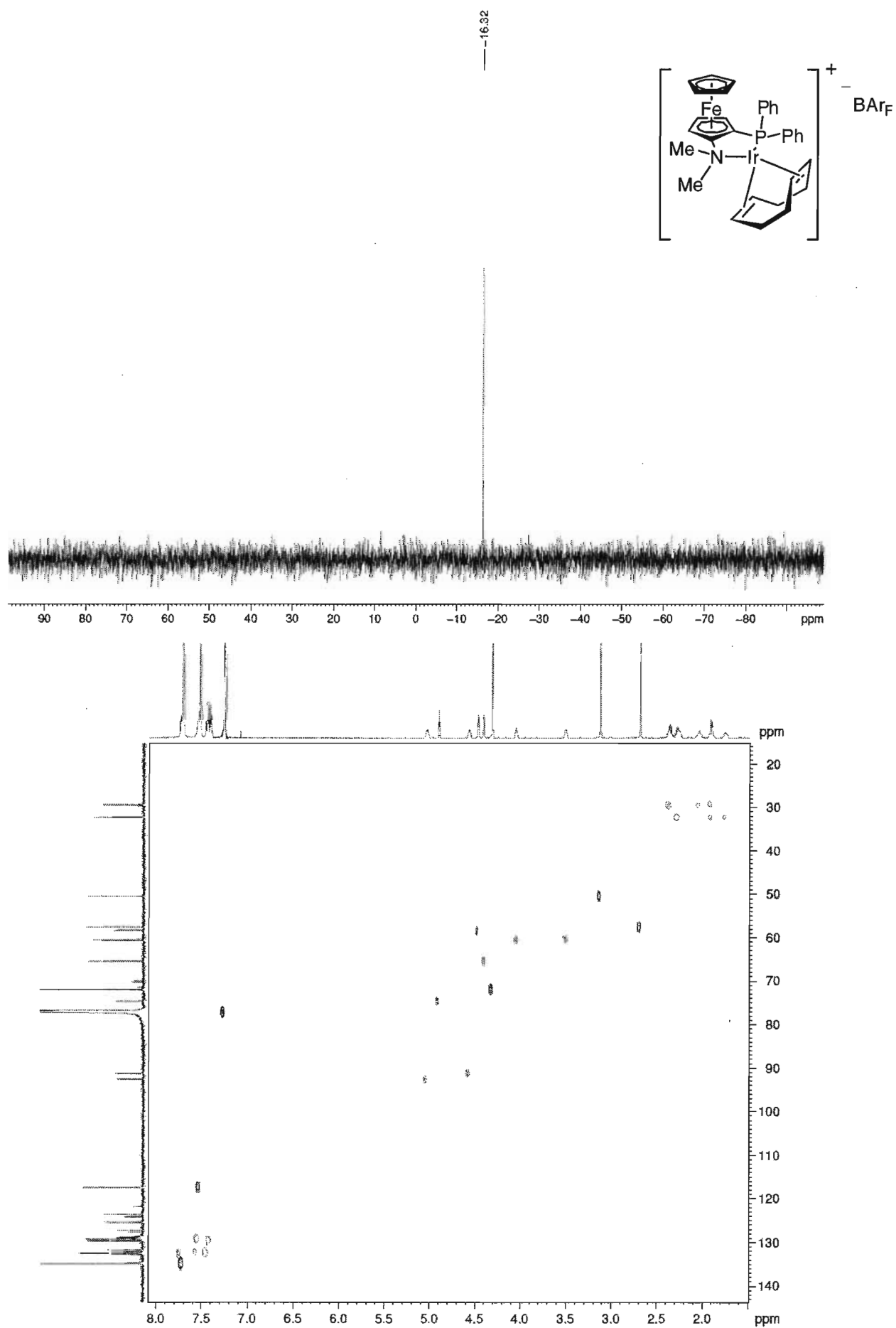


139.79
138.63
137.98
137.83
135.40
135.11
132.29
132.05
128.93
128.13
128.06
128.01
127.91
127.63
116.81
116.59

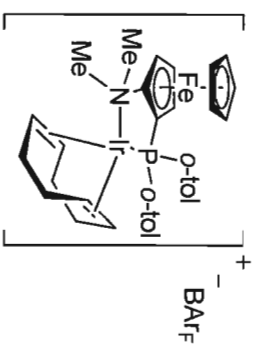
77.42
77.00
76.58
68.02
67.92
67.67
64.66
62.21
62.04
60.25
60.20
52.43
52.28

24.85
24.82





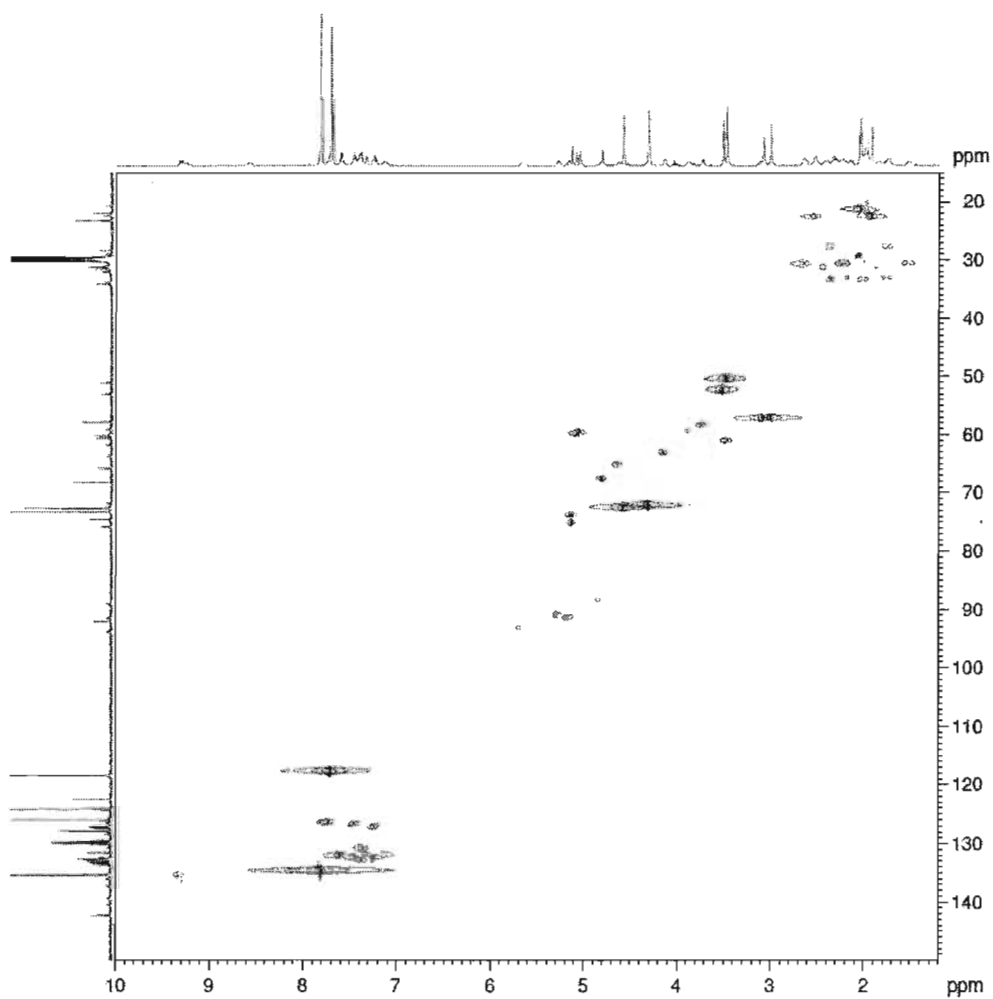
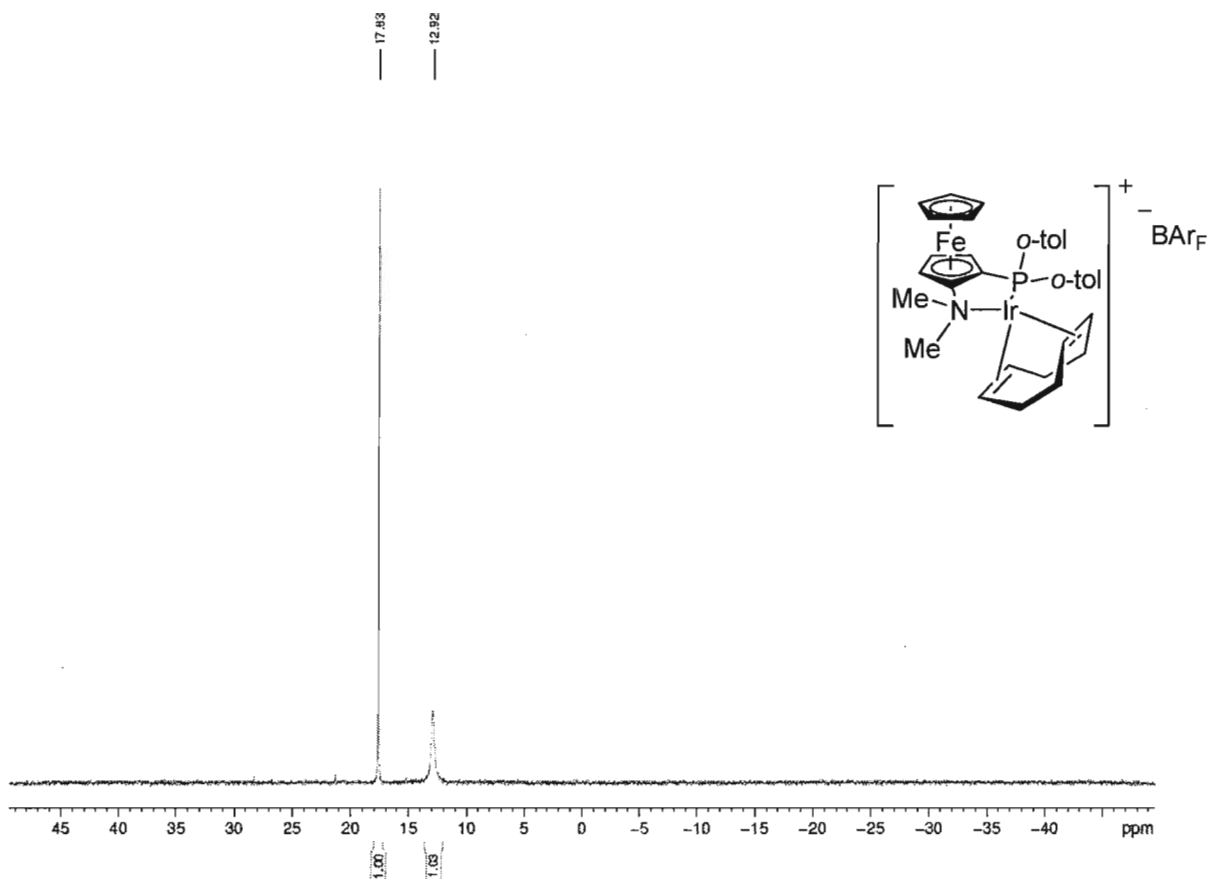
9.329
9.316
9.307
9.293
7.821
7.706
7.619
7.607
7.594
7.591
7.474
7.461
7.447
7.434
7.408
7.399
7.386
7.373
7.341
7.333
7.321
7.283
7.252
7.238
7.226
7.140
5.275
5.185
5.128
5.120
5.080
5.042
4.992
4.828
4.573
4.303
4.130
3.874
3.790
3.504
3.466
3.112
3.072
2.995
2.896
2.825
2.821
2.414
2.406
2.401
2.357
2.338
2.328
2.313
2.285
2.262
2.253
2.235
2.225
2.211
2.203
2.153
2.141
2.124
2.050
2.036
1.992
1.916
1.835
1.787
1.755
1.748
1.739
1.531
1.516



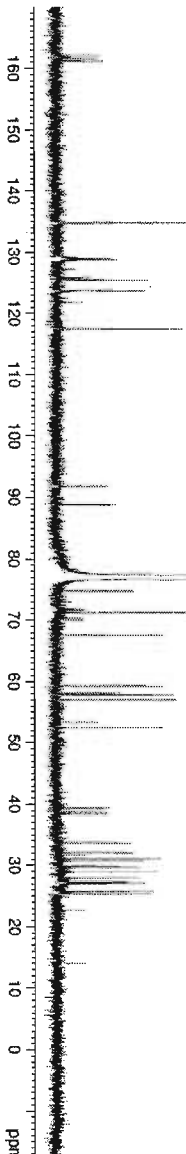
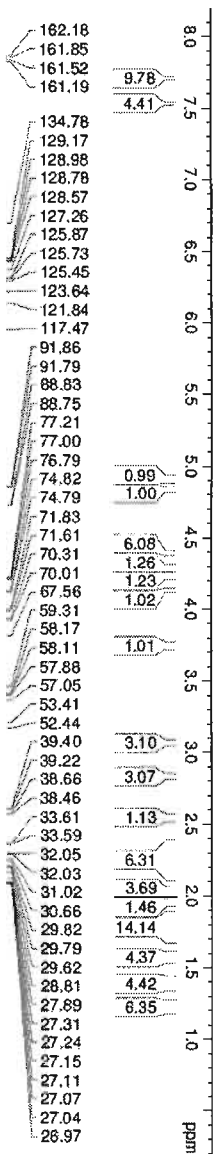
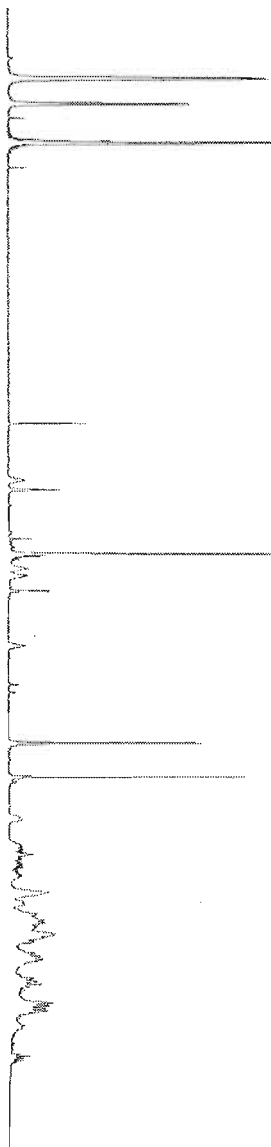
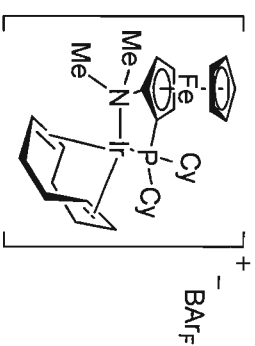
9.5
9.0
8.5
8.0
7.5
7.0
6.5
6.0
5.5
5.0
4.5
4.0
3.5
3.0
2.5
2.0
1.5
ppm

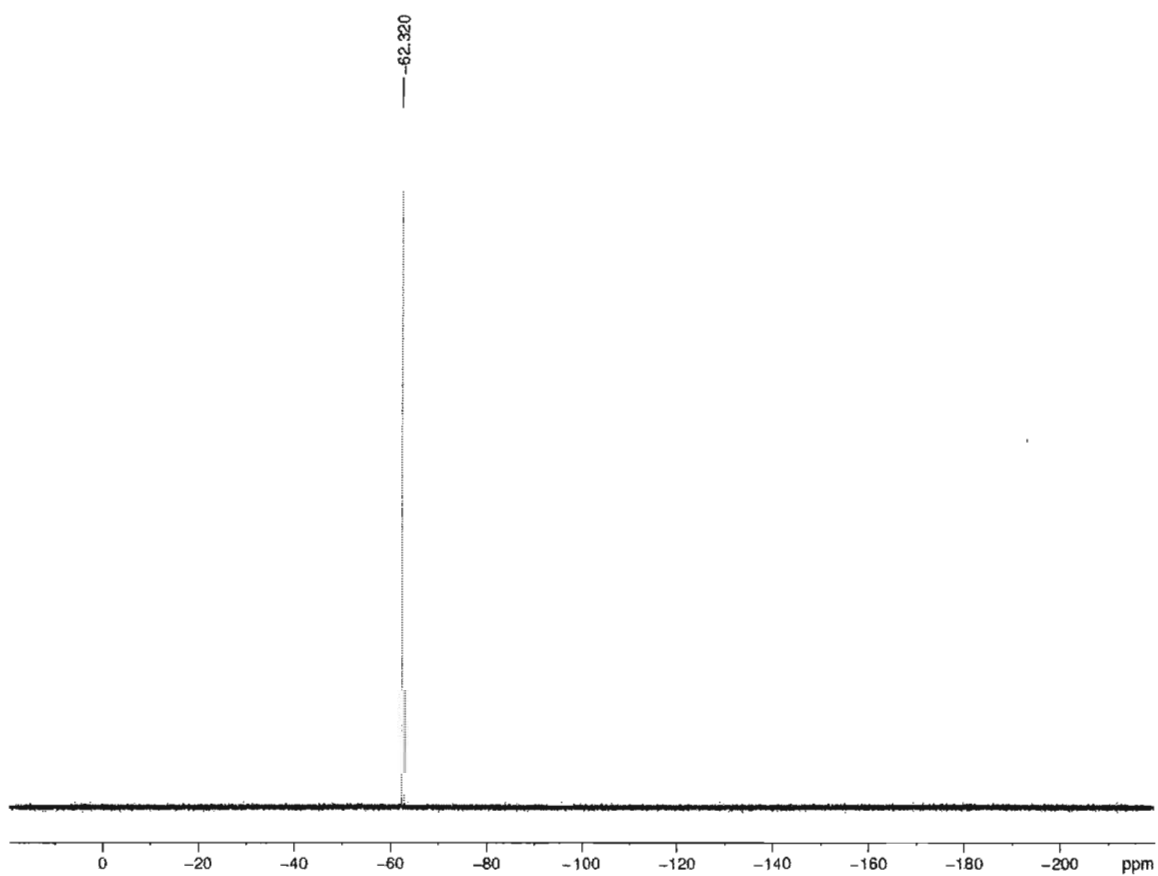
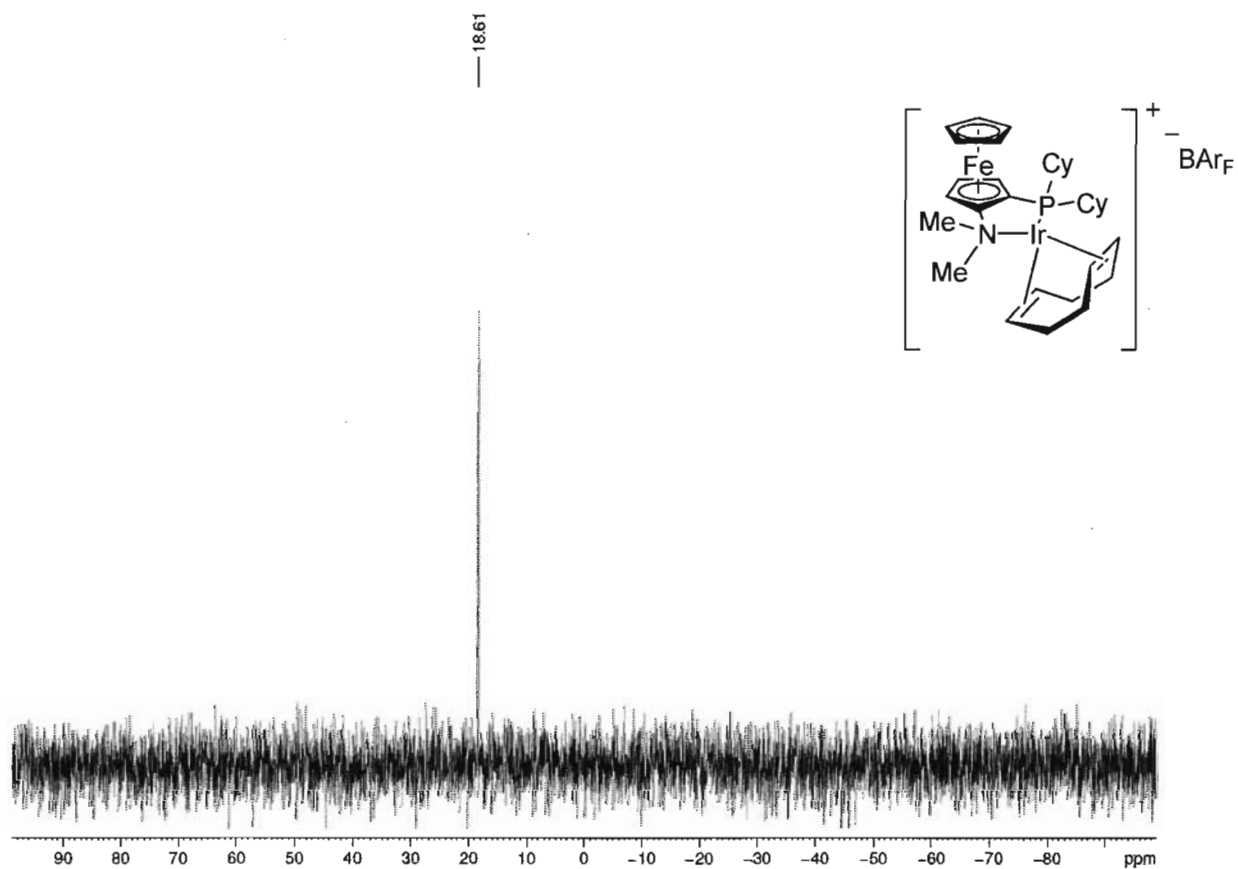
162.92
162.59
162.28
161.93
142.42
142.36
142.21
142.18
136.36
133.65
133.59
133.32
133.27
133.11
133.06
132.99
132.73
132.65
132.48
131.59
130.14
129.93
129.91
129.89
129.74
129.72
129.70
129.68
129.49
128.56
128.17
127.89
127.44
127.34
127.22
127.13
127.10
127.03
126.09
124.29
122.49
118.46
118.43
118.41
92.10
92.02
75.77
74.56
74.52
73.23
72.65
68.24
65.79
61.83
60.71
60.65
60.24
60.18
57.96
57.82
53.04
51.14
34.21
33.87
32.02
31.93
31.27
28.84
28.05
28.42
23.26
23.23
22.34
21.98
21.94

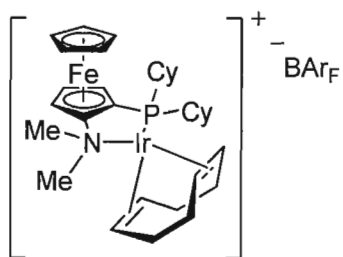
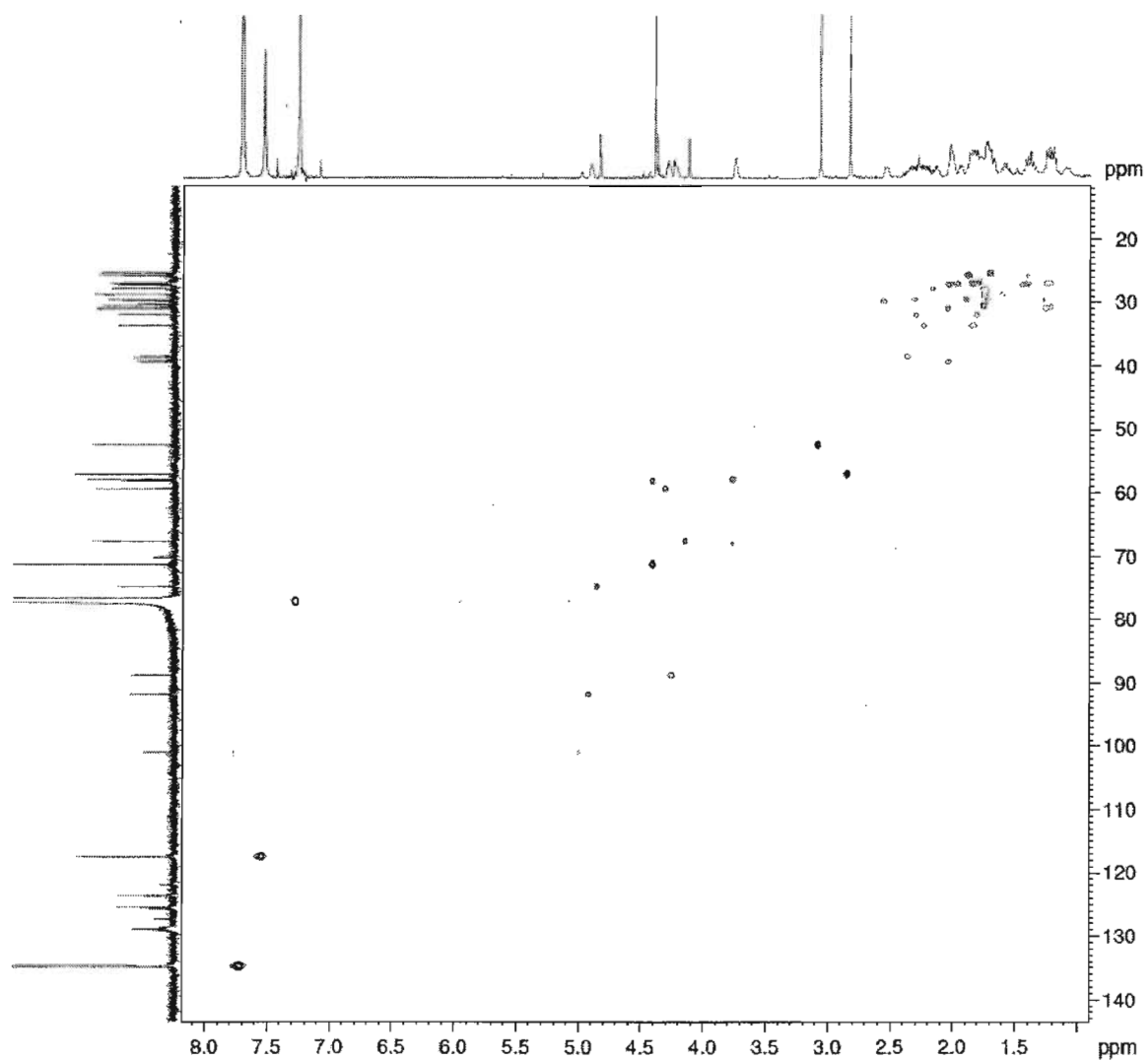
160
150
140
130
120
110
100
90
80
70
60
50
40
30
ppm

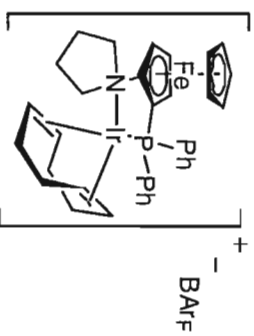


7.707
7.531
7.260
4.904
4.840
4.835
4.831
4.389
4.287
4.241
4.234
4.229
4.131
4.128
3.752
3.747
3.065
2.829
2.341
2.323
2.312
2.300
2.289
2.282
2.267
2.263
2.255
2.251
2.239
2.223
2.211
2.199
2.150
2.142
2.137
2.028
1.941
1.878
1.833
1.815
1.742
1.734
1.706
1.680
1.600
1.578
1.557
1.546
1.428
1.423
1.407
1.403
1.385
1.367
1.345
1.255
1.233
1.217
1.197
1.181



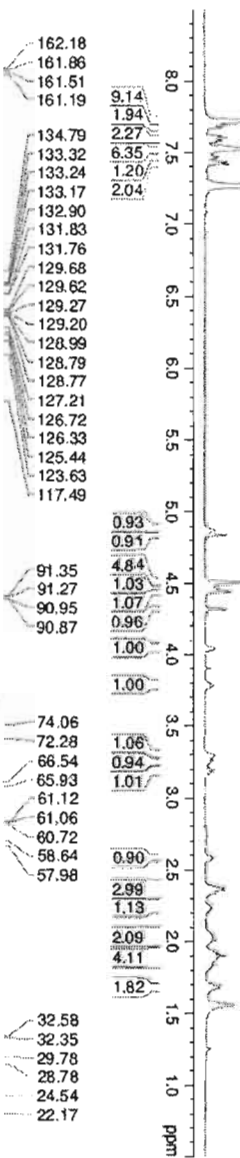






7.675
7.662
7.606
7.593
7.587
7.574
7.521
7.506
7.477
7.464
7.452
7.431
7.419
7.408
7.260

4.872
4.838
4.493
4.457
4.438
4.313
4.043
3.799
3.785
3.770
3.296
3.291
3.267
3.251
3.232
3.213
3.195
3.180
3.163
2.596
2.584
2.371
2.358
2.239
2.227
2.215
2.203
2.049
2.043
2.027
2.009
1.917
1.900
1.883
1.831
1.691
1.679



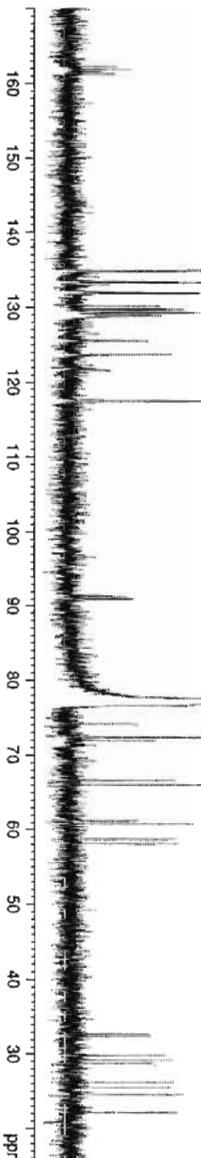
162.18
161.86
161.51
161.19

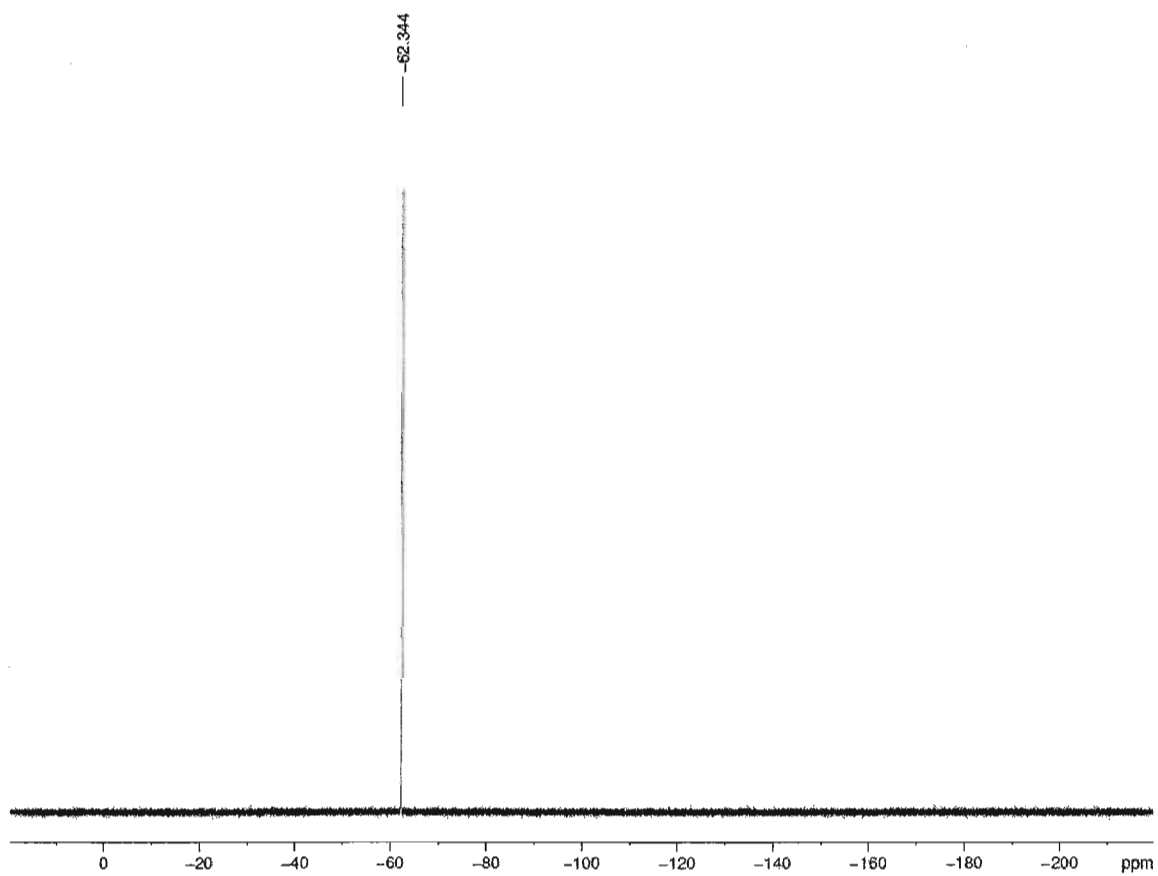
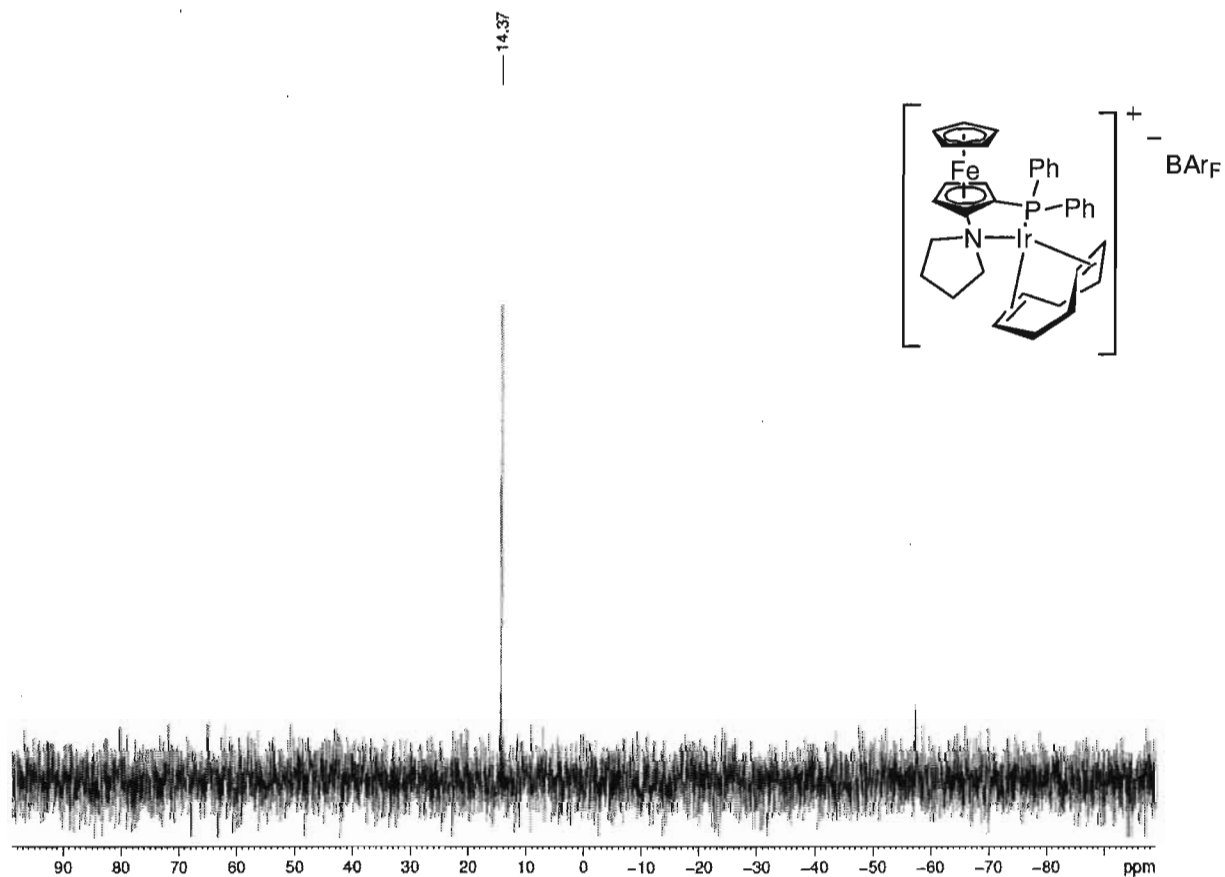
134.79
133.32
133.24
133.17
132.90
131.83
131.76
129.68
129.62
129.27
129.20
128.99
128.79
128.77
127.21
126.72
126.33
125.44
123.63
117.49

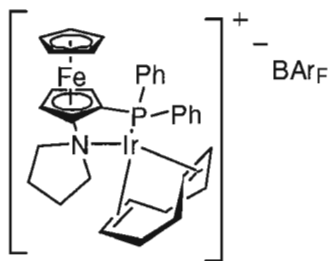
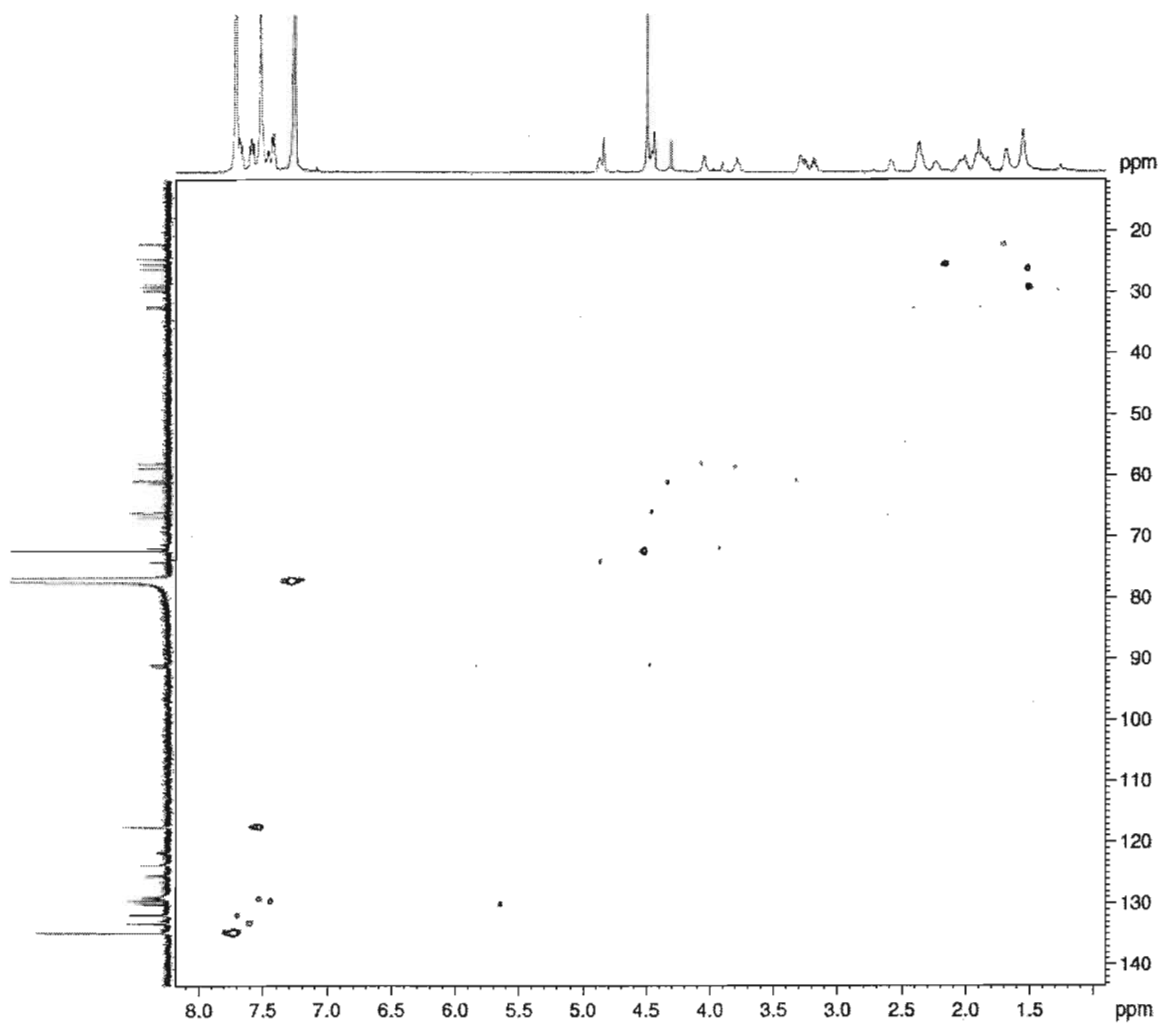
91.35
91.27
90.95
90.87

74.06
72.28
66.54
65.83
61.12
61.06
60.72
58.64
57.98

32.58
32.35
29.78
28.78
24.54
22.17







7.2 Appendix 2 – X-ray data.

X-ray data for racemic complex (S)-221

data_costadec2008b

```
_audit_creation_method      SHELXL-97
_chemical_name_systematic
;
?
;
_chemical_name_common       ?
_chemical_melting_point     ?
_chemical_formula_moiety    'C32 H36 Fe Ir N P, C32 H12 B F24'
_chemical_formula_sum
'C64 H48 B F24 Fe Ir N P'
_chemical_formula_weight    1576.86
```

```
loop_
  _atom_type_symbol
  _atom_type_description
  _atom_type_scatter_dispersion_real
  _atom_type_scatter_dispersion_imag
  _atom_type_scatter_source
'C' 'C' 0.0033 0.0016
'International Tables Vol C Tables 4.2.6.8 and 6.1.1.4'
'H' 'H' 0.0000 0.0000
'International Tables Vol C Tables 4.2.6.8 and 6.1.1.4'
'B' 'B' 0.0013 0.0007
'International Tables Vol C Tables 4.2.6.8 and 6.1.1.4'
'N' 'N' 0.0061 0.0033
'International Tables Vol C Tables 4.2.6.8 and 6.1.1.4'
'F' 'F' 0.0171 0.0103
'International Tables Vol C Tables 4.2.6.8 and 6.1.1.4'
'P' 'P' 0.1023 0.0942
'International Tables Vol C Tables 4.2.6.8 and 6.1.1.4'
'Fe' 'Fe' 0.3463 0.8444
'International Tables Vol C Tables 4.2.6.8 and 6.1.1.4'
'Ir' 'Ir' -1.4442 7.9887
'International Tables Vol C Tables 4.2.6.8 and 6.1.1.4'
```

```
_symmetry_cell_setting      Triclinic
_symmetry_space_group_name_Hall '-P 1'
_symmetry_space_group_name_H-M 'P -1'
loop_
  _symmetry_equiv_pos_as_xyz
```

'x, y, z'
'-x, -y, -z'

_cell_length_a 12.7697(6)
_cell_length_b 12.8455(6)
_cell_length_c 19.8377(10)
_cell_angle_alpha 74.724(2)
_cell_angle_beta 76.026(3)
_cell_angle_gamma 87.188(2)
_cell_volume 3045.8(3)
_cell_formula_units_Z 2
_cell_measurement_temperature 150(2)
_cell_measurement_reflns_used 9579
_cell_measurement_theta_min 2.609
_cell_measurement_theta_max 28.34

_exptl_crystal_description 'plate'
_exptl_crystal_colour 'orange'
_exptl_crystal_size_max 0.30
_exptl_crystal_size_mid 0.26
_exptl_crystal_size_min 0.04
_exptl_crystal_density_meas 'not measured'
_exptl_crystal_density_diffn 1.719
_exptl_crystal_density_method 'not measured'
_exptl_crystal_F_000 1556
_exptl_absorpt_coefficient_mu 2.563
_exptl_absorpt_correction_type 'multi-scan'
_exptl_absorpt_correction_T_min 0.5136
_exptl_absorpt_correction_T_max 0.9044
_exptl_absorpt_process_details 'SADABS, Bruker 2001'

_exptl_special_details

;
?
;

_diffn_ambient_temperature 150(2)
_diffn_radiation_wavelength 0.71073
_diffn_radiation_type MoK α
_diffn_radiation_source 'fine-focus sealed tube'
_diffn_radiation_monochromator graphite
_diffn_measurement_device_type 'Bruker Kappa Apex II area detector'
_diffn_measurement_method 'phi and omega scans'
_diffn_detector_area_resol_mean ?
_diffn_standards_number ?
_diffn_standards_interval_count ?

```

_diffn_standards_interval_time ?
_diffn_standards_decay_% ?
_diffn_reflns_number 81694
_diffn_reflns_av_R_equivalents 0.0341
_diffn_reflns_av_sigmaI/netI 0.0274
_diffn_reflns_limit_h_min -17
_diffn_reflns_limit_h_max 17
_diffn_reflns_limit_k_min -17
_diffn_reflns_limit_k_max 16
_diffn_reflns_limit_l_min -26
_diffn_reflns_limit_l_max 26
_diffn_reflns_theta_min 2.19
_diffn_reflns_theta_max 28.48
_reflns_number_total 15144
_reflns_number_gt 13709
_reflns_threshold_expression >2sigma(I)

_computing_data_collection 'Bruker SMART'
_computing_cell_refinement 'Bruker SMART'
_computing_data_reduction 'Bruker SAINT'
_computing_structure_solution 'SHELXS-97 (Sheldrick, 1990)'
_computing_structure_refinement 'SHELXL-97 (Sheldrick, 1997)'
_computing_molecular_graphics 'Bruker SHELXTL'
_computing_publication_material 'Bruker SHELXTL'

```

```
_refine_special_details
```

```
;
```

Refinement of F^2 against ALL reflections. The weighted R-factor wR and goodness of fit S are based on F^2 , conventional R-factors R are based on F , with F set to zero for negative F^2 . The threshold expression of $F^2 > 2\sigma(F^2)$ is used only for calculating R-factors(gt) etc. and is not relevant to the choice of reflections for refinement. R-factors based on F^2 are statistically about twice as large as those based on F , and R-factors based on ALL data will be even larger.

```
;
```

```

_refine_ls_structure_factor_coef Fsqd
_refine_ls_matrix_type full
_refine_ls_weighting_scheme calc
_refine_ls_weighting_details
'calc w=1/[\s^2^(Fo^2^)+(0.0658P)^2^+2.5190P] where P=(Fo^2^+2Fc^2^)/3'
_atom_sites_solution_primary direct
_atom_sites_solution_secondary difmap
_atom_sites_solution_hydrogens geom
_refine_ls_hydrogen_treatment constr
_refine_ls_extinction_method none

```

_refine_ls_extinction_coef	?
_refine_ls_number_reflns	15144
_refine_ls_number_parameters	840
_refine_ls_number_restraints	0
_refine_ls_R_factor_all	0.0413
_refine_ls_R_factor_gt	0.0352
_refine_ls_wR_factor_ref	0.1041
_refine_ls_wR_factor_gt	0.0985
_refine_ls_goodness_of_fit_ref	1.133
_refine_ls_restrained_S_all	1.133
_refine_ls_shift/su_max	0.003
_refine_ls_shift/su_mean	0.000

loop_

_atom_site_label
_atom_site_type_symbol
_atom_site_fract_x
_atom_site_fract_y
_atom_site_fract_z
_atom_site_U_iso_or_equiv
_atom_site_adp_type
_atom_site_occupancy
_atom_site_symmetry_multiplicity
_atom_site_calc_flag
_atom_site_refinement_flags
_atom_site_disorder_assembly
_atom_site_disorder_group

Ir1	Ir	0.819137(9)	0.732546(9)	0.724132(6)	0.01758(5)	Uani	1	1	d . . .
Fe1	Fe	0.65246(4)	0.63311(4)	0.61656(3)	0.02188(10)	Uani	1	1	d . . .
P1	P	0.65216(7)	0.65692(7)	0.78367(5)	0.01951(16)	Uani	1	1	d . . .
N1	N	0.8452(2)	0.5776(2)	0.69269(16)	0.0212(5)	Uani	1	1	d . . .
B1	B	0.1510(3)	0.1954(3)	0.75556(19)	0.0171(6)	Uani	1	1	d . . .
F1	F	0.1252(3)	-0.2253(2)	0.9334(2)	0.0740(11)	Uani	1	1	d . . .
F2	F	-0.0283(3)	-0.1550(3)	0.94970(19)	0.0630(9)	Uani	1	1	d . . .
F3	F	0.0539(3)	-0.1879(2)	1.03264(14)	0.0598(8)	Uani	1	1	d . . .
F4	F	0.3978(3)	0.0551(4)	0.9843(3)	0.1114(18)	Uani	1	1	d . . .
F5	F	0.3682(6)	0.2138(5)	0.9398(3)	0.177(4)	Uani	1	1	d . . .
F6	F	0.2764(3)	0.1309(6)	1.0372(3)	0.125(2)	Uani	1	1	d . . .
F7	F	0.3898(3)	0.5360(3)	0.5627(2)	0.0722(10)	Uani	1	1	d . . .
F8	F	0.2370(3)	0.5427(2)	0.53820(17)	0.0620(8)	Uani	1	1	d . . .
F9	F	0.2866(4)	0.6686(2)	0.5763(2)	0.0818(12)	Uani	1	1	d . . .
F10	F	0.1401(7)	0.4693(5)	0.9102(3)	0.191(4)	Uani	1	1	d . . .
F11	F	0.0270(4)	0.5587(3)	0.8631(2)	0.0849(12)	Uani	1	1	d . . .
F12	F	0.1795(4)	0.6307(4)	0.8357(3)	0.126(2)	Uani	1	1	d . . .
F13	F	0.5684(2)	0.1861(4)	0.6904(2)	0.0864(14)	Uani	1	1	d . . .

F14 F 0.6192(2) 0.0893(3) 0.6164(2) 0.0737(11) Uani 1 1 d ...
 F15 F 0.5777(2) 0.2509(3) 0.5814(2) 0.0833(13) Uani 1 1 d ...
 F16 F 0.2395(3) -0.1432(2) 0.62868(15) 0.0556(8) Uani 1 1 d ...
 F17 F 0.3577(2) -0.0730(2) 0.53292(16) 0.0496(7) Uani 1 1 d ...
 F18 F 0.1959(2) -0.0155(2) 0.54871(15) 0.0456(6) Uani 1 1 d ...
 F19 F -0.3102(3) 0.0884(3) 0.8488(3) 0.1108(19) Uani 1 1 d ...
 F20 F -0.3434(2) 0.2533(3) 0.81183(15) 0.0716(11) Uani 1 1 d ...
 F21 F -0.2557(2) 0.2037(3) 0.89133(14) 0.0635(10) Uani 1 1 d ...
 F22 F -0.01493(19) 0.20262(18) 0.53517(11) 0.0334(5) Uani 1 1 d ...
 F23 F -0.04654(19) 0.36663(17) 0.53893(11) 0.0321(5) Uani 1 1 d ...
 F24 F -0.17850(18) 0.2555(2) 0.56166(12) 0.0363(5) Uani 1 1 d ...
 C1 C 0.6403(3) 0.5765(3) 0.72443(19) 0.0245(7) Uani 1 1 d ...
 C2 C 0.7412(3) 0.5480(3) 0.68283(18) 0.0225(6) Uani 1 1 d ...
 C3 C 0.7195(3) 0.4840(3) 0.6395(2) 0.0285(7) Uani 1 1 d ...
 H3 H 0.7706 0.4541 0.6081 0.034 Uiso 1 1 calc R ..
 C4 C 0.6064(3) 0.4735(3) 0.6523(2) 0.0328(8) Uani 1 1 d ...
 H4 H 0.5705 0.4361 0.6301 0.039 Uiso 1 1 calc R ..
 C5 C 0.5564(3) 0.5291(3) 0.7043(2) 0.0285(7) Uani 1 1 d ...
 H5 H 0.4825 0.5341 0.7222 0.034 Uiso 1 1 calc R ..
 C1' C 0.6333(3) 0.7985(3) 0.5872(2) 0.0296(8) Uani 1 1 d ...
 H1' H 0.6177 0.8438 0.6178 0.036 Uiso 1 1 calc R ..
 C2' C 0.7378(3) 0.7706(3) 0.5532(2) 0.0280(7) Uani 1 1 d ...
 H2' H 0.8028 0.7942 0.5577 0.034 Uiso 1 1 calc R ..
 C3' C 0.7254(3) 0.7001(3) 0.5111(2) 0.0312(8) Uani 1 1 d ...
 H3' H 0.7808 0.6692 0.4832 0.037 Uiso 1 1 calc R ..
 C4' C 0.6132(4) 0.6855(3) 0.5191(2) 0.0338(8) Uani 1 1 d ...
 H4' H 0.5824 0.6437 0.4970 0.041 Uiso 1 1 calc R ..
 C5' C 0.5567(3) 0.7452(3) 0.5663(2) 0.0320(8) Uani 1 1 d ...
 H5' H 0.4820 0.7490 0.5811 0.038 Uiso 1 1 calc R ..
 C6 C 0.5355(3) 0.7401(3) 0.8007(2) 0.0267(7) Uani 1 1 d ...
 C7 C 0.4602(3) 0.7614(4) 0.7585(2) 0.0357(9) Uani 1 1 d ...
 H7 H 0.4642 0.7268 0.7223 0.043 Uiso 1 1 calc R ..
 C8 C 0.3784(3) 0.8355(4) 0.7712(3) 0.0487(12) Uani 1 1 d ...
 H8 H 0.3274 0.8495 0.7436 0.058 Uiso 1 1 calc R ..
 C9 C 0.3729(4) 0.8879(4) 0.8241(3) 0.0520(13) Uani 1 1 d ...
 H9 H 0.3187 0.9376 0.8316 0.062 Uiso 1 1 calc R ..
 C10 C 0.4466(4) 0.8677(4) 0.8661(3) 0.0492(12) Uani 1 1 d ...
 H10 H 0.4430 0.9036 0.9017 0.059 Uiso 1 1 calc R ..
 C11 C 0.5271(3) 0.7922(3) 0.8546(2) 0.0339(9) Uani 1 1 d ...
 H11 H 0.5760 0.7766 0.8837 0.041 Uiso 1 1 calc R ..
 C12 C 0.6481(3) 0.5621(3) 0.87001(18) 0.0245(7) Uani 1 1 d ...
 C13 C 0.5767(3) 0.4745(3) 0.8964(2) 0.0336(8) Uani 1 1 d ...
 H13 H 0.5263 0.4666 0.8711 0.040 Uiso 1 1 calc R ..
 C14 C 0.5799(4) 0.3989(4) 0.9602(2) 0.0430(10) Uani 1 1 d ...
 H14 H 0.5326 0.3399 0.9771 0.052 Uiso 1 1 calc R ..
 C15 C 0.6523(4) 0.4106(4) 0.9985(2) 0.0510(12) Uani 1 1 d ...

H15 H 0.6535 0.3603 1.0417 0.061 Uiso 1 1 calc R . .
 C16 C 0.7237(5) 0.4972(5) 0.9728(3) 0.0646(16) Uani 1 1 d . . .
 H16 H 0.7737 0.5047 0.9985 0.077 Uiso 1 1 calc R . .
 C17 C 0.7214(4) 0.5734(4) 0.9088(2) 0.0467(11) Uani 1 1 d . . .
 H17 H 0.7692 0.6320 0.8921 0.056 Uiso 1 1 calc R . .
 C18 C 0.8756(3) 0.4907(3) 0.7517(2) 0.0286(7) Uani 1 1 d . . .
 H18A H 0.8169 0.4775 0.7938 0.043 Uiso 1 1 calc R . .
 H18B H 0.9385 0.5134 0.7629 0.043 Uiso 1 1 calc R . .
 H18C H 0.8909 0.4256 0.7362 0.043 Uiso 1 1 calc R . .
 C19 C 0.9312(3) 0.5811(3) 0.6259(2) 0.0297(8) Uani 1 1 d . . .
 H19A H 0.9370 0.5112 0.6165 0.045 Uiso 1 1 calc R . .
 H19B H 0.9989 0.6011 0.6323 0.045 Uiso 1 1 calc R . .
 H19C H 0.9129 0.6332 0.5861 0.045 Uiso 1 1 calc R . .
 C20 C 0.9631(3) 0.8183(3) 0.64605(19) 0.0246(7) Uani 1 1 d . . .
 H20 H 0.9574 0.7756 0.6158 0.029 Uiso 1 1 calc R . .
 C21 C 0.9888(3) 0.7673(3) 0.7109(2) 0.0249(7) Uani 1 1 d . . .
 H21 H 0.9995 0.6932 0.7204 0.030 Uiso 1 1 calc R . .
 C22 C 1.0009(3) 0.8223(3) 0.7675(2) 0.0309(8) Uani 1 1 d . . .
 H22A H 1.0695 0.8612 0.7516 0.037 Uiso 1 1 calc R . .
 H22B H 1.0017 0.7679 0.8118 0.037 Uiso 1 1 calc R . .
 C23 C 0.9087(3) 0.9018(3) 0.7824(2) 0.0321(8) Uani 1 1 d . . .
 H23A H 0.9007 0.9110 0.8304 0.039 Uiso 1 1 calc R . .
 H23B H 0.9271 0.9717 0.7483 0.039 Uiso 1 1 calc R . .
 C24 C 0.8032(3) 0.8616(3) 0.7761(2) 0.0265(7) Uani 1 1 d . . .
 H24 H 0.7615 0.8131 0.8159 0.032 Uiso 1 1 calc R . .
 C25 C 0.7647(3) 0.8939(3) 0.7127(2) 0.0253(7) Uani 1 1 d . . .
 H25 H 0.6971 0.8680 0.7145 0.030 Uiso 1 1 calc R . .
 C26 C 0.8242(3) 0.9665(3) 0.6429(2) 0.0264(7) Uani 1 1 d . . .
 H26A H 0.8192 1.0404 0.6468 0.032 Uiso 1 1 calc R . .
 H26B H 0.7893 0.9622 0.6053 0.032 Uiso 1 1 calc R . .
 C27 C 0.9436(3) 0.9384(3) 0.6209(2) 0.0283(7) Uani 1 1 d . . .
 H27A H 0.9682 0.9617 0.5690 0.034 Uiso 1 1 calc R . .
 H27B H 0.9857 0.9775 0.6412 0.034 Uiso 1 1 calc R . .
 C28 C 0.1592(2) 0.1237(3) 0.83538(17) 0.0192(6) Uani 1 1 d . . .
 C29 C 0.1059(3) 0.0236(3) 0.86819(17) 0.0212(6) Uani 1 1 d . . .
 H29 H 0.0582 0.0006 0.8461 0.025 Uiso 1 1 calc R . .
 C30 C 0.1222(3) -0.0423(3) 0.93275(18) 0.0238(7) Uani 1 1 d . . .
 C31 C 0.1916(3) -0.0104(3) 0.96741(19) 0.0298(8) Uani 1 1 d . . .
 H31 H 0.2019 -0.0540 1.0108 0.036 Uiso 1 1 calc R . .
 C32 C 0.2455(3) 0.0875(3) 0.9364(2) 0.0297(8) Uani 1 1 d . . .
 C33 C 0.2305(3) 0.1527(3) 0.87166(19) 0.0240(7) Uani 1 1 d . . .
 H33 H 0.2688 0.2177 0.8516 0.029 Uiso 1 1 calc R . .
 C34 C 0.0698(3) -0.1521(3) 0.9625(2) 0.0300(8) Uani 1 1 d . . .
 C36 C 0.1766(3) 0.3241(3) 0.74316(18) 0.0211(6) Uani 1 1 d . . .
 C41 C 0.1467(3) 0.3768(3) 0.7983(2) 0.0332(9) Uani 1 1 d . . .
 H41 H 0.1123 0.3376 0.8443 0.040 Uiso 1 1 calc R . .

C40 C 0.1674(4) 0.4871(4) 0.7856(3) 0.0422(11) Uani 1 1 d ...
 C39 C 0.2122(4) 0.5498(3) 0.7180(3) 0.0415(11) Uani 1 1 d ...
 H39 H 0.2245 0.6232 0.7101 0.050 Uiso 1 1 calc R ...
 C37 C 0.2221(3) 0.3894(3) 0.6748(2) 0.0254(7) Uani 1 1 d ...
 H37 H 0.2422 0.3577 0.6366 0.030 Uiso 1 1 calc R ...
 C43 C 0.1314(7) 0.5345(5) 0.8512(4) 0.083(3) Uani 1 1 d ...
 C38 C 0.2389(3) 0.5006(3) 0.6613(2) 0.0317(8) Uani 1 1 d ...
 C42 C 0.2865(4) 0.5634(3) 0.5861(3) 0.0457(11) Uani 1 1 d ...
 C45 C 0.2438(2) 0.1453(2) 0.69967(17) 0.0169(6) Uani 1 1 d ...
 C46 C 0.3528(3) 0.1706(3) 0.68947(18) 0.0197(6) Uani 1 1 d ...
 H45 H 0.3710 0.2177 0.7134 0.024 Uiso 1 1 calc R ...
 C47 C 0.4345(3) 0.1282(3) 0.64510(18) 0.0206(6) Uani 1 1 d ...
 C48 C 0.4113(3) 0.0570(3) 0.60826(19) 0.0221(6) Uani 1 1 d ...
 H47 H 0.4660 0.0291 0.5779 0.027 Uiso 1 1 calc R ...
 C49 C 0.3050(3) 0.0294(3) 0.61828(17) 0.0190(6) Uani 1 1 d ...
 C50 C 0.2222(3) 0.0718(3) 0.66408(17) 0.0182(6) Uani 1 1 d ...
 H50 H 0.1512 0.0501 0.6708 0.022 Uiso 1 1 calc R ...
 C51 C 0.5492(3) 0.1607(4) 0.6349(2) 0.0335(8) Uani 1 1 d ...
 C52 C 0.2751(3) -0.0495(3) 0.5817(2) 0.0271(7) Uani 1 1 d ...
 C53 C 0.0317(2) 0.1960(2) 0.73875(17) 0.0170(6) Uani 1 1 d ...
 C58 C 0.0215(2) 0.2220(2) 0.66740(17) 0.0175(6) Uani 1 1 d ...
 H58 H 0.0838 0.2313 0.6305 0.021 Uiso 1 1 calc R ...
 C57 C -0.0781(2) 0.2343(2) 0.64986(17) 0.0169(6) Uani 1 1 d ...
 C56 C -0.1729(2) 0.2230(3) 0.70280(18) 0.0188(6) Uani 1 1 d ...
 H56 H -0.2397 0.2314 0.6911 0.023 Uiso 1 1 calc R ...
 C55 C -0.1655(3) 0.1986(3) 0.77419(17) 0.0196(6) Uani 1 1 d ...
 C54 C -0.0657(3) 0.1850(3) 0.79179(17) 0.0188(6) Uani 1 1 d ...
 H54 H -0.0633 0.1681 0.8399 0.023 Uiso 1 1 calc R ...
 C59 C -0.2682(3) 0.1863(4) 0.8315(2) 0.0343(9) Uani 1 1 d ...
 C60 C -0.0807(3) 0.2638(3) 0.57222(18) 0.0207(6) Uani 1 1 d ...
 C35 C 0.3213(4) 0.1240(4) 0.9735(3) 0.0472(12) Uani 1 1 d ...

loop_

_atom_site_aniso_label
 _atom_site_aniso_U_11
 _atom_site_aniso_U_22
 _atom_site_aniso_U_33
 _atom_site_aniso_U_23
 _atom_site_aniso_U_13
 _atom_site_aniso_U_12

Ir1 0.01716(7) 0.01637(7) 0.01950(7) -0.00589(5) -0.00358(5) 0.00046(4)
 Fe1 0.0270(2) 0.0186(2) 0.0216(2) -0.00413(18) -0.00970(19) -0.00110(18)
 P1 0.0197(4) 0.0192(4) 0.0177(4) -0.0033(3) -0.0024(3) 0.0002(3)
 N1 0.0226(13) 0.0186(13) 0.0222(14) -0.0049(11) -0.0059(11) 0.0032(10)
 B1 0.0180(15) 0.0186(16) 0.0173(16) -0.0073(13) -0.0070(13) 0.0038(12)

F1 0.080(2) 0.0349(15) 0.089(3) -0.0293(16) 0.0295(19) -0.0041(15)
 F2 0.0561(18) 0.0512(17) 0.074(2) 0.0139(15) -0.0300(16) -0.0218(14)
 F3 0.100(2) 0.0526(17) 0.0222(12) 0.0050(11) -0.0165(14) -0.0247(16)
 F4 0.074(3) 0.154(4) 0.166(5) -0.096(4) -0.089(3) 0.043(3)
 F5 0.271(8) 0.136(4) 0.145(5) 0.067(4) -0.176(5) -0.133(5)
 F6 0.078(3) 0.253(7) 0.098(3) -0.122(4) -0.034(2) -0.006(3)
 F7 0.0483(18) 0.0558(19) 0.090(3) 0.0045(18) 0.0017(17) -0.0020(15)
 F8 0.086(2) 0.0472(17) 0.0485(17) 0.0068(13) -0.0249(17) -0.0177(16)
 F9 0.123(3) 0.0182(13) 0.092(3) -0.0029(15) -0.014(2) -0.0093(16)
 F10 0.395(11) 0.145(5) 0.134(4) -0.122(4) -0.192(6) 0.173(6)
 F11 0.103(3) 0.092(3) 0.073(2) -0.053(2) -0.013(2) 0.022(2)
 F12 0.097(3) 0.134(4) 0.200(5) -0.149(4) -0.017(3) -0.009(3)
 F13 0.0270(14) 0.182(4) 0.077(2) -0.077(3) -0.0113(15) -0.0179(19)
 F14 0.0204(12) 0.079(2) 0.143(4) -0.066(2) -0.0222(16) 0.0154(13)
 F15 0.0371(16) 0.082(3) 0.106(3) 0.023(2) -0.0152(18) -0.0327(16)
 F16 0.093(2) 0.0276(13) 0.0459(16) -0.0139(11) -0.0060(15) -0.0218(14)
 F17 0.0317(12) 0.0676(18) 0.0610(17) -0.0522(15) 0.0068(12) -0.0034(12)
 F18 0.0421(14) 0.0552(16) 0.0591(17) -0.0361(14) -0.0269(13) 0.0074(12)
 F19 0.087(3) 0.083(3) 0.119(4) -0.031(3) 0.071(3) -0.050(2)
 F20 0.0307(13) 0.138(3) 0.0318(14) -0.0084(17) -0.0025(11) 0.0393(17)
 F21 0.0348(14) 0.130(3) 0.0265(13) -0.0286(16) -0.0045(11) 0.0230(17)
 F22 0.0475(13) 0.0361(12) 0.0204(10) -0.0138(9) -0.0108(9) 0.0155(10)
 F23 0.0479(13) 0.0236(10) 0.0203(10) 0.0011(8) -0.0062(9) -0.0039(9)
 F24 0.0291(11) 0.0548(15) 0.0256(11) -0.0010(10) -0.0169(9) -0.0049(10)
 C1 0.0309(18) 0.0206(15) 0.0226(16) -0.0040(13) -0.0089(14) -0.0007(13)
 C2 0.0273(16) 0.0185(15) 0.0222(16) -0.0040(12) -0.0088(13) 0.0012(12)
 C3 0.041(2) 0.0191(16) 0.0301(19) -0.0081(14) -0.0151(16) 0.0022(14)
 C4 0.046(2) 0.0199(16) 0.037(2) -0.0042(15) -0.0205(18) -0.0061(15)
 C5 0.0316(18) 0.0228(16) 0.0293(18) 0.0006(14) -0.0101(15) -0.0081(14)
 C1' 0.039(2) 0.0205(16) 0.0279(18) -0.0012(14) -0.0112(16) 0.0016(14)
 C2' 0.0321(18) 0.0243(17) 0.0254(18) 0.0013(14) -0.0101(15) -0.0054(14)
 C3' 0.039(2) 0.0313(19) 0.0203(17) -0.0035(14) -0.0052(15) -0.0006(16)
 C4' 0.045(2) 0.0322(19) 0.0271(19) -0.0012(15) -0.0188(17) -0.0075(17)
 C5' 0.0303(19) 0.0302(19) 0.034(2) 0.0013(16) -0.0144(16) 0.0009(15)
 C6 0.0197(15) 0.0253(17) 0.0259(17) 0.0009(14) 0.0035(13) 0.0006(13)
 C7 0.0228(17) 0.042(2) 0.032(2) 0.0019(17) -0.0012(15) 0.0032(16)
 C8 0.027(2) 0.054(3) 0.045(3) 0.010(2) 0.0003(18) 0.0135(19)
 C9 0.038(2) 0.047(3) 0.050(3) 0.000(2) 0.010(2) 0.021(2)
 C10 0.048(3) 0.043(3) 0.045(3) -0.014(2) 0.011(2) 0.013(2)
 C11 0.0243(17) 0.033(2) 0.040(2) -0.0118(17) 0.0022(16) 0.0049(15)
 C12 0.0268(17) 0.0258(17) 0.0170(15) -0.0027(13) -0.0015(13) 0.0027(13)
 C13 0.037(2) 0.0309(19) 0.0260(19) 0.0010(15) -0.0026(16) -0.0057(16)
 C14 0.052(3) 0.035(2) 0.031(2) 0.0043(17) -0.0013(19) -0.0032(19)
 C15 0.066(3) 0.053(3) 0.023(2) 0.0077(19) -0.009(2) 0.007(2)
 C16 0.072(4) 0.087(4) 0.033(3) 0.007(3) -0.031(3) -0.016(3)
 C17 0.052(3) 0.053(3) 0.031(2) 0.005(2) -0.018(2) -0.017(2)

C18 0.0332(19) 0.0196(16) 0.035(2) -0.0049(14) -0.0159(16) 0.0059(14)
 C19 0.0294(18) 0.0272(18) 0.0321(19) -0.0145(15) -0.0003(15) 0.0060(14)
 C20 0.0214(16) 0.0241(16) 0.0266(17) -0.0064(14) -0.0019(13) -0.0056(13)
 C21 0.0191(15) 0.0223(16) 0.0331(19) -0.0069(14) -0.0060(14) -0.0009(12)
 C22 0.0256(17) 0.0343(19) 0.038(2) -0.0103(16) -0.0167(16) 0.0025(15)
 C23 0.036(2) 0.0286(18) 0.039(2) -0.0187(16) -0.0112(17) -0.0004(15)
 C24 0.0266(17) 0.0234(16) 0.0306(18) -0.0127(14) -0.0022(14) -0.0034(13)
 C25 0.0245(16) 0.0163(15) 0.037(2) -0.0100(14) -0.0076(14) 0.0015(12)
 C26 0.0260(17) 0.0199(16) 0.0331(19) -0.0042(14) -0.0093(15) -0.0008(13)
 C27 0.0267(17) 0.0252(17) 0.0283(18) -0.0012(14) -0.0031(14) -0.0051(14)
 C28 0.0156(14) 0.0258(16) 0.0183(15) -0.0102(12) -0.0043(11) 0.0068(12)
 C29 0.0220(15) 0.0265(16) 0.0181(15) -0.0099(13) -0.0069(12) 0.0071(13)
 C30 0.0252(16) 0.0282(17) 0.0181(15) -0.0077(13) -0.0050(13) 0.0075(13)
 C31 0.038(2) 0.037(2) 0.0161(16) -0.0045(14) -0.0126(14) 0.0080(16)
 C32 0.0322(19) 0.038(2) 0.0237(17) -0.0088(15) -0.0155(15) 0.0042(15)
 C33 0.0219(16) 0.0295(17) 0.0228(16) -0.0075(14) -0.0093(13) 0.0032(13)
 C34 0.039(2) 0.0304(19) 0.0194(17) -0.0055(14) -0.0062(15) 0.0051(16)
 C36 0.0218(15) 0.0227(15) 0.0258(17) -0.0123(13) -0.0132(13) 0.0070(12)
 C41 0.041(2) 0.034(2) 0.038(2) -0.0239(17) -0.0235(18) 0.0202(17)
 C40 0.051(2) 0.038(2) 0.064(3) -0.037(2) -0.042(2) 0.0245(19)
 C39 0.045(2) 0.0239(18) 0.077(3) -0.026(2) -0.043(2) 0.0150(17)
 C37 0.0253(16) 0.0193(15) 0.037(2) -0.0108(14) -0.0147(15) 0.0031(13)
 C43 0.144(6) 0.051(3) 0.111(5) -0.061(4) -0.104(5) 0.059(4)
 C38 0.0305(18) 0.0172(16) 0.054(3) -0.0098(16) -0.0220(18) 0.0030(14)
 C42 0.045(2) 0.0206(18) 0.069(3) -0.0025(19) -0.017(2) -0.0046(17)
 C45 0.0184(14) 0.0158(13) 0.0161(14) -0.0025(11) -0.0054(11) 0.0026(11)
 C46 0.0178(14) 0.0208(15) 0.0225(16) -0.0056(12) -0.0087(12) 0.0014(12)
 C47 0.0161(14) 0.0214(15) 0.0245(16) -0.0043(13) -0.0070(12) 0.0013(12)
 C48 0.0188(15) 0.0221(15) 0.0245(16) -0.0069(13) -0.0032(13) 0.0044(12)
 C49 0.0185(14) 0.0184(14) 0.0208(15) -0.0087(12) -0.0024(12) 0.0019(11)
 C50 0.0173(14) 0.0172(14) 0.0184(15) -0.0046(12) -0.0010(12) 0.0016(11)
 C51 0.0178(16) 0.045(2) 0.042(2) -0.0205(19) -0.0056(15) 0.0027(15)
 C52 0.0234(16) 0.0277(17) 0.0314(19) -0.0165(15) 0.0009(14) -0.0004(13)
 C53 0.0184(14) 0.0167(14) 0.0171(14) -0.0067(11) -0.0045(11) 0.0032(11)
 C58 0.0171(14) 0.0183(14) 0.0163(14) -0.0042(11) -0.0033(11) 0.0007(11)
 C57 0.0195(14) 0.0155(13) 0.0169(14) -0.0041(11) -0.0069(12) 0.0019(11)
 C56 0.0171(14) 0.0190(14) 0.0198(15) -0.0038(12) -0.0053(12) 0.0015(11)
 C55 0.0176(14) 0.0210(15) 0.0177(15) -0.0034(12) -0.0016(12) 0.0030(11)
 C54 0.0195(14) 0.0220(15) 0.0156(14) -0.0050(12) -0.0057(12) 0.0033(12)
 C59 0.0254(18) 0.049(2) 0.0221(18) -0.0034(16) -0.0001(14) 0.0045(16)
 C60 0.0199(15) 0.0235(15) 0.0195(15) -0.0059(12) -0.0063(12) 0.0028(12)
 C35 0.054(3) 0.056(3) 0.040(3) -0.006(2) -0.034(2) -0.003(2)

_geom_special_details

;

All esds (except the esd in the dihedral angle between two l.s. planes)

are estimated using the full covariance matrix. The cell esds are taken into account individually in the estimation of esds in distances, angles and torsion angles; correlations between esds in cell parameters are only used when they are defined by crystal symmetry. An approximate (isotropic) treatment of cell esds is used for estimating esds involving l.s. planes.

;

loop_	F7 C42 1.350(6) . ?
_geom_bond_atom_site_label_1	F8 C42 1.346(6) . ?
_geom_bond_atom_site_label_2	F9 C42 1.314(5) . ?
_geom_bond_distance	F10 C43 1.273(8) . ?
_geom_bond_site_symmetry_2	F11 C43 1.333(8) . ?
_geom_bond_publ_flag	F12 C43 1.335(8) . ?
	F13 C51 1.306(5) . ?
Ir1 C25 2.125(3) . ?	F14 C51 1.309(5) . ?
Ir1 C24 2.148(3) . ?	F15 C51 1.344(6) . ?
Ir1 C21 2.173(3) . ?	F16 C52 1.335(5) . ?
Ir1 C20 2.217(3) . ?	F17 C52 1.330(4) . ?
Ir1 N1 2.225(3) . ?	F18 C52 1.330(5) . ?
Ir1 P1 2.2951(9) . ?	F19 C59 1.317(6) . ?
Fe1 C2 2.012(3) . ?	F20 C59 1.318(5) . ?
Fe1 C1 2.040(4) . ?	F21 C59 1.312(5) . ?
Fe1 C3' 2.043(4) . ?	F22 C60 1.343(4) . ?
Fe1 C3 2.044(4) . ?	F23 C60 1.353(4) . ?
Fe1 C4' 2.048(4) . ?	F24 C60 1.329(4) . ?
Fe1 C4 2.050(4) . ?	C1 C2 1.441(5) . ?
Fe1 C5 2.055(4) . ?	C1 C5 1.441(5) . ?
Fe1 C5' 2.055(4) . ?	C2 C3 1.415(5) . ?
Fe1 C2' 2.060(4) . ?	C3 C4 1.411(6) . ?
Fe1 C1' 2.068(4) . ?	C3 H3 0.9300 . ?
P1 C1 1.792(4) . ?	C4 C5 1.417(6) . ?
P1 C6 1.807(4) . ?	C4 H4 0.9300 . ?
P1 C12 1.812(4) . ?	C5 H5 0.9300 . ?
N1 C2 1.470(4) . ?	C1' C2' 1.417(5) . ?
N1 C19 1.494(4) . ?	C1' C5' 1.417(5) . ?
N1 C18 1.502(4) . ?	C1' H1' 0.9300 . ?
B1 C28 1.634(5) . ?	C2' C3' 1.421(5) . ?
B1 C53 1.636(5) . ?	C2' H2' 0.9300 . ?
B1 C36 1.643(5) . ?	C3' C4' 1.418(6) . ?
B1 C45 1.647(4) . ?	C3' H3' 0.9300 . ?
F1 C34 1.320(5) . ?	C4' C5' 1.408(6) . ?
F2 C34 1.341(5) . ?	C4' H4' 0.9300 . ?
F3 C34 1.314(4) . ?	C5' H5' 0.9300 . ?
F4 C35 1.304(6) . ?	C6 C11 1.384(6) . ?
F5 C35 1.267(7) . ?	C6 C7 1.394(6) . ?
F6 C35 1.279(6) . ?	C7 C8 1.401(6) . ?

C7 H7 0.9300 . ?
 C8 C9 1.376(8) . ?
 C8 H8 0.9300 . ?
 C9 C10 1.374(8) . ?
 C9 H9 0.9300 . ?
 C10 C11 1.398(5) . ?
 C10 H10 0.9300 . ?
 C11 H11 0.9300 . ?
 C12 C17 1.382(6) . ?
 C12 C13 1.390(5) . ?
 C13 C14 1.386(6) . ?
 C13 H13 0.9300 . ?
 C14 C15 1.366(7) . ?
 C14 H14 0.9300 . ?
 C15 C16 1.381(8) . ?
 C15 H15 0.9300 . ?
 C16 C17 1.389(7) . ?
 C16 H16 0.9300 . ?
 C17 H17 0.9300 . ?
 C18 H18A 0.9600 . ?
 C18 H18B 0.9600 . ?
 C18 H18C 0.9600 . ?
 C19 H19A 0.9600 . ?
 C19 H19B 0.9600 . ?
 C19 H19C 0.9600 . ?
 C20 C21 1.390(5) . ?
 C20 C27 1.520(5) . ?
 C20 H20 0.9300 . ?
 C21 C22 1.515(5) . ?
 C21 H21 0.9300 . ?
 C22 C23 1.546(5) . ?
 C22 H22A 0.9700 . ?
 C22 H22B 0.9700 . ?
 C23 C24 1.511(5) . ?
 C23 H23A 0.9700 . ?
 C23 H23B 0.9700 . ?
 C24 C25 1.413(5) . ?
 C24 H24 0.9300 . ?
 C25 C26 1.499(5) . ?
 C25 H25 0.9300 . ?
 C26 C27 1.534(5) . ?
 C26 H26A 0.9700 . ?
 C26 H26B 0.9700 . ?
 C27 H27A 0.9700 . ?
 C27 H27B 0.9700 . ?
 C28 C29 1.404(5) . ?

C28 C33 1.406(4) . ?
 C29 C30 1.393(5) . ?
 C29 H29 0.9300 . ?
 C30 C31 1.381(5) . ?
 C30 C34 1.498(5) . ?
 C31 C32 1.381(6) . ?
 C31 H31 0.9300 . ?
 C32 C33 1.387(5) . ?
 C32 C35 1.506(5) . ?
 C33 H33 0.9300 . ?
 C36 C37 1.395(5) . ?
 C36 C41 1.402(5) . ?
 C41 C40 1.399(6) . ?
 C41 H41 0.9300 . ?
 C40 C39 1.371(7) . ?
 C40 C43 1.542(7) . ?
 C39 C38 1.395(6) . ?
 C39 H39 0.9300 . ?
 C37 C38 1.399(5) . ?
 C37 H37 0.9300 . ?
 C38 C42 1.491(7) . ?
 C45 C50 1.392(4) . ?
 C45 C46 1.399(4) . ?
 C46 C47 1.383(4) . ?
 C46 H45 0.9300 . ?
 C47 C48 1.393(5) . ?
 C47 C51 1.494(5) . ?
 C48 C49 1.375(5) . ?
 C48 H47 0.9300 . ?
 C49 C50 1.407(4) . ?
 C49 C52 1.502(4) . ?
 C50 H50 0.9300 . ?
 C53 C58 1.403(4) . ?
 C53 C54 1.407(4) . ?
 C58 C57 1.390(4) . ?
 C58 H58 0.9300 . ?
 C57 C56 1.383(4) . ?
 C57 C60 1.494(4) . ?
 C56 C55 1.393(5) . ?
 C56 H56 0.9300 . ?
 C55 C54 1.392(4) . ?
 C55 C59 1.498(5) . ?
 C54 H54 0.9300 . ?

loop_
 _geom_angle_atom_site_label_1

_geom_angle_atom_site_label_2
 _geom_angle_atom_site_label_3
 _geom_angle
 _geom_angle_site_symmetry_1
 _geom_angle_site_symmetry_3
 _geom_angle_publ_flag

C25 Ir1 C24 38.60(14) .. ?
 C25 Ir1 C21 96.97(13) .. ?
 C24 Ir1 C21 80.63(13) .. ?
 C25 Ir1 C20 80.81(13) .. ?
 C24 Ir1 C20 88.20(13) .. ?
 C21 Ir1 C20 36.91(14) .. ?
 C25 Ir1 N1 153.97(13) .. ?
 C24 Ir1 N1 167.22(13) .. ?
 C21 Ir1 N1 95.84(12) .. ?
 C20 Ir1 N1 96.35(12) .. ?
 C25 Ir1 P1 94.25(10) .. ?
 C24 Ir1 P1 95.35(10) .. ?
 C21 Ir1 P1 155.94(10) .. ?
 C20 Ir1 P1 167.12(10) .. ?
 N1 Ir1 P1 82.84(8) .. ?
 C2 Fe1 C1 41.66(14) .. ?
 C2 Fe1 C3' 119.36(16) .. ?
 C1 Fe1 C3' 157.18(16) .. ?
 C2 Fe1 C3 40.84(13) .. ?
 C1 Fe1 C3 69.30(14) .. ?
 C3' Fe1 C3 104.23(16) .. ?
 C2 Fe1 C4' 153.27(16) .. ?
 C1 Fe1 C4' 162.01(16) .. ?
 C3' Fe1 C4' 40.57(17) .. ?
 C3 Fe1 C4' 117.31(16) .. ?
 C2 Fe1 C4 68.42(15) .. ?
 C1 Fe1 C4 68.82(15) .. ?
 C3' Fe1 C4 121.13(16) .. ?
 C3 Fe1 C4 40.31(16) .. ?
 C4' Fe1 C4 104.70(16) .. ?
 C2 Fe1 C5 69.13(15) .. ?
 C1 Fe1 C5 41.21(14) .. ?
 C3' Fe1 C5 158.40(16) .. ?
 C3 Fe1 C5 68.38(16) .. ?
 C4' Fe1 C5 123.24(16) .. ?
 C4 Fe1 C5 40.39(16) .. ?
 C2 Fe1 C5' 165.38(15) .. ?
 C1 Fe1 C5' 127.45(16) .. ?
 C3' Fe1 C5' 67.95(16) .. ?

C3 Fe1 C5' 153.15(15) .. ?
 C4' Fe1 C5' 40.15(17) .. ?
 C4 Fe1 C5' 120.18(16) .. ?
 C5 Fe1 C5' 108.98(16) .. ?
 C2 Fe1 C2' 108.76(15) .. ?
 C1 Fe1 C2' 123.96(14) .. ?
 C3' Fe1 C2' 40.53(15) .. ?
 C3 Fe1 C2' 123.86(16) .. ?
 C4' Fe1 C2' 67.90(15) .. ?
 C4 Fe1 C2' 158.86(17) .. ?
 C5 Fe1 C2' 160.03(15) .. ?
 C5' Fe1 C2' 67.75(15) .. ?
 C2 Fe1 C1' 128.13(15) .. ?
 C1 Fe1 C1' 111.64(15) .. ?
 C3' Fe1 C1' 67.79(16) .. ?
 C3 Fe1 C1' 162.46(16) .. ?
 C4' Fe1 C1' 67.51(16) .. ?
 C4 Fe1 C1' 157.20(17) .. ?
 C5 Fe1 C1' 124.64(16) .. ?
 C5' Fe1 C1' 40.19(15) .. ?
 C2' Fe1 C1' 40.15(15) .. ?
 C1 P1 C6 112.12(18) .. ?
 C1 P1 C12 105.58(16) .. ?
 C6 P1 C12 104.26(16) .. ?
 C1 P1 Ir1 98.32(12) .. ?
 C6 P1 Ir1 121.11(12) .. ?
 C12 P1 Ir1 114.61(12) .. ?
 C2 N1 C19 109.6(3) .. ?
 C2 N1 C18 108.7(3) .. ?
 C19 N1 C18 106.7(3) .. ?
 C2 N1 Ir1 106.17(19) .. ?
 C19 N1 Ir1 115.1(2) .. ?
 C18 N1 Ir1 110.5(2) .. ?
 C28 B1 C53 115.1(3) .. ?
 C28 B1 C36 112.2(3) .. ?
 C53 B1 C36 103.1(2) .. ?
 C28 B1 C45 104.4(2) .. ?
 C53 B1 C45 112.3(2) .. ?
 C36 B1 C45 109.8(3) .. ?
 C2 C1 C5 106.4(3) .. ?
 C2 C1 P1 115.0(3) .. ?
 C5 C1 P1 138.6(3) .. ?
 C2 C1 Fe1 68.13(19) .. ?
 C5 C1 Fe1 69.9(2) .. ?
 P1 C1 Fe1 125.43(19) .. ?
 C3 C2 C1 108.8(3) .. ?

C3 C2 N1 129.6(3) . . ?
 C1 C2 N1 121.4(3) . . ?
 C3 C2 Fe1 70.8(2) . . ?
 C1 C2 Fe1 70.22(19) . . ?
 N1 C2 Fe1 128.6(2) . . ?
 C4 C3 C2 107.8(3) . . ?
 C4 C3 Fe1 70.1(2) . . ?
 C2 C3 Fe1 68.38(19) . . ?
 C4 C3 H3 126.1 . . ?
 C2 C3 H3 126.1 . . ?
 Fe1 C3 H3 127.0 . . ?
 C3 C4 C5 109.1(3) . . ?
 C3 C4 Fe1 69.6(2) . . ?
 C5 C4 Fe1 70.0(2) . . ?
 C3 C4 H4 125.5 . . ?
 C5 C4 H4 125.5 . . ?
 Fe1 C4 H4 126.5 . . ?
 C4 C5 C1 107.9(3) . . ?
 C4 C5 Fe1 69.6(2) . . ?
 C1 C5 Fe1 68.9(2) . . ?
 C4 C5 H5 126.0 . . ?
 C1 C5 H5 126.0 . . ?
 Fe1 C5 H5 127.0 . . ?
 C2' C1' C5' 108.1(3) . . ?
 C2' C1' Fe1 69.6(2) . . ?
 C5' C1' Fe1 69.4(2) . . ?
 C2' C1' H1' 126.0 . . ?
 C5' C1' H1' 126.0 . . ?
 Fe1 C1' H1' 126.6 . . ?
 C1' C2' C3' 107.8(3) . . ?
 C1' C2' Fe1 70.3(2) . . ?
 C3' C2' Fe1 69.1(2) . . ?
 C1' C2' H2' 126.1 . . ?
 C3' C2' H2' 126.1 . . ?
 Fe1 C2' H2' 126.1 . . ?
 C4' C3' C2' 107.8(4) . . ?
 C4' C3' Fe1 69.9(2) . . ?
 C2' C3' Fe1 70.3(2) . . ?
 C4' C3' H3' 126.1 . . ?
 C2' C3' H3' 126.1 . . ?
 Fe1 C3' H3' 125.2 . . ?
 C5' C4' C3' 108.3(3) . . ?
 C5' C4' Fe1 70.2(2) . . ?
 C3' C4' Fe1 69.6(2) . . ?
 C5' C4' H4' 125.9 . . ?
 C3' C4' H4' 125.9 . . ?

Fe1 C4' H4' 125.9 . . ?
 C4' C5' C1' 108.1(4) . . ?
 C4' C5' Fe1 69.6(2) . . ?
 C1' C5' Fe1 70.4(2) . . ?
 C4' C5' H5' 126.0 . . ?
 C1' C5' H5' 126.0 . . ?
 Fe1 C5' H5' 125.6 . . ?
 C11 C6 C7 119.1(3) . . ?
 C11 C6 P1 117.3(3) . . ?
 C7 C6 P1 123.3(3) . . ?
 C6 C7 C8 119.3(4) . . ?
 C6 C7 H7 120.3 . . ?
 C8 C7 H7 120.3 . . ?
 C9 C8 C7 120.6(5) . . ?
 C9 C8 H8 119.7 . . ?
 C7 C8 H8 119.7 . . ?
 C10 C9 C8 120.7(4) . . ?
 C10 C9 H9 119.6 . . ?
 C8 C9 H9 119.6 . . ?
 C9 C10 C11 118.9(5) . . ?
 C9 C10 H10 120.5 . . ?
 C11 C10 H10 120.5 . . ?
 C6 C11 C10 121.3(4) . . ?
 C6 C11 H11 119.3 . . ?
 C10 C11 H11 119.3 . . ?
 C17 C12 C13 119.0(4) . . ?
 C17 C12 P1 119.5(3) . . ?
 C13 C12 P1 121.4(3) . . ?
 C14 C13 C12 120.5(4) . . ?
 C14 C13 H13 119.8 . . ?
 C12 C13 H13 119.8 . . ?
 C15 C14 C13 120.3(4) . . ?
 C15 C14 H14 119.8 . . ?
 C13 C14 H14 119.8 . . ?
 C14 C15 C16 119.7(4) . . ?
 C14 C15 H15 120.1 . . ?
 C16 C15 H15 120.1 . . ?
 C15 C16 C17 120.5(5) . . ?
 C15 C16 H16 119.8 . . ?
 C17 C16 H16 119.8 . . ?
 C12 C17 C16 120.0(5) . . ?
 C12 C17 H17 120.0 . . ?
 C16 C17 H17 120.0 . . ?
 N1 C18 H18A 109.5 . . ?
 N1 C18 H18B 109.5 . . ?
 H18A C18 H18B 109.5 . . ?

N1 C18 H18C 109.5 .. ?
 H18A C18 H18C 109.5 .. ?
 H18B C18 H18C 109.5 .. ?
 N1 C19 H19A 109.5 .. ?
 N1 C19 H19B 109.5 .. ?
 H19A C19 H19B 109.5 .. ?
 N1 C19 H19C 109.5 .. ?
 H19A C19 H19C 109.5 .. ?
 H19B C19 H19C 109.5 .. ?
 C21 C20 C27 124.9(3) .. ?
 C21 C20 Ir1 69.8(2) .. ?
 C27 C20 Ir1 111.5(2) .. ?
 C21 C20 H20 117.5 .. ?
 C27 C20 H20 117.5 .. ?
 Ir1 C20 H20 88.6 .. ?
 C20 C21 C22 125.5(3) .. ?
 C20 C21 Ir1 73.3(2) .. ?
 C22 C21 Ir1 109.5(2) .. ?
 C20 C21 H21 117.3 .. ?
 C22 C21 H21 117.3 .. ?
 Ir1 C21 H21 87.2 .. ?
 C21 C22 C23 112.3(3) .. ?
 C21 C22 H22A 109.2 .. ?
 C23 C22 H22A 109.2 .. ?
 C21 C22 H22B 109.2 .. ?
 C23 C22 H22B 109.2 .. ?
 H22A C22 H22B 107.9 .. ?
 C24 C23 C22 111.3(3) .. ?
 C24 C23 H23A 109.4 .. ?
 C22 C23 H23A 109.4 .. ?
 C24 C23 H23B 109.4 .. ?
 C22 C23 H23B 109.4 .. ?
 H23A C23 H23B 108.0 .. ?
 C25 C24 C23 123.3(3) .. ?
 C25 C24 Ir1 69.80(19) .. ?
 C23 C24 Ir1 114.4(2) .. ?
 C25 C24 H24 118.4 .. ?
 C23 C24 H24 118.4 .. ?
 Ir1 C24 H24 85.9 .. ?
 C24 C25 C26 125.2(3) .. ?
 C24 C25 Ir1 71.6(2) .. ?
 C26 C25 Ir1 111.0(2) .. ?
 C24 C25 H25 117.4 .. ?
 C26 C25 H25 117.4 .. ?
 Ir1 C25 H25 87.3 .. ?
 C25 C26 C27 113.5(3) .. ?

C25 C26 H26A 108.9 .. ?
 C27 C26 H26A 108.9 .. ?
 C25 C26 H26B 108.9 .. ?
 C27 C26 H26B 108.9 .. ?
 H26A C26 H26B 107.7 .. ?
 C20 C27 C26 112.3(3) .. ?
 C20 C27 H27A 109.1 .. ?
 C26 C27 H27A 109.1 .. ?
 C20 C27 H27B 109.1 .. ?
 C26 C27 H27B 109.1 .. ?
 H27A C27 H27B 107.9 .. ?
 C29 C28 C33 115.7(3) .. ?
 C29 C28 B1 122.4(3) .. ?
 C33 C28 B1 121.5(3) .. ?
 C30 C29 C28 122.1(3) .. ?
 C30 C29 H29 118.9 .. ?
 C28 C29 H29 118.9 .. ?
 C31 C30 C29 120.6(3) .. ?
 C31 C30 C34 119.4(3) .. ?
 C29 C30 C34 119.9(3) .. ?
 C30 C31 C32 118.7(3) .. ?
 C30 C31 H31 120.7 .. ?
 C32 C31 H31 120.7 .. ?
 C31 C32 C33 120.8(3) .. ?
 C31 C32 C35 119.5(4) .. ?
 C33 C32 C35 119.6(4) .. ?
 C32 C33 C28 122.1(3) .. ?
 C32 C33 H33 119.0 .. ?
 C28 C33 H33 119.0 .. ?
 F3 C34 F1 107.8(4) .. ?
 F3 C34 F2 104.6(3) .. ?
 F1 C34 F2 104.6(4) .. ?
 F3 C34 C30 113.7(3) .. ?
 F1 C34 C30 112.5(3) .. ?
 F2 C34 C30 112.9(3) .. ?
 C37 C36 C41 115.9(3) .. ?
 C37 C36 B1 121.1(3) .. ?
 C41 C36 B1 122.8(3) .. ?
 C40 C41 C36 121.4(4) .. ?
 C40 C41 H41 119.3 .. ?
 C36 C41 H41 119.3 .. ?
 C39 C40 C41 121.6(4) .. ?
 C39 C40 C43 122.3(4) .. ?
 C41 C40 C43 116.0(5) .. ?
 C40 C39 C38 118.4(4) .. ?
 C40 C39 H39 120.8 .. ?

C38 C39 H39 120.8 .. ?	F18 C52 F17 106.9(3) .. ?
C36 C37 C38 122.9(3) .. ?	F18 C52 F16 105.2(3) .. ?
C36 C37 H37 118.6 .. ?	F17 C52 F16 106.3(3) .. ?
C38 C37 H37 118.6 .. ?	F18 C52 C49 113.3(3) .. ?
F10 C43 F11 103.7(8) .. ?	F17 C52 C49 113.0(3) .. ?
F10 C43 F12 115.4(6) .. ?	F16 C52 C49 111.6(3) .. ?
F11 C43 F12 102.8(4) .. ?	C58 C53 C54 115.7(3) .. ?
F10 C43 C40 113.7(4) .. ?	C58 C53 B1 120.0(3) .. ?
F11 C43 C40 111.8(4) .. ?	C54 C53 B1 123.8(3) .. ?
F12 C43 C40 108.8(7) .. ?	C57 C58 C53 122.4(3) .. ?
C39 C38 C37 119.7(4) .. ?	C57 C58 H58 118.8 .. ?
C39 C38 C42 121.7(4) .. ?	C53 C58 H58 118.8 .. ?
C37 C38 C42 118.6(4) .. ?	C56 C57 C58 120.9(3) .. ?
F9 C42 F8 106.9(4) .. ?	C56 C57 C60 120.5(3) .. ?
F9 C42 F7 106.6(4) .. ?	C58 C57 C60 118.5(3) .. ?
F8 C42 F7 103.3(5) .. ?	C57 C56 C55 118.0(3) .. ?
F9 C42 C38 114.7(5) .. ?	C57 C56 H56 121.0 .. ?
F8 C42 C38 112.8(4) .. ?	C55 C56 H56 121.0 .. ?
F7 C42 C38 111.8(4) .. ?	C54 C55 C56 121.0(3) .. ?
C50 C45 C46 115.9(3) .. ?	C54 C55 C59 121.0(3) .. ?
C50 C45 B1 124.1(3) .. ?	C56 C55 C59 118.0(3) .. ?
C46 C45 B1 119.9(3) .. ?	C55 C54 C53 121.8(3) .. ?
C47 C46 C45 122.5(3) .. ?	C55 C54 H54 119.1 .. ?
C47 C46 H45 118.7 .. ?	C53 C54 H54 119.1 .. ?
C45 C46 H45 118.7 .. ?	F21 C59 F19 106.4(4) .. ?
C46 C47 C48 120.9(3) .. ?	F21 C59 F20 105.8(4) .. ?
C46 C47 C51 119.9(3) .. ?	F19 C59 F20 106.3(4) .. ?
C48 C47 C51 119.2(3) .. ?	F21 C59 C55 113.2(3) .. ?
C49 C48 C47 117.8(3) .. ?	F19 C59 C55 111.7(4) .. ?
C49 C48 H47 121.1 .. ?	F20 C59 C55 112.8(3) .. ?
C47 C48 H47 121.1 .. ?	F24 C60 F22 107.1(3) .. ?
C48 C49 C50 121.1(3) .. ?	F24 C60 F23 106.4(3) .. ?
C48 C49 C52 120.3(3) .. ?	F22 C60 F23 105.3(3) .. ?
C50 C49 C52 118.6(3) .. ?	F24 C60 C57 113.4(3) .. ?
C45 C50 C49 121.7(3) .. ?	F22 C60 C57 112.4(3) .. ?
C45 C50 H50 119.1 .. ?	F23 C60 C57 111.8(3) .. ?
C49 C50 H50 119.1 .. ?	F5 C35 F6 106.9(6) .. ?
F13 C51 F14 109.2(4) .. ?	F5 C35 F4 106.0(6) .. ?
F13 C51 F15 103.3(4) .. ?	F6 C35 F4 102.4(5) .. ?
F14 C51 F15 104.2(4) .. ?	F5 C35 C32 114.4(4) .. ?
F13 C51 C47 113.6(3) .. ?	F6 C35 C32 113.7(4) .. ?
F14 C51 C47 113.7(3) .. ?	F4 C35 C32 112.4(4) .. ?
F15 C51 C47 111.9(3) .. ?	

_diffn_measured_fraction_theta_max 0.983
 _diffn_reflns_theta_full 28.48


```

_diffrn_measured_fraction_theta_full  0.983
_refine_diff_density_max    6.129
_refine_diff_density_min    -0.790
_refine_diff_density_rms    0.138

```

X-ray data for salt (S)-230·HBF₄

data_costa4_0m

```

_audit_creation_method      SHELXL-97
_chemical_name_systematic
;
?
;
_chemical_name_common      ?
_chemical_melting_point    ?
_chemical_formula_moiety   'C24 H25 Fe N P S, B F4'
_chemical_formula_sum
'C24 H25 B F4 Fe N P S'
_chemical_formula_weight   533.14
_chemical_absolute_configuration 'S'

```

```

loop_
_atom_type_symbol
_atom_type_description
_atom_type_scatter_dispersion_real
_atom_type_scatter_dispersion_imag
_atom_type_scatter_source
'C' 'C'  0.0033  0.0016

```

```

'International Tables Vol C Tables 4.2.6.8 and 6.1.1.4'
'H' 'H'  0.0000  0.0000

```

```

'International Tables Vol C Tables 4.2.6.8 and 6.1.1.4'
'B' 'B'  0.0013  0.0007

```

```

'International Tables Vol C Tables 4.2.6.8 and 6.1.1.4'
'N' 'N'  0.0061  0.0033

```

```

'International Tables Vol C Tables 4.2.6.8 and 6.1.1.4'
'F' 'F'  0.0171  0.0103

```

```

'International Tables Vol C Tables 4.2.6.8 and 6.1.1.4'
'P' 'P'  0.1023  0.0942

```

'International Tables Vol C Tables 4.2.6.8 and 6.1.1.4'
'S' 'S' 0.1246 0.1234

'International Tables Vol C Tables 4.2.6.8 and 6.1.1.4'
'Fe' 'Fe' 0.3463 0.8444

'International Tables Vol C Tables 4.2.6.8 and 6.1.1.4'

_symmetry_cell_setting Orthorhombic
_symmetry_space_group_name_H-M P2(1)2(1)2(1)
_symmetry_space_group_name_Hall 'P 2ac 2ab'

loop_
_symmetry_equiv_pos_as_xyz
'x, y, z'
'-x+1/2, -y, z+1/2'
'-x, y+1/2, -z+1/2'
'x+1/2, -y+1/2, -z'

_cell_length_a 10.3605(13)
_cell_length_b 12.6260(16)
_cell_length_c 17.967(2)
_cell_angle_alpha 90.00
_cell_angle_beta 90.00
_cell_angle_gamma 90.00
_cell_volume 2350.3(5)
_cell_formula_units_Z 4
_cell_measurement_temperature 100(2)
_cell_measurement_reflns_used 9973
_cell_measurement_theta_min 2.27
_cell_measurement_theta_max 32.47

_exptl_crystal_description block
_exptl_crystal_colour orange
_exptl_crystal_size_max 0.33
_exptl_crystal_size_mid 0.23
_exptl_crystal_size_min 0.21
exptl_crystal_density_meas 'not measured'
_exptl_crystal_density_diffn 1.507
_exptl_crystal_density_method 'not measured'
_exptl_crystal_F_000 1096
_exptl_absorpt_coefficient_mu 0.843
_exptl_absorpt_correction_type numerical
_exptl_absorpt_correction_T_min 0.7659
_exptl_absorpt_correction_T_max 0.8401

_exptl_absorpt_process_details SADABS

_exptl_special_details

;
?
;

_diffn_ambient_temperature 100(2)
_diffn_radiation_wavelength 0.71073
_diffn_radiation_type MoK α
_diffn_radiation_source 'fine-focus sealed tube'
_diffn_radiation_monochromator graphite
_diffn_measurement_device_type 'CCD area detector'
_diffn_measurement_method 'phi and omega scans'
_diffn_detector_area_resol_mean ?
_diffn_standards_number ?
_diffn_standards_interval_count ?
_diffn_standards_interval_time ?
_diffn_standards_decay_% ?
_diffn_reflns_number 35112
_diffn_reflns_av_R_equivalents 0.0332
_diffn_reflns_av_sigmaI/netI 0.0295
_diffn_reflns_limit_h_min -12
_diffn_reflns_limit_h_max 14
_diffn_reflns_limit_k_min -14
_diffn_reflns_limit_k_max 17
_diffn_reflns_limit_l_min -25
_diffn_reflns_limit_l_max 24
_diffn_reflns_theta_min 2.27
_diffn_reflns_theta_max 30.00
_reflns_number_total 6841
_reflns_number_gt 6435
_reflns_threshold_expression >2sigma(I)

_computing_data_collection 'Bruker SMART'
_computing_cell_refinement 'Bruker SMART'
_computing_data_reduction 'Bruker SAINT'
_computing_structure_solution 'SHELXS-97 (Sheldrick, 1990)'
_computing_structure_refinement 'SHELXL-97 (Sheldrick, 1997)'
_computing_molecular_graphics 'Bruker SHELXTL'
_computing_publication_material 'Bruker SHELXTL'

_refine_special_details

;

Refinement of F^2 against ALL reflections. The weighted R-factor wR and goodness of fit S are based on F^2 , conventional R-factors R are based

on F , with F' set to zero for negative F^2 . The threshold expression of $F^2 > 2\sigma(F^2)$ is used only for calculating R-factors(gt) etc. and is not relevant to the choice of reflections for refinement. R-factors based on F^2 are statistically about twice as large as those based on F , and R-factors based on ALL data will be even larger.

;

```
_refine_ls_structure_factor_coef Fsqd
_refine_ls_matrix_type full
_refine_ls_weighting_scheme calc
_refine_ls_weighting_details
'calc w=1/[s^2(Fo^2)+(0.0358P)^2+0.0000P] where P=(Fo^2+2Fc^2)/3'
_atom_sites_solution_primary direct
_atom_sites_solution_secondary difmap
_atom_sites_solution_hydrogens geom
_refine_ls_hydrogen_treatment mixed
_refine_ls_extinction_method none
_refine_ls_extinction_coef ?
_refine_ls_abs_structure_details
'Flack H D (1983), Acta Cryst. A39, 876-881'
_refine_ls_abs_structure_Flack 0.000(7)
_refine_ls_number_reflns 6841
_refine_ls_number_parameters 358
_refine_ls_number_restraints 0
_refine_ls_R_factor_all 0.0262
_refine_ls_R_factor_gt 0.0238
_refine_ls_wR_factor_ref 0.0590
_refine_ls_wR_factor_gt 0.0578
_refine_ls_goodness_of_fit_ref 1.021
_refine_ls_restrained_S_all 1.021
_refine_ls_shift/su_max 0.001
_refine_ls_shift/su_mean 0.000
```

```
loop_
_atom_site_label
_atom_site_type_symbol
_atom_site_fract_x
_atom_site_fract_y
_atom_site_fract_z
_atom_site_U_iso_or_equiv
_atom_site_adp_type
_atom_site_occupancy
_atom_site_symmetry_multiplicity
_atom_site_calc_flag
_atom_site_refinement_flags
```

_atom_site_disorder_assembly
_atom_site_disorder_group

Fe1 Fe 0.140704(17) 0.379757(13) 0.797601(10) 0.01101(5) Uani 1 1 d ...
S1 S 0.42003(3) 0.45211(3) 0.63891(2) 0.01927(8) Uani 1 1 d ...
P1 P 0.24910(3) 0.39648(2) 0.614823(19) 0.01303(7) Uani 1 1 d ...
N1 N 0.37892(11) 0.24541(9) 0.75177(7) 0.0161(2) Uani 1 1 d ...
H1A H 0.4160(16) 0.3071(13) 0.7432(9) 0.015(4) Uiso 1 1 d ...
C1 C 0.23908(13) 0.26488(10) 0.74667(8) 0.0137(2) Uani 1 1 d ...
C1' C 0.26598(15) 0.47476(12) 0.85523(9) 0.0221(3) Uani 1 1 d ...
H1' H 0.349(2) 0.4680(15) 0.8570(11) 0.036(5) Uiso 1 1 d ...
C2 C 0.17623(12) 0.33175(10) 0.69249(7) 0.0128(2) Uani 1 1 d ...
C2' C 0.19206(15) 0.53620(11) 0.80509(9) 0.0194(3) Uani 1 1 d ...
H2' H 0.2263(17) 0.5743(13) 0.7655(10) 0.016(4) Uiso 1 1 d ...
C3 C 0.04008(13) 0.32567(10) 0.70815(8) 0.0139(2) Uani 1 1 d ...
H3A H -0.0241(19) 0.3649(15) 0.6845(10) 0.024(5) Uiso 1 1 d ...
C3' C 0.05925(14) 0.52266(11) 0.82310(9) 0.0180(3) Uani 1 1 d ...
H3' H -0.0080(19) 0.5496(15) 0.7961(11) 0.026(5) Uiso 1 1 d ...
C4' C 0.05143(15) 0.45274(11) 0.88474(9) 0.0186(3) Uani 1 1 d ...
H4' H -0.0224(19) 0.4301(14) 0.9032(11) 0.025(5) Uiso 1 1 d ...
C4 C 0.02081(14) 0.25635(11) 0.76942(8) 0.0150(3) Uani 1 1 d ...
H4A H -0.0586(16) 0.2402(12) 0.7914(10) 0.011(4) Uiso 1 1 d ...
C5 C 0.14318(13) 0.21709(10) 0.79292(8) 0.0153(2) Uani 1 1 d ...
H5A H 0.1583(16) 0.1685(12) 0.8338(9) 0.012(4) Uiso 1 1 d ...
C5' C 0.17919(16) 0.42323(11) 0.90484(8) 0.0217(3) Uani 1 1 d ...
H5' H 0.2038 0.3745 0.9463 0.026 Uiso 1 1 calc R ..
C6 C 0.41659(16) 0.20448(13) 0.82680(9) 0.0255(3) Uani 1 1 d ...
H6A H 0.3850 0.2529 0.8653 0.038 Uiso 1 1 calc R ..
H6B H 0.5108 0.1995 0.8299 0.038 Uiso 1 1 calc R ..
H6C H 0.3787 0.1342 0.8344 0.038 Uiso 1 1 calc R ..
C7 C 0.42744(15) 0.17153(12) 0.69226(10) 0.0247(3) Uani 1 1 d ...
H7A H 0.4029 0.1989 0.6432 0.037 Uiso 1 1 calc R ..
H7B H 0.3894 0.1012 0.6994 0.037 Uiso 1 1 calc R ..
H7C H 0.5217 0.1664 0.6954 0.037 Uiso 1 1 calc R ..
C8 C 0.13837(15) 0.49643(10) 0.57985(8) 0.0163(3) Uani 1 1 d ...
C9 C 0.03104(15) 0.46729(12) 0.53725(9) 0.0219(3) Uani 1 1 d ...
H9A H 0.0158(19) 0.3907(16) 0.5302(11) 0.033(5) Uiso 1 1 d ...
C10 C -0.04583(17) 0.54427(15) 0.50454(10) 0.0280(3) Uani 1 1 d ...
H10A H -0.110(2) 0.5240(16) 0.4730(11) 0.029(5) Uiso 1 1 d ...
C11 C -0.01608(17) 0.65014(14) 0.51333(9) 0.0276(4) Uani 1 1 d ...
H11A H -0.0680 0.7027 0.4901 0.033 Uiso 1 1 calc R ..
C12 C 0.08966(18) 0.68000(12) 0.55601(9) 0.0274(3) Uani 1 1 d ...
H12A H 0.1090 0.7529 0.5626 0.033 Uiso 1 1 calc R ..
C13 C 0.16714(15) 0.60351(11) 0.58906(9) 0.0207(3) Uani 1 1 d ...
H13A H 0.2377(18) 0.6198(14) 0.6167(11) 0.025(5) Uiso 1 1 d ...
C14 C 0.24465(13) 0.29594(10) 0.54316(8) 0.0143(2) Uani 1 1 d ...

C15 C 0.30523(14) 0.31742(11) 0.47550(8) 0.0166(3) Uani 1 1 d ...
 H15A H 0.3492(17) 0.3807(14) 0.4704(10) 0.020(4) Uiso 1 1 d ...
 C16 C 0.29305(14) 0.24781(11) 0.41647(8) 0.0185(3) Uani 1 1 d ...
 H16A H 0.3324(16) 0.2640(12) 0.3708(9) 0.012(4) Uiso 1 1 d ...
 C17 C 0.22192(15) 0.15524(12) 0.42444(9) 0.0206(3) Uani 1 1 d ...
 H17A H 0.2130(16) 0.1100(13) 0.3858(10) 0.013(4) Uiso 1 1 d ...
 C18 C 0.16389(15) 0.13200(12) 0.49173(9) 0.0233(3) Uani 1 1 d ...
 H18A H 0.1170 0.0679 0.4975 0.028 Uiso 1 1 calc R ..
 C19 C 0.17393(14) 0.20213(12) 0.55106(9) 0.0199(3) Uani 1 1 d ...
 H19A H 0.132(2) 0.1816(15) 0.5955(11) 0.033(5) Uiso 1 1 d ...
 B1 B 0.69375(15) 0.38085(14) 0.79917(10) 0.0219(3) Uani 1 1 d ...
 F1 F 0.70622(10) 0.28031(8) 0.76822(6) 0.0343(2) Uani 1 1 d ...
 F2 F 0.75342(11) 0.45508(8) 0.75371(6) 0.0354(2) Uani 1 1 d ...
 F3 F 0.74856(10) 0.38200(11) 0.86926(6) 0.0446(3) Uani 1 1 d ...
 F4 F 0.56193(8) 0.40524(7) 0.80543(6) 0.0254(2) Uani 1 1 d ...

loop_

_atom_site_aniso_label
 _atom_site_aniso_U_11
 _atom_site_aniso_U_22
 _atom_site_aniso_U_33
 _atom_site_aniso_U_23
 _atom_site_aniso_U_13
 _atom_site_aniso_U_12

Fe1 0.01185(8) 0.01028(8) 0.01088(9) -0.00118(7) -0.00096(7) -0.00011(7)
 S1 0.01519(15) 0.01870(15) 0.02393(19) -0.00266(14) 0.00115(14) -0.00528(13)
 P1 0.01349(14) 0.01275(14) 0.01285(16) -0.00097(12) 0.00153(12) -0.00178(12)
 N1 0.0143(5) 0.0125(5) 0.0214(6) -0.0007(4) -0.0005(4) 0.0016(4)
 C1 0.0136(6) 0.0117(5) 0.0158(6) -0.0022(5) -0.0008(5) 0.0008(5)
 C1' 0.0166(7) 0.0214(7) 0.0282(8) -0.0117(6) -0.0046(6) -0.0006(6)
 C2 0.0133(5) 0.0127(5) 0.0124(7) -0.0010(5) -0.0004(5) -0.0017(4)
 C2' 0.0260(7) 0.0125(6) 0.0197(8) -0.0039(5) 0.0033(6) -0.0054(5)
 C3 0.0125(5) 0.0163(6) 0.0129(6) -0.0033(5) -0.0020(5) -0.0009(5)
 C3' 0.0188(7) 0.0131(6) 0.0222(8) -0.0048(5) -0.0040(6) 0.0023(5)
 C4' 0.0219(7) 0.0161(6) 0.0177(7) -0.0067(5) 0.0061(5) -0.0036(5)
 C4 0.0152(6) 0.0146(6) 0.0152(7) -0.0021(5) 0.0012(5) -0.0035(5)
 C5 0.0187(6) 0.0112(5) 0.0160(6) -0.0010(5) -0.0013(6) -0.0004(5)
 C5' 0.0354(8) 0.0159(6) 0.0139(7) -0.0041(5) -0.0056(6) 0.0034(6)
 C6 0.0213(7) 0.0264(7) 0.0287(8) 0.0072(6) -0.0059(6) 0.0071(7)
 C7 0.0213(7) 0.0205(7) 0.0322(9) -0.0097(6) 0.0026(6) 0.0059(6)
 C8 0.0200(6) 0.0166(6) 0.0124(6) 0.0020(5) 0.0032(5) 0.0016(6)
 C9 0.0213(7) 0.0230(7) 0.0213(8) 0.0026(6) -0.0005(6) -0.0004(6)
 C10 0.0249(8) 0.0373(9) 0.0219(8) 0.0060(7) -0.0006(6) 0.0065(7)
 C11 0.0300(8) 0.0304(8) 0.0223(8) 0.0085(6) 0.0080(7) 0.0144(7)
 C12 0.0405(9) 0.0197(7) 0.0222(8) 0.0012(6) 0.0105(7) 0.0087(7)

C13 0.0275(7) 0.0185(7) 0.0161(7) -0.0015(5) 0.0050(6) 0.0010(6)
 C14 0.0151(6) 0.0146(5) 0.0133(6) -0.0011(5) 0.0002(5) 0.0002(5)
 C15 0.0176(6) 0.0139(6) 0.0183(7) 0.0018(5) 0.0052(5) 0.0011(5)
 C16 0.0217(7) 0.0191(6) 0.0147(7) -0.0002(5) 0.0050(5) 0.0031(5)
 C17 0.0213(7) 0.0239(7) 0.0165(7) -0.0050(6) 0.0007(5) 0.0006(6)
 C18 0.0253(7) 0.0215(7) 0.0230(8) -0.0064(6) 0.0041(6) -0.0093(6)
 C19 0.0228(7) 0.0216(7) 0.0152(7) -0.0022(6) 0.0041(5) -0.0071(6)
 B1 0.0148(6) 0.0272(8) 0.0237(8) -0.0064(8) -0.0012(6) 0.0038(6)
 F1 0.0299(5) 0.0274(5) 0.0455(6) -0.0107(4) 0.0060(5) 0.0064(4)
 F2 0.0297(5) 0.0337(5) 0.0427(6) -0.0034(5) 0.0096(5) -0.0042(5)
 F3 0.0254(5) 0.0814(9) 0.0270(6) -0.0122(6) -0.0088(4) 0.0137(6)
 F4 0.0134(4) 0.0251(4) 0.0376(6) -0.0039(4) -0.0033(4) 0.0047(3)

_geom_special_details

;

All esds (except the esd in the dihedral angle between two l.s. planes)
 are estimated using the full covariance matrix. The cell esds are taken
 into account individually in the estimation of esds in distances, angles
 and torsion angles; correlations between esds in cell parameters are only
 used when they are defined by crystal symmetry. An approximate (isotropic)
 treatment of cell esds is used for estimating esds involving l.s. planes.

;

loop_	N1 C7 1.5053(18) . ?
_geom_bond_atom_site_label_1	N1 H1A 0.882(17) . ?
_geom_bond_atom_site_label_2	C1 C5 1.4289(19) . ?
_geom_bond_distance	C1 C2 1.4438(18) . ?
_geom_bond_site_symmetry_2	C1' C2' 1.414(2) . ?
_geom_bond_publ_flag	C1' C5' 1.423(2) . ?
	C1' H1' 0.87(2) . ?
Fe1 C1 1.9950(13) . ?	C2 C3 1.4404(18) . ?
Fe1 C2 2.0173(14) . ?	C2' C3' 1.424(2) . ?
Fe1 C3 2.0337(14) . ?	C2' H2' 0.929(18) . ?
Fe1 C4' 2.0386(15) . ?	C3 C4 1.420(2) . ?
Fe1 C5' 2.0427(15) . ?	C3 H3A 0.932(19) . ?
Fe1 C3' 2.0439(14) . ?	C3' C4' 1.419(2) . ?
Fe1 C1' 2.0482(15) . ?	C3' H3' 0.915(19) . ?
Fe1 C2' 2.0500(14) . ?	C4' C5' 1.422(2) . ?
Fe1 C5 2.0557(12) . ?	C4' H4' 0.88(2) . ?
Fe1 C4 2.0560(14) . ?	C4 C5 1.425(2) . ?
S1 P1 1.9537(5) . ?	C4 H4A 0.935(16) . ?
P1 C2 1.7847(14) . ?	C5 H5A 0.970(16) . ?
P1 C14 1.8087(14) . ?	C5' H5' 1.0000 . ?
P1 C8 1.8176(15) . ?	C6 H6A 0.9800 . ?
N1 C1 1.4723(18) . ?	C6 H6B 0.9800 . ?
N1 C6 1.4954(19) . ?	C6 H6C 0.9800 . ?

C7 H7A 0.9800 . ?	C2 Fe1 C5' 158.15(6) . . ?
C7 H7B 0.9800 . ?	C3 Fe1 C5' 159.34(6) . . ?
C7 H7C 0.9800 . ?	C4' Fe1 C5' 40.77(6) . . ?
C8 C13 1.3944(19) . ?	C1 Fe1 C3' 162.86(6) . . ?
C8 C9 1.399(2) . ?	C2 Fe1 C3' 123.40(6) . . ?
C9 C10 1.387(2) . ?	C3 Fe1 C3' 105.18(6) . . ?
C9 H9A 0.99(2) . ?	C4' Fe1 C3' 40.67(6) . . ?
C10 C11 1.381(3) . ?	C5' Fe1 C3' 68.41(6) . . ?
C10 H10A 0.91(2) . ?	C1 Fe1 C1' 109.50(6) . . ?
C11 C12 1.389(3) . ?	C2 Fe1 C1' 122.25(6) . . ?
C11 H11A 0.9500 . ?	C3 Fe1 C1' 157.06(6) . . ?
C12 C13 1.389(2) . ?	C4' Fe1 C1' 68.56(6) . . ?
C12 H12A 0.9500 . ?	C5' Fe1 C1' 40.72(7) . . ?
C13 H13A 0.907(19) . ?	C3' Fe1 C1' 68.37(6) . . ?
C14 C15 1.3946(19) . ?	C1 Fe1 C2' 126.73(6) . . ?
C14 C19 1.4000(19) . ?	C2 Fe1 C2' 107.67(6) . . ?
C15 C16 1.383(2) . ?	C3 Fe1 C2' 120.56(6) . . ?
C15 H15A 0.925(18) . ?	C4' Fe1 C2' 68.40(6) . . ?
C16 C17 1.389(2) . ?	C5' Fe1 C2' 68.19(6) . . ?
C16 H16A 0.939(17) . ?	C3' Fe1 C2' 40.70(6) . . ?
C17 C18 1.382(2) . ?	C1' Fe1 C2' 40.37(6) . . ?
C17 H17A 0.903(17) . ?	C1 Fe1 C5 41.28(6) . . ?
C18 C19 1.390(2) . ?	C2 Fe1 C5 70.07(5) . . ?
C18 H18A 0.9500 . ?	C3 Fe1 C5 68.81(5) . . ?
C19 H19A 0.95(2) . ?	C4' Fe1 C5 119.26(6) . . ?
B1 F3 1.382(2) . ?	C5' Fe1 C5 107.74(6) . . ?
B1 F2 1.388(2) . ?	C3' Fe1 C5 153.67(6) . . ?
B1 F1 1.392(2) . ?	C1' Fe1 C5 126.72(6) . . ?
B1 F4 1.4046(17) . ?	C2' Fe1 C5 164.17(6) . . ?
loop_	C1 Fe1 C4 69.19(6) . . ?
_geom_angle_atom_site_label_1	C2 Fe1 C4 69.63(5) . . ?
_geom_angle_atom_site_label_2	C3 Fe1 C4 40.64(5) . . ?
_geom_angle_atom_site_label_3	C4' Fe1 C4 104.93(6) . . ?
_geom_angle	C5' Fe1 C4 123.63(6) . . ?
_geom_angle_site_symmetry_1	C3' Fe1 C4 118.34(6) . . ?
_geom_angle_site_symmetry_3	C1' Fe1 C4 162.01(6) . . ?
_geom_angle_publ_flag	C2' Fe1 C4 154.58(6) . . ?
C1 Fe1 C2 42.18(5) . . ?	C5 Fe1 C4 40.56(6) . . ?
C1 Fe1 C3 69.84(6) . . ?	C2 P1 C14 102.97(6) . . ?
C2 Fe1 C3 41.65(5) . . ?	C2 P1 C8 108.74(6) . . ?
C1 Fe1 C4' 155.88(6) . . ?	C14 P1 C8 103.01(6) . . ?
C2 Fe1 C4' 159.65(6) . . ?	C2 P1 S1 112.02(5) . . ?
C3 Fe1 C4' 121.74(6) . . ?	C14 P1 S1 115.67(5) . . ?
C1 Fe1 C5' 121.89(6) . . ?	C8 P1 S1 113.52(5) . . ?
	C1 N1 C6 111.76(12) . . ?
	C1 N1 C7 112.82(11) . . ?

C6 N1 C7 109.81(11) . . ?
 C1 N1 H1A 105.7(11) . . ?
 C6 N1 H1A 110.4(11) . . ?
 C7 N1 H1A 106.2(11) . . ?
 C5 C1 C2 108.99(12) . . ?
 C5 C1 N1 125.28(12) . . ?
 C2 C1 N1 125.69(12) . . ?
 C5 C1 Fe1 71.64(8) . . ?
 C2 C1 Fe1 69.74(7) . . ?
 N1 C1 Fe1 126.55(9) . . ?
 C2' C1' C5' 107.91(13) . . ?
 C2' C1' Fe1 69.88(8) . . ?
 C5' C1' Fe1 69.43(8) . . ?
 C2' C1' H1' 128.0(14) . . ?
 C5' C1' H1' 124.1(14) . . ?
 Fe1 C1' H1' 126.3(13) . . ?
 C3 C2 C1 106.18(12) . . ?
 C3 C2 P1 126.26(10) . . ?
 C1 C2 P1 127.17(10) . . ?
 C3 C2 Fe1 69.78(8) . . ?
 C1 C2 Fe1 68.09(8) . . ?
 P1 C2 Fe1 132.19(7) . . ?
 C1' C2' C3' 108.23(14) . . ?
 C1' C2' Fe1 69.75(8) . . ?
 C3' C2' Fe1 69.42(8) . . ?
 C1' C2' H2' 124.4(11) . . ?
 C3' C2' H2' 127.2(11) . . ?
 Fe1 C2' H2' 123.3(10) . . ?
 C4 C3 C2 108.78(12) . . ?
 C4 C3 Fe1 70.52(8) . . ?
 C2 C3 Fe1 68.56(8) . . ?
 C4 C3 H3A 125.5(12) . . ?
 C2 C3 H3A 125.6(12) . . ?
 Fe1 C3 H3A 123.2(11) . . ?
 C4' C3' C2' 107.89(13) . . ?
 C4' C3' Fe1 69.46(8) . . ?
 C2' C3' Fe1 69.88(8) . . ?
 C4' C3' H3' 127.0(12) . . ?
 C2' C3' H3' 124.8(12) . . ?
 Fe1 C3' H3' 121.6(12) . . ?
 C3' C4' C5' 107.95(13) . . ?
 C3' C4' Fe1 69.87(8) . . ?
 C5' C4' Fe1 69.77(8) . . ?
 C3' C4' H4' 123.0(13) . . ?
 C5' C4' H4' 128.9(13) . . ?
 Fe1 C4' H4' 122.4(12) . . ?

C3 C4 C5 108.59(12) . . ?
 C3 C4 Fe1 68.83(8) . . ?
 C5 C4 Fe1 69.71(7) . . ?
 C3 C4 H4A 125.8(10) . . ?
 C5 C4 H4A 125.6(10) . . ?
 Fe1 C4 H4A 126.4(10) . . ?
 C4 C5 C1 107.43(12) . . ?
 C4 C5 Fe1 69.73(7) . . ?
 C1 C5 Fe1 67.08(7) . . ?
 C4 C5 H5A 126.0(10) . . ?
 C1 C5 H5A 126.6(10) . . ?
 Fe1 C5 H5A 127.1(9) . . ?
 C4' C5' C1' 108.01(13) . . ?
 C4' C5' Fe1 69.46(8) . . ?
 C1' C5' Fe1 69.85(8) . . ?
 C4' C5' H5' 126.0 . . ?
 C1' C5' H5' 126.0 . . ?
 Fe1 C5' H5' 126.0 . . ?
 N1 C6 H6A 109.5 . . ?
 N1 C6 H6B 109.5 . . ?
 H6A C6 H6B 109.5 . . ?
 N1 C6 H6C 109.5 . . ?
 H6A C6 H6C 109.5 . . ?
 H6B C6 H6C 109.5 . . ?
 N1 C7 H7A 109.5 . . ?
 N1 C7 H7B 109.5 . . ?
 H7A C7 H7B 109.5 . . ?
 N1 C7 H7C 109.5 . . ?
 H7A C7 H7C 109.5 . . ?
 H7B C7 H7C 109.5 . . ?
 C13 C8 C9 119.33(14) . . ?
 C13 C8 P1 119.82(12) . . ?
 C9 C8 P1 120.54(11) . . ?
 C10 C9 C8 120.25(15) . . ?
 C10 C9 H9A 122.7(12) . . ?
 C8 C9 H9A 117.0(12) . . ?
 C11 C10 C9 120.11(17) . . ?
 C11 C10 H10A 120.4(13) . . ?
 C9 C10 H10A 119.1(13) . . ?
 C10 C11 C12 120.12(15) . . ?
 C10 C11 H11A 119.9 . . ?
 C12 C11 H11A 119.9 . . ?
 C13 C12 C11 120.20(15) . . ?
 C13 C12 H12A 119.9 . . ?
 C11 C12 H12A 119.9 . . ?
 C12 C13 C8 119.98(15) . . ?

C12 C13 H13A 122.8(12) .. ?
 C8 C13 H13A 117.2(11) .. ?
 C15 C14 C19 119.24(13) .. ?
 C15 C14 P1 118.20(10) .. ?
 C19 C14 P1 122.34(11) .. ?
 C16 C15 C14 120.25(13) .. ?
 C16 C15 H15A 121.2(11) .. ?
 C14 C15 H15A 118.4(11) .. ?
 C15 C16 C17 120.25(14) .. ?
 C15 C16 H16A 119.5(10) .. ?
 C17 C16 H16A 120.3(9) .. ?
 C18 C17 C16 119.99(14) .. ?
 C18 C17 H17A 119.6(11) .. ?
 C16 C17 H17A 120.4(11) .. ?
 C17 C18 C19 120.21(14) .. ?
 C17 C18 H18A 119.9 .. ?
 C19 C18 H18A 119.9 .. ?
 C18 C19 C14 120.03(14) .. ?
 C18 C19 H19A 116.1(12) .. ?
 C14 C19 H19A 123.9(12) .. ?
 F3 B1 F2 110.25(14) .. ?
 F3 B1 F1 109.62(14) .. ?
 F2 B1 F1 109.83(13) .. ?
 F3 B1 F4 108.93(13) .. ?
 F2 B1 F4 109.39(14) .. ?
 F1 B1 F4 108.80(12) .. ?

loop_

_geom_torsion_atom_site_label_1
 _geom_torsion_atom_site_label_2
 _geom_torsion_atom_site_label_3
 _geom_torsion_atom_site_label_4
 _geom_torsion
 _geom_torsion_site_symmetry_1
 _geom_torsion_site_symmetry_2
 _geom_torsion_site_symmetry_3
 _geom_torsion_site_symmetry_4
 _geom_torsion_publ_flag

C6 N1 C1 C5 -22.08(17) ?
 C7 N1 C1 C5 102.25(16) ?
 C6 N1 C1 C2 160.56(13) ?
 C7 N1 C1 C2 -75.12(16) ?
 C6 N1 C1 Fe1 70.46(14) ?
 C7 N1 C1 Fe1 -165.22(10) ?
 C2 Fe1 C1 C5 -119.21(11) ?

C3 Fe1 C1 C5 -80.48(8) ?
 C4' Fe1 C1 C5 42.98(17) ?
 C5' Fe1 C1 C5 80.51(10) ?
 C3' Fe1 C1 C5 -156.36(18) ?
 C1' Fe1 C1 C5 123.91(9) ?
 C2' Fe1 C1 C5 165.83(9) ?
 C4 Fe1 C1 C5 -36.96(8) ?
 C3 Fe1 C1 C2 38.73(7) ?
 C4' Fe1 C1 C2 162.19(13) ?
 C5' Fe1 C1 C2 -160.28(8) ?
 C3' Fe1 C1 C2 -37.2(2) ?
 C1' Fe1 C1 C2 -116.88(8) ?
 C2' Fe1 C1 C2 -74.97(10) ?
 C5 Fe1 C1 C2 119.21(11) ?
 C4 Fe1 C1 C2 82.24(8) ?
 C2 Fe1 C1 N1 120.03(15) ?
 C3 Fe1 C1 N1 158.76(13) ?
 C4' Fe1 C1 N1 -77.78(19) ?
 C5' Fe1 C1 N1 -40.25(14) ?
 C3' Fe1 C1 N1 82.9(2) ?
 C1' Fe1 C1 N1 3.15(14) ?
 C2' Fe1 C1 N1 45.06(15) ?
 C5 Fe1 C1 N1 -120.76(15) ?
 C4 Fe1 C1 N1 -157.73(13) ?
 C1 Fe1 C1' C2' 124.25(9) ?
 C2 Fe1 C1' C2' 79.17(10) ?
 C3 Fe1 C1' C2' 40.07(18) ?
 C4' Fe1 C1' C2' -81.44(10) ?
 C5' Fe1 C1' C2' -119.16(13) ?
 C3' Fe1 C1' C2' -37.57(9) ?
 C5 Fe1 C1' C2' 167.33(9) ?
 C4 Fe1 C1' C2' -153.19(17) ?
 C1 Fe1 C1' C5' -116.58(9) ?
 C2 Fe1 C1' C5' -161.67(8) ?
 C3 Fe1 C1' C5' 159.23(13) ?
 C4' Fe1 C1' C5' 37.73(9) ?
 C3' Fe1 C1' C5' 81.60(9) ?
 C2' Fe1 C1' C5' 119.16(13) ?
 C5 Fe1 C1' C5' -73.51(11) ?
 C4 Fe1 C1' C5' -34.0(2) ?
 C5 C1 C2 C3 1.48(14) ?
 N1 C1 C2 C3 179.21(12) ?
 Fe1 C1 C2 C3 -59.69(9) ?
 C5 C1 C2 P1 -171.71(10) ?
 N1 C1 C2 P1 6.02(19) ?
 Fe1 C1 C2 P1 127.11(11) ?

C5 C1 C2 Fe1 61.18(9) ?
 N1 C1 C2 Fe1 -121.10(13) ?
 C14 P1 C2 C3 -85.91(12) ?
 C8 P1 C2 C3 22.88(14) ?
 S1 P1 C2 C3 149.16(10) ?
 C14 P1 C2 C1 85.97(12) ?
 C8 P1 C2 C1 -165.24(11) ?
 S1 P1 C2 C1 -38.96(13) ?
 C14 P1 C2 Fe1 179.13(9) ?
 C8 P1 C2 Fe1 -72.08(10) ?
 S1 P1 C2 Fe1 54.20(10) ?
 C1 Fe1 C2 C3 117.93(11) ?
 C4' Fe1 C2 C3 -41.01(19) ?
 C5' Fe1 C2 C3 168.25(13) ?
 C3' Fe1 C2 C3 -74.39(9) ?
 C1' Fe1 C2 C3 -158.30(8) ?
 C2' Fe1 C2 C3 -116.41(8) ?
 C5 Fe1 C2 C3 80.16(8) ?
 C4 Fe1 C2 C3 36.83(8) ?
 C3 Fe1 C2 C1 -117.93(11) ?
 C4' Fe1 C2 C1 -158.94(15) ?
 C5' Fe1 C2 C1 50.32(17) ?
 C3' Fe1 C2 C1 167.69(8) ?
 C1' Fe1 C2 C1 83.78(9) ?
 C2' Fe1 C2 C1 125.67(8) ?
 C5 Fe1 C2 C1 -37.77(8) ?
 C4 Fe1 C2 C1 -81.10(8) ?
 C1 Fe1 C2 P1 -120.95(13) ?
 C3 Fe1 C2 P1 121.12(13) ?
 C4' Fe1 C2 P1 80.11(19) ?
 C5' Fe1 C2 P1 -70.63(18) ?
 C3' Fe1 C2 P1 46.73(12) ?
 C1' Fe1 C2 P1 -37.17(12) ?
 C2' Fe1 C2 P1 4.71(11) ?
 C5 Fe1 C2 P1 -158.72(11) ?
 C4 Fe1 C2 P1 157.95(11) ?
 C5' C1' C2' C3' -0.29(16) ?
 Fe1 C1' C2' C3' 58.93(10) ?
 C5' C1' C2' Fe1 -59.23(10) ?
 C1 Fe1 C2' C1' -76.44(11) ?
 C2 Fe1 C2' C1' -119.33(9) ?
 C3 Fe1 C2' C1' -163.06(9) ?
 C4' Fe1 C2' C1' 81.89(10) ?
 C5' Fe1 C2' C1' 37.85(9) ?
 C3' Fe1 C2' C1' 119.65(13) ?
 C5 Fe1 C2' C1' -40.1(3) ?

C4 Fe1 C2' C1' 161.07(13) ?
 C1 Fe1 C2' C3' 163.91(9) ?
 C2 Fe1 C2' C3' 121.02(9) ?
 C3 Fe1 C2' C3' 77.29(10) ?
 C4' Fe1 C2' C3' -37.76(9) ?
 C5' Fe1 C2' C3' -81.80(10) ?
 C1' Fe1 C2' C3' -119.65(13) ?
 C5 Fe1 C2' C3' -159.78(19) ?
 C4 Fe1 C2' C3' 41.42(18) ?
 C1 C2 C3 C4 -0.61(15) ?
 P1 C2 C3 C4 172.66(10) ?
 Fe1 C2 C3 C4 -59.21(10) ?
 C1 C2 C3 Fe1 58.60(9) ?
 P1 C2 C3 Fe1 -128.13(11) ?
 C1 Fe1 C3 C4 81.18(8) ?
 C2 Fe1 C3 C4 120.38(11) ?
 C4' Fe1 C3 C4 -75.19(10) ?
 C5' Fe1 C3 C4 -47.21(18) ?
 C3' Fe1 C3 C4 -116.05(9) ?
 C1' Fe1 C3 C4 173.76(13) ?
 C2' Fe1 C3 C4 -157.28(8) ?
 C5 Fe1 C3 C4 36.93(8) ?
 C1 Fe1 C3 C2 -39.20(7) ?
 C4' Fe1 C3 C2 164.43(8) ?
 C5' Fe1 C3 C2 -167.59(14) ?
 C3' Fe1 C3 C2 123.57(8) ?
 C1' Fe1 C3 C2 53.38(17) ?
 C2' Fe1 C3 C2 82.34(9) ?
 C5 Fe1 C3 C2 -83.45(8) ?
 C4 Fe1 C3 C2 -120.38(11) ?
 C1' C2' C3' C4' 0.14(16) ?
 Fe1 C2' C3' C4' 59.28(10) ?
 C1' C2' C3' Fe1 -59.14(10) ?
 C1 Fe1 C3' C4' -168.01(18) ?
 C2 Fe1 C3' C4' 162.93(8) ?
 C3 Fe1 C3' C4' 121.38(9) ?
 C5' Fe1 C3' C4' -37.90(9) ?
 C1' Fe1 C3' C4' -81.85(10) ?
 C2' Fe1 C3' C4' -119.12(13) ?
 C5 Fe1 C3' C4' 48.60(17) ?
 C4 Fe1 C3' C4' 79.70(10) ?
 C1 Fe1 C3' C2' -48.9(2) ?
 C2 Fe1 C3' C2' -77.95(10) ?
 C3 Fe1 C3' C2' -119.50(9) ?
 C4' Fe1 C3' C2' 119.12(13) ?
 C5' Fe1 C3' C2' 81.22(10) ?

C1' Fe1 C3' C2' 37.27(9) ?
 C5 Fe1 C3' C2' 167.72(12) ?
 C4 Fe1 C3' C2' -161.18(9) ?
 C2' C3' C4' C5' 0.07(16) ?
 Fe1 C3' C4' C5' 59.61(10) ?
 C2' C3' C4' Fe1 -59.54(10) ?
 C1 Fe1 C4' C3' 171.38(13) ?
 C2 Fe1 C4' C3' -44.82(19) ?
 C3 Fe1 C4' C3' -75.67(10) ?
 C5' Fe1 C4' C3' 119.01(12) ?
 C1' Fe1 C4' C3' 81.33(10) ?
 C2' Fe1 C4' C3' 37.79(9) ?
 C5 Fe1 C4' C3' -157.59(8) ?
 C4 Fe1 C4' C3' -116.34(9) ?
 C1 Fe1 C4' C5' 52.37(17) ?
 C2 Fe1 C4' C5' -163.83(14) ?
 C3 Fe1 C4' C5' 165.32(8) ?
 C3' Fe1 C4' C5' -119.01(12) ?
 C1' Fe1 C4' C5' -37.68(9) ?
 C2' Fe1 C4' C5' -81.22(9) ?
 C5 Fe1 C4' C5' 83.40(10) ?
 C4 Fe1 C4' C5' 124.65(9) ?
 C2 C3 C4 C5 -0.48(15) ?
 Fe1 C3 C4 C5 -58.50(9) ?
 C2 C3 C4 Fe1 58.01(9) ?
 C1 Fe1 C4 C3 -82.91(8) ?
 C2 Fe1 C4 C3 -37.71(8) ?
 C4' Fe1 C4 C3 121.69(9) ?
 C5' Fe1 C4 C3 161.88(8) ?
 C3' Fe1 C4 C3 80.12(9) ?
 C1' Fe1 C4 C3 -172.11(17) ?
 C2' Fe1 C4 C3 50.77(17) ?
 C5 Fe1 C4 C3 -120.51(12) ?
 C1 Fe1 C4 C5 37.59(8) ?
 C2 Fe1 C4 C5 82.80(9) ?
 C3 Fe1 C4 C5 120.51(12) ?
 C4' Fe1 C4 C5 -117.80(9) ?
 C5' Fe1 C4 C5 -77.62(10) ?
 C3' Fe1 C4 C5 -159.37(9) ?
 C1' Fe1 C4 C5 -51.6(2) ?
 C2' Fe1 C4 C5 171.27(13) ?
 C3 C4 C5 C1 1.40(15) ?
 Fe1 C4 C5 C1 -56.56(9) ?
 C3 C4 C5 Fe1 57.96(9) ?
 C2 C1 C5 C4 -1.79(14) ?
 N1 C1 C5 C4 -179.53(12) ?

Fe1 C1 C5 C4 58.20(9) ?
 C2 C1 C5 Fe1 -59.99(9) ?
 N1 C1 C5 Fe1 122.27(13) ?
 C1 Fe1 C5 C4 -120.19(12) ?
 C2 Fe1 C5 C4 -81.62(9) ?
 C3 Fe1 C5 C4 -37.01(8) ?
 C4' Fe1 C5 C4 78.44(10) ?
 C5' Fe1 C5 C4 121.37(9) ?
 C3' Fe1 C5 C4 44.36(17) ?
 C1' Fe1 C5 C4 162.42(9) ?
 C2' Fe1 C5 C4 -166.2(2) ?
 C2 Fe1 C5 C1 38.56(8) ?
 C3 Fe1 C5 C1 83.18(9) ?
 C4' Fe1 C5 C1 -161.38(8) ?
 C5' Fe1 C5 C1 -118.44(9) ?
 C3' Fe1 C5 C1 164.54(12) ?
 C1' Fe1 C5 C1 -77.39(10) ?
 C2' Fe1 C5 C1 -46.0(2) ?
 C4 Fe1 C5 C1 120.19(12) ?
 C3' C4' C5' C1' -0.25(16) ?
 Fe1 C4' C5' C1' 59.42(10) ?
 C3' C4' C5' Fe1 -59.67(10) ?
 C2' C1' C5' C4' 0.34(16) ?
 Fe1 C1' C5' C4' -59.18(10) ?
 C2' C1' C5' Fe1 59.51(10) ?
 C1 Fe1 C5' C4' -157.60(8) ?
 C2 Fe1 C5' C4' 164.92(13) ?
 C3 Fe1 C5' C4' -37.65(19) ?
 C3' Fe1 C5' C4' 37.80(9) ?
 C1' Fe1 C5' C4' 119.30(12) ?
 C2' Fe1 C5' C4' 81.76(9) ?
 C5 Fe1 C5' C4' -114.51(9) ?
 C4 Fe1 C5' C4' -72.68(10) ?
 C1 Fe1 C5' C1' 83.11(10) ?
 C2 Fe1 C5' C1' 45.62(18) ?
 C3 Fe1 C5' C1' -156.94(14) ?
 C4' Fe1 C5' C1' -119.30(12) ?
 C3' Fe1 C5' C1' -81.49(9) ?
 C2' Fe1 C5' C1' -37.53(9) ?
 C5 Fe1 C5' C1' 126.20(9) ?
 C4 Fe1 C5' C1' 168.02(8) ?
 C2 P1 C8 C13 110.06(12) ?
 C14 P1 C8 C13 -141.17(12) ?
 S1 P1 C8 C13 -15.34(13) ?
 C2 P1 C8 C9 -76.38(13) ?
 C14 P1 C8 C9 32.39(13) ?

S1 P1 C8 C9 158.22(11) ?
 C13 C8 C9 C10 0.0(2) ?
 P1 C8 C9 C10 -173.58(13) ?
 C8 C9 C10 C11 0.6(3) ?
 C9 C10 C11 C12 -1.1(3) ?
 C10 C11 C12 C13 1.0(2) ?
 C11 C12 C13 C8 -0.4(2) ?
 C9 C8 C13 C12 -0.1(2) ?
 P1 C8 C13 C12 173.54(12) ?
 C2 P1 C14 C15 -174.48(11) ?
 C8 P1 C14 C15 72.47(12) ?
 S1 P1 C14 C15 -51.96(12) ?

C2 P1 C14 C19 11.01(14) ?
 C8 P1 C14 C19 -102.04(13) ?
 S1 P1 C14 C19 133.53(11) ?
 C19 C14 C15 C16 1.4(2) ?
 P1 C14 C15 C16 -173.28(11) ?
 C14 C15 C16 C17 -0.9(2) ?
 C15 C16 C17 C18 -0.5(2) ?
 C16 C17 C18 C19 1.5(2) ?
 C17 C18 C19 C14 -1.0(2) ?
 C15 C14 C19 C18 -0.5(2) ?
 P1 C14 C19 C18 173.99(12) ?

_diffn_measured_fraction_theta_max 1.000
 _diffn_reflns_theta_full 30.00
 _diffn_measured_fraction_theta_full 1.000
 _refine_diff_density_max 0.297
 _refine_diff_density_min -0.201
 _refine_diff_density_rms 0.049